ISSN: 2795-1944

Date of Printing: June, 2022

Date of Publishing: June, 2022

Editor: Er. Bikesh Kunwar

Publication:

SET – Advanced College of Engineering and Management

Kalanki, Kathmandu

Proceedings

of

2nd National Conference

on

Science, Engineering and Technology

(SET Conference 2019- Innovation in Science, Engineering & Technology)

Vol: 2

November 23, 2019

Associate Editors:

Er. Prabin Dawadi

Er. Subeksha Khanal

Er. Bigyan Karki

Er. Laxmi Prasad Bhatt

Er. Sameer Sitoula

Committee Members of Set Conference – 2019

Advisory Board

Prof. Dr. Subarna Shakya
Prof. Shashidhar Ram Joshi, PhD
Assoc. Prof. Dr. Vinod Parajuli
Er. Santosh Kumar Shrestha
Assoc. Prof. Laxmi Bhakta Maharjan

Executive Committee

President
Er. Ajaya Shrestha

Vice President
Er. Amit Kumar Rauniyar

Secretary
Er. Prerana Khwaunju

Joint Secretary
Er. Narayan K.C.

Media Coordinator
Er. Pradip Khanal

Technical Coordinator
Er. Ram Prasad Sapkota

Finance Coordinator
Er. Prem Chandra Roy

Conference Coordinator
Er. Anku Jaiswal

Members

Er. Pradip Khanal
Er. Neha Karn
Er. Bikash Acharya
Er. Abhishesh Dahal
Er. Laxmi K.C.
Er. Sujata Dahal
Er. Deepak Kumar Singh
Mr. Gunanidhi Gyawali
Er. Prathana Khakurel
Er. Kushal Dahal
Er. Prakash Upadhyaya
Er. Gopal Dutta Bhatta
Er. Lok Bahadur Mijar
Er. Sagar Dharel
Er. Anil Panjiyar
Er. Abcon Budhathoki
Er. Nishant Bhatta
Er. Pankaj Shrestha
Er. Aviral Upadhya

Table of Contents

Part I: AI and Decision Support System

Part II: Fuzzy Logic ANN and Genetic Algorithms

Part III: Data Science, Analysis and Mining

Part IV: Communication System

Part V: Construction Field and Building Techniques

Part VI: Soil Mechanics and Irrigation

Part VII: Electrical Engineering

Part VIII: Applied Sciences

Part I: AI and Decision Support System

Application of Machine Learning in Stock Market

Narayan K.C.[1]

[1]*Department of Graduate Studies, NCIT, Lalitpur, Nepal*

narayanck@gmail.com

Abstract

Stock market is very vast and difficult to understand as it isn't certain either it will increase or decrease the following day as there is huge fluctuation of the market. Investing in a stock market is very tedious task as one can earn tons of profit also one can face loss? Investing in a good stock can help to outcome profit, similarly investing in a bad one can bear loss. Financial investors nowadays are facing problem of trading as they do not properly understand where to invest.

The goal of this paper is to investigate the machine learning technique is able to retrieve information from past prices and predict price movement and future trends. We explore using trend trading indicators in a machine learning based model. We propose algorithms that combine different technical and fundamental indicators in order to provide accurate positive indicators for financial market movements. In this paper, machine learning technique called the Artificial Intelligence is applied to big data from the financial market that is of high volume, high velocity, high variety and high variability using real time and off-line data of different time granularities. The results of predictive algorithms were analyzed and presented. Experimental results confirmed that the use of machine learning and artificial intelligence methods can help to select top performing result in financial markets.

Keywords*: machine learning, finance, fraud, deep learning, financial markets.*

1. Introduction

Stock market predication is the act of trying to determine the future value of a company stock. Stock market plays vital role in the growth of the economy condition. To raise funds for a company stock market is considered as a primary source. Stock market is based on the concept of demand and supply. If the demand for a company's stock is higher, then the company share increase and vice-versa.

The New York Stock Exchange is an American stock exchange located at 11 Wall Street, Lower Manhattan, New York City, New York. It is by far the world's largest stock exchange by market capitalization of its listed companies at US$30.1 trillion as of February 2018. The average daily trading value was approximately US$169 billion in 2013. The NYSE trading floor is located at 11 Wall Street and is composed of 21 rooms used for the

facilitation of trading.

The Nepal stock exchange limited (NEPSE) is the only stock exchange of Nepal. NEPSE opened its trading floor on 13th January 1994. The basic objective of NEPSE is to impart free marketability and liquidity to the government and corporate securities by facilitating transactions in its trading floor through member, market intermediaries, such as broker, market makers etc.

Stock market prediction system will allow us to predict the market pattern and predict the time to purchase stock. If predicted successfully it can provide huge profit. This can have done by using large market data to represent varying condition so that generate pattern have statistically significant predictive power for high probability of prediction the right amount.

2. Literature Review

Over the past time many important changes have taken place in the environment of financial markets. In order to be able to extract such relationship from available data, data mining technique are used with involvement of advance math and science. Some models have been proposed and implemented using the above mentioned techniques, the authors of [5] made an empirical study on building a stock buying/selling alert system using back propagation neural networks (BPNN), their NN was codenamed NN5. The system was trained and tested with past price data from Hong Kong and Shanghai Banking Corporation Holdings over the period from January 2004 to December 2005. The empirical results showed that the implemented system was able to predict short-term price movement directions with accuracy about 74%.

Wilson and Sharda studied prediction firm bankruptcy using neural networks and classical multiple discriminant analysis, where neural networks performed significantly better than multiple discriminant analysis [1].

Min and Lee were doing prediction of bankruptcy using machine learning. They evaluated methods based on Support Vector Machine, multiple discriminant analysis, logistic regression analysis, and three-layer fully connected back-propagation neural networks. Their results indicated that support vector machines outperformed other approaches. Lee was trying to predict credit rating of a company using support vector machines. They used various financial indicator and ratios such as interest coverage ratio, ordinary income to total assets, Net income to stakeholders' equity, current liabilities ratio, etc. and achieved accuracy of around 60%. Predicting credit rating of the companies were also studied using neural networks achieving accuracy between 75% and 80% for the United States and Taiwan markets [2].

Tsai and Wang did a research where they tried to predict stock prices by using ensemble learning, composed of decision trees and artificial neural networks. They created dataset from Taiwanese stock market data, taking into account fundamental indexes, technical indexes, and macroeconomic indexes. The performance of Decision Tree and

Artificial Neural Network trained on Taiwan stock exchange data showed F-score performance of 77%. Single algorithms showed F-score performance up to 67% [3].

Kim and Han used a genetic algorithm to transform continuous input values into discrete ones. The genetic algorithm was used to reduce the complexity of the feature space. This paper proposes a novel evolutionary computing method called a genetic quantum algorithm. Genetic Quantum Algorithm is based on the concept and principles of quantum computing such as qubits and superposition of states. Instead of binary, numeric, or

symbolic representation, by adopting bit chromosome as a representation Genetic Quantum Algorithm can represent a linear superposition of solutions due to its probabilistic representation. As genetic operators, quantum gates are employed for the search of the best solution [4].

3. Methodology

In this section, we will review various purposed method that have been planned to be used for the completion of the stock prediction system to be designed. Its development consists of various phases ranging from selection of software development approach to the algorithms used. The various methods of the system are described as below in details.

a. Software Development Approach

As we are trying to develop a stock prediction system, we have to use training data to the system and make changes to the system as per our need to get a more efficient architecture with minimum number of neurons and maximum efficiency with a small period of time, the software development model best for us was found to be Incremental Model.

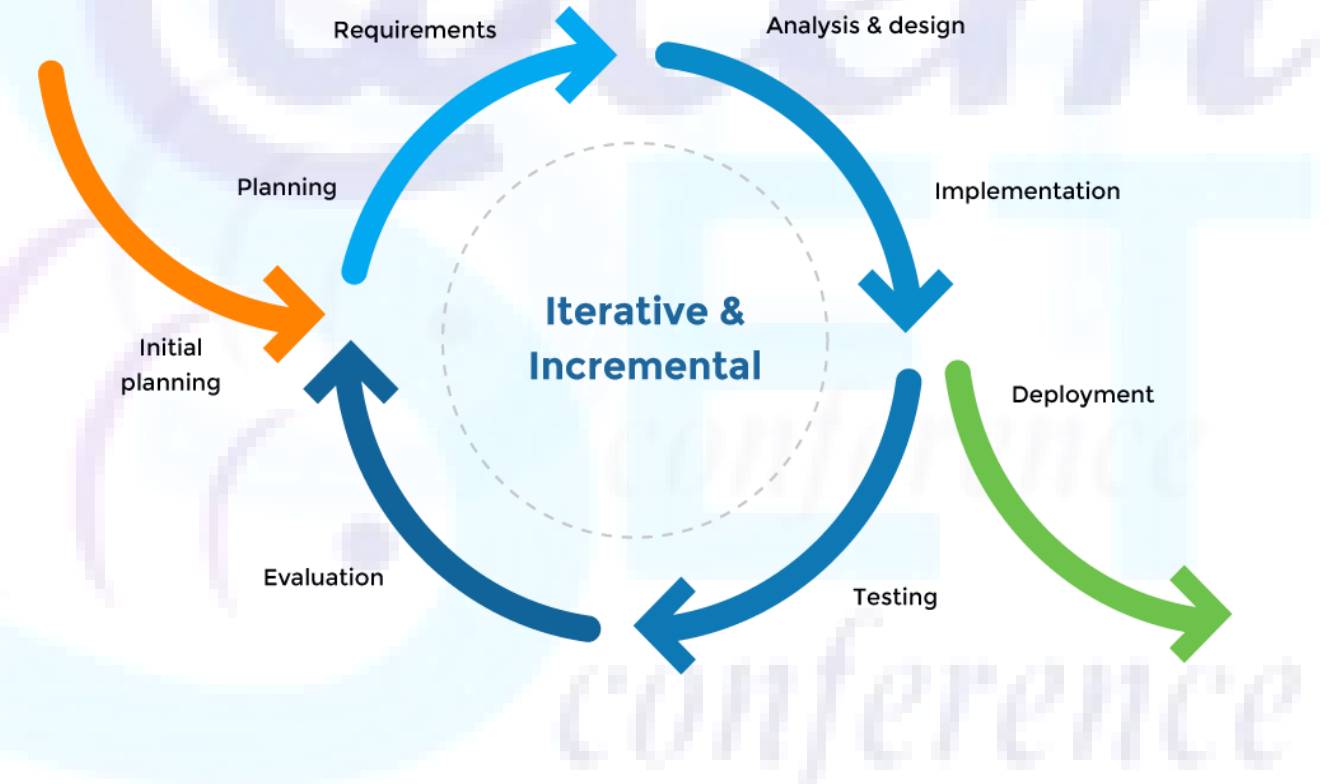

Figure 1: Incremental Model

(Source: https://www.quora.com/What-is-the-difference-between-Waterfall-and-Incremental-Model)

b. Data Collection

For the prediction of stock, we need large amount of data for training purpose of the system of developed. The data needs to be correct and should be obtained from a reliable source so as to increase the accuracy of the

prediction system. We were able to collect data as per our required parameters. We collected data related to opening value, closing value, stock volume, highest price and lowest price and then the correct stock value for the various mentioned parameters were categorized as required in the project. The collected data could be fed to the predicting system for training purpose and for testing the results.

c. Parameters

i. Opening Price

The opening price is the price at which a security first trades upon the opening of an exchange on a trading day; for example, the Nepse opens at precisely 11:00 a.m. Nepalese time. The price of the first trade for any listed stock is its daily opening price.

ii. Closing Price

The closing price is the final price at which a share is traded on a given trading day. The closing price represents the most up-to-date price of a share until trading commences again on the next trading day. For example, NEPSE closes precisely at 3:00 pm on working days.

iii. Highest Price

The highest price that a stock has attained is also one of the key parameter while predicting the system's future. It can be different from the highest or lowest price and sometimes equal to them.

iv. *Lowest Price*

General Index is the weighted average of price of all the listed companies. It is a tool used by investors and financial managers to describe the market. Increasing index indicates bullish trend and decreasing index indicates bearish trend**.**

v. Volume

The total number of stocks traded within a span in a trading day is the volume of the stock. The company has a specified portion of the share distributed to the public and the number of shares that are traded by the general people in a day is the total volume.

d. Data Preprocessing

The raw data that had been previously collected aren't always in the required format to be fed into the artificial neural network. If wrong data is fed into the system, the system gets changed according to the wrong data which decreases the accuracy of the system. So, the data were preprocessed and the incorrect data, missing data were corrected and added in the system.

e. Data Normalization

The data collected for different parameters vary from each other over a wide range which may reduce the efficiency of the system. So, the data needs to be normalized before being fed into the system. The data are

normalized in the range [0, 1] using min-max function as below:

$$\text{Normalized value of X} = \frac{X - \text{Min value of } X}{\text{Max value of } X - \text{Min value of } X}$$

f. Neural Network Implementation

The neural network selected to be worked for this project is Multilayer Perceptron Network, which is a class of feedforward neural network, consisting of input layer, hidden layer and output layer. The implementation of neural network is discussed further below.

g. *Neural Network Architecture*

The multilayer feed forward neural network that we decided to use initially consists of three layers: input layer, hidden layer and output layer. The input layer consists of 6 neurons as we will be taking 6 parameters as input, the number of neurons in the hidden layer will depends on the training phase as the number of neurons which gives maximum accuracy will be used in the final application, and the output layer will only contain one neuron which will give the predicted stock value.

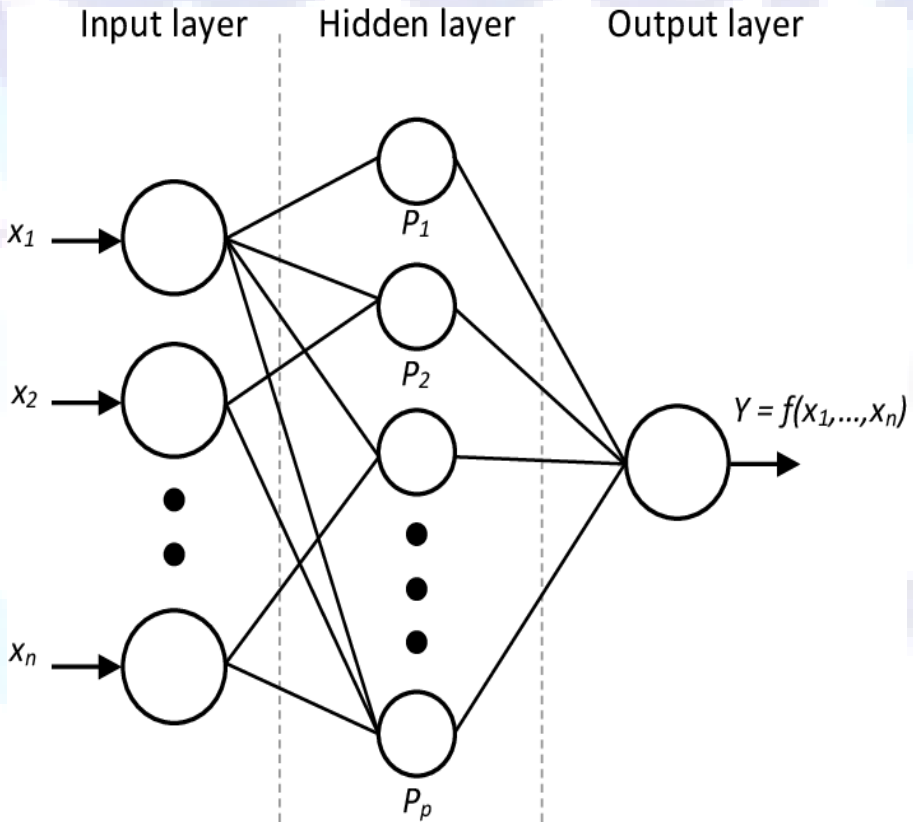

Figure 2: Neural Network Architecture
(Source: ioenotes.edu.np)

i. Activation Function

Activation function is needed for our neural network as it adds non-linearity to the system, which allows the neural network to compute and learn any problem. Activation function is used in hidden layer. The activation function that we used for this project is sigmoid function which is as below:

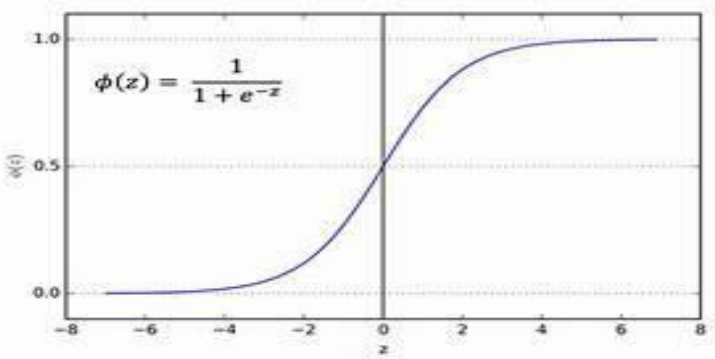

$$F(x) = \frac{1}{1+e^{-x}}$$

Sigmoid function is used as it gives output between 0 and 1 which allows the output to be seen as a probability, and this function can be easily differentiable.

ii. Feedforward neural network with backpropagation

A feedforward neural network consists of three layers: input layer, hidden layer and output layer. Each neuron in one layer is connected to every other neuron of neuron in another layer. The path connecting the neurons are called synapse. Each synapse has some weight assigned to it. The weights of these synapses are responsible for predicting the final output.

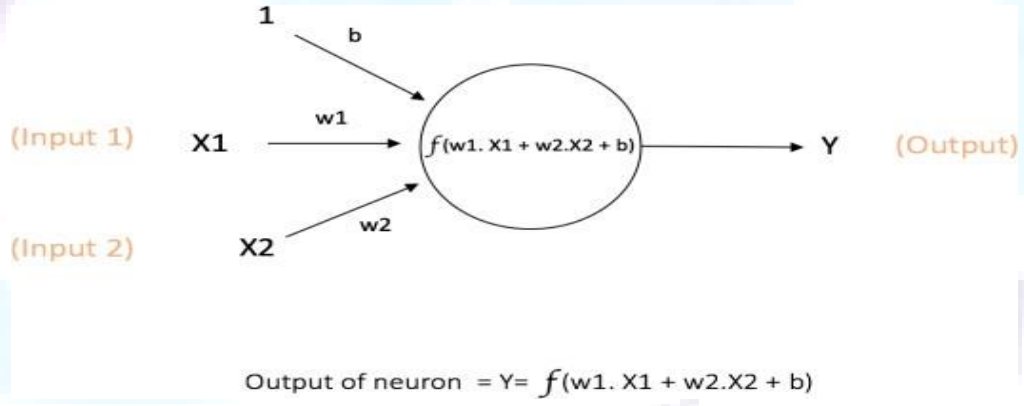

Figure 3: Representation of Neuron

(Source: https://towardsdatascience.com/deep-learning-feedforward-neural-network-26a6705dbdc7)

Neural network needs some sort of algorithm for it to be able to learn and mimic certain functions by adding training data to it. Backpropagation is one of the learning algorithm used with multilayer perceptron neural network. It is supervised learning algorithm used to train a feed forward network. The process of backpropagation is repeated until a satisfactory error is obtained by the neural network.

The Algorithm for backpropagation is as below:

Step1: Initialize some small random value as weight for the synapse.
Step2: Feed training data to the neural network and obtain the output.
Step3: Compute the error for each output unit as the difference between required output and obtained output.
Step4: The mean square error reflects the effectiveness of training done on the neural network.
Step5: Back propagate the errors till the input layer.
Step6: Calculate the weight to be updated (delta) for all the weights on the synapses across the network.
Step7: Update the old weight and replace it by new weight on all the synapses.
Step8: Feed another test data and repeat the process to make the neural network more accurate.
Step9: Repeat all the processes till the required accuracy is obtained.

4. Result and Analysis

The stock market prediction system has been developed and can predict the values of various companies. One of the example of this is as shown below which is of the Intel company.

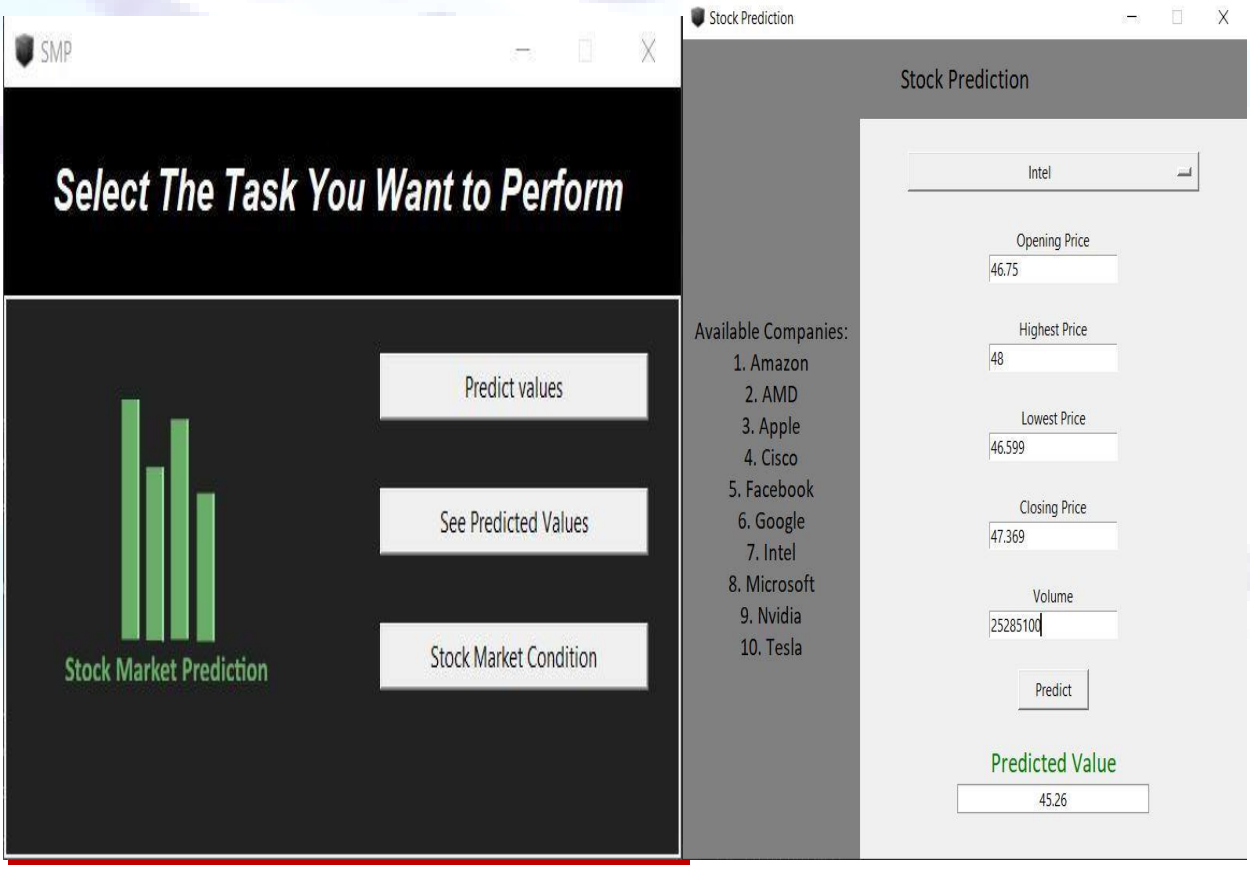

Figure 4: Stock market prediction system

data

Stock Prediction

S.N.	Traded Companies	Open price	Highest Price	Lowest price	Close Price	Volume	Predicted Average Stock (1 Day)	Predicted Average Stock (3 Days)
1	Amazon	1901.3499760000002	1921.6700440000002	1899.790039	1901.369995	3871900.0	1566.671557260609	1528.8592601385071
2	AMD	29.76	30.969998999999998	29.58	30.450001	85779500.0	18.982705416261226	24.731468419249595
3	Apple	196.050003	200.28999299999998	195.21000700000002	198.449997	26087900.0	167.30812797307854	176.12509579252608
4	Cisco	56.07	56.650002	55.75	56.049999	21039600.0	46.24085151516866	46.82191509623988
5	Facebook	194.0	194.529999	187.279999	188.470001	37231600.0	162.86344406575802	173.27423716076254
6	Google	1109.689941	1116.390015	1098.98999	1103.599976	1378700.0	1182.3529597967372	1173.9631342501461
7	Intel	46.75	48.0	46.599998	47.369999	25285100.0	45.26369798890444	45.94762972026032
8	Microsoft	125.260002	125.760002	124.779999	125.730003	16829600.0	108.1732862338014	105.74996571540808
9	Nvidia	147.5	155.110001	147.059998	152.880005	14268200.0	151.41173623928717	152.14276218126855
10	Tesla	228.72000099999997	234.74000499999997	222.559998	224.74000499999997	12668900.0	257.0861524157525	256.79346361131167

Figure 5: Predicted data

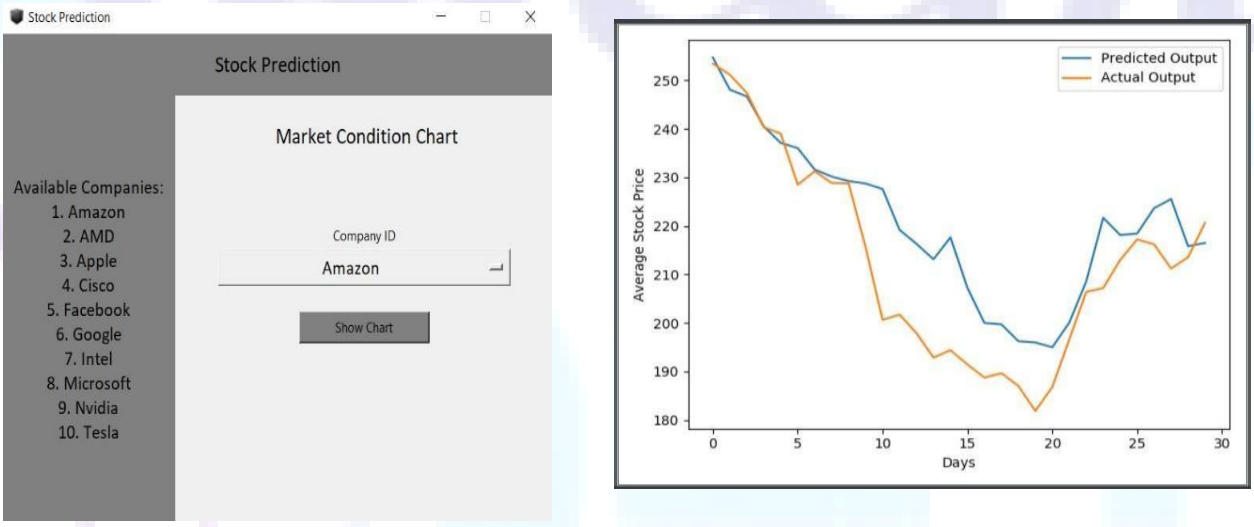

Figure 6: Actual vs Predicted Graph

Here we can see the graphs of predicted and actual value of the company. X- axis represents time and Y-axis represents the average stock price. There exists a reasonable degree of accuracy which we desire.

In this way, we have designed Stock Market Prediction System using ANN and have learnt various things during this time. We learned to analyze the components of neural network and also of the various stocks. We have also achieved a fair degree of accuracy and the nature of the stock has been predicted using the prediction system.

5. Conclusion

Hence we can conclude that we are able to design the stock market prediction application using artificial neural network i.e. multilayer perceptron neural network. We also have identified the parameters effecting the share market.

We can also predict the value of any company's share with a reasonable degree of accuracy.

References

[1] R. L. Wilson and S. Ramesh, "Bankruptcy Prediction using Neural Networks," Elsevier, June, 1994.

[2] J. MIn and Y. Lee, "The Prediction Model of Financial Crisis Based on the Combination Principle Component Analysis and Support Vector Machines," Open Journal of Social Sciences, vol. Vol.2, 2014.

[3] K.-H. Tsai and J.-C. Wang, "External technology sourcing and innovation performance in LMT sectors: An analysis based on the Taiwanese Technological Innovation Survey," Elsevier, vol. 38, no. 3, 2009.

[4] K.-H. Han and J.-H. Kim, "Genetic Quantum Algorithm and its Application to Combinational Optimization Problem".

[5] Tsang, P.M., Kwok, P., Choy, S.O., Kwan, R., Ng, S.C., Mak, J., Tsang, J., Koong, K., and Wong, T.L. (2007) "Design and implementation of NN5 for Hong Kong stock price forecasting", Engineering Applications of Artificial Intelligence, 20, pp. 453-461.

[6] Web Search Engine.

Deep Learning Based Seed Quality Tester

Manish Bhurtel[1], Jabeen Shrestha[2], Niten Lama[3], Sajan Bhattarai[4], Aashma Uprety[5], Manoj Kumar Guragain[6]

[1,2,3,4,5]*Students of Department of Electronics and Computer Engineering, Institute of Engineering, Purwanchal Campus, Dharan Sub-Metropolitan City, Sunsari, Nepal*

[6]*Lecturer at Department of Electronics and Computer Engineering, Institute of Engineering, Purwanchal Campus, Dharan Sub-Metropolitan City, Sunsari, Nepal*

[1]manish.bhurtel09@gmail.com, [2]jabeenshrestha@gmail.com, [3]nitenlama46@gmail.com, [4]sajanbhatte@gmail.com, [5]aashmauprety99@gmail.com, [6]manojkguragai@ioepc.edu.np

Abstract

The paper presents a novel solution to the problem faced by the commercial farmers and seed packaging industries. It is very inconvenient to filter out every damaged seed and foreign elements by winnowing in industries and commercial farming. This issue can be minimized if the seeds are filtered in clusters. The paper presents an approach to enhance the efficiency in seed cultivation and seed packaging processes. We created a high-quality dataset which includes fine maize seeds, damaged maize seeds, and foreign elements. By using the Deep Learning technique, the system categorizes an input image as Excellent, Good, Average, Bad and Worst quality seed cluster. The Excellent and Good clusters (sometimes Average) can be cultivated or packaged, and the Bad and Worst clusters can be rejected. We also have recommended the use of object detection to detect and filter out damaged seeds and foreign elements from good quality seed clusters.

Keywords: *Seed Quality Tester, Deep Learning, Convolutional Neural Network, Optimizers, Dropout, Hidden Neuron*

1. Introduction

In the commercial seed cultivation sector, it is not feasible to filter out the individual damaged seeds and foreign elements in the case of the voluminous amount of seeds. Moreover, in the seed packaging industries, the seed filtering is done by the manual labor force which leads to poor quality seeds in the packets and waste of a large amount of fine quality seeds. In this context, efficient and automated seed testing [17] is the most important part of all other seeds technologies. Seed testing facilities need to evaluate tens of thousands of seed lots each year [17]. To make ease in all the sectors of seeds, there should be some efficiency and automation in the seed filtering and packaging sectors. All these problems motivated us to enhance efficiency and bring automation by the use of Deep Learning technique. This would help to cultivate the fine quality seeds and reject the bad quality seeds without much effort. On the other hand, packaging of only fine quality seeds in seed packaging industries can be ensured by the use of our system. In this regard, we came across various solutions but the deep learning technique was an ideal approach to implement the system efficiently. Furthermore, use of Artificial Intelligence and Machine Learning is quite rare in the context of agriculture and industry, especially in Nepal. We also aimed to synchronize

the Artificial Intelligence, Agriculture and Seed Packaging Industry, which would be a novel solution in Nepal. Therefore, the purpose of the paper is to use the deep learning technique to generate a system that can enhance ease in the commercial seed cultivation and seed packaging industries. In this context, we are also motivated to carry out research on object detection in the future. By the use of object detection, we can detect few damaged seeds and foreign elements present in the cluster of good quality seeds, and detect the few fine quality seeds present in the bad quality cluster. In this way, we can easily separate the fine-quality cultivable seeds from the damaged seeds and foreign elements.

2. Literature Review

With the reference of the paper [16], we found the idea of processing the images of the seed which would also be highly practical in the context of Nepal. In this paper, Digital Image Processing and MATLAB were used for the processing of the image and classifying it as Bad Purity or Good Purity or Excellent Purity. But we felt that the cluster made for the image processing would not give accurate results as the seeds underneath would not be visible.

In the paper [3], they have used Computer Vision to detect the germination of Lettuce Seeds. They have created the image dataset by placing the seeds distinctly. They used the Edge Detection method and principle of counting to detect the germinated seeds. But still, the counting would not be feasible for implementing our concept.

Furthermore, in the paper [9], they have proposed the automation idea of seed testing using Image Analysis Software and Edge Detection but still, the dominating features in the images could not be extracted with just image analysis software.

With the paper published in 2018 [1], we were enlightened by the very convincing method of using deep learning technique in the agricultural purposes. They proposed a systematic approach of using a deep learning model for the prediction of a category of an image. Furthermore, with the reference of the handbook of Julianna Bányai [8], we came across the idea about creating a seed lot which could be a very novel concept and useful for the commercial farmers and seed packaging industries.

Deep Learning or Hierarchical Learning has been emerging as a new area of research on Machine Learning [2]. Deep learning discovers detailed structure in huge datasets by using the backpropagation [23] and updating the internal parameters that are used to predict certain categories.

With the amalgamation of all the concepts and techniques, we finally came across the idea of using Convolutional Neural Network (CNN) for detecting the quality of the image Seed Lot (16 seeds) as Excellent, Good, Average, Bad and Worst quality. CNN is an extension of the Artificial Neural Network (ANN) that is comprised of neurons that optimize itself through continuous learning [13]. In the paper [13], CNN composed of 3 layers viz. convolution layers, pooling layers and fully connected layers. They implemented it for the MNIST dataset for detecting the hand-written digits.

We were also inclined towards the concept cited in the paper [21] which compared the different results obtained from Transfer Learning of ResNet, Inception v3, Xception and VGG 19 [21] but we believed that it would be effective to adjust the hyperparameters and design the CNN architecture on our own as per our dataset and requirements.

3. Methodology

The paper proposes the system to detect the quality of a seed lot using Convolutional Neural Network (CNN). The system has been developed in four stages: Dataset Preparation, Image Pre - processing, Building CNN, and Compiling and Training CNN.

3.1 Dataset Preparation

To generate our dataset, we used the maize variety, Super 900 M - F1, which is largely available at the Eastern Terai Region of Nepal. We included fine seeds, damaged seeds and foreign elements in the dataset and categorized the seed lot in percentage basis (Table 1) as Excellent, Good, Average, Bad and Worst as in figure 1. First, we clicked the images of the seed lot with a normal camera with not so good resolution. But the detailing that the system require to distinguish between the fine seed and damaged seeds, were not good enough which could make our system vulnerable to inaccurate predictions. So we again clicked 3000 images with high-quality camera and generated high-quality dataset with sharp detailing. We tried to accommodate all the possible orientations of the seeds in the seed lot so that the model learns all the different positions of the seeds in the cluster. Finally, we separated the dataset as 2500 training data and 500 testing data belonging to five categories as in Table 1.

(a) Excellent Quality (b) Good Quality (c) Average Quality

(d) Bad Quality (e) Worst Quality

Figure 1: Different Qualities of the Seed Lots based on the percentage of Fine Quality Seeds

3.2 Image Pre-processing

Table 1: Percentage of fine seeds, and damaged seeds or foreign elements in different seed lots

Categories (Seed Lot)	Fine Seeds (%)	Damaged Seeds or Foreign Elements (%)
Excellent Quality	100	0
Good Quality	61 – 99	1 – 39
Average Quality	40 – 60	40 – 60
Bad Quality	1 – 39	61 – 99
Worst Quality	0	100

The dataset should be processed before feeding it into the neural network. We augmented the dataset using the library function provided by Keras and processed all the images to uniform 256 *256 resolution. Increasing the input shape beyond this resolution could give more accuracy but slows down the speed. This resolution keeps the distinguishing features of the damaged seeds which makes the machine easy to learn. The adjusted parameters are rescale, shear, zoom, width and height shifting, rotation, horizontal and vertical flip. After the dataset preparation, all the images are of uniform attributes and are ready to be fed into the Convolutional Neural Network.

3.3 Building Convolutional Neural Network (CNN)

Building a neural network was a great challenge because we need to make sure that in any of the layers, the detailing of the damaged and fine seeds is not lost. So we built our CNN keeping the high resolution for the input images.

3.3.1 Convolution and Pooling Layer

We used three convolution layers, each layer followed by a max-pooling Layer. In the convolution layer, feature detectors slide thoroughly and rapidly in the image searching for certain features within the image. The pooling function reduces the resolution of the feature maps to achieve spatial invariance [7]. We used the max-pooling function to extract the dominating or maximum features from the feature map. We used 64, 128 and 256 feature detectors in the corresponding three convolution layers and initialized the convolution layer to accept the image of 256 * 256 resolution and depth of 3 RGB color channels. The feature detector of the 3 * 3 matrix slides over the image and searches extensively for the features in the image. In max-pooling layers, the matrix of 2 * 2 pool size rolls over the feature map with a stride of 2 and collects the maximum values which are the respective dominating features in the image.

ReLU Activation

Rectified Linear Unit (ReLU) rectifies the linearities in the non – linear images. ReLU boosts up the training process [12] so as to converge to accurate predictions. 3cm.The graphical representation of ReLU in figure 2.

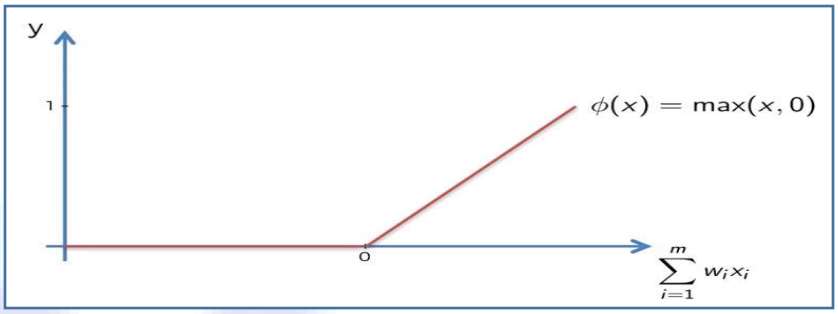

Figure 2: Rectified Linear Unit (ReLU) Activation Function

3.3.2 Dropout Layer

The dataset we created were high in quality but low in quantity. In the initial training procedure, our system was vulnerable to a high degree of overfitting. The input data must pass through a number of hidden layers which could cause the model to learn complicated relationships resulting in sampling noise and ultimately overfitting problem [19]. We overcome the issue by placing a dropout layer before the hidden layer. The dropout layer drops different units randomly from the neural architecture preventing the units from excessive co-adaptation [19]. With the placement of a dropout layer, there was no overfitting and the model predicted accurately.

3.3.3 Flattening Layer

The images after penetrating the convolution and max-pooling layers are in a two-dimensional pooled feature map. But the images should be fed into the series of artificial neurons which takes the input as a one-dimensional single vector representing the dominating features of the input image. This is achieved by performing the flattening operation to all the pooled feature maps. Finally, we have the flattened array of the input images ready to be fed into the fully connected layer.

3.3.4 Full Connection

The full connection is the addition of a general artificial neural network (ANN) with a fully connected hidden layer. With the reference of paper [10] and the number of experiments with hidden neurons, we assigned one fully connected layer with 512 hidden neurons for our system. The flattened data is passed through the number of hidden neurons and the predictive probability is passed to the final output layer. The output layer is assigned a softmax function whose output range is between 0 and 1 [4]. The softmax function designates the input image into five different output classes in our system. The softmax function with any input 'x' is calculated by using the following mathematical formula [6]:

$$f(x_i) = \frac{\exp(x_i)}{\sum_j \exp(x_j)}$$

3.4 Compiling and Training CNN

The compilation of the CNN architecture is done designating the following parameters:

Loss Function

In every iteration of the training and validation process, there arises a certain loss. The loss cannot be ignored as it is an important entity to determine the inconsistency between the predicted value and actual value. Since have used categorical cross-entropy function to calculate the errors and loss in the training of our multi-class classification approach. The error is calculated and then propagated backward from the network which updates the previous weights. The optimizer grabs a learning rate, propagates the error and updates the weights in each neuron. This helps to increase the accuracy of our training model. With the reference of the paper [20], to classify γ - dimensional input x_i to one of the C categories, then the Categorical Cross-Entropy (CCE) loss can be defined as [20]:

$$E_{CC} = -\frac{1}{N}\sum_{i=1}^{N}\sum_{c=1}^{C}(p_{ic}\log(y_{ic})),$$

Where N is the number of training data, y is the output and p_{ic} is the binary indicator function that validates the accuracy of ith training pattern to cth category.

Optimizer

We experimented with our system on adam, adagrad and adadelta optimizers. Adam optimizer had big time Complexity in our system. Furthermore, in adagrad [11], continuous decay of the learning rates throughout the training process was a major problem. Adadelta adapts the learning rate dynamically using only the first order information [24]. So we used adadelta optimizer which is the adaptive learning rate method [24] surpassing adam and adagrad optimizers.

Evaluation Metric

The training of the neural network should be evaluated with a certain metric to improve the system performance. We have chosen accuracy metric to evaluate our CNN model. After running for 100 epochs, the model finally ensued 81% training accuracy and 80% testing accuracy.

4. Experiments and Results

We experimented with our model by using different numbers of hidden nodes and dropout layers with different probabilities (p).

4.1 Experiment with different number of hidden nodes

The number of hidden nodes is to be computed from the experiments. We took 5 sets of hidden nodes with 64, 128, 256, 512 and 1024 nodes, running for 100 epochs. The accuracy increased with an increase in the number of hidden nodes. There was no huge difference in using 512 and 1024 number nodes, so we decided to take 512 number of hidden nodes for our convolutional neural network design. The results are demonstrated in the following

chart 1.

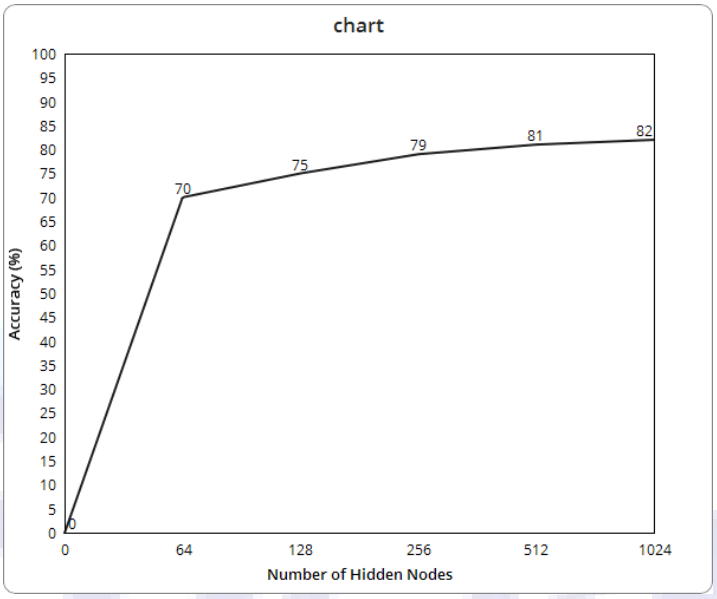

Chart 1: Change in Accuracy with increasing number of hidden nodes\

4.2 Experiment with addition of dropout layer

First, we tested the model without any dropout layer. We came across the issue of overfitting which must be addressed very carefully. Then we used the dropout layer before the hidden layer and gradually increased the probability ranging from 0.1 to 0.5. We got varying results which finally overcome the issue of overfitting and underfitting. The results are demonstrated in the following Table 2.

Table 2: Use of Dropout Layer to overcome overfitting and underfitting

	Training Accuracy (%)	**Testing Accuracy (%)**	**Remarks**
No dropout layer	77	69	Overfitting
Dropout(0.1)	76	70	Overfitting
Dropout(0.2)	76	74	Decrease in Overfitting
Dropout(0.3)	77	75	Slight Overfitting
Dropout(0.4)	78	80	Slight Underfitting
Dropout(0.5)	81	80	Almost perfect Fit

4.3 Output

After the model generation, we tested our system for the 20 test images in GUI developed using Django Framework. In the scenario, class prediction for 15 images were correct (figure 3) while the class prediction for 5 images were slightly different (figure 4) i.e. the CNN model predicted the category one step up or down.

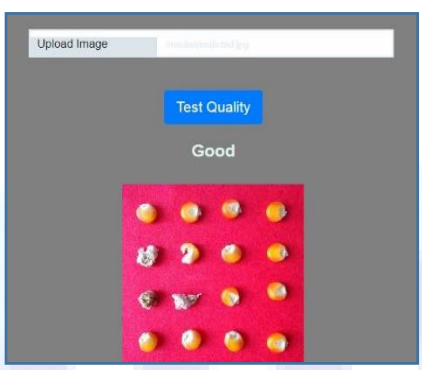

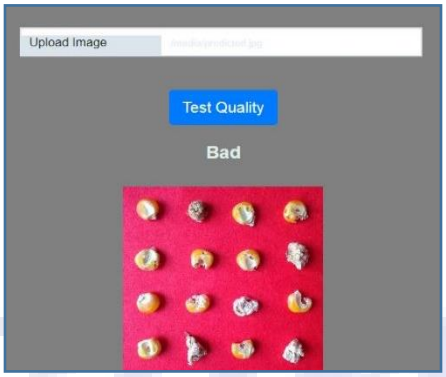

(a) Model predicting Good accurately (b) Model predicting bad accurately

Fig 3: Model showing accurate predictions

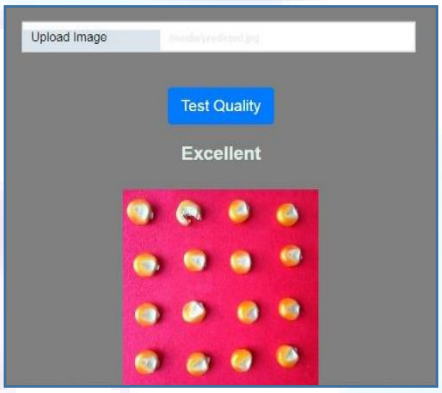

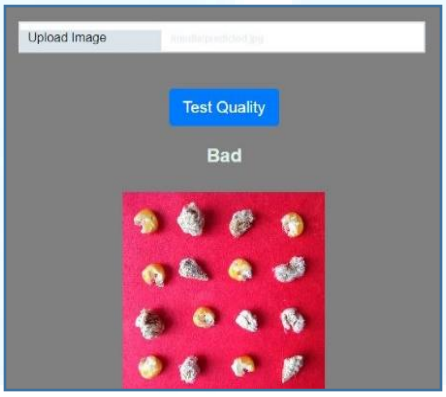

(c) Model predicting Good Quality as Excellent (d) Model predicting Worst Quality as Bad

Fig 4: Model predicting one – step up category

5. Conclusion

This paper presents an implementation of a seed quality testing system to detect the quality of a seed lot as excellent, good, average, bad and worst on the basis of the percentage of fine quality seeds in the seed lot. The decision of categorization is based on the flow of the dataset through the various neurons in the convolutional neural network (CNN). The summary of the CNN architecture used in our system is explained in the following table 3.

Table 3: Summary of the CNN Architecture in our system

Keywords	**Details**	**Remarks**
Number of Convolution Layers	3	Feature Detectors: 64, 128, 256; Input Shape: 256 * 256; Activation: ReLU
Number of Pooling Layers	3	Use of Max – Pooling
Number of Hidden Layer	1	
Number of Hidden Neurons	512	Selected with multiple experiments
Dropout layer	p=0.5	Before the Hidden Layer
Optimizer	Adadelta	
Loss Function	Cross Entropy	Categorical
Performance Metric	Accuracy	81% training accuracy; 80% testing accuracy
Output Classes	5	Excellent, Good, Average, Bad, Worst; Use of Softmax Function

6. Suggestions and Recommendations

With extensive research and experiments, we came to the conclusion that the model with small number of dataset can predict accurately if the images in the dataset are of high quality and all the hyperparameters like number of convolution layers, number of hidden neurons, use of dropout layers, etc. are properly adjusted as per the requirement of the system. In the initial phase, we did not have good accuracy, then we adjusted the hyperparameters but still, we were facing the problem of overfitting and underfitting. The problems were overcome by the use of dropout layers.

The final model of our system still ensued some inaccurate results. Those inaccuracies can also still be improved by adjusting the following parameters:

- Increasing the input shape in the convolution layer beyond 256 * 256.
- Training for higher number of epochs i.e. beyond 100.

We recommend the following future research activities to direct our project:

- Implementation using the emerging Rectified Adam optimizer (RAdam).
- Implementation and coverage of a wide variety of seeds.
- Implementation of Object Detection to detect damaged seeds and foreign elements in good quality seed lot, and fine seeds in the bad quality seed lot.
- Research to encompass different other criteria for seed quality detection like temperature, humidity, soil type and germinating nature of seed [18].

Acknowledgements

We would like to express our deep gratitude to our project supervisor Mr. Manoj Kumar Guragain for his relentless guidance and encouragement during our research project. We would also like to thank our friends Ujjawal Poudel and Saroj Raj Sharma who helped us with our research project without a frown.

We would also like to extend our thanks to Mr. Heros Silva Araujo, who is working as a Data Scientist at Gupy, Sao Paulo, Brazil, for his solicitous assistance and positive encouragement.

References

[1] Andreas Kamilaris, F. X.-B. (2018). Deep Learning in Agriculture: A Survey. *Computers and Electronics in Agriculture, 147*(1). doi: 10.1016/j.compag.2018.02.016

[2] Bengio, Y. (2009, January). Learning Deep Architectures for AI. *Foundations and Trends® in Machine Learning, 2*(1), 1-127 .

[3] Chao Li, A. R. (2012). Application of Computer Vision for Lettuce Seeds Germination Detection.

[4] Chigozie Enyinna Nwankpa, W. I. (2018). Activation Functions: Comparison of Trends in Practice and Research for Deep Learning. *ArXiv*.

[5] Chollet, F. (2017). *Deep Learning with Python.* Manning Publications.

[6] Courville, I. G. (2016). *Deep Learning*. MIT Press. Retrieved from http://www.deeplearningbook.org

[7] Dominik Scherer, A. M. (2010). Evaluation of pooling operations in convolutional architectures for object recognition. *ICANN'10 Proceedings of the 20th international conference on Artificial neural networks: Part III* (pp. 92-101). Thessaloniki, Greece: Springer-Verlag Berlin, Heidelberg.

[8] Dr. Julianna Bányai, D. J. (2002). *Handbook On Statistics In Seed Testing.*

[9] IHemender, S. S. (2018, April). Image Analysis: A Modern Approach to Seed Quality Testing. *Current Journal of Applied Science and Technology*. doi:10.9734/CJAST/2018/40945

[10] Jha, G. (2019). Artificial Neural Networks and Its Applications.

[11] John Duchi, E. H. (2011). Adaptive Subgradient Methods for Online Learning and Stochastic Optimization. (T. Zhang, Ed.) *Journal of Machine Learning Research, 12*, 2121-2159.

[12] Kaiming He, X. Z. (2015). Delving Deep into Rectifiers: Surpassing Human-Level Performance on ImageNet Classification. *2015 IEEE International Conference on Computer Vision (ICCV)*, 1026-1034.

[13] Keiron Teilo O'Shea, R. N. (2015). An Introduction to Convolutional Neural Networks. *ArXiv e-prints*.

[14] Kuo, C.-C. J. (2016). Understanding Convolutional Neural Networks with A Mathematical Model. *Journal of Visual Communication and Image Representation, 41*, 406 - 413. doi:DOI: 10.1016/j.jvcir.2016.11.003

[15] Li Deng, D. Y. (2014, June 30). Deep Learning: Methods and Applications. *Foundations and Trends® in Signal Processing, 7*(3-4), 197 - 387. doi:10.1561/2000000039

[16] Ms. Mrinal Sawarkar, D. S. (2017 , May). Digital Image Processing Applied to Seed Purity Test . *International Journal of Innovative Research in Electrical, Electronics, Instrumentation and Control Engineering, 5*(5).

[17] Ms. Prajakta Pradip Belsare, P. M. (2013, February). Application Of Image Processing For Seed Quality Assessment: A Survey. *International Journal of Engineering Research & Technology (IJERT), 2*(2).

[18] Nathaniel Narra, P. T. (2018). Deep Learning in Agriculture – what's happening.

[19] Nitish Srivastava, G. H. (2014). Dropout: A Simple Way to Prevent Neural Networks from Overfitting. *Journal of Machine Learning Research, 15*, 1929-1958. Retrieved from http://jmlr.org/papers/v15/srivastava14a.html

[20] Rusiecki, A. (2019, March 21). Trimmed categorical cross-entropy for deep learning with label noise. *Electronics Letters, 55*(6), 319 – 320. doi:10.1049/el.2018.7980

[21] Samer Alashhab, A.-J. G. (2019). Hand Gesture Detection with Convolutional Neural Network. *Distributed Computing and Artificial Intelligence, 15th International Conference*. Springer International Publishing.

[22] Y. Lecun, L. B. (1998, Nov). Gradient-based learning applied to document recognition. *Proceedings of the IEEE, 86*, 2278-2324. doi:10.1109/5.726791

[23] Yann LeCun, Y. B. (2015, 5). Deep learning. *Nature, 521*(7553). doi:10.1038/nature14539

[24] Zeiler, M. D. (2012). ADADELTA: An Adaptive Learning Rate Method. *ArXiv, abs/1212.5701*.

Fake News Stance Recognition Using Machine Learning

Sneha Karki, Rakshya Basnet, Abhishesh Dahal, Shreya Tamrakar

Department of Computer and Electronics Engineering Advanced College of Engineering and Management (Tribhuvan University)

Abstract

Fake news surfaces on the internet rapidly, as it can be shared and accessed easily online. On one hand, it's low cost, and easy accessibility with rapid share of information draws more attention of people to read news from it. On the other hand, it enables wide spreading of Fake news, which are nothing but false information to mislead people. Fake news detection has recently become an emerging research that is attracting tremendous attention. Fake news detection can help reduce the rate of online propagandas and frauds. In this work, Machine-learning methods have been employed to detect the credibility of news based on the text content and URLs provided by users. In the first step, the provided contents are analyzed so that they can be converted to quantified values using various text mining techniques (Count Vectorizer, TF-IDF). After that, classifiers are trained using datasets, containing both real and fake news so they can differ the two. When the classifier achieved a decent level of accuracy and performed better than other classifiers, then it was ready for detecting fake news from the user inputs.

Keywords*: Fake News; Naive Bayes Classifier; Artificial Intelligence*

1.Introduction

Fake News has been defined in multiple ways. The New York Times defines it as "a made-up story with an intention to deceive". This definition focuses on two dimensions: the intentionality (very difficult to prove) and the fact that the story is made up. The challenge lies on how to prove the intentionality behind it. Fake News can be a profitable business, generating large sums of advertising revenue for publishers who create and publish stories that go viral. This problem is not only prevalent across social media sites but even sites of popular newspaper publications provide it readers with fake information many a times. Today it is enormously being fed and triggered through the Internet. Fake news detection presents its own unique characteristics and challenges from simply contrasting fake news from genuine news, or collecting data (fake news articles). Some examples of fake news that circulated abruptly across the Internet: "Michael Jordan resigns from the board at Nike and takes Air-Jordans with him", "North Korea opens its doors to Christianity", etc.

Unlike the traditional media which is bound by regulations and code of ethics of journalism, stating and spreading false news is a lot easier in digital media. Therefore, we can conclude that detecting fake news has become the need of the hour. With the idea of tackling this arising issue, this project was taken up. Fake News Detector is a research-based project that primarily focuses on analyzing news content shared and read online, and thereby detecting whether it is fake. This project uses the machine learning approach to vary fake news from robust

news. Machine Learning (AI) is providing effectual ways to tackle this issue. NLP techniques can now parse through the given text and perform all sorts of human-level tasks [1]. Previously, multiple machine learning and Artificial Intelligence based attempts have been made in the context of fake news detection. Some approaches were focused on algorithm performance while some worked on manual datasets. Each of these attempts have leveraged the way for further research and progress in the field of AI and Machine learning: categorically in fake news detection. Hence, picking up from past papers and articles, we have incorporated the Natural Language Processing approach to classify the articles based on the terms used in the articles.

The ability of ML algorithms to make classifications has been utilized to the maximum in this work. The Machine Learning Algorithm has been employed to actually detect the authenticity of a given piece of news article. These algorithms have been trained well enough to make future predictions potent. Each input text body will be analyzed for several features such as number of overlapped words, number of negative words in headline, similarity features of headlines, text body, etc. The system uses NLP approaches like Count Vectorization and TF-IDF Vectorization before passing the text through Passive Aggressive Classifier that gives the authenticity of an article in percentage for classification.

The main objective of this research is to detect the integrity and authenticity of news articles shared online. The project is aimed at assessing various ML algorithms at hand in order to identify the most fitting one for fake news detection. The goal of the research is to examine how this particular method works for this particular problem and whether it supports the use of artificial intelligence for fake news detection. The difference between this paper and other papers on the similar topics is that in this composition Passive Aggressive Classifier was specifically used for fake news detection.

The rest of the paper is organized in Section II, Section III, Section IV, Section V, Section VI and Section VII. Section II consists the related work in past. Section III consists the datasets and features utilized. Section IV consists models and algorithms followed in the task. Section V consists implementation detail. Section VI consists results of the task and Section VII consist conclusion of the work.

2. Related Work

A. Related Research

Various attempts have been made at fake news detection. News articles have been categorized under various types: bias (443), bs (11492), conspiracy (430), fake (19), hate (246) and so on.

1. Fake news detection on Social media: A data mining perspective, arXiv,2017

The issue of fake news was tackled using concepts of machine learning. Features such as: publisher (author, domain, name, age), and the content, with features: common linguistic features, Domain specific linguistic features, Visual-based features, user-based features, etc. were used as parameters for detection. Publicly available datasets such as BuzzFeed News, LIAR, BSDETECTOR, CREDBANK, etc. were used. The achieved results were finally tested as per the conditions: True Positive (when predicted fake news pieces were actually annotated as fake news), True Negative (when predicted true news pieces were actually annotated as true news), False Positive (when predicted true news pieces were actually annotated as fake news), False Negative (when predicted fake news pieces were actually annotated as true news). [2]

2. Fake Bananas:

At HackMIT 2017,a fake news detection system was developed by Kastan Day and his team using machine learning based stance detection.A machine learning model was built which accurately discerned between fake and legitimate news by comparing the given article or user phrase to known reputable and unreputable news sources.A more general approach of classifying articles from unknown sources was used as generally agreeing or generally disagreeing with sources of known (high and low) credibility. Moreover, A link to an article OR as any arbitrary claim to be fact checked like (Obama is not a US citizen) was given as user input to the system. In this way their program acted as a fact-finding search engine and links to relevant articles along with that article's stance (agree/disagree/is-neutral) on that topic were returned. Tremendous research and discovery potential were offered to users along with the ability of simply checking claims. The application was called Fake Bananas. [3]

3. QCRI -MIT system based on Media Bias/Fact check

The best approach to adequately differ real news from hoax was believed to focus not only on individual claims, but on the news sources themselves as per the Researchers from MIT's Computer Science and Artificial Intelligence Lab (CSAIL) and the Qatar Computing Research Institute (QCRI). Using this tack a new system, that used machine learning to determine if a source was accurate or politically biased, was demonstrated. The system was a collaboration between computer scientists at MIT CSAIL and QCRI, which is part of the Hamad Bin Khalifa University in Qatar.Data was first taken by Researchers from Media Bias/Fact Check (MBFC), a website with human fact-checkers who analyze the accuracy and biases of more than 2,000 news sites; from MSNBC and Fox News; and from low-traffic content farms.

Collected data was then fed to a machine learning algorithm, and programmed to classify news sites the same way as MBFC. When given a new news outlet, the system was then 65 percent accurate at detecting whether it had a high, low or medium level of factuality, and roughly 70 percent accurate at detecting if it was left-leaning, right-leaning, or moderate. The most reliable ways to detect both fake news and biased reporting were derived as to look at the common linguistic features across the source's stories, including sentiment, complexity, and structure. [4]

a. Text Classification

Text classification is the process of assigning tags or categories to text according to its content. It's one of the fundamental tasks in Natural Language Processing (NLP). Text classification also known as text tagging or text categorization is the process of categorizing text into organized groups. By using Natural Language Processing (NLP), text classifiers can automatically analyze text and then assign a set of pre-defined tags or categories based on its content. Unstructured text is everywhere, such as emails, chat conversations, websites, and social media but it's hard to extract value from this data unless it's organized in a certain way. Text classifiers with NLP have proven to be a great alternative to structure textual data in a fast, cost-effective, and scalable way. Some of the most common examples and use cases for automatic text classification include Sentiment Analysis, Topic Detection, etc. [5]

b. Web scraping

Web Scraping (also termed Screen Scraping, Web Data Extraction, Web Harvesting, etc.) is a technique employed to extract large amounts of data from websites whereby the data is extracted and saved to a local file in your computer or to a database in table (spreadsheet) format.

Data displayed by most websites can only be viewed using a web browser. They do not offer the functionality to save a copy of this data for personal use. The only option then is to manually copy and paste the data - a very tedious job which can take many hours or sometimes days to complete. Web Scraping is the technique of automating this process, so that instead of manually copying the data from websites, the Web Scraping software will perform the same task within a fraction of the time.

Web scraping is essentially a form of data mining. Items like weather reports, auction details, market pricing, or any other list of collected data can be sought in Web scraping efforts. The practice of Web scraping has drawn a lot of controversy because the terms of use for some websites do not allow certain kinds of data mining. Despite the legal challenges, Web scraping promises to become a popular way of collecting information as these kinds of aggregated data resources become more capable. [6]

3. Dataset and Features

a. Data Collection

The dataset named Fake_or_Real_News was retrieved from Kaggle. It had 7797 datasets in tabular form which contained the title, content, Id and label as its attributes. Furthermore, some 600+ URLs were acquired for detection of fake news using the URL in our system. The datasets contained news from various domain like sports, politics, health, business etc. Majority of available text data was highly unstructured and noisy in nature. In order to achieve better insights or to build better algorithms, data was cleaned and made workable. Informal communication like typos, bad grammar, usage of slang, presence of unwanted content like URLs, stopwords, and expressions etc. were present in the data, which was removed from the textual data.

b. ***Feature Extraction***

Feature Extraction is an essential stage in preprocessing data.

1. Removal of Stop-words

When data analysis needs to be data driven at the word level, the commonly occurring words (stop-words) should be removed. One can either create a long list of stop-words or one can use predefined language specific libraries. For our system, the stop words were chosen from python libraries and set to English. The stop words were then removed easily from our articles for further processing. [7]

2. Bag-Of-Words

A bag-of-words model, or BoW for short, is a way of extracting features from text for use in modeling, such as with machine learning algorithms. The approach is very simple and flexible, and can be used in a myriad of ways for extracting features from documents. The bag-of-words model is one of the simplest language models used in NLP. It makes a unigram model of the text by keeping track of the number of occurrences of each word. This can later be used as a feature for Text Classifiers. In this bag-of-words model only individual words are taken into account and each word is given a specific subjectivity score. This subjectivity score can be looked up in a sentiment lexicon. If the total score is negative the text will be classified as negative and if it is positive the text will be classified as positive. It is simple to make, but is less accurate because it does not take the word order or grammar into account. [7]

In our system, the Bag-Of-Words allowed us to correspond the importance of a word with respect to the whole text as well as the context in which the word is being used. BoW is divided into two parts:

a. *Count Vector*

The words were tokenized using count vector and the number of times a word appeared in the whole text was counted. It was done in order to check the authenticity of the article. The higher the number count of a particular word, the more significant it is in the article. However, it is to be noted, that the stop-words like 'the', 'was', 'him' or the words which are frequent in the general English writings are already removed leaving us with more sophisticated words.

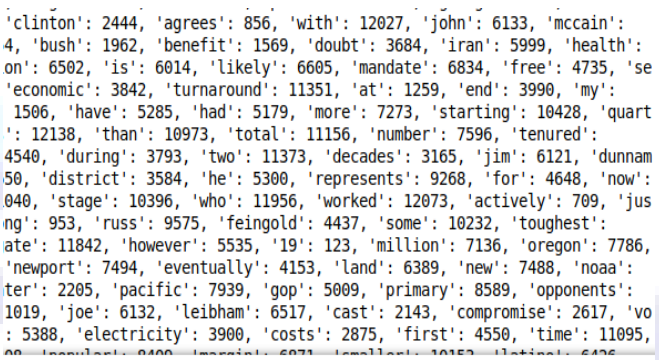

Figure 1: Preprocessing After Count Vectorization

Count Vectors as feature

Count Vector is a matrix notation of the dataset in which every row represents a document from the corpus, every column represents a term from the corpus, and every cell represents the frequency count of a particular term in a particular document. It creates vectors that have a dimensionality equal to the size of our vocabulary, and if the text data features that vocab word, we will put a one in that dimension. The result of this will be very large vectors, if we use them on real text data, however, we will get very accurate counts of the word content of our text data. [8]

b. *Tf-idf:*

The tf-idf weight is a weight often used in information retrieval and text mining. This weight is a statistical measure used to evaluate how important a word is to a document in a collection or corpus. The importance increases proportionally to the number of times a word appears in the document but is offset by the frequency of the word in the corpus. In our system, the threshold for the frequency is set 0.7 which means that if the word occurs 7 out of 10 times, the word is occurring more than it needs to leads us to believe that there might be something wrong with the article itself.

TF-IDF as a feature

A problem with scoring word frequency is that highly frequent words start to dominate in the document (e.g. larger score), but may not contain as much "informational content" to the model as rarer but perhaps domain specific words. One approach is to rescale the frequency of words by how often they appear in all documents, so that the scores for frequent words like "the" that are also frequent across all documents are penalized. [8]

This approach to scoring is called Term Frequency – Inverse Document Frequency, or TF-IDF for short, where:

- ***Term Frequency:*** is a scoring of the frequency of the word in the current document.

- ***Inverse Document Frequency***: is a scoring of how rare the word is across documents.

The scores are a weighting where not all words are equally as important or interesting.

$$w_{i,j} = tf_{i,j} \times \log\left(\frac{N}{df_i}\right) \quad (1)$$

Term Frequency-Inverse document frequency uses all the tokens in the dataset as vocabulary. Frequency of occurrence of a token from vocabulary in each document consists of the term frequency and number of documents in which token occurs determines the Inverse document frequency. What this ensures is that, if a token occurs frequently in a document that token will have high TF but if that token occurs frequently in majority of documents then it reduces the IDF, so stop words like an, the, I which occur frequently are penalized and important words which contain the essence of document get a boost .Both these TF and IDF matrices for a particular document is multiplied and normalized to form TF-IDF of a document. [8]

4. Model and Algorithm

After the preprocessing is complete, the data is then fed to the model. Now, for our system we have chosen SVM model since, it was found more suitable for text data mining. Even in SVM, we have chosen Passive Aggressive Classifier.

"Support Vector Machine" (SVM) is a supervised machine learning algorithm which can be used for both classification and regression challenges. However, it is mostly used in classification problems which deemed appropriate for our project.

Passive Aggressive Algorithms are a family of online learning algorithms (for both classification and regression) proposed by Crammer at al. Classification.

Let's suppose to have a dataset:

$$\begin{cases} X = \{\bar{x}_0, \bar{x}_1, \dots, \bar{x}_t, \dots\} \; where \; \bar{x}_i \in \mathbb{R}^n \\ Y = \{y_0, y_1, \dots, y_t, \dots\} \; where \; y_i \in \{-1, +1\} \end{cases} \quad (2)$$

The index t has been chosen to mark the temporal dimension. In this case, in fact, the samples can continue arriving for an indefinite time. Of course, if they are drawn from same data generating distribution, the algorithm will keep learning (probably without large parameter modifications), but if they are drawn from a completely different distribution, the weights will slowly forget the previous one and learn the new distribution. For simplicity, we also assume we're working with a binary classification based on bipolar labels.

Given a weight vector w, the prediction is simply obtained as:

$$\tilde{y}_t = sign(\bar{w}^T \cdot \bar{x}_t) \quad (3)$$

All these algorithms are based on the Hinge loss function (the same used by SVM):

$$L(\bar{\theta}) = max\left(0, 1 - y \cdot f(\bar{x}_t; \bar{\theta})\right) \quad (4)$$

The value of L is bounded between 0 (meaning perfect match) and K depending on f(x(t), θ) with K>0 (completely

wrong prediction). A Passive-Aggressive algorithm works generically with this update rule:

$$\begin{cases} \bar{w}_{t+1} = argmin_{\bar{w}} \frac{1}{2} \|\bar{w} - \bar{w}_t\|^2 + C\xi^2 \\ L(\bar{w}; \bar{x}_t, y_t) \leq \xi \end{cases} \quad (5)$$

To understand this rule, let's assume the slack variable ξ=0 (and L constrained to be 0). If a sample x(t) is presented, the classifier uses the current weight vector to determine the sign. If the sign is correct, the loss function is 0 and the argmin is w(t). This means that the algorithm is passive when a correct classification occurs. Let's now assume that a misclassification occurred: The angle θ > 90°, therefore, the dot product is negative and the sample is classified as -1, however, its label is +1. In this case, the update rule becomes very aggressive, because it looks for a new w which must be as close as possible as the previous (otherwise the existing knowledge is immediately lost), but it must satisfy L=0 (in other words, the classification must be correct). [9]

Our system has 3 search fields which are: -

1) Search by article content.
2) Search using key terms.
3) Search for website in database.

In the first search field, SVM was used to detect the authenticity of the news article and the process is as mentioned above. In simple words, articles can be analyzed by feeding them to a machine learning model (Passive Aggressive Classifier) which predicts the reliability of the content after it's trained through predefined datasets of classified real vs. fake news.

For the second search field, the site asks for specific keywords to be searched on the net upon which it provides a suitable output for the percentage probability of that term actually being present in an article or a similar article with those keyword references in it. The second search field asks for keywords to be searched on the net to find sources for those particular keywords in articles. For this the python package request is used to pull and provide the HTML and then another python package Beautiful Soup to parse the HTML to extract the headers and the body of the links. Search terms are analyzed by doing a Google search (first 100 entries) and ensuring if the news corresponding to the keywords have been covered by reliable news sources and aggregators. For every search term covered by a reliable news source it receives a score of +1, while fake sources are heavily penalized. If multiple fake sources cover the news, then the truth score is penalized even harder. Keywords like 'hoax', 'fake', etc. are also looked up in the payload content.

The third search field of the site accepts a specific website domain name upon which the implementation looks for the site in our true sites database or the blacklisted sites database. The true sites database holds the domain names which regularly provide proper and authentic news and vice versa. If the site isn't found in either of the databases, then the implementation doesn't classify the domain it simply states that the news aggregator does not exist. The third search field asks for a domain name from the user and tells him/her if the domain is reliable or not. The domain name is taken as input and the implementation searches for it in manually created databases of blacklisted sites which have a high probability of providing fake news and another database containing the domains which provide reliable news and information.

5. Implementation Details

SVM is used to detect the authenticity of the news article and the process is as mentioned above. In simple words, articles can be analyzed by feeding them to a machine learning model (Passive Aggressive Classifier) which predicts the reliability of the content after it's trained through predefined datasets of classified real vs. fake news. The stages of implementation are presented below:

1. Training Datasets

The datasets were taken from Kaggle, as Kaggle has been providing an optimum number of datasets and within required frequency. These data samples were then preprocessed following various steps. Then, the preprocessed data were split into two parts: Training Dataset and Testing Dataset, in a ratio of (70:30). Training Dataset is the actual dataset that we used to train the model. The model sees and learns from this data.

2. Testing Datasets

It was tested once our model was completely trained. The test dataset is the sample of data that provides an unbiased evaluation of the final model. It is only used once a model is completely trained (using the train and validation sets).

These datasets were pre-processed to a similar level so that the model could identify the test datasets during final evaluation and work with it, as it did with training datasets (or validation datasets). The division of the sample data into these datasets was done after shuffling, in a random fashion.

3. Classification

The system makes a very simple distinction among the datasets after all of the above-mentioned steps are completed. The dataset is then shown the percentage as to how true the news actually is. This is the foundation for classification.

6.The Experimental Result

Vector representation test on term frequency-inverted document frequency, frequency count was conducted. The algorithm used in the test is the passive aggressive classifier with linear support vector machine.

The model's overall performance was evaluated with classification accuracy. Classification accuracy is simply the rate of correct classifications, either for an independent test set, or using some variation of the cross-validation idea.

When the model makes prediction, there are 4 possible types of outcomes:

- The article was actually FAKE and the model classified it as FAKE: This is called a True Negative
- The article was actually FAKE and the model classified it as TRUE: This is called a False Positive
- The article was actually TRUE and the model classified it as FAKE: This is called a False Negative
- The article was actually TRUE and the model classified it as TRUE: This is called a True Positive

The confusion matrix for the same was constructed based on these parameters.

Accuracy=(TP+TN)/(TP+TN+FP+FN)

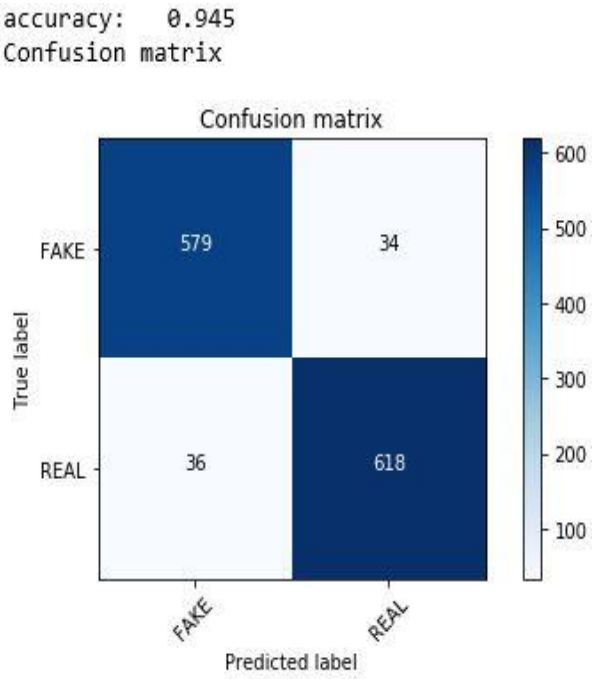

Figure 2: Confusion Matrix

For the tfidf_vectorizer the threshold is set to 0.7 which means that the words which appear more than 70% of the time in the articles are not counted in. The stop words parameter is used for avoiding the various stop words used commonly in the English language.

- Among various ML algorithms, Passive Aggressive Classifier was our best option as it was providing accuracy scores as high as 93% on the test data set.

- Fake_or_Real_News dataset was used and performed news detection using SVM that was able to extract count vector and tf-idf as features. The model received a high accuracy score of 94.5% on the training set.

7. Conclusion

Often sensational news is created and spread through social media to achieve intended end. On the other hand, it may also involve narration of a true fact however being deliberately exaggerated. This may also affect the importance of serious news media. The problem is to identify the authenticity of the news and online content. Equally important problem is to identify the bots involved in spreading false news. Thus, this project comes up with the applications of NLP (Natural Language Processing) techniques for detecting the 'fake news', that is, misleading news stories that comes from the non-reputable sources. After the data is acquired through web scraping, the data is preprocessed using BoW and Count Vectorizer and Tf-idf is used as extraction feature. Passive Aggressive model was found to be giving high accuracy as compared to other models so it was trained with 7797 articles to detect the misleading news. Therefore, fake news recognition using machine learning proved to be very helpful in this case to track the real news and fake news and provide the reliable accuracy.

References

[1] 19 04 2019. [Online]. Available: https://www.analyticsvidhya.com/blog/datahack-radio-machine-learning-identify-fake-news-mike-tamir/.

[2] "researchgate," [Online]. Available: https://www.researchgate.net/publication/318981549_Fake_News_Detection_on_Social_Media_A_Data_Mining_Perspective.

[3] 07 2018. [Online]. Available: https://github.com/likeaj6/FakeBananas/blob/master/Fake%20Bananas%20Blog%20Post.md.

[4] "shack15," 4 10 2018. [Online]. Available: https://news.shack15.com/machine-learning-software-mit-qatari-can-detect-fake-news-sites/.

[5] 2018. [Online]. Available: https://monkeylearn.com/what-is-text-classification/ .

[6] 2018. [Online]. Available: https://monkeylearn.com/what-is-text-classification/ .

[7] 04 2019. [Online]. Available: https://www.kdnuggets.com/text-preprocessing-nlp-machine-learning.html.

[8] P. Pantola, 14 07 2019. [Online]. Available: https://medium.com/natural-language-processing-text-data-vectorization-af2520529cf7.

[9] "Giuseppe Bonaccorso," 06 10 2017. [Online]. Available: https://www.bonaccorso.eu/2017/10/06/ml-algorithms-addendum-passive-aggressive-algorithms..

[10] "science direct," [Online]. Available: https://www.sciencedirect.com/topics/engineering/classification-accuracy

Spam Mail Identification Using Machine Learning Technique

Praveen Kumar Karn[1], Neha Karna[2]

[1]*Assistant Lecturer, Department of Computer Engineering, Lalitpur Engineering College, Chakupat, Lalitpur,* [2]*Lecturer, Department of Electronics & Computer Engineering, Advanced College of Engineering & Management, Kupondole, Lalitpur*

[1]karnpraveen1@gmail.com, [2]er.karna.nehaa@gmail.com

Abstract

Electronic spamming is the use of electronic messaging systems to send an unsolicited message (spam), especially advertising, as well as sending messages repeatedly on the same site. While the most widely recognized form of spam is email spam, the term is applied to similar abuses in other media: instant messaging spam, Usenet newsgroup spam, Web search engine spam, spam in blogs, wiki spam, online classified ads spam, mobile phone messaging spam, Internet forum spam, junk fax transmissions, social spam, spam mobile apps, television advertising and file sharing spam. Support Vector Machine (SVM) is used to detect spam in an email. Support Vector Machines are based on the conceptof decision planes that define decision boundaries. This paper will show that SVM can be simply implemented for a reasonably accurate text classifier and that it can be modified to make a significant impact on the accuracy, precision, recall, confusion matrix, F1 score of the filter.

Keywords*: E-mail, Non-spam, Spam, Support Vector Machine.*

1. Introduction

Electronic mail, or E-mail is an effective, fastest and cheaper way of communication to exchange information between people using electronic device such as computers, tablets, mobile phones etc. E- mail provide a way for internet users to easily transfer information globally. It is very much useful for personal as well as professional communication purpose. However, the increase of email users have resulted in the dramatic increase of spam mails during the past few years. Also, it causes traffic jam, decreases productivity, and phishing that has become a heavy problem. E-mail spam has rapidly grownsince the early 1990s [1]. E-mail spam is also known as uninvited e-mail. the quantity of spam is increased extraordinarily that causes varied downside like overflow of user's mailbox, utilization of network information measure and space for storing, wastage of user's time and energy to spot the mailor in removing the spam mails [3]. The spam can additionally have an effect on the financial infolike checking account variety, password and alternative private info.

Spam can be defined as unsolicited (unwanted, junk) email for a recipient or any email that the user donot wanted to have in his inbox. Spam mail means the mail which contains the symbol and word like: *,$,#,@,!,-,==,xxx, £ ,dollar,pound,sexually,free,Viagra,moneyetc.To filter spam with ancient strategies such as

domains, IP address, mailing address is not possible. The fact that out of 80 billion emails received everyday 48 billion of them being spam highlighted. According to a report from FerrisResearch, the global sum of losses from spam made about 130 billion dollars, and in the USA, 42 billionin 2009.With the more usage of internet, it is necessary to create efficient spam filters. Therefore, emailclassification is a most trending research area to classify spam and non-spam messages using different algorithms. A spam filter is an email service feature designed to find uninvited and unwanted email andstop those messages from a user's inbox.

2. Literature Review

In August 2002, Paul Graham published an influential paper, "A plan for spam", describing a spam- filtering technique using improved Bayesian filtering. Later spam was being a challenge to control it.Soresearchers had focused on this topics to control and classify it using different techniques. The differentrelated papers and journal in the past are "Comparative Study on Email Spam Classifier using Data Mining Techniques (2012A.D.)" was published which focused on exploring the efficient classifier for email spam classification using TANAGRA data mining tool. From the obtained results, fisher filtering and runs filtering feature selection algorithms performs better classification for many classifiers. The Rnd tree classifier is also tested with test dataset which gives accurate results than other classifiers for this spam dataset. Finally, best classifier for email spam is identified based on the error rate, precision and recall [1].

Similarly, the author of [2] used Spam data and SPAMBASE datasets for the evaluation of Naïve Bayes Algorithm for email spam filtering getting higher precision The performance of the datasets is evaluatedbased on their accuracy, recall, precision and F-measure. The result shows that the type of email and the number of instances of the dataset has an influence towards the performance of Naive Bayes.

Also in 2016 A.D. the author of [3] provides particle swarm optimization algorithm to evaluate the emails as spammed or non-spam in more accurate manner. The proposed technique has integrated particle swarm optimization based on decision tree algorithm with unsupervised filtering to enhance theaccuracy rate further. The experiments are done using MATLAB 2010 and Weka 7.0. Also to improve the accuracy rate, further the unsupervised filtering is used as pre-processing tool while classifying mail spam.

In 2017 A.D. the author of [4] describe the development and implementation of an open source tool that provides a flexible way to extract a large number of features from any email corpus to produce cleanseddataset which can be used to train and test various classification algorithms. A total of 140 features areextracted from Spam as in email corpus using the developed tool. Also in 2016 A.D. the author of [5] was focused on using keyword-based corpus that were built from training datasets to classify new incoming email message. It was seen that proposed algorithm with an accuracy, recall, false positive rate, false negative rate and f-measure of 92.8%, 93.9%, 84.6%, 7.8%, 6.1% and 89.1% respectively [5].

3. Methodology

3.1 ***Training Dataset***: In this paper, mail dataset has been collected from Ling-spam corpus which consist of 962 mail files. Mail files are divided equally between spam and ham messages. The dataset is available at the website [10].Dataset is divided into training set which is always higher.

3.2 ***Pre-processing*:**

3.2.1 ***Stop word Removal***: This is the stop word list which consist of terms including articles, prepositions, conjunctions and certain high frequency words (such as some verbs, adverbs).These words are not very meaningful in deciding spam and ham, so these words are removed from the emails.These words are called stop words and the technique is called stop removal. Some of the examples of stop-word are: a, an, the, and, are, as, at, be, for, from, has, he, in, is, it, its, of, on, that, the, to, was, were, will, with etc.

3.2.2 ***Tokenization*:** Lexical analysis also named as Tokenizing. Tokenization is the process of breaking a stream of text up into words, phrases, symbols, string or other meaningful elements called tokens. Filtering techniques uses white space (blank) removal and removal of punctuation symbols in tokenizing.

3.2.3 ***Lemmatization***: In computational linguistics, lemmatization is the algorithmic process of determining the lemma for a given word. Since the process may involve complex tasks such as understanding context and determining the part of speech of a word in a sentence. For instance: 1. the word "better" has "good" as its lemma. , 2. The word "walk" is the base form for word "walking", and hence this is matched in both stemming and lemmatization.

3.2.4 ***Noise removal***: Unclear terms in email cause noise. An intentional action of misplaced space, misspelling or embedding particular characters into a word is pointed to as obfuscation. For instance, spammers obfuscated the word Free into “fr33” or Viagra into “VIagra” or “V|agra”.spammers employthis approach in an effort to bypass the right recognition of these words by spam filtering.

3.2.5 ***Word Frequency*:** This counts the frequency of words depending on its occurrence, it helps in deriving the word probability for spam and legitimate mails.

3.3 ***Feature Extraction*:** Extraction of specific features (here words) which can very much represent is represented in numerical features in matrix form. Here for this project word count vector is being used for extraction of mails. This model consists on receiving a list of labeled text corpora, making a word count on each corpus and determining with how much frequency each word appears for every given label.

3.4 ***Support Vector Machine*:** Support vector machines (SVMs) are a set of supervised learning methods used for classification, regression and detection. Support Vector Machines are based on the concept of decision planes that define decision boundaries. A decision plane is one that separates between a set of objects having different class memberships. The standard SVM takes a set of input data and predicts, for each given input, which of two possible classes comprises the input, making the SVM a non-probabilistic binary linear classifier. A Support Vector Machine (SVM) is a discriminative classifier formally defined by a separating hyper plane. In other words, given labeled training data (*supervised learning*), the algorithm outputs an optimal hyper plane which categorizes new examples. In two dimensional space this hyper plane is a line dividing a plane in two parts where in each class layin either side.

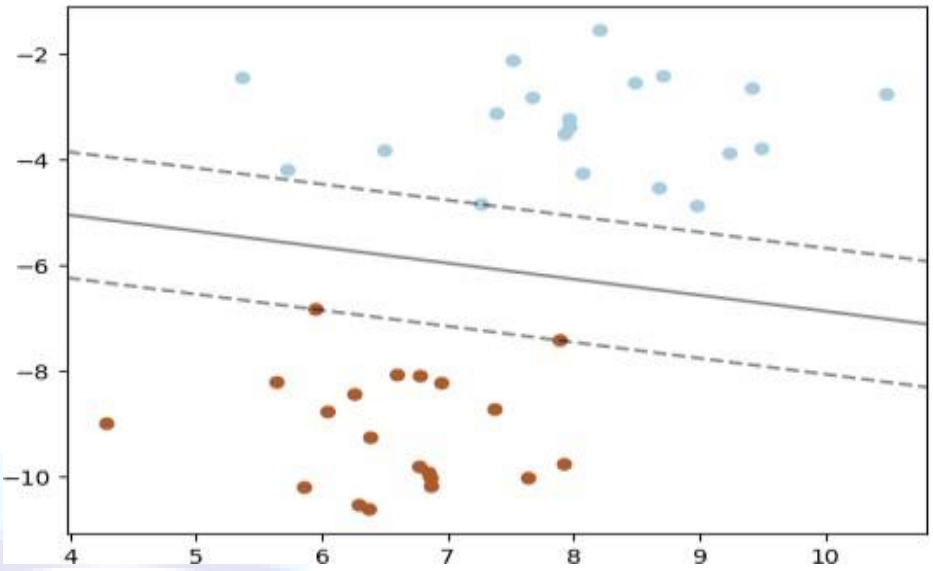

Figure 1: Support Vector Representation

3.5 ***Testing the dataset*****:** Once the classifiers dataset are trained, the performance of the models havebeen checked on test-set. Word count vector will be extracted for each mail in test-set and predict its class (ham or spam) with the trained SVM model. Testing dataset is192 mails files which consist of equal number of spam and ham messages.

3.6 ***Performance Evaluation*****:** For the evaluation of this techniques Accuracy, F1 Score, Recall, Precision, Confusion matrix will be evaluated.

i) ***Accuracy:*** Accuracy of a classifier is defined as the percentage of the dataset correctly classifiedby the method.

$$\text{Accuracy} = \frac{\text{Number of correct prediction}}{\text{Total number of prediction made}}$$

ii) ***F1 score:*** - F1 Score is the Harmonic Mean between precision and recall. The range for F1 Score is [0, 1]. It tells you how precise your classifier is (how many instances it classifies correctly), as well as how robust it is (it does not miss a significant number of instances). The greater the F1 Score, the betteris the performance of our model. Mathematically, it can be expressed as:

$$\text{F1 Score} = 2 * \frac{Precision * Recall}{Precision + Recall}$$

iii) ***Recall:*** - It is the number of correct positive results divided by the number of *all* relevant samples(all samples that should have been identified as positive).

iv) ***Confusion matrix:*** - Confusion Matrix as the name suggests gives us a matrix as output and describes the complete performance of the model. It is used for Classification problem where the output can be of two or more types of classes.

		Predicted Class	
		Negative(0)	Positive(1)
Actual Class	Negative(0)	TN	FP
	Positive(1)	FN	TP

The overall design of the project is:

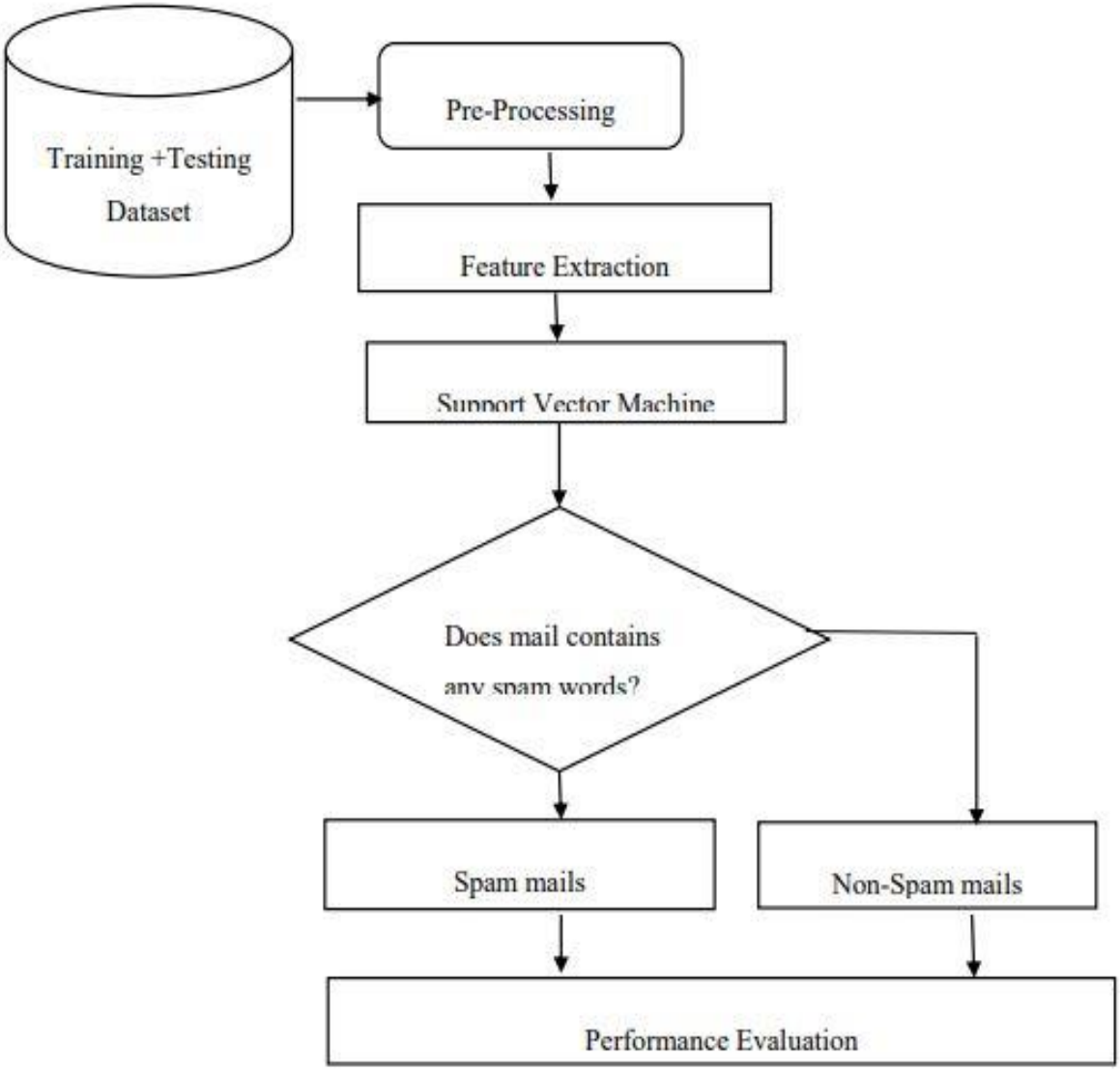

Figure 2: Project Methodology

4. Results and Discussions

Firstly, dataset is collected from Ling-spam corpus that is divided into training and testing mails respectively. Then all the process of pre-processing has been done, in which stop word removal, lemmatization, noise removal, word frequency counts and preparing dictionary has been done. In preparing dictionary step, 3000 most frequently words have been used. Feature extraction process has been also done, in which word count vector (Bag of words) model has been used. Which represent each word in the numerical form in matrix model. Similarly, others dataset are also trained. Support Vector Machine (SVM) algorithm is realized with training dataset. Then after, we can check the performance of the models on test-set. We extract word count vector for each mail in test-set and predict its class (ham or spam) with the trained SVM model.

4.1 Creating Word Dictionary

As a first step, a dictionary of words and their frequency is created. For this task, training set of 770 mails is utilized. Here, 3000 most frequently used words is chosen in the dictionary.

4.2 Feature Extraction Process

Once the dictionary is ready, we can extract word count vector (our feature here) of 3000 dimensions for each email of training set. Each word count vector contains the frequency of 3000 words in the training file.

4.3 Training, Testing Classifiers and checking the performance

For training the classifiers, Support Vector Machine (SVMs) are used which is supervised binary classifiers is very effective. The goal of Support Vector Machine (SVM) is to separate some subset of training data from rest called the support vectors (boundary of separating hyper-plane). The decision function of SVM model that predicts the class of the test data is based on support vectors and makes use of a kernel trick. Once the classifiers are trained, the performance of the models is tested on test- set. Word count vector for each mail is extracted in test-set and predict its class (ham or spam) with the trained Support Vector Machine (SVM) model.

Support Vector Machine (SVM) is trained and tested with different ranges of dataset ratio and which accuracy have been compared. And higher accuracy dataset ratio has been taken. Training with 60 %(577) dataset files and testing with 40 %(385) dataset files of total mail files with SVM gives accuracy of 93.51%.

Training with 70 %(673) dataset files and testing with 30 %(289) dataset files of total mail files with SVM gives accuracy of 96.19%.

Training with 80 %(770) dataset files and testing with 30 %(192) dataset files of total mail files with SVM gives accuracy of 98.96% which is shown in figure below.

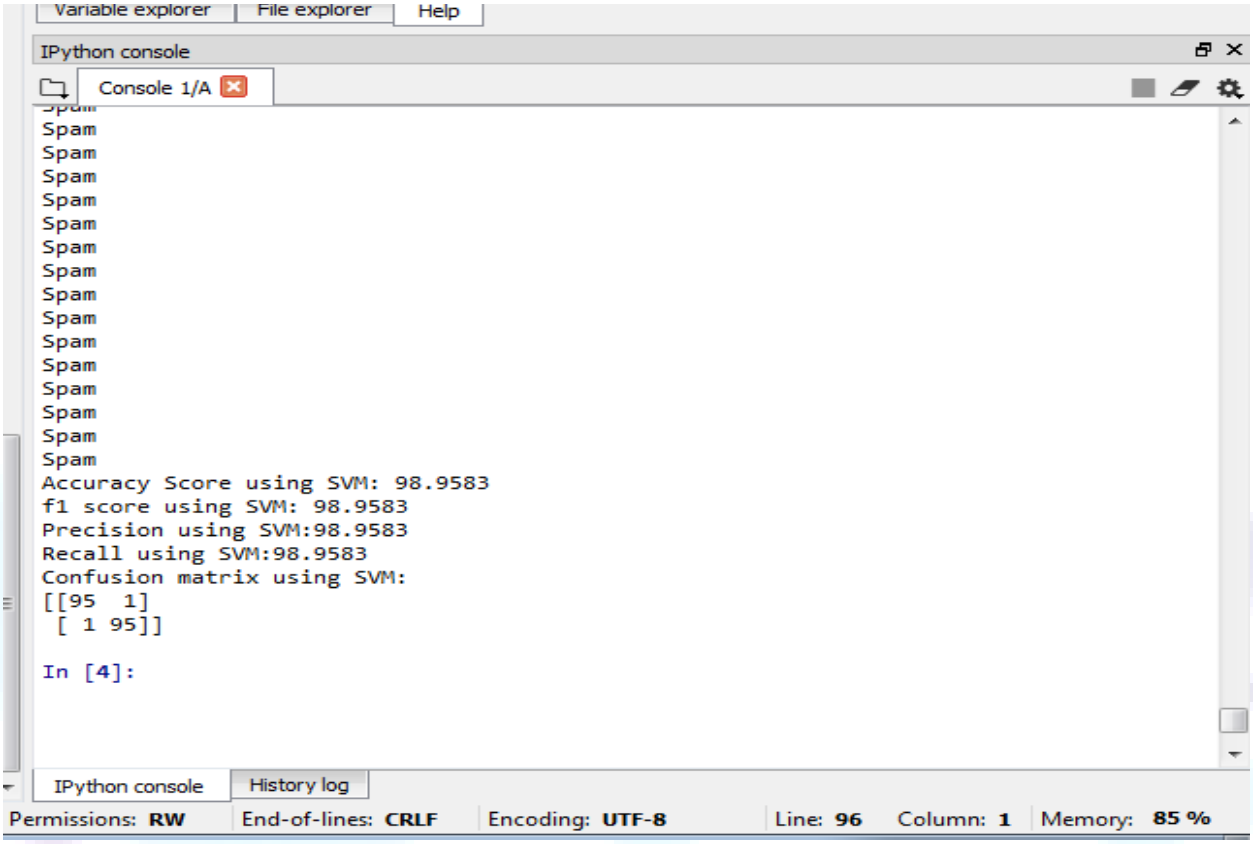

Figure 3: Training &Testing dataset with ratio of (80%-20%)

Figure 4: Comparison of Training &Testing dataset ratio with accuracy

4.4 Checking Performance

Above figure 4 shows that comparison of training and testing dataset ratio with accuracy. Among themit has been concluded that training and testing ratio of (80%-20%) is more accurate which gives Accuracy of 98.9583%, Precision of 98.9583%, Recall of 98.9583% is shown clearly in figure 3.In

Figure 3, Confusion matrix has been also shown above. In confusion matrix, True Negative (TN) is in matrix of position (1×1matrix),which signifies out of 96 non-spam mail files 95 mail files are non-spam detected. Similarly True Positive (TP) is in matrix of position (2×2matrix),which signifies out of 96 spam mail files 95 mail files are spam detected. False Positive (FP) is in matrix of position (1×2 matrix),which signifies out of 96 non-spam mail files only1 file is detected as spam. False Negative (FN) is in matrix of position (2×1 matrix), which signifies out of 96 spam mails files only 1 is identified as non- spam.

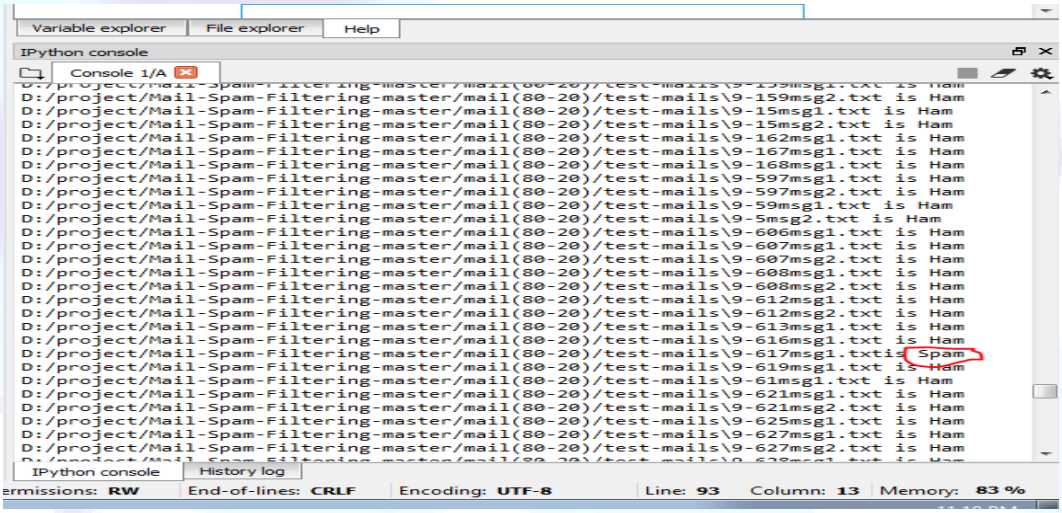

Figure 5: Final Output

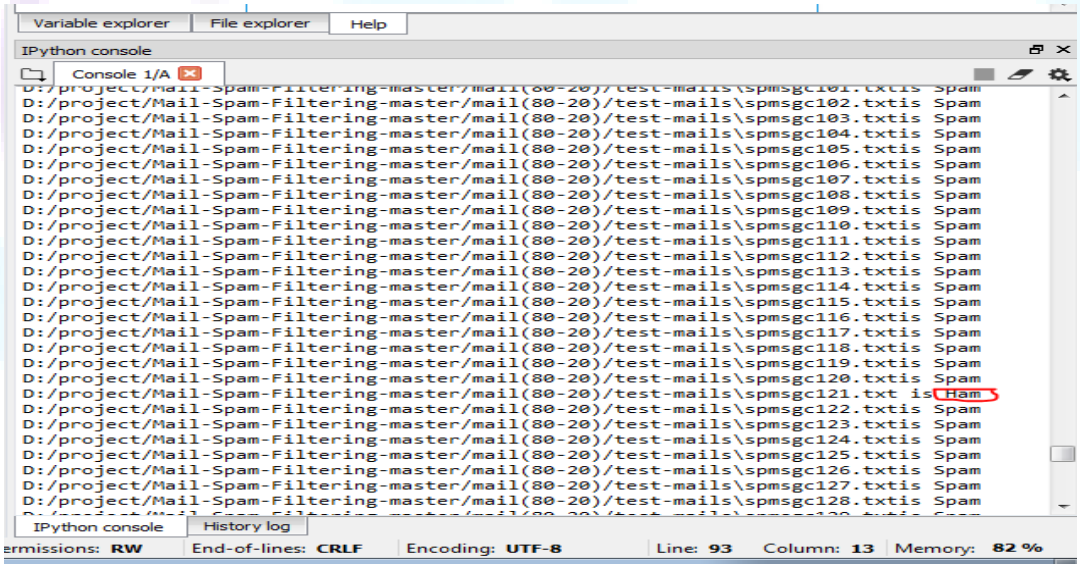

Figure 6: Final output

Above figure show that out of total 192 dataset mail files are divided into equal number of files that is 96 spam mail files and 96 non-spam mail files. Figure 5 shows that out of 96 spam mail files 95 mail files are identified as spam and only 1 file is identified as non-spam(ham). Similarly figure 6 shows thatout of 96 non-spam(ham) mails files, 95 mail files are identified as non-spam(ham) and only 1 file is identified as spam which is output.

5. Conclusion and Future Work

5.1 Conclusion

E-mail spam filtering is an important issue in the network security and machine learning techniques. This paper represents an approach to spam classification using Support Vector Machine (SVM).SupportVector Machine (SVM) classifier algorithm applied on relevant features has produced 98.9583% accuracy in spam detection. Beside Accuracy, Different performance measures such as the Precision, Recall-score, and Confusion matrix etc. are observed. The experiments are done using Python 3.6.4.

The experiment clearly states that the fact that suggested technique has better accuracy than existing techniques. In this paper, dataset is separated into training and testing sets. Typically, most of the datais used for training and a smaller portion of the data is used for testing. After a model has been processedby using the training set, the models are being predicted against the test set. Because the data in the testing set already contains known values for the attribute that prediction is made. In this paper spam and non-spam (ham) mails are identified, which gives high accuracy in detection part.

5.2 Future work

The work presented in this paper can be further extended & can be tested with different algorithmsand varying size of large data sets. In future, filtering of spam will be done on the basis of contents. Also real time detection will be more effective in the future work. If the email can be classified before it is sent to a receiver, it can help to reduce the workload of both networks and servers. For instance, a rating system can be applied to determine if user is spammer or not based on user historical behavior. The rating system keeps track of user behavior and set a threshold that how many emails are classifiedas spam in given amount of time. If the number of spam emails reach or exceed the threshold, system can automatically either send a warning to customer or freeze this account. Then the workload of networks or servers can be reduced from spams.

References

[1] R. K. Kumar, G. Poonkuzhali, and P. Sudhakar, "Comparative study on email spam classifier using data mining techniques," *Proc. Int. MultiConference Eng. Comput. Sci.*, vol. 1, pp. 14–16,2012.

[2] N. F. Rusland, N. Wahid, S. Kasim, and H. Hafit, "Analysis of Naïve Bayes Algorithm for EmailSpam Filtering across Multiple Datasets," *IOP Conf. Ser. Mater. Sci. Eng.*, vol. 226, no. 1, 2017.

[3] H. Kaur and A. Sharma, "Improved Email Spam Classification Method Using Integrated ParticleSwarm Optimization and Decision Tree," no. October, pp. 516–521, 2016.

[4] W. Hijawi, H. Faris, J. Alqatawna, A. M. Al-zoubi, and I. Aljarah, "Improving Email Spam Detection Using Content Based Feature Engineering Approach," *2017 IEEE Jordan Conf. Appl. Electr. Eng. Comput. Technol.*, pp. 1–6, 2016.

[5] P. Liu and T. S. Moh, "Content based spam E-mail filtering," *Proc. - 2016 Int. Conf. Collab. Technol. Syst. CTS 2016*, pp. 218–224, 2016.

[6] S. Naksomboon *et al.*, "An adaptive fusion algorithm for spam detection," *Data Min. Probl. Semin. MTAT.03.177*, vol. 23, no. 1, p. 27, 2015.

[7] M. Rathi and V. Pareek, "Spam Mail Detection through Data Mining – A ComparativePerformance Analysis," *Int. J. Mod. Educ. Comput. Sci.*, vol. 5, no. 12, pp. 31–39, 2013.

[8] M. Basavaraju and R. Prabhakar, "A Novel Method of Spam Mail Detection using Text Based Clustering Approach," *Int. J. Comput. Appl.*, vol. 5, no. 4, pp. 15–25, 2010.

[9] R. M. Alguliev, R. M. Aliguliyev, and S. A. Nazirova, "Classification of Textual E-Mail Spam Using Data Mining Techniques," *Appl. Comput. Intell. Soft Comput.*, vol. 2011, pp. 1–8, 2011.

[10] Dataset Retrieved from: https://www.dropbox.com/s

Part II: Fuzzy Logic ANN and Genetic Algorithms

Automatic Text Summarizer Using LSTM

Lisa Rajkarnikar[1], Lujina Maharjan[2], Monika Pokharel[3], Prakash Chandra Prasad[4]

Advanced College of Engineering and Management, Tribhuvan University, Nepal[1], Pulchowk Campus, Institute of Engineering, Nepal[2]

lisarajkarnikar@gmail.com[1], mhrzn6luzi@gmail.com[2], monikapokharel1@gmail.com[3], infymee@gmail.com[4]

Abstract

In this new era, there has been an explosion in the amount of text data available from different sources. Extracting only the meaningful and useful information from massive texts could be time consuming. Our system proposes the solution by automatically generating the summary of huge chunks of texts preserving their overall meaning. It starts with preprocessing and text cleaning. Next, the tokenizer is prepared which builds the vocabulary and the text sequences are converted to integer sequences. Considering our system as Many-to-Many Seq2Seq problem, we have used the 3 stacked LSTM for both encoder and decoder as our model. Finally, the summary of the text data is generated and displayed which extracts only the meaningful and useful information. With this, our system provides the ease to get the summarized version of huge chunks of data. In addition, it saves the valuable time of people and serves as the boon to mankind.

Keywords*: Text summarizer, Seq2Seq, LSTM, Encoder, Decoder*

1. Introduction

Text summarization is the procedure in which important information are extracted from the original text and converted into its short summary. The summary preserves the overall meaning of the text. In the recent years, text summarization has gained much more importance because of the flooding of information over the web. Hence, this information brings the massive need for more genuine and competent text summarizers. In recent years, need for summarization can be seen in various purpose and in many domains such as news articles summary, email summary, short message of news on mobile, and information summary for businessman, government officials, researchers online search through search engine to receive the summary of relevant pages found, medical field for tracking patient's medical history for further treatment [1].

This research study was initiated by examining the content of the text document, extracting the important meanings from the text and presenting in the summarized yet, meaningful form. The main objective of our paper

was to provide the helping aid to understand the content within the large document in very short period of time. It has twin advantage: the short summary shown as output enables the user to acknowledge the gist of document and reduces the reading time of massive documents serving as the boon to mankind.

2. Literature Review

Research on text summarizer is the need of present speedy emergent information age. Many techniques have been developed so far. Using the graph-based method, the paper [2], introduced the methodology of Text Rank method. This method used the shortest path algorithm for the generation of the summaries. It generates better summaries but it only used the shortest path. Also, the paper [3] merged the content feature with surface feature i.e., location and length of sentence, cue phrase etc. The final summary will be generated on basis of score of each sentence but it wasn't easy to find the subtopics.

Text Summarizer, being one of the fields of Natural Language processing, the cluster-based approach can also be used for it. Using the clustering-based approach, the paper [4] (2012) has introduced a clear approach for multi document summarization by linking simple summary of the document using the phrase clustering. It used both syntactic and semantic similarity for sentence summarizing.

Using the Term Frequency Based Methods, the paper [5] proposed the technique for multi document summarization using TF-IDF based extraction. Categories were into three topics - one topic, multi topic and others. Summaries for individual documents are generated and same summaries will be used for generating multi-document summary.

3. Methodology

Text summarization is the procedure in which important information are extracted from the original text and converted into its short summary. The summary preserves the overall meaning of the text. Text summarization is one of the popular tasks in the field of Natural Language processing. It can be broadly divided as: Abstractive summarization and Extractive summarization.

An extractive summarization technique consists of selecting vital sentences, paragraphs, etc., from the original manuscript and concatenating them into a shorter form. The significance of sentences is strongly based on statistical and linguistic features of sentences.

In contrast, abstractive summarization methods aim at generating new sentences from the original text producing important material in a new way. In other words, they interpret and examine the text using advanced natural language techniques in order to generate a new shorter text that conveys the most critical information from the original text. Even though summaries created by humans are usually not extractive, most of the summarization research today has focused on extractive summarization. The sentences generated through abstractive summarization might not be present in the original text. Abstractive Summarization is suitable in our projects as we generate new sentences from the original text as shown in Figure 1.

Figure 1: Abstractive text summarization

Sequence to sequence modeling

Sequence to sequence modeling refers to a special class modeling problem, where the input as well as the output are a sequence. Seq2Seq model can be used in any problem which carries the information in sequential format. This includes Sentiment classification, Neural Machine Translation, and Named Entity Recognition – some very common applications of sequential information. In the case of Neural Machine Translation, the input is a text in one language and the output is also a text in another language while in the Named Entity Recognition, the input is a sequence of words and the output is a sequence of tags for every word in the input sequence [7].

There are two major components in a Sequence-to-sequence modeling architecture: Encoder and Decoder. It can also be referred as Encoder Decoder problem. The Encoder Decoder architecture can be used to solve the Sequence-to-sequence problem where input and output sequences are of different lengths. Encoder Decoder architecture refers to the architecture in which the input is fed into the encoder which is capable of generating the internal state and fed to the decoder for the output. Varieties of Recurrent Neural Networks (RNNs) can be used such as Gated Recurrent Neural Network (GRU) or Long Short-Term Memory (LSTM) can be used as the encoder and Decoder components. The RNNs can overcome the problem of vanishing gradient by capturing the long-term dependencies.

LSTM

Long short-term memory (LSTM) is an artificial Recurrent Neural Network (RNN) architecture used in the field of deep learning. Unlike standard feed forwarding, LSTM has feedback connections. It can not only process single data points (such as images), but also entire sequences of data (such as speech or video). A common LSTM unit is composed of a cell, an input gate, an output gate and a forget gate. The cell remembers values over arbitrary time intervals and the three gates regulate the flow of information into and out of the cell.

$$i(t) = F(wi[ht\text{-}1, xt]+bi) \quad \ldots (1)$$
$$f(t) = F(wf[ht\text{-}1, xt]+bf) \quad \ldots (2)$$
$$o(t) = F(wo[ht\text{-}1, xt]+bo) \quad \ldots (3)$$

Here, x(t) represents the input, f(t) represents the forget gate which is used to disable all the stored information. The input gate i(t) is used to take all the inputs and present the output through the output gate o(t). The final result is obtained through h(t) which is also referred as the hidden layer.

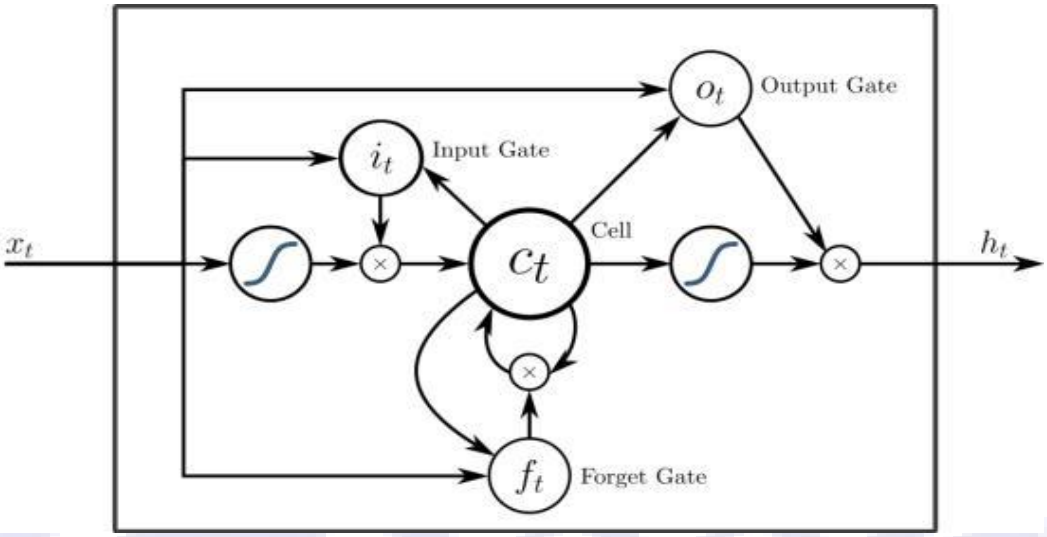

Figure 2: LSTM Architecture

Working of Text Summarizer

Our system builds a text summarizer using the Many-to-Many Sequence to Sequence Modeling. It takes the long sequence of words generally in the text body as its input. It generates the output as a short meaningful summary which conveys the overall meaning of the text. The output is a sequence as well. The input is a long sequence of words and the output will be a short version of the input sequence. The requirement for the difference in lengths of output and input enables to use the Encoder Decoder architecture. For the purpose of capturing the long-term dependencies, Long Short-Term Memory (LSTM) model is used as the Encoder and Decoder components. Here, we set up the Encoder and Decoder in two stages: Training Stage and Inference stage.

Training phase

In the training phase, the encoder and decoder is set up. Then the model is trained to predict the target sequence. The target sequence is made offset by one timestep. The two different sets of the LSTM architecture: encoder and decoder

Encoder

The Encoder Long Short-Term Memory model (LSTM) takes the input sequence where a single word is taken up by the encoder in each time step. The information is then processed using the LSTM hidden layers that produce a fixed-length representation of the source document. The contextual information is extracted from the input sequence every time step. This process undergoes into number of states from one time step to the other. The final state is then allowed to feed into the decoder. The hidden state (hi) and cell state (ci) of the last time step are used to initialize the decoder as shown in the figure.

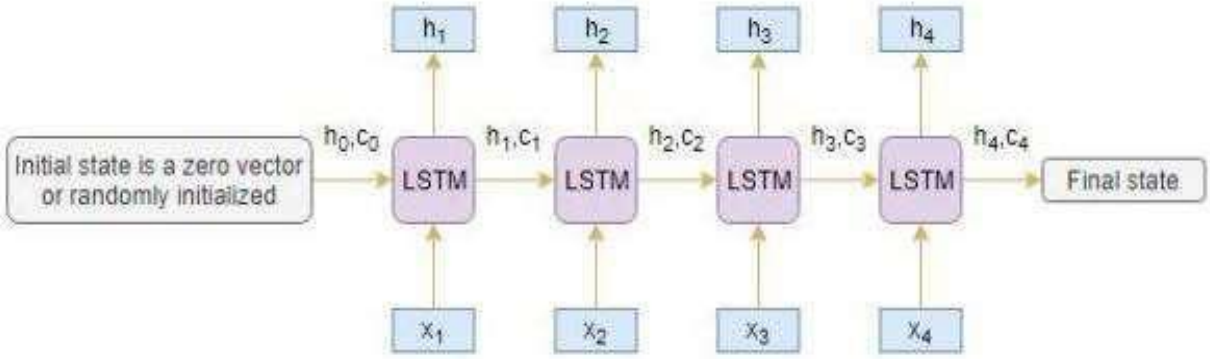

Figure 3: Encoder Architecture

Decoder

The Decoder Long Short-Term Memory model takes the intermediate target sequence one word in a single timestep. It reads the representation of the last generated word and uses these inputs to generate each word in the output summary. The decoder predicts the same sequence offset. It is capable of predicting the next word in the sequence when the previous work is available. The decoder uses the special tokens namely <start> and <end> attached with the target sequence. The <start> token denotes the starting of the sentence. The <end> token denotes the end of the sentence. The target sequence is unknown while decoding the test sequence. For predicting the target sequence, the first word is passed into the decoder which would be always the <start> token and the <end> token signals the end of the sentence.

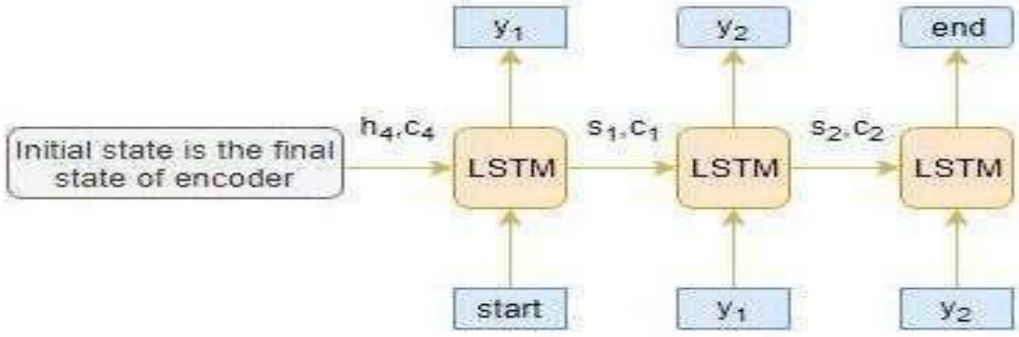

Figure 4: Decoder Architecture

Inference Phase

During the inference phase, the test data is fed into the model for which the target sequence is unknown. It is sent into the encoder phase for processing the information. Then a decoder is set up to decode a test sequence: The Following steps are used to decode the test sequence:

[1] Encode the entire input sequence and initialize the decoder with internal states of the encoder

[2] Pass <start> token as an input to the decoder
[3] Run the decoder for one timestep with the internal states
[4] The output will be the probability for the next word. The word with the maximum probability will be selected
[5] Pass the sampled word as an input to the decoder in the next timestep and update the internal states with the current time step
[6] Repeat steps 3 – 5 until we generate <end> token or hit the maximum length of the target sequence.

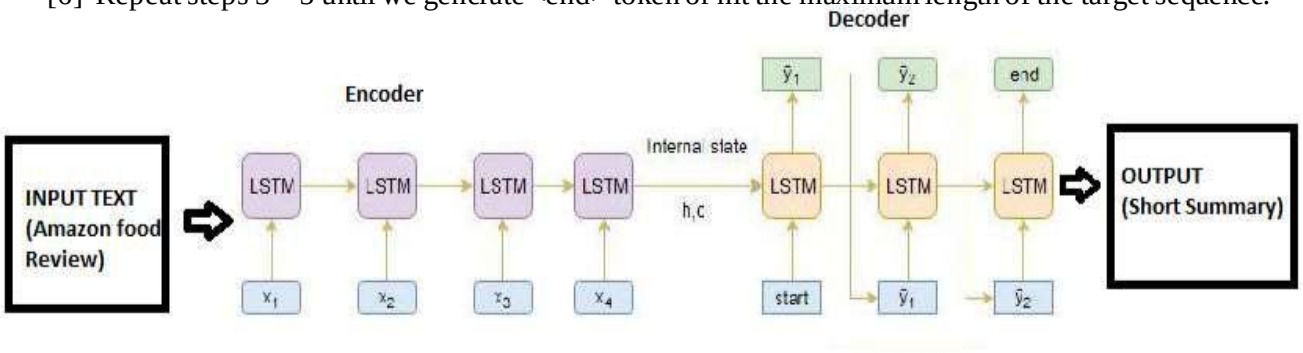

Figure 5: Architecture of Text Summarization System

About the dataset

This project requires the textual data of huge length as the project also emphasizes on generating the summaries and extracting the gist of the content. So, it is necessary to have a trusted source having relevant and necessary data required for the summary. We are using the Kaggle Amazon Fine Food reviews dataset which involves the reviews of fine foods from Amazon. The data span a period of more than 10 years, including all ~500,000 reviews up to October 2012. Reviews include product and user information, ratings, and a plain text review. It also includes reviews from all other Amazon categories [6].

4. Result

The "Automatic Text Summarizer" presents the model which is capable of generating the summary of the lengthy reviews of "Amazon Food Reviews" dataset.

The sparse categorical cross-entropy has been used as the loss function since it converts the integer sequence to a one-hot vector on the fly which overcomes the memory issues. The train and test graph can be visualized as shown in Figure 6 where we observed the validation loss increase after tenth epoch and hence, we stopped training the model.

The outcome of the Text summarizer can be analyzed by comparing the actual summary with the predicted summary as shown in the Figure 7. Although the summary predicted by the model does not match the word by word to the actual summary, but they convey the same meaning. Hence the model is capable of generating the legible summary based on the context present in the text.

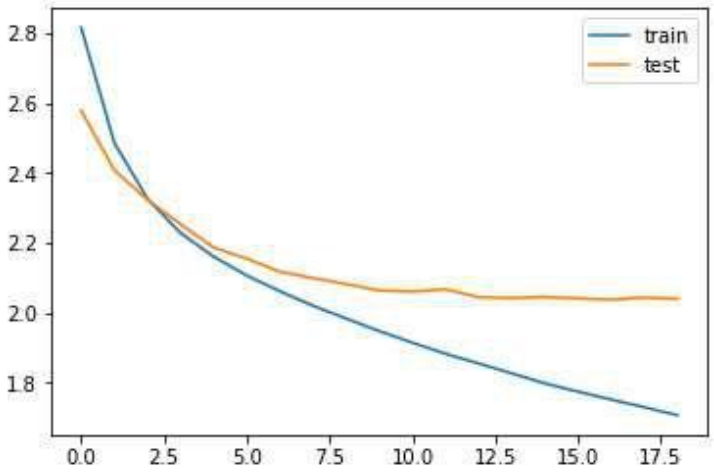

Figure 6: Visualization of Train and Test modeling

```
Review: gave caffeine shakes heart anxiety attack plus tastes unbelievably bad stick coffee tea soda thank
s
Original summary: hour
Predicted summary:  not worth the money


Review: got great course good belgian chocolates better
Original summary: would like to give it stars but
Predicted summary:  good


Review: one best flavored coffees tried usually like flavored coffees one great serve company love
Original summary: delicious
Predicted summary:  great coffee
```

Figure 7: Result of Text Summarizer shown in terms of Original and predicted summary

5. Conclusion

Because of the increasing growth of the information, it has become difficult for the people to extract the gist of the entire lengthy document. It is time consuming to analyze the huge texts. Thus, there is immense requirement of text summarizer. In this paper, we have emphasized the use of extractive summarization techniques using the Long Short Term Memory approach. It examines the content of the text document, extracts the important meanings from the text and presents in the summarized yet, meaningful form. It reduces the valuable time of the readers in this fast-moving technological world serving as the boon to mankind.

6. Future Enhancement

We can increase the training dataset size and build the model due to which the generalization capability of a deep learning model enhances. Also; we can implement Bi-Directional LSTM which is capable of capturing the context from both the directions and results in a better context vector. The beam search strategy can be used for decoding the test sequence instead of using the greedy approach (argmax). The performance of our model can be evaluated based on the BLEU score for better accuracy and we can also implement pointer-generator networks and coverage mechanisms for model development.

Acknowledgements

We would like to express our deepest gratitude to "SET conference 2019" and its team for providing us such a wonderful opportunity to publish our research paper in their well-recognized platform. We thank our Research Department of Advanced College of Engineering and Management. We are immensely grateful to the Department of Electronics and Communication, Advanced College of Engineering and Management for sharing their wisdom and providing this great opportunity. Also, we would like to thank our colleagues who provided us insights and comments that helped to improve our project. The initiation of this project would not have been successful and reached to this level in the absence of their continuous support. Their work, determination and valuable guidelines are really praiseworthy. Finally, any modifications, valuable suggestions and recommendation for further improvement will be highly appreciated and warmly welcomed.

References

[1] Saranyamol C S, Sindhu L, "A Survey on Automatic Text Summarization", International Journal of Computer Science and Information Technologies, Vol. 5 Issue 6, 2014.

[2] K. S. Thakkar, R. V. Dharaskar, and M. Chandak, "Graph-based algorithms for text summarization, " in Emerging Trends in Engineering and Technology (lCETET), 2010 3rd International Conference on, pp.516-519, IEEE, 2010.

[3] S. S. Ge, Z. Zhang, and H. He, "Weighted graph model based sentence clustering and ranking for document summarization, " in Interaction Sciences (ICIS), 2011 4th International Conference on, pp. 90-95, IEEE, 2011.

[4] V. K. Gupta and T. J. Siddiqui, "Multi-document summarization using sentence clustering, in Intelligent Human Computer Interaction (IHCI), 2012 4th International Conference on, pp. 1-5, IEEE, 2012

[5] Jun'ichi Fukumoto, "Multi-Document Summarization Using Document Set Type Classification," Proceedings of NTCIR- 4, Tokyo, pp. 412-416, 2004.

[6] https://www.kaggle.com/snap/amazon-fine-food-reviews

[7] https://www.analyticsvidhya.com/blog/2019/06/comprehensive-guide-text-summarization-using-deep-learning-python/

Pneumonia Detection Using Convolution Neural Network

Sitam Gautam[1],Pabitra Thapa[2],Prakriti Paudel[3],Surakshya Guragain[4]

Department of Electronics and Computer Engineering, Advanced College of Engineering and Management, Kupondole, Lalitpur, Nepal

[1]gautamsitam5@gmail.com, mailto:pabitrathapa972@gmail.com, iprakriti.paudel0@gmail.com, mailto:surakshya.114@gmail.com

Abstract

Chest diseases are very serious health problems in the life of people Pneumonia affects 7% of the global population, resulting in 2 million pediatric deaths every year. Pneumonia is often diagnosed with chest X-Rays and kills around 50,000 people each year. The timely diagnosis of chest diseases is very important. Many methods have been developed for this purpose. Unlike other methods that rely solely on transfer learning approaches or traditional handcrafted techniques to achieve a remarkable classification performance, we constructed a convolutional neural network model to extract features from a given chest X-ray image and classify it to determine if a person is infected with pneumonia. We trained our model on the recently released Chest X-ray dataset, which contains frontal-view chest X-ray images individually labeled with up to different thoracic diseases, including pneumonia. We use dense connections and batch normalization to make the optimization of such a deep network tractable. Detection of disease through some automatic technique is beneficial at very early stage as it itself detects the presence of the diseases i.e. when they appear on chest x-ray. This paper depicts an approach for analysis of pneumonia classification techniques that can be used for diseases detection using image analysis. Thus, we hope that this technology can improve healthcare delivery and increase access to medical imaging expertise in parts of the world where access to skilled radiologists is limited.

Keywords*: Pneumonia, X ray, Datasets, Convolution neural network, Artificial intelligence*

1. Introduction

Pneumonia is an infection of lungs and most commonly caused by viruses or bacteria and spreads by direct contact with infected people. Pneumonia affects approximately 450 million people globally (7% of the population) and results in about 4 million deaths per year. Pneumonia, a common lower respiratory infection accounted for 2.7 million deaths worldwide being the leading cause in children under 5 years, adults over 65 years, and immune compromised subjects. The risk factors include poverty, lack of measles immunization, indoor air pollution, overcrowding, malnutrition, poor nutritional practices. [1] Chestradiographs are taken according to usual clinical practice, which included all children with pneumonia suspected on clinical grounds. All chestradiographs were evaluated by an experienced radiologist. Chest X-rays are currently the best available method for diagnosing

pneumonia playing a crucial role in clinical are andepidemiological studies. Pneumonia causes over 15% of all deaths of children under 5 years old internationally. The appearance of pneumonia in X-ray images is often vague, can overlap with other diagnoses. Detecting pneumonia in chest radiography can be difficult for radiologists and also access to skilled radiologists is limited. Therefore, detecting pneumonia in chest X- rays is a challenging task that relies on the availability of expert radiologists. The purpose of this paper is to present a model that can automatically detect pneumonia from chest X-rays at a level exceeding practicing radiologist. [2] This model is a convolutional neural network that inputs a chest X-ray image and outputs the probability of pneumonia. Detecting pneumonia in chest radiography can be difficult for radiologists. The appearance of pneumoniain X-ray images is often vague, can overlap with other diagnoses, and can mimic many other benign abnormalities. These discrepancies cause considerable variability among radiologists in the diagnosis of pneumonia. Automated detection of pneumonia from chest X-rays at the level of expert radiologists would not only have tremendous benefit in clinical settings, it would also be invaluable in delivery of health care to populations with inadequate access to diagnostic imaging specialists. In this paper, we construct a system which detects pneumonia from frontal-view chest X-ray images at a level exceeding practicing radiologist. This technology can improve healthcare delivery and increase access to medical imaging expertise in parts of the world where access to skilled radiologists is limited. [3]

2. Literature Review

Prediction of pneumonia using Artificial intelligence is an advance approach in the field of medicine. In this approach of advance science, chest diseases can be shown in images in the form of cavitation, consolidations, infiltrates, blunted costophrenic angles, and small broadly distributed nodules. By analyzing the chest X-ray image, the radiologists can diagnose many conditions and diseases such as pleurisy, effusion, pneumonia, bronchitis, infiltration, nodule, atelectasis, pericarditis, cardiomegaly, pneumothorax, fractures, andmanyothers. Classifying the chest X-ray abnormalities is considered as a tedious task for radiologists; hence, many algorithms were proposed by researchers to accurately perform this task.[4]

Medical X-rays are images which are generally used to diagnose some sensitive human body parts such as bones, chest, teeth, skull, and so on. Medical experts have used this technique for several decades to explore and visualize fractures or abnormalities in body organs. X-rays are very effective diagnostic tools in revealing the pathological alterations, in addition to its noninvasive characteristics and economic considerations. Still there may be defects and error occurred while handling x-rays from the naked eyes. In the advancement of technology, medical x-rays can play vital role when collaborating with machine learning algorithms.[5]

Community-acquired pneumonia is a common cause of hospitalization, and pneumococcal vaccinations are recommended for high-risk individuals. Although risk factors for pneumonia have been identified, there are currently no pneumonia hospitalization prediction models based on the risk profiles of healthy subjects. This study aimed to develop a predictive model for pneumonia hospitalization in adults to accurately identify high-risk individuals to facilitate the efficient prevention of pneumonia. It conducted a retrospective database analysis using health checkup data and health insurance claims data for residents of Kyoto prefecture, Japan, between April 2010 and March 2015 choosing adults who had undergone health checkups in the first year of the study period, and tracked pneumonia hospitalizations over the next 5 years. Subjects were randomly divided into training and test sets. The outcome measure was pneumonia hospitalization, and candidate predictors were obtained from the health checkup data.The prediction model was developed and internally validated using a LASSO logistic regression

analysis. Lastly, it compared the new model with comparative models. The study sample comprised 54,907 people who had undergone health checkups. Amongthese,921 were hospitalized for pneumonia during the study period. The c-statistic for the prediction model in the test set was 0.71(95%confidence interval:0.69–0.73). In contrast, a comparative model with only age and comorbidities as predictors had a lower c-statistic of 0.55 (95% confidence interval:0.54–0.56).[6]

CAD systems have been developed to extract useful information from X-rays to help doctors in having a quantitative in sight about an X-ray. However, these CAD systems could not have achieved a significance level to make decisions on the type of conditions of diseases in an X-ray. Thus, the role of them was left as visualization functionality that helps doctors in making decisions.

A numberof research works have been carried out on the diagnosis of chest diseases using artificial intelligence methodologies. In, multilayer probabilistic, learning vector quantization, and generalized regression neural networks have been used for diagnosis chest diseases. The diagnosis of chronic obstructive pulmonary and pneumonia diseases was implemented using neural networks and artificial immune system. In the detection of lung diseases such as TB, pneumonia, and lung cancer using chest radiographs is considered. The histogram equalization in image segmentation was applied for image preprocessing, and feed forward neural network is used for classification purpose. The above research works have been efficiently used in classifying medical diseases; however, their performance was not as efficient as the deep networks in terms of accuracy, computation time, and minimum square error achieved. Deep-Learning based systems have been applied to increase the accuracy of image classification. These deep networks showed superhuman accuracies in performing such tasks. This success motivated the researchers to apply these networks to medical images for diseases classification tasks, and the results showed that deep networks can efficiently extract useful features that distinguish different classes of images. Most commonly used deep learning architecture is the convolutional neural network.CNN has been applied to various medical images classification due to its power of extracting different level features from images Having gone through the related research studies, in this paper, a deep convolutional neural network is employed to improve the performance of the diagnosis of the chest diseases in terms of accuracy and minimum square error achieved. For this purpose, traditional and deep learning-based networks are employed to classify most common thoracic diseases and to present comparative results. Back propagation neural network, and convolutional neural network are examined to classify 12 common diseases that may be found in the chest X-ray, that is, atelectasis, cardiomegaly, effusion, infiltration, mass, nodule, pneumonia, pneumothorax, consolidation, edema, emphysema, and fibrosis. In this paper, we aim at training both traditional and deep network using the same chest X-ray data set and evaluating their performances.The data used in the paper are obtained from the Kaggle, online community of data scientists and machine learning. The data set contains 25,684 frontal-view X-ray images of 30,229 unique patients. [7]

3. Feasibility study

This paper has passed through various feasibility scrutinization in order to make sure the use of this paper can be implied on real world problems efficiently.

Economics study: We have conducted economic feasibility studies to determine the operational and maintenance cost. This project consists of a laptop with more processing power to process and analyze the data.

Technical Feasibility: This project requires large amount of database space and processing power to store and cluster user info and process each of them in small time.

Social Feasibility: This project is socially feasible as it targets the health sector. Radiologist and patient can use this technology to check their health without the technical help and easily can take appropriate actions based on the type of stage of pneumonia. On the other hand, this approach helps in modernizing the health sector.

Operational Feasibility: The project requires setting up some devices as mentioned above and a server to manage and analysis of the data.

4. System Architecture and Design

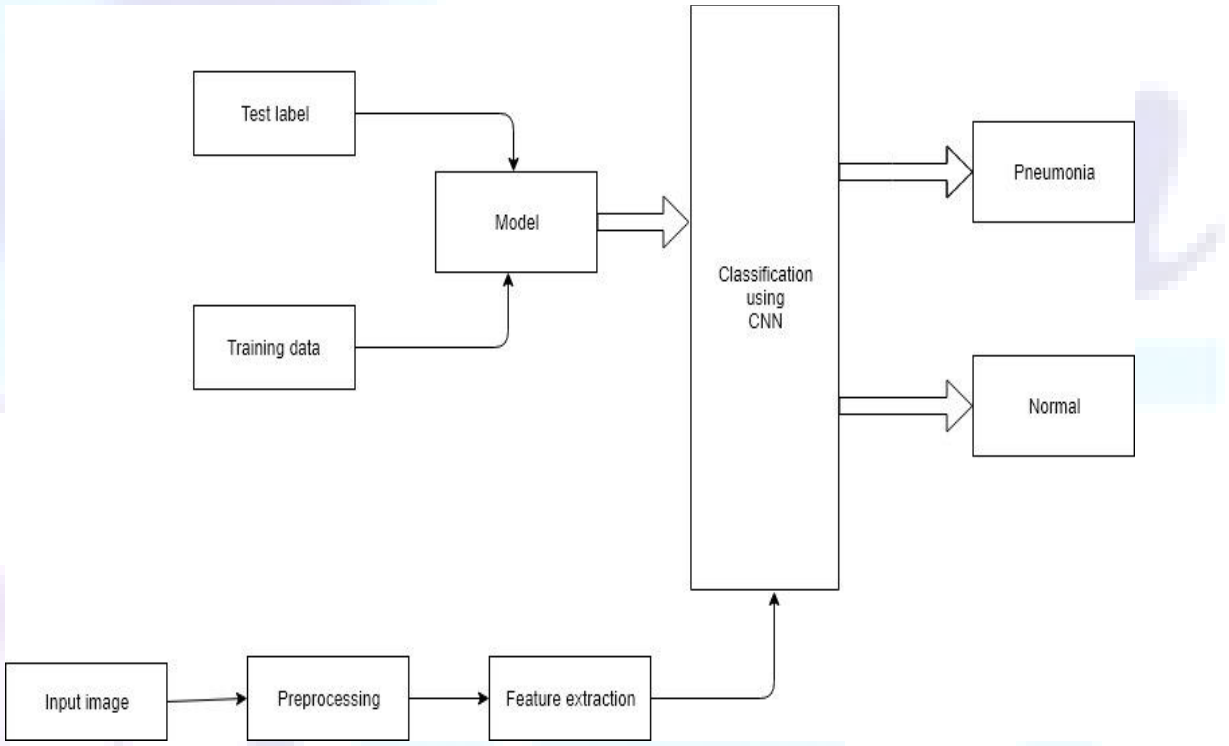

Figure 3: ***System Diagram***

Training data: From the preprocessed data, we selected 70% of the data for training the models.

Testing data: The remaining 30% data are used as testing data.

Now after getting the dataset we need to preprocess the data and provide labels to each of the image given there during training the data set. Firstly, the input datasets are trained. To extract features from CNN model first we need to train the CNN network with last sigmoid/logistic dense layer with respect to target variable. The objective of the training network is to identify the correct weights for the network by multiple forward and backward iterations, which eventually try to minimize binary cross entropy (misclassification cost). The input to the proposed system consists of some trained images with their respective patient id. The feature gets extracted i.e. it

figures out what part of image is distinctive from the trained datasets for further classification. The input image is preprocessed through preprocessing techniques and classified further for feature extraction. Finally, the result is delivered based on CNN model.

5. Proposed Model

The overall architecture of the proposed CNN model which consists of two major parts: the feature extractors and a classifier (sigmoid activation function). Each layer in the feature extraction layer takes its immediate preceding layer's output as input, and its output is passed as an input to the succeeding layers. The proposed architecture in Figure 3 consists of the convolution, max-pooling, and classification layers combined together. The feature extractors comprise conv 3×3,16; conv3 × 3, 32; conv3 × 3, 64; conv3 × 3, 96; conv3 × 3, 128, max-pooling layer of size 2 × 2, and a RELU activator between them. .e output of the convolution and max-pooling operations are assembled into 2D planes called feature maps, and we obtained 16×150 × 150, 32 × 75 × 75, 64 × 37×37, 96 × 18 × 18,and 128 × 8 × 8 sizes of feature maps, respectively, for the convolution operations and 16 × 75 × 75, 32 × 37 × 37, 64 × 18 ×18, 96 ×8 ×8 and , 128 × 3×3 sizes of feature maps from the pooling operations, respectively, with an input of image of size 150×150 × 3 .It is worthy to note that each plane of a layer in the network was obtained by combining one or more planes of previous layers. The classifier is placed at the far end of the proposed convolutional neural network (CNN) model. It is simply an artificial neural network (ANN) often referred to as a dense layer. This classifier requiring individual features (vectors) to perform computations like any other classifier. Therefore, the output of the feature extractor (CNN part) is converted into a 1D feature vector for the classifiers. .is process is known as flattening where the output of the convolution operation is flattened to generate one lengthy feature vector for the dense layer to utilize in its final classification process. The classification layer contains a flattened layer, a dropout of size 0.4, two dense layers of size 64 and 2, respectively, a RELU between the two dense layers and a sigmoid activation function that performs the classification tasks.

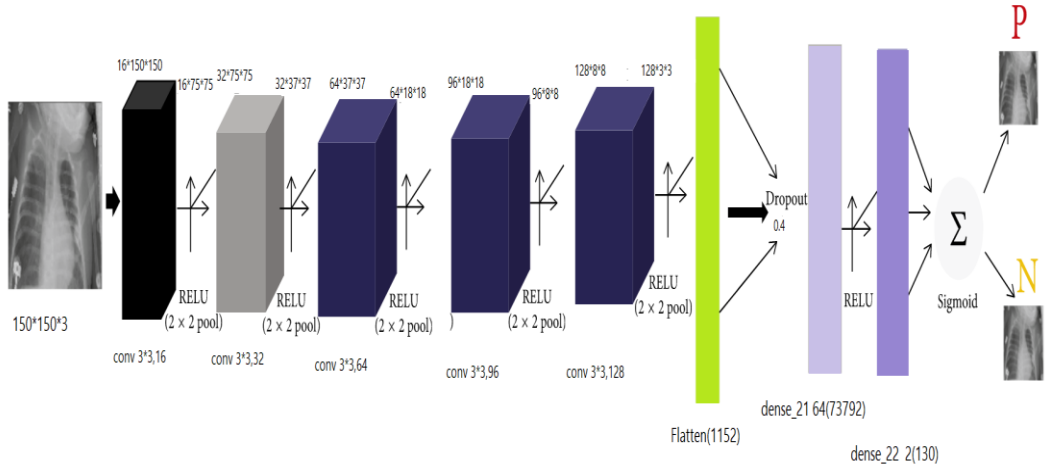

Figure 2: ***Proposed Model architecture***

6. Result and Analysis

The final output of our project is to detect the pneumonia accurately with the help of iterations obtained, loss and accuracy graph and the confusion matrix.

The given figure shows the histogram evaluated based on RGB intensities of the given dataset.

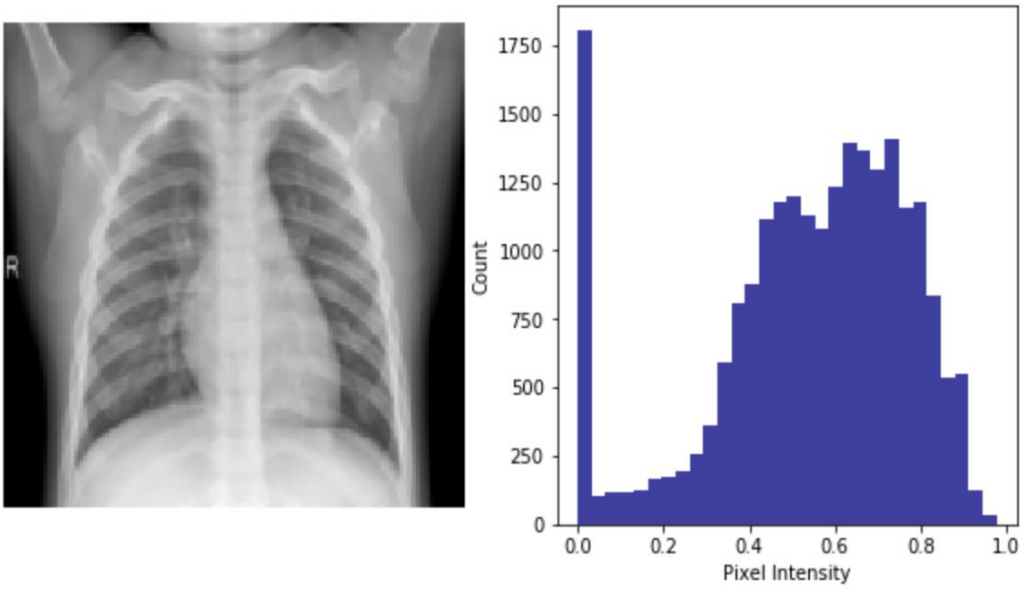

After preprocessing and data augmentation process, we passed our datasets as input and evaluated whether the given input X-ray image is classified as either No Pneumonia or Pneumonia as show in the below diagrams which were obtained as an output:

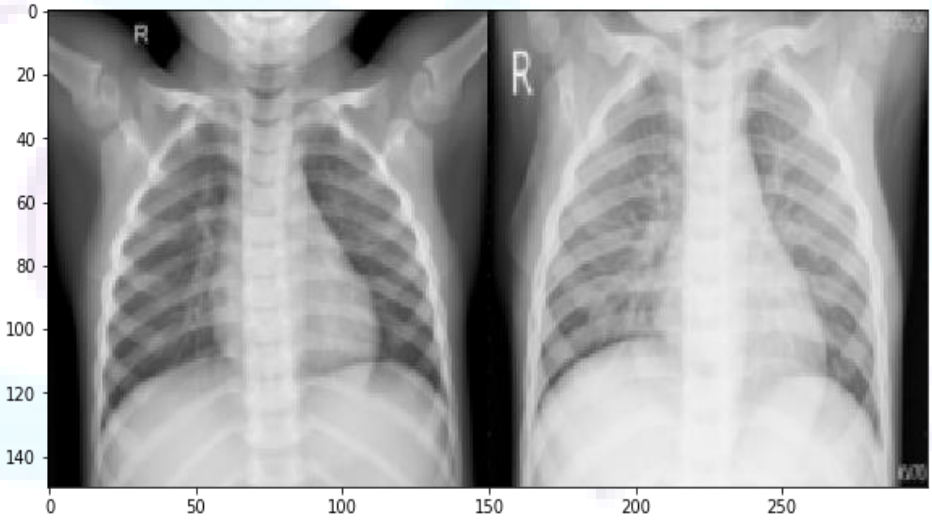

Figure 3: ***(Left) - No Pneumonia Vs (Right) - Pneumonia***

We have performed six series of iteration from which we can clearly observe that the loss is decreasing with each iteration. Loss is about how much right the model is. So, we wanted to minimize the loss function and as a result our model has perfectly declined the loss value straight from starting point and at every iteration, we get closer to minimum.

Next we evaluated learning curves for the best result of our model. These learning curves (Learning curve for Training set & Learning curve for Validation set) shows the performance of our model on training and validation set as a function of number of training iterations.

We have learning curve for validation set which is decreasing with each iteration which shows that loss is minimizing giving the best result. On the other hand, we have performed learning curve for training set which is increasing with each iteration that means our model is getting better and better at learning.

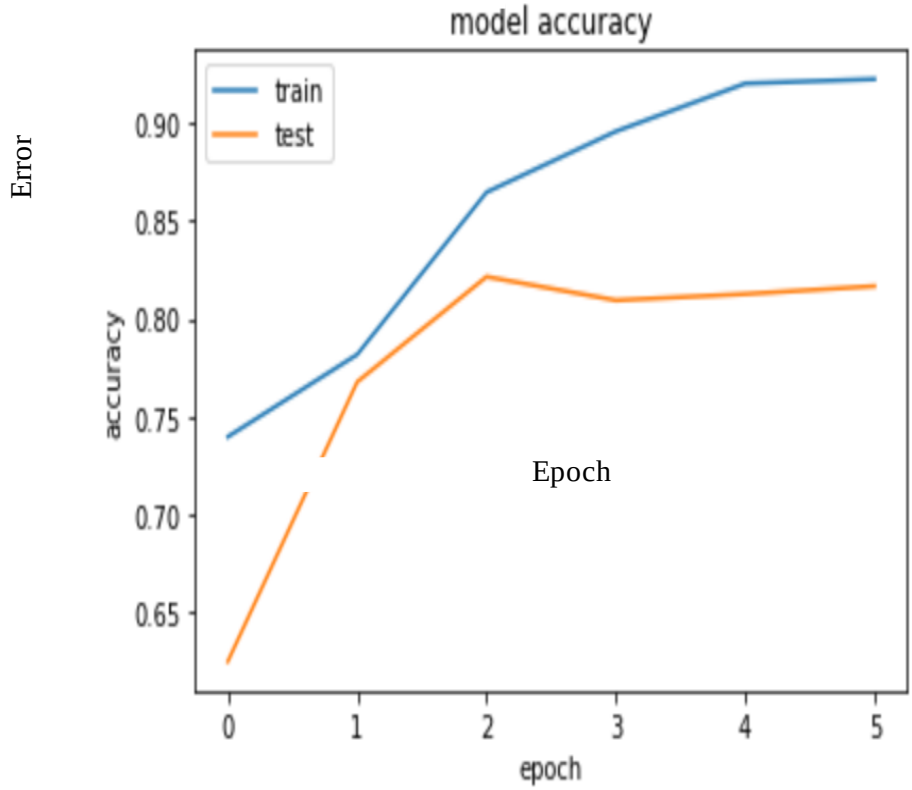

Figure 4: Learning curve for Training Set

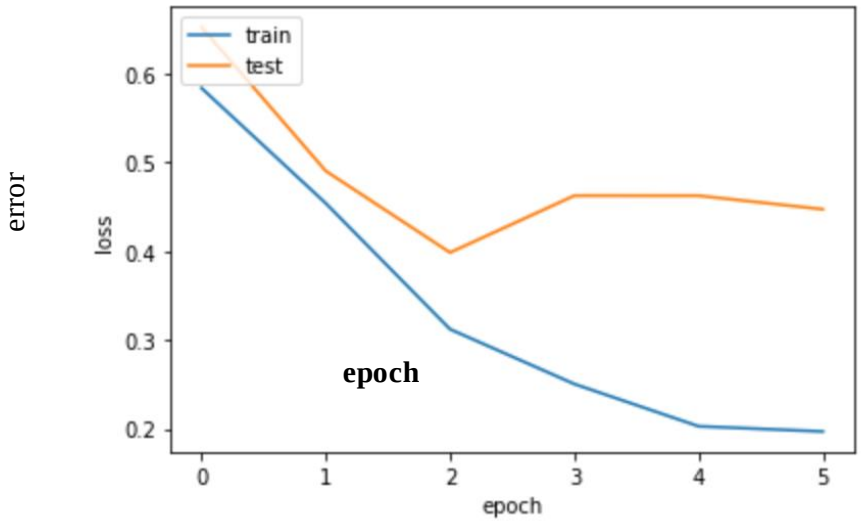

Figure 5: Learning curve for Validation set

Finally, we evaluated confusion matrix to describe the performance of our classification model. We then calculated precision, accuracy and recall value from the obtained confusion matrix to measure our model accurate performance.

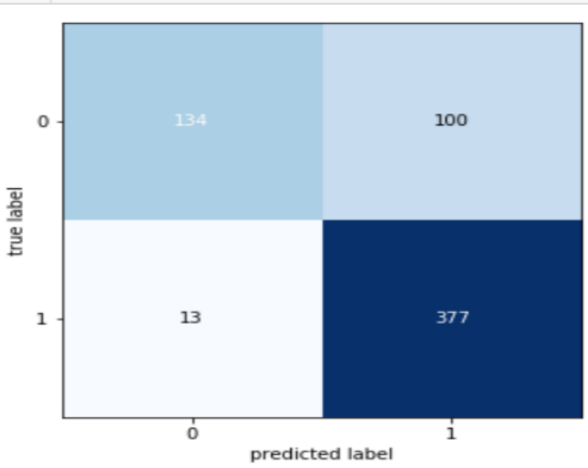

Figure 6. Confusion matrix

Here the 0 belongs to class of people not having Pneumonia and 1 belongs to class of people having Pneumonia. The confusion matrix consists of True positive, True negative, False positive and False negative values according to which different parameters are calculated which is shown in figure below:

```
#precision= (TP/(TP+FP))

377/(377+100)
```

```
0.790356394129979
```

```
#Recall =(TP/(TP+FN))

377/ (377 + 13)
```

```
0.9666666666666667
```

```
#Accuracy = (TP+TN)/(TP+TN+FP+FN)

(134+377)/(134+377+100+13)
```

```
0.8189102564102564
```

Figure 7: *Screenshot*

Here, the recall is most significant quantity even more than accuracy and precision. Since we are having unequal number of people in both the classes, therefore we can't take accuracy as an alone metric to calculate model accuracy. Also, we must minimize the false negative which is in the denominator of recall increasing the value for recall.

False negative has to be intuitively minimized because falsely diagnosing a patient of Pneumonia as not having Pneumonia is much larger deal than falsely diagnosing a healthy person as a Pneumonia patient which is our major concern. That is why we are making this model to reduce the mistakes done by doctors accidentally.

7. Conclusion

We have created the model using convolution neural network that detects pneumonia with a good value of accuracy and recall. Data were collected from different sources and were preprocessed and further trained and tested the large amount of data obtained. We created our own weights and biases to pass into defined CNN function. CNN different layers were performed to extract the image features. This model helps us to detect pneumonia through x rays. We also evaluated the confusion matrix, learning curve to see how accurate our model is. After training, a separate test set was used to evaluate the performance of the CNN classifier. The test set is a little unbalanced. We also use this number as baseline accuracy. The CNN classifier achieved an accuracy of 82.13%, which is substantially better than the baseline accuracy. By analyzing the confusion matrix, we can see that the CNN classifier is particularly good at identifying pneumonia images as 377 out of 390 pneumonia images were correctly classified.

8. Future work

In the future we can implement our model in real world data as well as providing 100% accuracy. Normal people can also make their life facilitated with such model and also, they will be able to predict different stages of pneumonia. In our future enhancement we will be trying to integrate our model in a suitable website or mobile application so that normal users get facilitated by our projects. In context of Nepal, we can use this technique in the rural areas where there are lack of health centers and hospitals so that infected people in the rural areas will be able to get early treatment for pneumonia. In future we will also be working to add more features to our model so that it'll be able to predict the type of pneumonia whether it is Bacterial pneumonia

or Viral pneumonia or Mycoplasma pneumonia or Other pneumonias such that person can quickly get the treatment according to the type as detected by the model.

References

[1] https://www.google.com/search?q=pneumonia&rlz=1C1DVJR_enNP828NP828&oq=peum&aqs=chrome.1.69i57j0l5.4265j0j7&sourceid=chrome&ie=UTF-8

[2] Stanfordmlgroup.github.io.(2018). CheXNet:Radiologist-Level PneumoniaDetectiononChest X-RayswithDeepLearning. [online]Available at: https://stanfordmlgroup.github.io/projects/chexnet/

[3] Rajpurkar,P.,Irvin,J.,Zhu,K.,Yang, B.,Mehta,H.,Duan,T.,Ding,D.,Bagul,A., Langlotz,C., Shpanskaya,K.,Lungren,M.andNg,A.(2018). CheXNet:Radiologist- LevelPneumonia DetectiononChestX-RayswithDeepLearning. [online] arXiv.org. Available at:https://arxiv.org/abs/1711.05225

[4] The diagnosisof pneumonia requiresa chestradiograph(x-ray)—yes,n.(2018). Pneumonia.[online]Pneumonia.Availableat:https://pneumonia.biomedcentral.com/articles?tab=keyword&sort=PubDateAscending

[5] Centre, N.(2018).Diagnosis of pneumonia in children maybe confirmedby ultrasound. [online] Discover.dc.nihr.ac.uk. Available at: https://discover.dc.nihr.ac.uk/content/signal-000624/diagnosis-of-pneumonia-in- children-may-be-confirmed-by-ultrasound

[6] Access NCBI through the world wide web(WWW).(1995).MolecularBiotechnology, 3(1), pp.75-75.

[7] Portal.inf.ufg.br(2018).http://www.portal.inf.ufg.br/~leandroluis/aqruivos/leandro.pdf

[8] Learning,D.andWith,2.(2018).25OpenDatasetsforDeepLearningEvery Data Scientist Must Work With. [online] Analytics Vidhya. Available at: https://www.analyticsvidhya.com/blog/2018/03/comprehensive-collection-deep- learning-datasets/

[9] .Cs231n.github.io.(2018). CS231nConvolutionalNeuralNetworksfor Visual Recognition. [online]Available at:http://cs231n.github.io/convolutional-networks/

[10] .solver.(2018).NeuralNetworkClassification.[online] Available at:

[11] https://www.solver.com/xlminer/help/neural-networks-classification-intro

Real-Time Stock Prediction Using Neural Network

Abhishek Sharma[1]

[1]*Department of Electronics and Computer*
Pulchowk Engineering Campus, IOE
Tribhuvan University, Lalitpur, Nepal

Abstract

Stock price prediction has been a trending yet mystifying topic for a very long time now. The fact that the stock price on short-term are the result of public reaction to rumors and are moreover, associated with public psychology, has made it tricky for the general people to get an insight on the market. This paper presents a method to predict stock prices of companies listed under Nepal Stock Exchange Limited at an interval of every two minutes. The paper describes an approach to comprehend instant public preferences through traded share volume, number of transactions and price fluctuation analysis. The result of these analysis is fed to Neural Network, which then predicts the percentage change in stock price.

Keywords: Stock price prediction, *Neural Network*

1. Introduction

One of the most fundamental concepts of economics is the rule of supply and demand. Stock market also works on the same principle. With the increase in demand, prices of the stocks tend to increase and with the decrease in demand, they tend to decrease. Factors like economic news, corporate policy and interest rates tend to affect the demand for stock. While demand for stock can change rapidly with change in corporate policy, economic shifts and government change, the supply of stocks shows only leisure change [1]. Manual assessment of supply and demand to get insight on the future stock price used to be a trend in the past. However, with the advancement in computing capabilities, research on computational method using Neural Networks to assess the behavior of stock market is an area of concern today.

2. Literature Survey

Regarding the prediction of the future prices of Stock Market securities, several theories have been put forward. The first is Efficient Market Hypothesis (EMH). In EMH, it is assumed that the price of a security reflects all the information available and that everyone has some degree of access to the information [2]. Famas theory further breaks EMH into three forms: Weak, Semi-strong, and Strong. In Weak EMH, only historical information is embedded in the current price. The Semi-Strong form goes a step further by incorporating all historical and currently public information in the price. The Strong form includes historical, public, and private information, such as insider information, in the share price. From the tenets of EMH, it is believed that the market reacts instantaneously to any given news and that it is impossible to consistently outperform the market.

A different perspective on prediction comes from Random Walk Theory. In this theory, Stock Market prediction is believed to be impossible where prices are determined randomly and outperforming the market is non-feasible [3]. Random Walk Theory has similar theoretical underpinnings to Semi- Strong EMH where, all public information is assumed to be available to everyone. However, Random Walk Theory declares that even with such information, future prediction is ineffective.

It is from these theories that two distinct trading philosophies emerged; the fundamental analysis and the technical analysis. Fundamental analysis involves assessment of companies in- transit value in regards to its quarter, semi-annual or annual report. This analysis is however more relevant to the long-term predictions and is usually discarded for short-term predictions. Technical analysis on other hand takes account of the historical patterns in order to predict the future stock value. A similar research in a paper 'Stock prediction using Artificial Neural Network' by Kar [4] depicts the way to predict stock market indices as a part of Technical analysis. The paper, on contrary, incorporates the concept of real-time traded share volume, number of transactions and price fluctuation analysis to predict the stock price using feed-forward neural network.

3. Methodology

3.1 Data Collection

Both historical and real-time data are essential for devel- oping a model and predicting the stock price. This paper considers the following factors for building the prediction model–Number of transactions, Traded Volume and Last Traded Price. Each data set contained the data related to above mentioned factors, collected in every thirty minutes interval. A large number of these sets of data were collected by crawling the *Merolagani* website over six-months period.

3.2 Data Preprocessing

Redundant data were observed while crawling in the non- trading days. Those data were filtered and removed to maintain data integrity. Also, the prices were cross-checked with NEPSE website to validate the authenticity of data. The ambiguity in data, if found were filtered, removed and then replaced by linear interpolation technique.

3.3 Neural Network Model

An optimized feed-forward Neural Network model was built by tuning the number of neurons in hidden layer. 3-X-10 Neural network model was built with X tuned experimentally. A set of all possible input features were at first collected through rigorous study and from expert opinion. Considering the training time and complexity of model, only three best relevant features were selected using the wrapper method. The wrapper method [5] is explained in the figure 1.

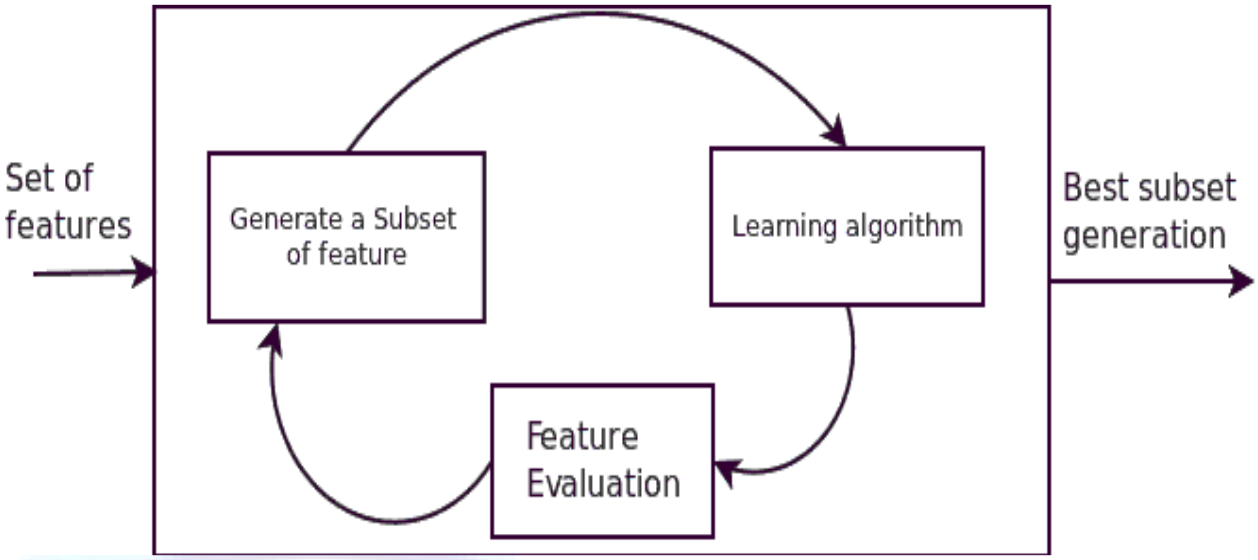

Figure 1: Feature Selection

The selected input features were:

- Number of transactions in 30 minutes
- Traded share volume in 30 minutes

The output of Network was divided into 10 class labels:

- Increase with (0-1) %
- Increase with (1-2) %
- Increase with (2-3) %
- Increase with (3-4) %
- Increase with (more than 4) %
- Decrease with (0-1) %
- Decrease with (1-2) %
- Decrease with (2-3) %
- Decrease with (3-4) %
- Decrease with (more than 4) %

Backpropagation algorithm was used to train the weights associated with the interconnected neurons.

3.4 Training and Testing Model

Around one thousand data sets were collected over six- months period. K-fold cross-validation was used over these data to evaluate the performance of the model. The value of k was chosen such that it lowered the variance of result of the cross validation, which after experiment was found out to be 12.

A visualization of the system proposed by the paper is shown in the figure 3. The system collects the historical data by crawling the NEPSE website. These data are divided into the data-chunks of thirty minutes each. For each chunk (30-minute interval), the system calculates the Total number of transactions, Traded share and Standard Deviation of Last Traded Price. Similarly, the class label for each vector is also determined by comparing the current price with latest price. Once a complete vector-set is simplied, the system is now ready for training and building a model. The training is achieved using Backpropagation algorithm, which gives refined synaptic weights as the output. These refined weights are then stored in the database for easy access during prediction. Whenever a prediction is to be made, the synaptic weights are read from the database alongside the recent real-time features. These features are then fed to Neural Network which on passing through series of synaptic weights and activation functions produces the predicted stock price for the second minute.

4. Result and Analysis

The change in accuracy while varying the hidden layer neuron is depicted in the table I.

From the table I, it can be seen that the prediction accuracy changes with change in number of neurons in the hidden layer. Also, the Neural network model that best fits one company may not fit other companies to the same extent. Thus, the number of neurons in hidden layer were tuned separately for the separate companies. On the basis of above analysis, it can be said that NABIL bank is best modeled by 3-30-10 neural network, ADBL bank is best modeled by 3-20-10 neural network, SCB is best modeled by 3-10-10 neural network and NTC is best modeled by 3-10-10 neural network. Same process was carried out for the remaining companies to model their respective network. The best result was found out for ADBL with an accuracy of 86.12 %, modeled by a 3-20-10 network. The result of stock prediction for NABIL Bank Limited for varying number of neurons in hidden layer are shown through figure 4, 5 and 6.

The change in Sum of Squared Error (SSE) as a function of number of iterations in training is depicted in figure 7. It is seen that provided the training iteration is sufficiently large, the value of α has no considerable effect on the SSE error.

5. Conclusion and Future Enhancement

The system attempts to design the framework for predicting minute-wise stock price by the analysis of those real-time market variables which inherently carry the information of supply and demand. From the analysis of prediction of several companies, it is seen that this approach of prediction of stock price, in fact, can potentially challenge the theory of Efficient Market Hypothesis and hence shows that stock price on short run, being a function of market supply and demand, can be predicted with considerable amount of

accuracy. The system performance can further be improved by increasing the depth of hidden layer in the network. The need for computationally strong servers arises with the increased depth in network. Hence, provided that the system is computationally well-equipped, it is only a matter of time before machines explore complex market to its core.

References

[1] Investopedia. (2015, April 2). How does the law of supply and demand affect the stock market? [Online].Available: http://www.investopedia.com/ask/answers/040215/how-does-law-supplyand-demand-affect-stock-market.asp

[2] E. Fama, "The Behavior of Stock-Market Prices".Journal of Business, vol. 38 (1965), pp. 34-105.

[3] B.G. Malkiel, "The firm-foundation theory of stock prices", in A Random Walk Down Wall Street. New York: W.W. Norton Company, Inc., 1973, ch. 4, pp. 47-57

A. Kar, "Stock Prediction using Artificial Neural Networks". Available: https://people.eecs.berkeley.edu/ akar/IITK website/EE671/report stock.pdf

[4] S. Kaushik. (2016, Dec 1). Introduction to Feature Selection methods with an example (or how to select the right variables?) [Online]. Available: https://www.analyticsvidhya.com/blog/2016/12/introductionto-feature-selection-methods-with-an-example-or-how-to-select-theright-variable

Part III: Data Science, Analysis and Mining

A Comparative Study on Performance of Centralized and Distributed Database System

Abhishesh Dahal[1], Shashidhar Ram Joshi[2]

Department of Computer and Electronics Engineering
Advanced College of Engineering and Management, Institute of Engineering
(Tribhuvan University)

[1] abhishesh.dahal@acem.edu.np, [2] mailto:srjoshi@ioe.edu.np

Abstract

Data are often collected, organized and stored in an electronic entity termed as database. The main idea behind this mechanism is to easily and efficiently access the data on demand. End user doesn't have direct access to database so a user interface bridging user and database named as Database Management System is brought in account which plays a great role to provide a platform to end user to access database. Beside these, architecture of database too plays a major role in how efficiently an end user access data from a database. Centralized and Distributed architecture are two of those architecture in which database can exist. Computer network is the major utility required for existence of both of the database architecture. Centralized Database System consist of a central master node who is responsible for managing all the affairs related in data access from the database whereas Distributed Database System consist each device in the system as an independent node able to manage the entire affairs related to data access. This research paper proposes an expressive method of comparing the performance of both centralized and distributed database architecture on the basis of cost spent while accessing the desired attributes of the database table. Numeric outcomes obtained clearly show that the distributed database system utilize less cost to access the attribute in comparison to that in centralized database system.

Keywords: *Database System, Centralized Database, Distributed Database, Site, User Query, Attribute Access Cost*

1. Introduction

A database is a composed accumulation of information which are stored and retrieved electronically from a computerized system. When databases design are increasingly complex they are regularly created utilizing formal plan and modelling procedures. The Database Management System (DBMS) is the product that communicates with end clients, applications, and the database itself to grab and break down the information. The DBMS programming furthermore includes the central functionalities to manage the entire database. The entirety of the database, the DBMS and the related applications can be alluded to as a "database system".

Regularly the term "database" is likewise used to freely allude to any of the DBMS, the database framework or an application related with the database. The sector of database can enlarge to a huge extent with variety of terminologies within it.

Centralized database is a type of database which is generally found in a solitary area [1]. This area is regularly a central PC or database framework, for instance a workstation, a server CPU, or a centralized server PC. A centralized database is utilized by an institution or an organization in several sectors. Users often get access to a centralized database through a single PC connected within a network.

Distributed database is a type of database system where not all storing elements are appended to a typical processing unit [2]. It might be put away in different PCs, situated in the equivalent physical area; or might be scattered over a system of interconnected PCs. In contrast to parallel frameworks, in which the processors are firmly coupled and comprise a solitary database framework, a distributed database framework comprises of loosely coupled destinations that doesn't share any physical components.

Database administrators can circulate accumulations of information over different physical areas. A distributed database can dwell on composed system servers or decentralized autonomous PCs on the Internet, on corporate intranets or extranets, or on other association systems. Since distributed databases holds ability to store information over various PCs, distributed databases may improve execution at end-client worksites by enabling transactions to be prepared on numerous machines, rather than being constrained to one.

Centralized database management system is any product that is just concerned to controls the capacity and the organization of information in a particular database, while distributed database management system comprise of a solitary database that is partitioned into numerous segments. Each segment termed as fragment is coordinated on at least one PC and constrained by autonomous database. In Distributed DBMS the information is disseminated over the system PCs, and the information is put away on numerous destinations under the administration duty of DDBMS. In Centralized DBMS, information is put away and controlled in a central site.

Both of distributed and concentrated DBMS give access to database utilizing a similar interf ace, yet for this capacity brought together centralized DBMS faces less inconvenience than DDBMS [3]. For circulating information over system we can utilize fragmentation or allocation. The target of fragmentation and replication is to maintain transparency to the user so that the implementation details are hidden away from the end users. Centralized database doesn't emphasize on transparency. DDBMS also discovers few issues which are not in centralized DBMS structure. These issues are: How to part the database to sections and in which site we can discover these sections.

The main objective of this research is to identify the best database architecture among the two specified architecture, i.e. centralized database architecture and distributed database architecture. Attribute access cost is obtained as an output to evaluate the performance of the two architecture of database. A comparison on the attribute access cost is made and the architecture with the less access cost value is marked as the better architecture in comparison to other.

The rest of the paper is organized in Section II, Section III, Section IV and Section V. Section II elaborates on the recent works done in this research context. Section III elaborates on the research methods used in this research. Section IV consists findings of the experiment and Section V consist conclusion of the research.

2. Related Work

Several researchers contributed a lot in comparing different architectures of the databases. In context to it, author of [4] looks at centralized, partially distributed, and fully distributed methodologies utilizing PCs associated with a campus wide enterprise framework. The outcomes demonstrate that distributed methodologies can be utilized to limit the measure of information transmitted between frameworks, without essentially lessening the general nature of the impact examination. These distributed methodologies supports a proficient and adaptable effect assessment in present day enterprise systems. The author concludes that the effect assessment procedures can be adequately dispersed among the end frameworks. All the more explicitly, the information transmission and evaluation quality outcomes demonstrated that the distributed methodologies produce sway appraisal results similar in quality to the centralized approach while fundamentally decreasing the measure of information moved. The author feel that these underlying, littler scale results are worthy and legitimate for further examination. These methodologies were tried in bigger scale situations, as far as framework multifaceted complex nature (for example the quantity of end frameworks, including more multi-level and shared applications) and time (for example utilizing multi-month and multi-year informational indexes).

Authors of [5] presents a case study, e-learning portal performance optimization by using distributed databases technology. In this phase of improvement wherein institutions consist branches conveyed over a wide geographic territory, distributed database systems become progressively suitable to utilize, on the grounds that they offer a higher level of adaptability and versatility at that point than centralized ones. Distributed databases take out demerits of centralized databases and offer a few benefits, for example, accessibility, unwavering quality, execution, measured improvement and so on. In any case, distributed architecture conditions face new issues that are not applicable in centralized situations, for example, fragmentation and replication. The utilization of distributed databases in e-Learning frameworks improves access to data and offer fast information accumulation. Present day colleges, with geologically circulated areas, must accept the accountability to present new advances in the instructive procedure and must embrace learning strategies dependent on the new innovations that are more effective than the conventional ones.

Authors of [6] introduce and evaluates biometric access control systems based on centralized and distributed architectures. It compares these two architectures, presents their strong and weak aspects, and discuss applications where one among the two are more appropriate. Biometric access control frameworks can be designed in centralized architectures, distributed architectures or some mixture of them too. Each architectural approach offers few advantages and disadvantages. The plan of the architecture fitting for every specific circumstance should adjust the requirements for central control, failure-resistant operation, autonomous operation, override capability, robust operation, expansion requirements and resistance to compromise.

3. Research Method

A. Database Table Setup

This define the structure of table which is utilized in the experiment. It includes 8 attributes representing a table of a relational database. Every attribute are named as A1, A2, A3, A4, A5, A6, A7, A8. Attributes of this table are accessed from certain sites in the network. In centralized database, this table resides on one of the site in network where as in distributed database, this table is divided as per fragmentation strategy and those fragments pieces are allocated to several sites in the network.

B. User Query

It is a list of query performed by different user from different sites. This list includes information of attribute accessed by every query, information regarding the site where query was initiated and also the type of query operation performed to particular attribute.

Table 1: User Query List

Query	Site	A1	A2	A3	A4	A5	A6	A7	A8
1	S5	r				r		r	
2	S4		r		r	r			
3	S1	r		r		r		r	
4	S8		r		r		r		
5	S2		r					r	
6	S7	r				r			r
7	S6		r		r		r		
8	S3	r		r		r			

The value r in Table 1 indicates read (select query) operation.

C. Centralized Data Access

Centralized database implementation is on the basis of placing the entire table of a database onto one of the site in the network. This site acts as the server and process the request from all other sites of the network. Any site requesting for the attribute data of the table invokes a request from their respective site to the server site where the server in return process the request received and provides the requesting site with necessary outcome.

D. Distributed Data Access

Distributed database implementation is on the basis of performing fragmentation and allocation of the database table. Instead of placing the entire table of a database onto one of the site in the network like in centralized database; in distributed database it first dissects the table into multiple fragments on the basis of the user query. Then it allocates the fragments onto desired sites from where the access to the respective fragments are high. There is no any concept of client and server mechanism rather the migration strategy that can be adopted here which allows migration of those fragment into several sites of the network as per requirement making each site act like a server and client as well.

The single table used here for distributed database is fragmented into two fragments based on Graphical Fragmentation Algorithm. The two fragments are Fragment1 (F1) and Fragment2 (F2). The attributes present in fragment1 are F1(A1,A3,A5,A7,A8) and in fragment2 are F2(A2, A4,A6). Also, the adopted allocation strategy ensures the allocation of fragment1 (F1) onto Site 1 and fragment2 onto Site 4.

E. Access Cost Evaluation

The attribute access of the database table is computed with the help of Attribute Access Cost Evaluator (AACE). AACE is a cost indicator equation which is utilized to identify the cost occurred to access the attributes of the table. This cost is on the basis of the number of desired and undesired attributes accessed by a query.

The Attribute Access Cost Evaluator for centralized database is given as:

$$AACE = A * (1 - \frac{A}{T}) \quad (1)$$

where,

A is the total number of attributes accessed by a query T is the total number of attributes in a table

The Attribute Access Cost Evaluator for distributed database is given as:

$$AACE = \sum_{k=1}^{K} A_k * (1 - \frac{A_k}{T_k}) \quad (2)$$

where,

K is the total number of fragments

A_k is the total number of attributes of fragment k accessed by a query

T_k is the total number of attributes of fragment k

4. The Experimental Results

The experiment is carried out on the basis of the user query mentioned in Table I as its primary input.

In centralized database cost identification, 8 sites are connected in a network where one of them is considered as server and the remaining as client. The server is allowed to hold the entire table of the database and the clients access the attributes.

In distributed database cost identification, 8 sites are also connected in a network where none of them are neither client nor server. Each of the site at a certain instant can hold the entire table or some part of the table.

AACE is utilized to identify the access cost consumed by both of the database scheme as per the user query.

Table 2: Aace Value

Query	Centralized DB	Distributed DB
1	1.88	1.2
2	1.88	1.47
3	2.0	0.8
4	1.88	0
5	1.5	1.47
6	1.88	1.2
7	1.88	0
8	1.88	1.2

Based on the AACE value, the total cost occurred to access attribute in centralized and distributed database is mentioned on Table 2.

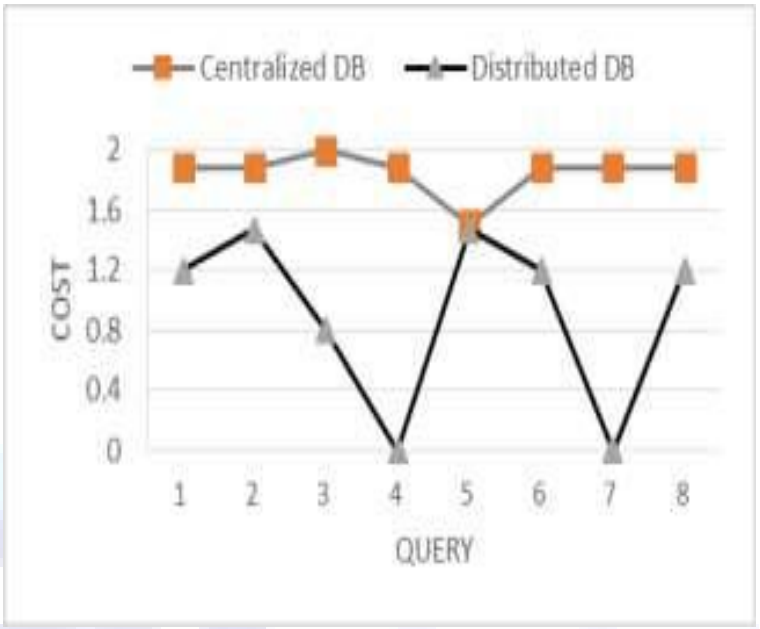

Figure 1. Attribute Access Cost Comparison

Figure 1 shows the comparison of attribute access cost of both centralized and distributed database schemes. From the figure, it can clearly be observed that in every case attribute access cost in distributed database is less than centralized database.

5. Conclusion

The outcome of experimental results shows that centralized database possess high attribute access cost as compared to that of distributed database. This shows that the use of centralized database requires much time to retrieve a data from the table than that in distributed database. In centralized database, since the entire table is on a single site so accessing the required attribute cause access of the entire attribute i.e. access of both desired and undesired attributes. Due to access of undesired attribute, here the access cost increases. But in case of distributed database, fragmentation strategy ensures proper division of attributes. As this division of attributes is on the basis of the same query used for identifying the access cost, therefore there is less chance of getting high cost. Here the desired attribute are grouped in a single fragment so that accessing the attribute by a single query have high chance of getting desired attribute and low chance of getting undesired attributes. Therefore, the cost occurred in this case is low. As [a] result, distributed database performance is far better than centralized database.

References

[1] H. Ibrahim, "Checking Integrity Constraints - How it Differs in Centralized, Distributed and Parallel Databases", Proceedings of the 17th International Conference on Database and Expert Systems Applications, 2006.

[2] M. T. Ozsu and P. Valduriez, Principles of Distributed Database Systems. New Jersey: Alan Apt, 1999.

[3] M. Sharma and G. Singh, "Analysis of Joins and Semi-joins in Centralized and Distributed Database Queries", International Conference on Computing Sciences, pp. 15–20, December 2012. [4] M. B.Moss, "Comparing Centralized and Distributed Approaches for Operational Impact Analysis in Enterprise Systems", IEEE International Conference on Granular Computing, pp. 765–769, 2007.

[5] N. M. Lacob and M. L. Moise, "Centralized vs. Distributed Databases. Case Study", Academic Journal of Economic Studies, vol. 1, no.4, pp. 119–130, December 2015.

[6] E. C. Driscoll and R. C. Fowler, "A Comparison of Centralized versus Distributed Architectures in Biometric Access Control
Systems", ICCST, 1989.

Comparative Analysis of Thyroid Disease Using Data Mining Techniques

Prapti Bhatta, Priya Pandey, Samjhana Kasaju, Smriti Shrestha

Department of Electronics and Computer Engineering, Advanced College of Engineering and Management, Kupondole, Lalitpur, Nepal

Abstract

Recently, thyroid diseases are more and more spread worldwide. Factors that affect the thyroid function are: stress, infection, trauma, toxins, low-calorie diet, certain medication etc. It is very important to prevent such diseases rather than cure them, because most treatments consist in long term medication or in chirurgical intervention. The current study refers to thyroid disease classification in two of the most common thyroid dysfunctions (hyperthyroidism and hypothyroidism) among the population. Thus, through this project we have analyzed and compared four classification models: Decision tree, Naïve Bayes, Multilayer Perceptron and Random Forest. The results indicate a significant accuracy for all classification models mentioned above. The dataset used to build and to validate the classifier is provided by UCI machine learning repository. The model built for testing and validating classifier is created using python and its libraries This paper depicts an approach for comparative analysis of thyroid disease techniques using data mining technique. Thus, through this analysis further study on thyroid disease on be done.

Keywords: *Data Mining, Classification Model, Thyroid diseases, Machine Learning, Random forest, Naïve Bayes, Artificial Neural Network, Decision Tree, Multi-layer Perceptron, Support Vector Machine (SVM)*

1. Introduction

Prevention in health care is a continuous concern for the doctors and the correct diagnostic at the right time for a patient is crucial, due to the implied risk. Recently, the usual medical report can be accompanied by an additional report given by a decision support system or other advanced diagnosis techniques based on symptoms. The authors focus their work on using classification methods and identifying the best algorithm for classification thyroid disorders. [1]

Thyroid is a butterfly-shaped gland, which is located at the bottom of the throat responsible for producing two active thyroid hormones, levothyroxine (T4) and triiodothyronine (T3) that affect some functions of the body such as: stabilizing body temperature, blood pressure, regulating the heart rate etc. Reverse T3 (RT3) is manufactured from thyroxine (T4), and its role is to block the action of T3. An abnormal function of the thyroid implies the occurrence of hyperthyroidism and hypothyroidism, two of the common thyroid affections. Hypothyroidism (underactive thyroid or low thyroid) means that the thyroid gland doesn't produce enough of certain important hormones. Without an adequate treatment, hypothyroidism can cause various health problems such as: obesity, joint pain, infertility and heart disease. Hyperthyroidism (overactive thyroid) refers to a condition in which the thyroid gland produces too much of the hormone thyroxin. In this case, the body's metabolism is accelerating significantly, causing sudden weight loss, a rapid or irregular heartbeat, sweating,

and nervousness or irritability (eMedonline, 2016). [3]

2. Literature Review

Data mining refers to extracting unknown patterns from an enormous volume of data involving different methods and algorithms which exist at the intersection of fields such as artificial intelligence, machine learning, statistics and database systems (Piatetsky-Shapiro & Parker, 2011). In literature are mentioned certain applications of data mining techniques in the health domain, some of them being presented in the following paragraphs.

Most examples refer to diagnosing diseases of thyroid using decision trees, artificial neural networks, support vector machine, expert systems etc. For example, the diagnosis of thyroid disorders using ANN's is discussed in Gharehchopogh, Molany & Mokri (2013), Anupama Shukla & Prabhdeep Kaur (2015).

The authors of the research work presented in Margret, Lakshmipathi & Kumar (2012) proposed the diagnosis of thyroid disease using decision tree splitting rules.

The classification of the thyroid nodules was performed with support vector machines in Chuan-Yu Chang, Ming-Fang Tsai & Shao-JerChen (2008), while a comparison study by data mining classification algorithms (C 4.5, C5.0) for thyroid cancer set is presented in Upadhayay, Shukla & Kumar (2013).

A diagnosis expert system based on fuzzy rules is described in Keleş & Keleş, (2008), while a three-stage expert system based on support vector machines is presented in Hui-Ling Chen et al. (2012).

All the mentioned studies have the same goal, namely the diagnosis of thyroid disorders and predicting the occurrence of a certain disease on population. We experimented on a database provided by UCI Machine Learning Repository, containing data about clinical history of patients with thyroid disorders. And we used that data for classification, using five data mining algorithms: Naive Bayes, Decision Trees, Multilayer Perceptron, Random Forest and SVM to build a robust classifier.

The goal of this study is to find the best classification model in order to make future classification of new patient data more accurately. In this paper more experiments are discussed and an interpretation of results (evaluation measurements) is given.

3. Feasibility study

We have been giving our dedication to make the proposed application feasible. The matter off feasibility is discussed in following main sectors.

a. Social Feasibility

This application will work as thyroid prediction system that seeks to predict the disease that a person might suffer from.

b. Economic feasibility

The costs and benefits associated with the proposed system are economically feasible as its benefits outweigh costs. All the development tools are also available free of cost.

c. Operational Feasibility

This project is feasible operationally. It requires running a single server for storage and analysis of collected data. This is not such a challenging requirement.

d. Technical feasibility

This project requires large amount of database space and processing power to store and process each of them in small time.

4. System Architecture and Design

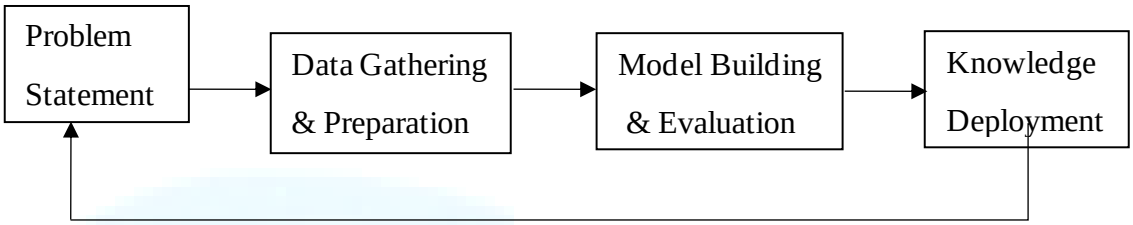

4.1. Block Diagram

a. Problem Statement

Recently, thyroid diseases are more and more spread worldwide. It is very important to prevent such diseases rather than cure them, because most treatments consist in long term medication or in chirurgical intervention.

b. Data Gathering

We used a data set (UCI) containing 756 records about persons with thyroid dysfunctions. The classification model has 22 attributes; the class attribute is the target and it has three possible values: hypothyroidism, hyperthyroidism and normal. The current data set was extracted and preprocessed from the original file.

c. Model Building & Evaluation

After the normalization of data set, the full data set was split into two partitions: the training set for model construction (70%) and the test set for model evaluation (30%). The training set are fed into the model by which the model leams the dataset.

d. Knowledge Deployment

The dataset after split into test and training set is fitted into models of classifier. The target is set as classes i.e., normal (1), hyperthyroidism (2) and hypothyroidism (3). After fitting into the models, we then measured the accuracy of each classifier and build confusion matric which include precision, recall, F1-score, and support by using test set. Steps for Developing System

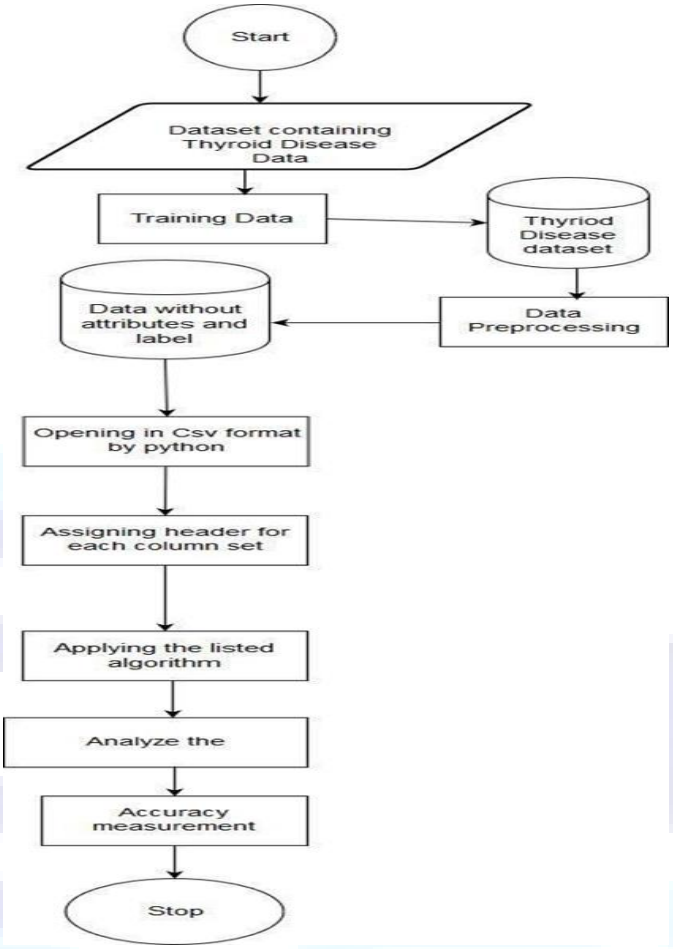

Figure 4: Flowchart for Building Model

5. Proposed Model

a. Data Collection

For our system, we have collected thyroid disease related data from UCI this process includes collecting data for hyperthyroidism and hypothyroidism for both male and female gender. The study has been carried to become familiar with data type and comparing is done between different dataset.

b. Data Preprocessing

Data preprocessing is the main process in the Data Mining. The phrase is "Garbage in, Garbage Out", Data Preprocessing includes cleaning, normalization, transformation, feature extraction and selection etc.

Real-world data tend to be incomplete, noisy and inconsistent. This can lead to a poor quality of collected data, and, further to a low quality of models built on such data.

c. Classification

So, we will be using twenty-two attribute and the class attribute is the final target and it has three possible values: hypothyroidism, hyperthyroidism and normal.

```
@attribute Age numeric
@attribute Sex {0, 1}
@attribute On_thyroxine {0, 1}
@attribute Query_on_thyroxine {0, 1}
@attribute On_antithyroid_medication {0, 1}
@attribute Sick {0, 1}
@attribute Pregnant {0, 1}
@attribute Thyroid_surgery {0, 1}
@attribute I131_treatment {0, 1}
@attribute Query_hypothyroid {0, 1}
@attribute Query_hyperthyroid {0, 1}
@attribute Lithium integer {0, 1}
@attribute Goitre {0, 1}
@attribute Tumor {0, 1}
@attribute Hypopituitary {0, 1}
@attribute Psych {0, 1}
@attribute TSH numeric
@attribute T3 numeric
@attribute TT4 numeric
@attribute T4U numeric
@attribute FTI numeric
@attribute Class {1,2,3}
```

Figure 5: Attributes of the classification models used in the experiments

6 attributes have numeric values (Age, TSH, T3, TT4, T4U, FTI), 15 attributes are categorical with two possible values (0/1). The *class* attribute is categorical too, but it can take three possible values (1-normal, 2-hyperthyroidism, 3- hypothyroidism).

6. Implementation Details

For model training, we would be using the different classifiers discussed below:

- ***Visualizing Features:***

Before building a model, we must first know the important feature that will have high impact in the preprocessing of result. So, below figure shows the visualization of important feature in the dataset with their respective score.

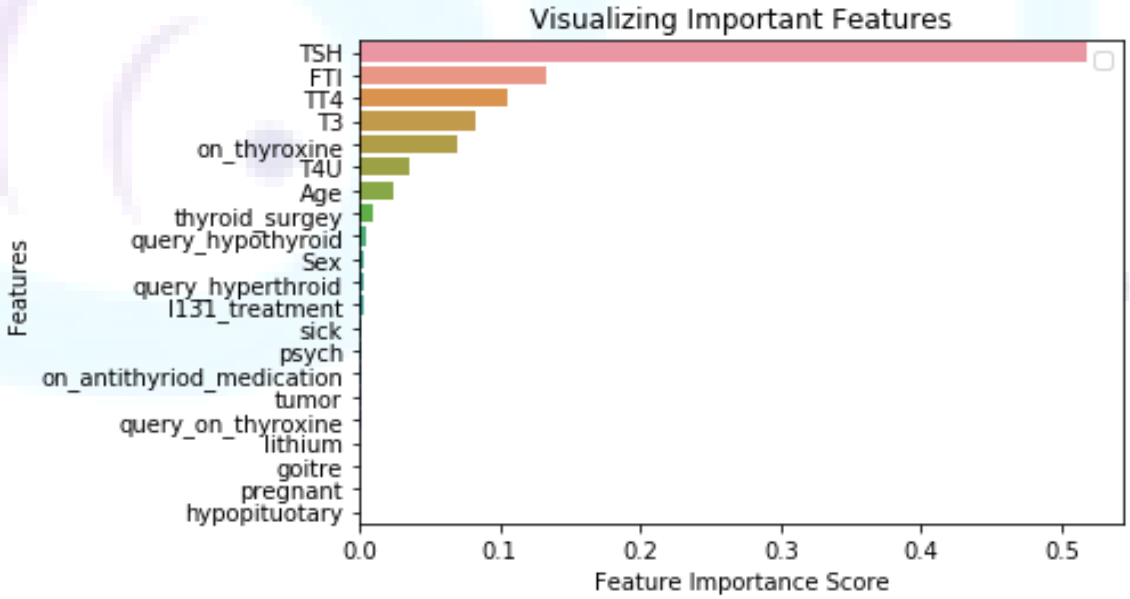

Figure 6: Visualization of Important Features

Table 1: Attributes with importance score

Attribute	Importance Score
TSH	0.517804
FTI	0.133056
TT4	0.105519
T3	0.082164
on_thyroxine	0.069706
T4U	0.035007
Age	0.024194
thyroid_surgey	0.009853
query_hypothyroid	0.005294
Sex	0.003242
query_hyperthroid	0.003088
I131_treatment	0.003013
sick	0.002009
psych	0.001618
on_antithyriod_medication	0.001372
tumor	0.001037
query_on_thyroxine	0.001000
lithium	0.000642
goitre	0.000203
pregnant	0.000181
hypopituotary	0.000000

- ***Building Model:***

The preprocessed data is fetched using panda's library. The data are fitted into the respected models i.e. Decision Tree, Naïve Bayes, Multilayer Perceptron, Random Forest Classifier, and Support Vector Machine.

- ***Training:***

The preprocessed data are separated for training and testing. For almost all model we have used, 70% of data as training set and 30% as test set.

Supervised learning is used to train the neural network. The training data include both the inputs and the desired outputs. The training procedure starts with a set of initial values for all biases and weights. The entire set of selected inputs are passed to the input layer. At the next epoch, the training is repeated with the new set of weights. The procedure is repeated until the error reaches an acceptable lower bound.

Many models have important parameters which cannot be directly estimated from the data. There are different approaches to searching for the best parameters. A general approach that can be applied to almost any model is to define a set of candidate values, generate reliable estimates of model utility across the candidate values, then choose the optimal settings.

- ***Decision Tree Algorithm***

CART is an alternative decision tree building algorithm. It can handle both classification and regression tasks. This algorithm uses a new metric named GINI index.

As we can see that tree node starts with TSH feature which is the root node, it start with TSH attribute because it have the highest importance score in the dataset and similarly having number of patient belonging to the class 3 i.e. hypothyroidism is high.

That is the reason why our model selected TSH feature and after that it split the node to form decision tree.

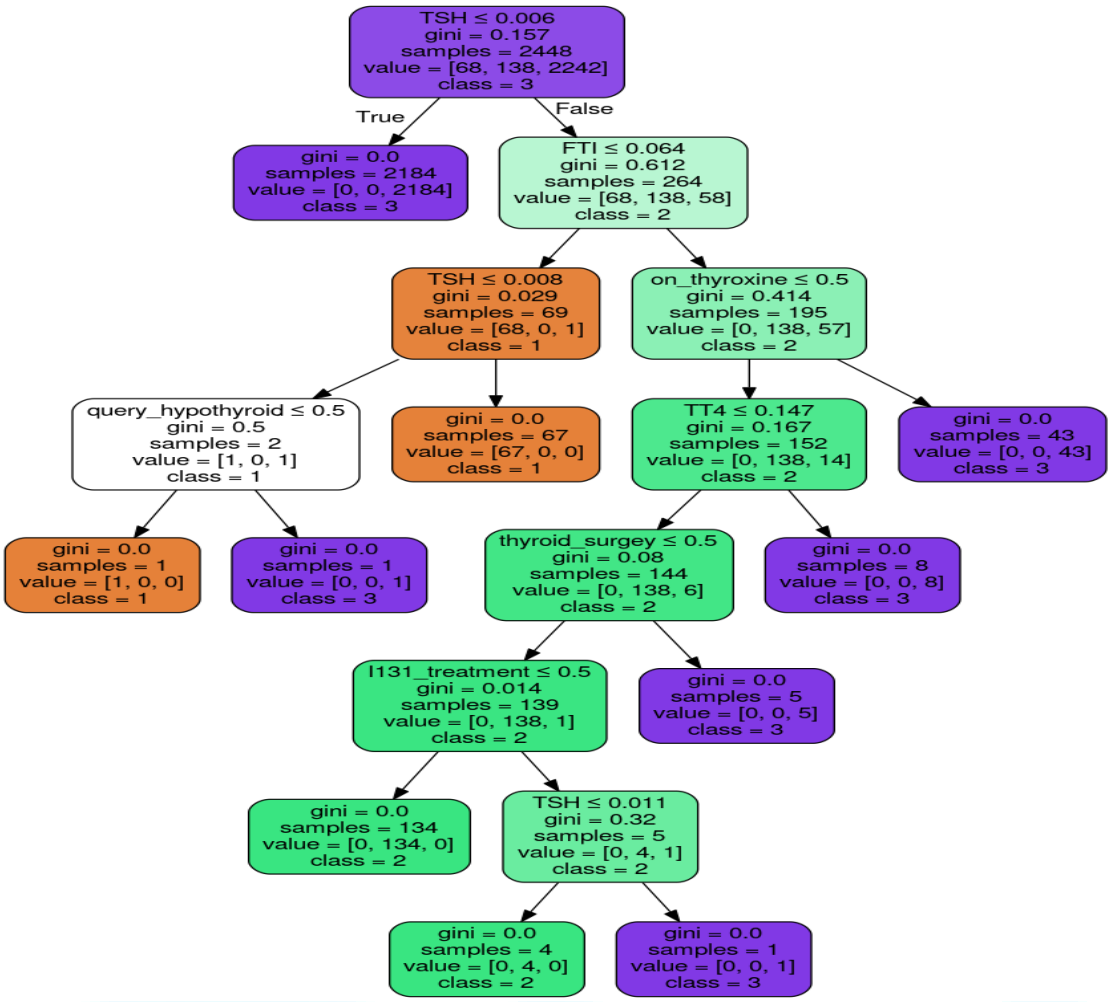

Figure 8: Decision tree generated by the model

- **Random forest Classifier**

The most important parameter of the Random Forest class is the n_estimators parameter. This parameter defines the number of trees in the random forest. We will start with n_estimators = 20. [8]

- **Multilayer Perceptron Development:**

The process involved in this neural network system are as follows:

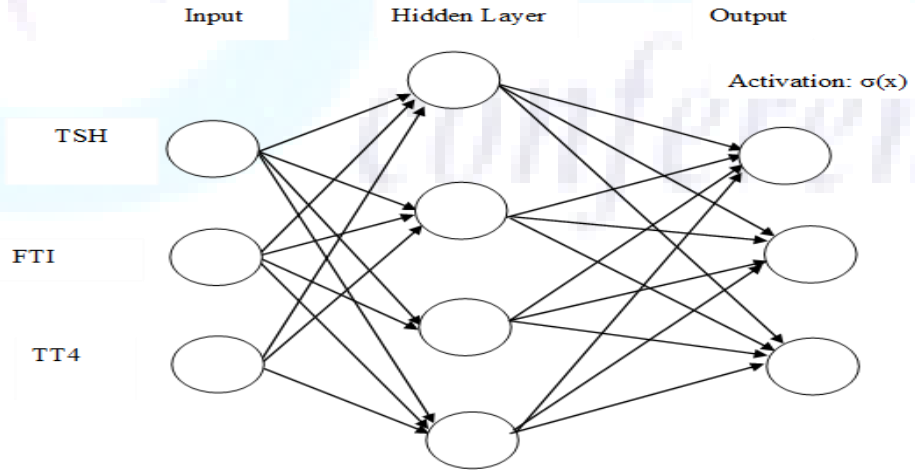

Figure 9: MLP of our System

There is an input layer with 21 input features. And two hidden layers, the 1st hidden having 16 nodes and

while the 2nd hidden layer having 32 nodes and an output layer with 4 nodes.

```
1 model.summary()
```

```
_________________________________________________________________
Layer (type)                 Output Shape              Param #
=================================================================
dense_1 (Dense)              (None, 16)                352
_________________________________________________________________
dense_2 (Dense)              (None, 32)                544
_________________________________________________________________
dense_3 (Dense)              (None, 4)                 132
=================================================================
Total params: 1,028
Trainable params: 1,028
```

Figure 10: Model Summary of MLP

Learnable parameters/parameter/params/trainable parameters
-is a parameter that is learned by the network during training
Learnable parameter calculation
inputs * outputs + biases
21 * 16 = 336 + 16 (biases) = 352

- ***Naïve Bayes:***

For the development of model using naïve bayes we can use 3 types of naïve Bayes.

In our model we have used multinomial Naïve bayes because it can be used for data set having multiple class and random sample.

- ***SVM***

SVM offers high accuracy. It is known for its kernel trick to handle nonlinear input spaces. We have used linear kernel to build SVM model.

- ***Validation:***

For the validation of the model, we compared the actual value and predicted value by preparing training and test set so in response we get (1-normal, 2-hyperthyroidism, 3- hypothyroidism), then we compute the accuracy of all the models, constructed confusion matrix which includes precision, recall, support and f1-score for the validation of the model.

7. Result and Analysis

Table 2: Evaluation measurements for classification models

		Accuracy Statistics	Classification Models				
			Naïve Bayes	***Decision Tree***	***MLP***	***Random Forest***	***SVM***
Classes	***Hypothyroidsm (3)***	Recall	1	1.00	1.00	1.00	1.00
		Precision	0.93	1.00	0.92	1.00	0.93
		Support	2007	4342	1324	1325	2258
		F1 - Score	0.96	1.00	0.96	1.00	0.96
	Hyperthyroidsm	Recall	0	0.99	0	1.00	0
		Precision	0	0.98	0	0.96	0
		Support	105	238	84	88	132
		F1 - Score	0	0.98	0	0.98	0
	Normal (1)	Recall	0	0.93	0	0.93	0.21
		Precision	0	0.89	0	0.96	1.00
		Support	48	100	32	27	58
		F1 - Score	0	0.91	0	0.93	0.34

Table 3: Accuracy for classification models

		Classification Models			
	Naïve Bayes	***Decision Tree***	***MLP***	***Random Forest***	***SVM***
Accuracy	92.91%	98.92%	91.94%	99.5%	92.12%

The accuracy of the classification models is over 90%, the best model being Decision Tree with 98.92% accuracy. If the number of epochs for MLP model increases to 500 (initial was set to 20) the accuracy of the classification model increases to %. Similarly, the accuracy of Naïve Bayes, Random Forest and SVM is 92.91%, 99.5%, 92.12% respectively.

The classification model based on **random forest classifier** obtained the best accuracy (99.5%), while MLP obtained the weakest classification. As we observed, random forest classifier model was the model with the highest accuracy for the classification of thyroid diseases, followed by Decision Tree, Naïve Bayes and SVM models.

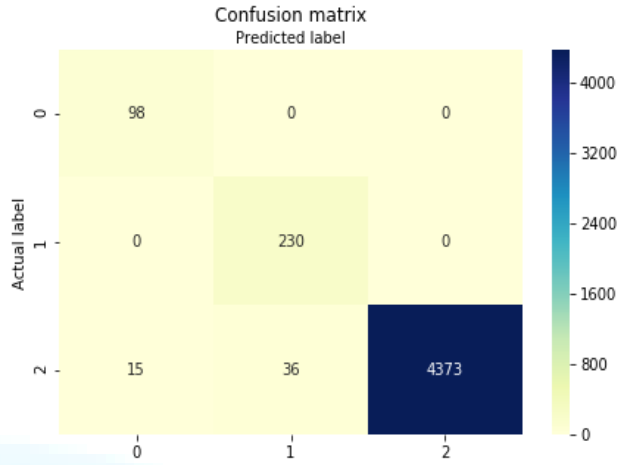

Figure 11: Confusion matrix of Decision tree

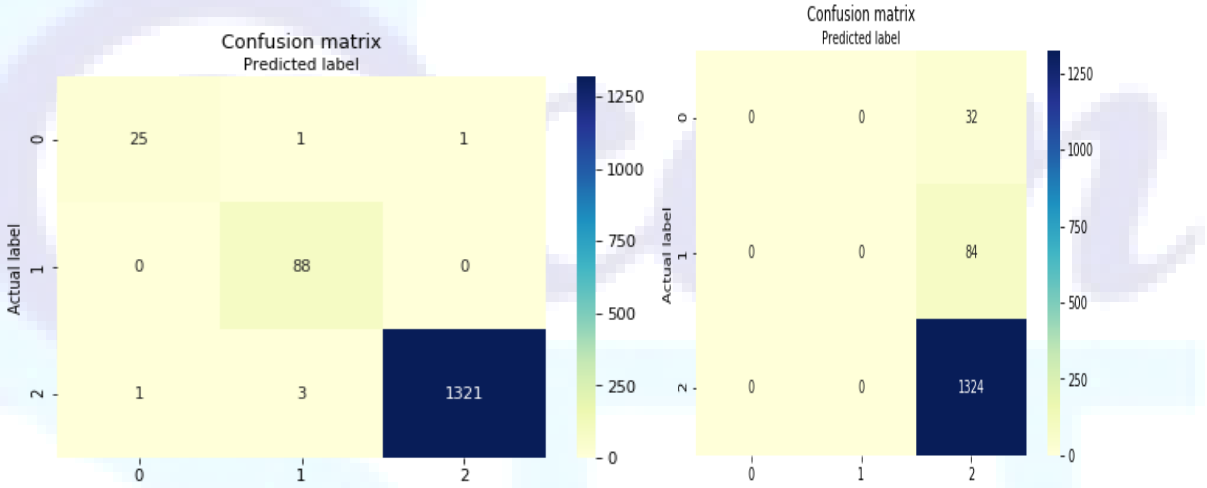

Figure12: Confusion matrix of Random Forest and Multilayer Perceptron

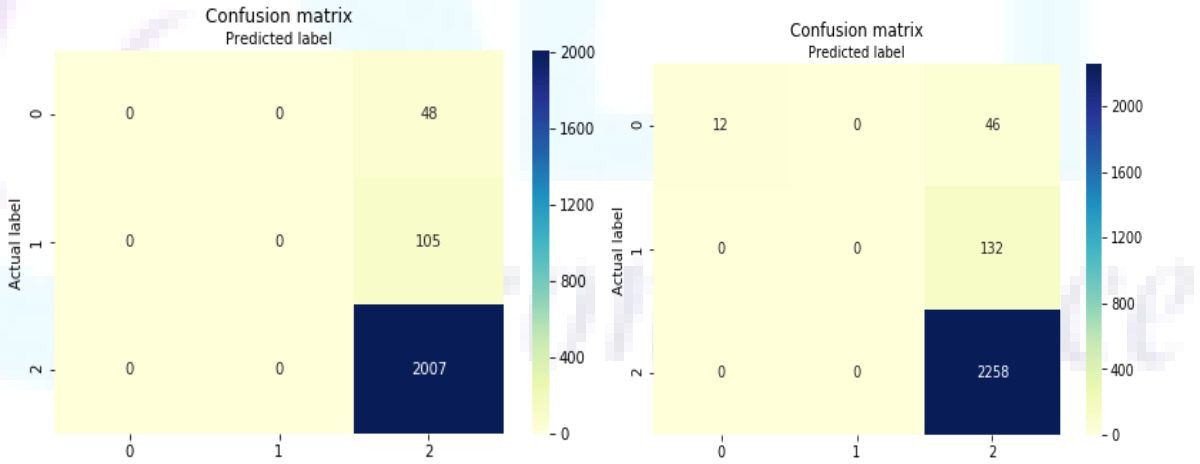

Figure13: Confusion matrix of Naïve Bayes and Support Vector Machine

8. Conclusion

In this analysis-based project we discussed about applying five classification models (Naïve Bayes, Decision Tree, MLP, Radom forest and SVM) on thyroid data set to identify more accurately the dysfunction of thyroid namely hyperthyroidism and hypothyroidism. The best classification model was the Random Forest model in all the experiments.

This project can be used as a prototype by hospital in the Nepali Scenario too, it can work as an efficient model to study thyroid disease analysis based on their acquired dataset.

9. Future Work

In future, we will focus on obtaining answers to questions like: What segment of age concentrates the thyroid cancer? How can we prevent thyroid diseases on the youth? by applying data mining more algorithms.

References

[1] F. Cold et al., "Slideshow: Thyroid Symptoms and Solutions", *WebMD*, 2019. [Online]. Available: https://www.webmd.com/women/ss/slideshow-thyroid-symptom sand-solution [Accessed: 16- Jan- 2019].

[2] "Decision tree", *En.wikipedia.org*, 2019. [Online]. Available: https://en.wikipedia.org/ wiki /Decision tree. [Accessed: 18- Jan- 2019].

[3] "A decision support system for prediction of thyroid disease", 2019. [Online]. Available: https://www.researchgate.net/publication/284887708_A_decision_support _system_for_prediction_of_thyroid_disease_A_comparison_of_multilayer_perceptron_neural_network _and_radial_basis_function_neural_network?fbclid=IwAR3deqyOntoV2fUDjXT-BFA pERLrrnrD_GyDdXpgy4SOkQStCaIF3mVDk8I. [Accessed:01-Mar-2019].

[4] "How Random Forest Algorithm Works in Machine Learning", *Medium*, 2019. [Online]. Available: https://medium.com/@Synced/how-random-forest-algorithm-worksin-machine-learning-3c0fe15b6674. [Accessed: 01- Mar- 2019].

[5] "Getting Started with TensorFlow", *O'Reilly | Safari*, 2019. [Online]. Available:

[6] https: //www.oreilly.com/library/view/getting-started-ith/9781786468574/ch04s04 .html.[Accessed: 18- Jan- 2019].

[7] "Decision Tree Classification in Python", *DataCamp Community*, 2019. [Online]. Available: https://www.datacamp.com/community/tutorials/decision-tree-clasification -python. [Accessed: 20- Jul- 2019]

[8] "Naive Bayes Classification using Scikit-learn", *DataCamp Community*, 2019. [Online]. Available: https://www.datacamp.com/community/tutorials/naive-bayes-scikit-learn. [Accessed: 20- Jul- 2019]

[9] "Random Forests Classifiers in Python", *DataCamp Community*, 2019. [Online]. Available: https://www.datacamp.com/community/tutorials/random-forests-classifier-python. [Accessed: 20- Jul- 2019]

[10] "Support Vector Machines in Scikit-learn", *DataCamp Community*, 2019. [Online]. Available: https://www.datacamp.com/community/tutorials/svm-classification-scikit-learn-python. [Accessed: 20- Jul- 2019]

Performance Analysis of Genome Sequence Alignment with Cloud-Enabled Hadoop MapReduce

Ashish Thapa[1], Dipinti Manandhar[2], Jnaneshwor Bohara[3]

[1,2]*Advanced College of Engineering and Management, Tribhuvan University, Nepal* [3]
Pulchowk Engineering College, Tribhuvan University, Nepal

[1]mailto:thapaashis110@gmail.com, [2]mailto:dipintimanandhar@gmail.com,
[3]mailto:dipintimanandhar@gmail.com

Abstract

Genome Sequence Alignment is a term defined under bioinformatics which deals with arranging the sequences of genome including DNA, RNA and protein to establish their similarities in terms of functional, structural and evolutionary relationships. Sequence Alignment of the huge volume of sequence data by standalone machine have not proved to be computationally efficient. Nowadays Distributed computing, with the increase in performance and acceptance, have influenced the sequence alignment processes to a great extent. In this paper, we thus present the performance analysis of implementation of such distributed computing through Cloud- enabled Hadoop MapReduce. CloudBurst algorithm is used to introduce the Cloud Computing concept which utilizes a number of nodes for processing and is more efficient than single node implementation.

Keywords*: Sequence Alignment, CloudBurst, Hadoop, MapReduce, Genome, DNA, RNA.*

1. Introduction

With the rapid evolution of big data technologies in the latest time, its scope and application has extended in a high rate. The big data technologies have served as a medium to store and process extremely large data sets that may be analyzed computationally to reveal patterns, trends, and associations between those huge data.

Similarly, the extension of big data to the domain of bioinformatics and cloud computing for genome analysis, sequencing, and alignment has really been proved as a boon such that those tasks which required a lot of computational time and space in the early days are now performed within very limited time and space with extended scalability. We can take reference from the 1,000 Genome project which explains that the cost of sequencing the human genome has decreased rapidly from $1 million in 2007 to $1 thousand in 2012 [13]. During the runtime of the project, the data deposited in its first 6 months was two times the sequence data that was collected in the last 30 years of time. In bioinformatics, even a single base pair difference can have a significant biological impact, so researchers require highly sensitive mapping algorithms to analyze the reads. As such, researchers are generating sequence data at an incredible rate and need highly scalable algorithms to analyze their data. This huge computational power and scalability of big data in bioinformatics using cloud computing platform served as the basic motivation for the initiation of this

project.

A sequence alignment is a way of arranging the sequences of DNA, RNA, or protein to identify regions of similarity between the sequences.[1] Multiple sequence alignment is an extension of pairwise alignment to incorporate more than two sequences at a time trying to align all of the sequences in a given query set.

Computational approaches to sequence alignment generally fall into two categories: global alignments and local alignments. Global alignment is a form of global optimization that spans the alignment to entire length of all query sequences. On the other hand, local alignments identify regions of similarity within long sequences that are often widely divergent overall.

Storage of sequence alignments can be done in a wide variety of text-based file formats out of which most were originally developed in conjunction with a specific alignment program or implementation. Most popular web-based tools such as FASTA format and GenBank format allow a limited number of input and output formats, where the output is not easily editable.

Scoring function:

Scoring function reflects how strong or weak is the alignment between any two sequences in terms of biological or statistical observations. It is much helpful and important to producing good alignments, compare the close alignments and optimize the alignment results. Protein sequences are frequently aligned using substitution matrices that reflect the probabilities of given character-to-character substitutions. PAM matrices encode evolutionary approximations regarding the rates and probabilities of particular amino acid mutations. Another common series of scoring matrix, known as BLOSUM (Blocks Substitution Matrix), encodes empirically derived substitution probabilities.

2. Literature Review

The history of development of read-alignment algorithms is not to far as compared to the level it has reached today. The first read-alignment was SSAHA brought at the near end of 2001. It was followed by BLAST in the early months of 2002 which was much more popular. However, the exploration of such algorithm initiated an era for Sequence alignment. The BLAST was much efficient for short reads mapping and for serial execution of those map tasks. But with the addition of a huge volume of data in the domain of genome sequencing from projects like Human Genome Project (HGP), scalable algorithms for mapping were felt necessary with less computational time and higher sensitivity. This need gave birth to various Next Generation Sequencing (NGS) algorithms which are most popular and have a wide application and is a much-viewed topic for further research. Among various NGS sequencing algorithms, CloudBurst is the sensitive read mapping algorithm based on Hadoop MapReduce on cloud platform.

Many of the currently used read-mapping programs, including BLAST, SOAP, MAQ, RMAP and ZOOM, use an algorithmic technique called *seed-and-extend* to accelerate the mapping process. Seeds are the sub-strings that exactly match in both the reads and the reference sequences. These seeds are then extended into longer, inexact alignments using a more sensitive algorithm that allows for a fixed number of mismatches or gaps. There are a variety of methods for finding and extending the seeds, each having different features and performance. However, each of these programs is designed for execution on a single computing node, and as such requires a long running time or limits the sensitivity of the alignments they find. To overcome such long running time various parallel read algorithms were developed which are extensively used these days.[13].

Till date more than 90 algorithms have been developed for the purpose of sequencing and the evolutionary history of such algorithm can be viewed in a chart as shown below:

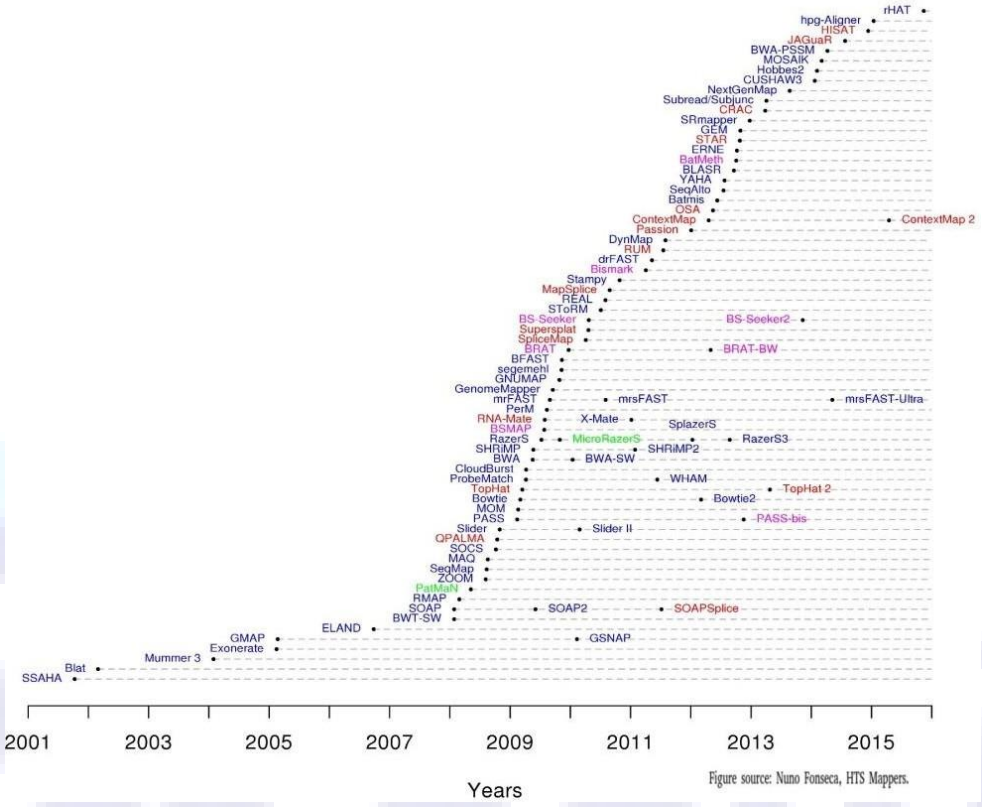

Figure 1: Timeline of NGS read aligners

3. Methodology

The sequence alignment process involves a large number of reads sequence compared with a number of reference sequence as input. As mentioned above there are various formats in which input sequences can be provided. FASTA format is the one that we use in this context which contains reads and multiple fasta files containing one or more reference sequences. These files are then converted to binary format and copied to HDFS storage. The files from HDFS are fed to MapReduce which aligns various sequences of reads to reference sequence. A general outline of workflow of Sequence Alignment is shown below:

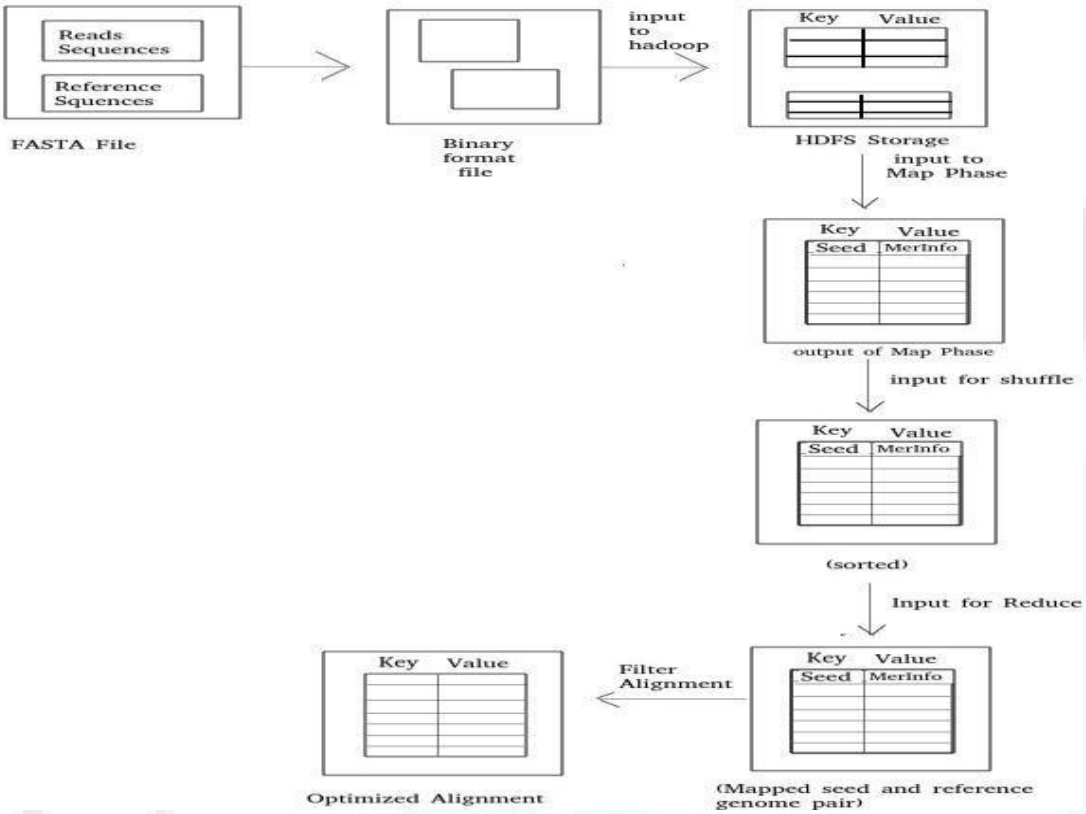

Figure 2: Workflow of Sequence Alignment

MapReduce

MapReduce is a parallel processing framework that works across huge datasets using a large number of computers (nodes), collectively referred to as a cluster or a grid. Cluster is a collection of nodes on the same local network and using similar hardware whereas grids are the collection of nodes shared across geographically and administratively distributed systems making use of more heterogeneous hardware. Processing can occur on data stored either in an unstructured filesystem or in a structured database. Data locality, processing of data near the place it is stored in is the concept used by MapReduce in order to minimize communication overhead.

A MapReduce framework is usually composed of three operations:

1. Map: During map phase, each worker node applies the map function to the local data, and writes the output to a temporary storage. A master node ensures that only one copy of the redundant input data is processed.
2. Shuffle: At this stage, worker nodes redistribute data based on the output keys produced by the map function, such that all data belonging to one key is located on the same worker node.
3. Reduce: Worker nodes now process each group of output data, per key, in parallel.

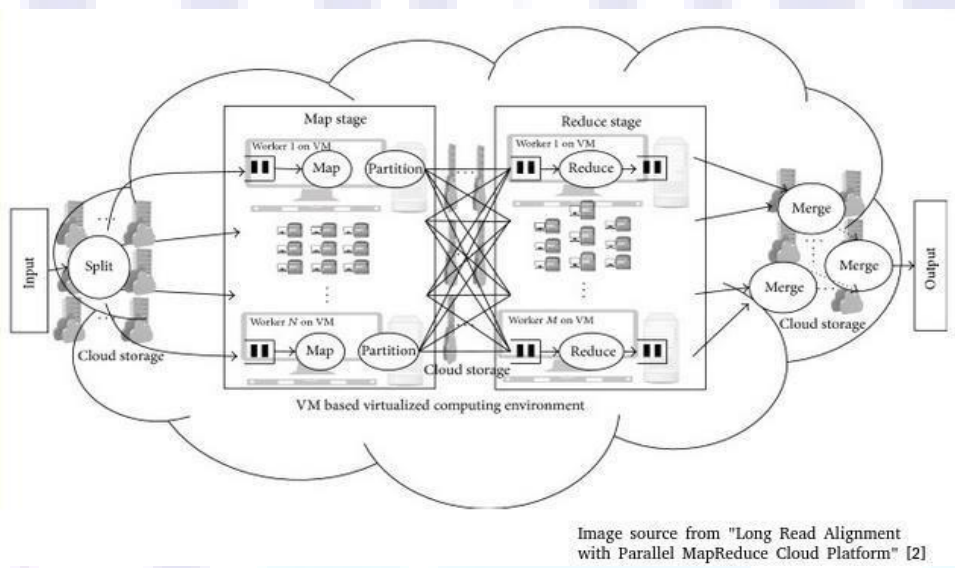

Figure 3: MapReduce model deployed using VM based computing environment

Hadoop

Hadoop MapReduce is an open source software framework based on MapReduce programmingmodel for implementing parallel computation in distributed environment.

The base Hadoop framework is composed of the following modules:

4. Hadoop Common – It contains libraries and utilities needed by other Hadoop modules.
5. Hadoop Distributed File System (HDFS) – It is a distributed file-system that stores data on commodity machines, providing very high aggregate bandwidth across the cluster.
6. Hadoop YARN – It is a platform responsible for managing computing resources in clusters and using them for scheduling users' applications.
7. Hadoop MapReduce – An actual implementation of the MapReduce programming model for large-scale data processing.

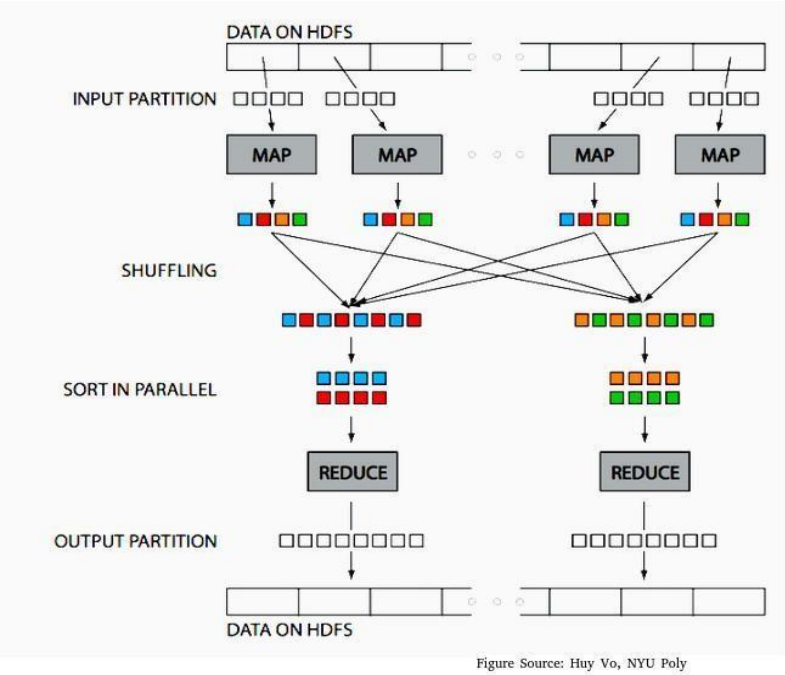

Figure 4: Hadoop in one picture

Cloudburst

Cloudburst is a parallel read-mappingalgorithm optimized for mapping next- generation sequence data to other reference sequences usually genome. It is modeled after the short-read mapping program RMAP, andreports either all alignments or the unambiguous best alignment resulted fromalignment filtering for each read with any number of allowed mismatches or differences. This level of sensitivity could be prohibitively time consuming, but CloudBurst uses the open- source Hadoop implementation of MapReduce to parallelize execution using multiple compute nodes. This implementation thus makes it effective for use in a variety of biological analyses including SNP discovery, genotyping, and personal genomics.

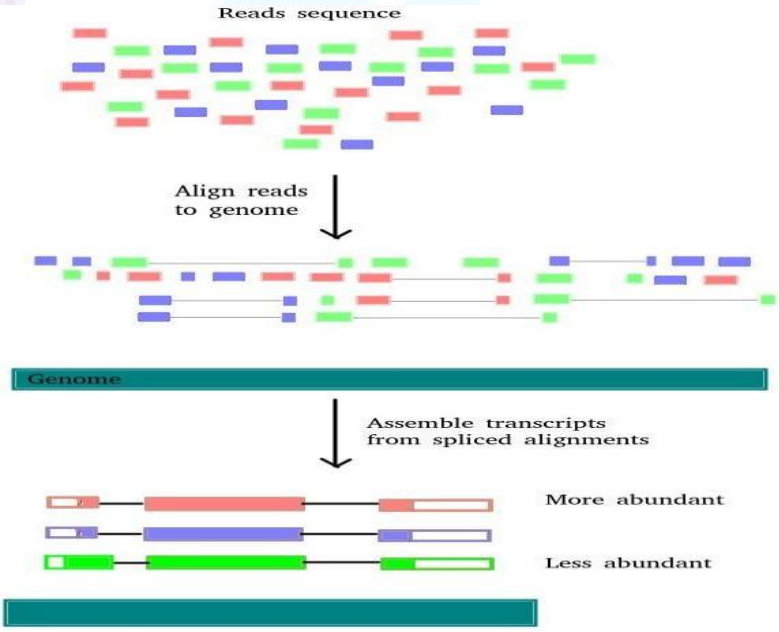

Figure 5: Sequence Alignment

Alignment Filtering

Alignment Filtering is introduced to produce only best and unambiguous alignment for each read sequence with a given reference sequences. By default, the number of best results provided by alignment filtering is 2. This would allow no any exact if there are a number of equally best results. The default setting can be modified to result alignments with any allowed number of mismatches or gaps. This would highly increase the readability of the output by removing a large number ofunwanted results. Alignment filtering is introduced with another MapReduce task where the output op MapReduce only list a certain sequence satisfying the provided number of mismatches. Although the computational time of filtering MapReduce is less and uses simple algorithm for implementation, it increases user's understandability and thus is added to sequence alignment.

4. Result

The execution of CloudBurst algorithm was performed at various stages with varying parameters. In short, the various iteration of our test consisted of parameters as follows:

1. Length of read sequences was taken as 40 bp.
2. Three different reference sequences corresponding to genome and chromosomes were taken where reference sequence was of 3.2billions bp (Gbp), and second and third reference sequences of length 348 millionbp (Mbp) and 30 millionbp (Mbp).
3. Different number of reads ranging from 1 million to 16million were taken during a single execution of a job. The data were recorded at R=1,2,4,8 and 16 million for each reference string.
4. Varying number of mismatches were allowed from k=0 to k=4.

In our experiment as the length of read sequence taken was fixed to 40 base pair(bp), it is assumed that the execution time is independent to read sequence size in this context. The seed size is varied from s=40 when k=0 to s=20,13.33,10,8 when k=1,2,3,4 respectively.

With this set of tests parameters, the graphs for the runtime (in seconds) vs the number of reads (in millions) for different reference sequences: Sequence 1, Sequence 2 and Sequence 3 was performed. mismatch 0 to mismatch 4 respectively.The graphs obtained are shown for various case in fig:6 to fig:10 for mismatch ranging from 0 to 4:

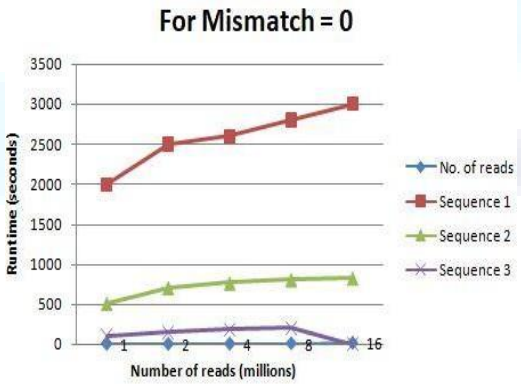

Figure 6: Runtime VS Number of reads for mismatch=0

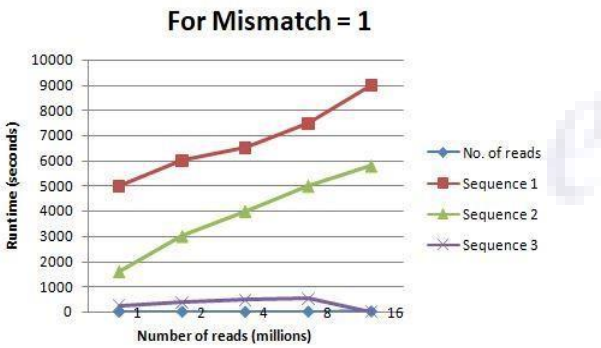

Figure 7: Runtime VS Number of reads for mismatch=1

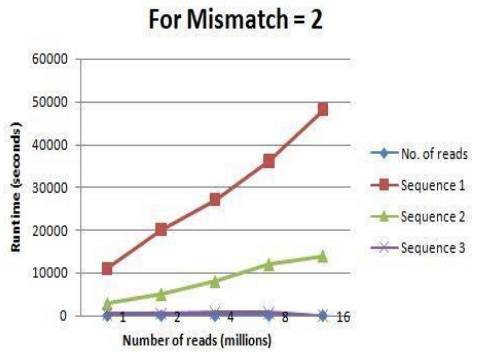

Figure 8: Runtime VS Number of reads for Mismatch=2

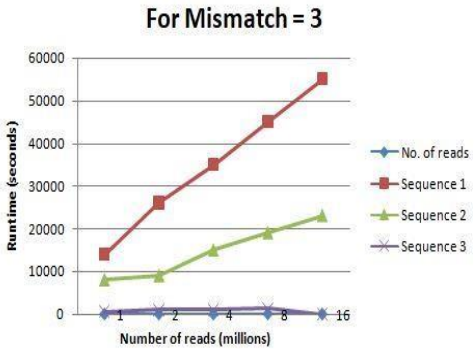

Figure 9: Runtime VS Number of reads for Mismatch=3

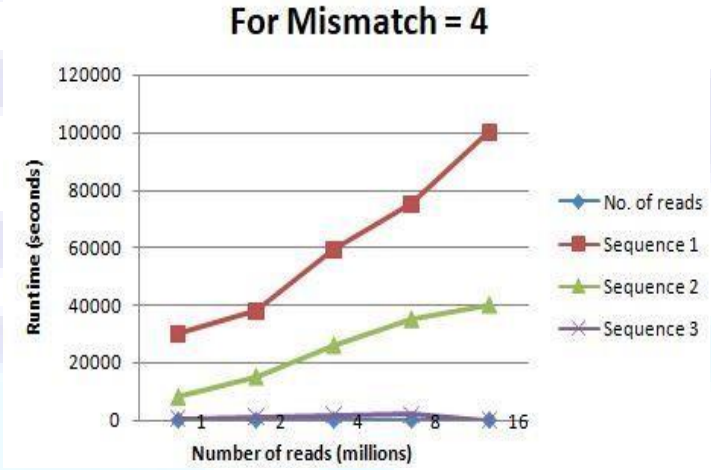

Figure 10: Runtime VS Number of reads for Mismatch=4

5. Discussion

The execution of the alignment jobs which would take a large number of days for short read mapping through RMAP can now be decreased to few numbers of hours with the use of CloudBurst.

The execution of CloudBurst algorithm was analyzed and found to be in accordance with the following set of statements:

1. The execution time of the job using cloudburst algorithm was found to be dependent on parameters like length of read sequence (m), length of reference sequence(L), number of read sequences(R), seed length(s) which is further dependent on number of mismatches allowed(k).
   Execution Time = f(m,L,R,s,k)
2. The relation between seed length(s) and read sequence length(m) is given by
   s=m/(k+1)
3. The probability of occurrence of a seed of length s in a subsequence of length L is P(O)=(L-s+1)/4^s. Thus, giving expected number of occurrence E(O) as:
   E(O)=P(O)*L

The use of CloudBurst algorithm is much faster and scalable with the increase of number of input reads allowing very high sensitivity.

5. Conclusion

The successful execution of CloudBurst Algorithm on different sets of reads and reference sequence led to following sets of performance-based conclusion:

4. Execution time decreases with the increase of length of reads sequence(m).
5. Execution time increases or scales linearly with the increase of number of reads sequence(R).
6. Execution time increases gradually with the increase of number of allowed mismatchesinitially and it increases rapidly (nearly exponentially) on later increases of allowed number of mismatches.
7. Execution time decreases with the increase of length of reads sequence. The decrease rate is high on further increase.

6. Future Works

The use of CloudBurst algorithm is highly recommended for read mapping and alignment with high scalability and much preference to sensitive data. This can further be used to various phylogenetic analysis and evolution patterns. The study of sensitive data can be extended in diagnostic phase to make a comparison between any sequences of an unhealthy person with that of healthy person. The result can be helpful for successful treatment of the defective gene with less complexity and in quick time. The mutation relationship and its pattern, which is like a mystery for biologist at present can get some help when using these analyses.

Acknowledgements

We would like to express our deepest gratitude to "SET conference 2019" and its team for providing us such a wonderful opportunity to publish our research paper in their well-recognized platform. We are thankful to Er. Anku Jaiswal and Er Narayan K.C. for leading us to the platform where we areable to finalize this project as a team. We are highly obliged to all the teachers of Advanced College of Engineering and Management who continuously provided much precise advice during the course of selection of the topic and guided us during the much-needed time. The initiation of this project would not have been successful and reached to this level in the absence of their continuous support. Their work, determination and valuable guidelines are really praiseworthy. Finally, any modifications, valuable suggestions and recommendation for further improvement will be highly appreciated and warmly welcomed.

References

[1] Arumugam, Krithika&Shyang, Yu & Lee, Bu &Kanagasabai, Rajaraman. (2012). "Cloud - enabling Sequence Alignment with Hadoop MapReduce: A Performance Analysis".

[2] Al-Absi, Ahmed Abdulhakim, and Dae-Ki Kang. "Long Read Alignment with Parallel MapReduce Cloud Platform". BioMed research international vol. 2015 (2015): 807407. doi:10.1155/2015/807407.

[3] Lee, Hyungro. "Using Bioinformatics Applications on the Cloud." (2014)

[4] AislingO'Driscoll, JurateDaugelaite, Roy D.Sleator. "Big data',Hadoop and cloudcomputing in genomics".(2013).

[5] Quan Zou, Xu-Bin Li, Wen-Rui Jiang, Zi-Yu Lin, Gui-Lin Li, Ke Chen. "Survey of MapReduce frame operation in bioinformatics." (2014).

[6] Ronald C Taylor. Article number: S1 "An overview of the Hadoop/MapReduce/HBase framework and its current applications in bioinformatics". (2010)

[7] Xin Feng, Robert Grossman&Lincoln Stein."PeakRanger: A cloud-enabled peak caller for ChIP-seq data". Article number: 139. (2011).

[8] David R Kelley,Michael C Schatz&Steven L Salzberg."Quake: quality-aware detection and correction of sequencing errors".*GenomeBiology*volume 11, Article number: R116 (2010).

[9] Ben Langmead, Kasper D Hansen&Jeffrey T Leek ."Cloud-scale RNA-sequencing differential expression analysis with Myrna".*GenomeBiology*volume 11, Article number: R83. (2010).

[10] Dennis P Wall, ParulKudtarkar, Vincent A Fusaro, RimmaPivovarov, Prasad Patil&Peter J Tonellato."Cloud computing for comparative genomics".BMCBioinformaticsvolume 11, Article number: 259 (2010).

[11] Michael C. Schatz. "BlastReduce: High Performance Short Read Mapping with MapReduce" (2013).

[12] Simone Leo ,Gianluigi Zanetti, Federico Santoni. "Biodoop: Bioinformatics on Hadoop," *41st International Conference on Parallel Processing Workshops*, Vienna, Austria, 2009 pp. 415 - 422. (2012).

[13] Michael C. Schatz. "CloudBurst: highly sensitive read mapping with MapReduce", *Bioinformatics*, Volume 25, Issue 11. (2009).

[14] Andréa Matsunaga, MaurícioTsugawa,José Fortes "CloudBLAST: Combining MapReduce and Virtualization on Distributed Resources for Bioinformatics Applications," *IEEE Fourth International Conference on eScience*, Indianapolis, IN, 2008, pp. 222-229. (2008).

[15] Ben Langmead, Michael C Schatz, Jimmy Lin, Mihai Pop&Steven L Salzberg. "Searching forSNPs with cloud computing". *Genome Biology* volume 10, Article number: R134 (2009).

Part IV: Communication System

A Decentralized Peer to Peer Messaging System Based on Blockchain Technology

Ashmita Pandey[1], Anku Jaiswal[2]

[1]*Department of Computer Engineering, Kathmandu Engineering College*
Ganeshman Singh Rd, Kathmandu 44614, Nepal
[2]*Department of Electronics and Communication, Advanced College of Engineering and Management, Kupondole, Lalitpur, Nepal*

[1]*ashmita.pandey.np@gmail.com* , [2]*jaiswalaku@gmail.com*

Abstract

"A decentralized peer to peer messaging system based on blockchain technology" is a distributed peer-to-peer messaging system that utilizes end-to-end encryption and blockchain for decentralized and secure messaging. The paper provides the ways of incorporating standard features of modern message transfer applications in a decentralized system. The network communication between nodes is established with the help of Distributed Hash Table (DHT). DHT implementation mainly uses Kademlia protocol. The encryption is provided using public key cryptography. Different techniques like Proof of Work (P0W), Proof of Authority(PoA) are implemented to prevent denial of service attacks. The system utilizes etherium blockchain to store user identity, addresses and contracts among users to ensure proper delivery of messages. The services of the blockchain are accessed and maintained by what is called the full ethereum nodes. An End-to-end encryption (E2EE) is performed for secure message transfer in overlay network. While transferring or receiving message, a json format of message is received with attributes message id and message. All details like message type, message contents, message status, sent date, etc. that are sent or received are encoded in the message. The system addresses the growing need of privacy, security and decentralization in the field of instant messaging ensuring the anonymity of the users in the network.

Keywords: *Blockchain, Distributed Hash Table, Ethereum, E2EE, PoW, PoA.*

1. Introduction

BlockChain Based Messaging System, in the simplest sense, is a messaging application but messages are sent and received on a peer-to-peer manner. The foundation of the application is based on end- to-end encryption, decentralization and effective use of blockchain technologies. Messages are transferred from node to node using socket programming with the help of nodes established on Distributed Hash Table(DHT) particularly Kademlia [1]. For the encryption it utilizes public key cryptography algorithm with custom protocol designs for shared secret establishment. In short, the blockchain address is also the identity of the user, and user can send/receive the messages through the messenger. For this, a separate distributed messaging layer is developed on top of peer-to-peer network to handle the message distribution and the validity of the message storage is done on the public blockchain.

Use of blockchain technology for chat app primarily serves the purpose of storing identity and public key

of the users. On the other hand, blockchain will also be used for bookkeeping of the contracts among nodes responsible for storing and delivering the message in the network (referred as postmen hereafter) and the end user clients. Postmen are full nodes who sign contracts with the clients to store the messages for fixed period of time as defined in the contract policy and allow the clients to retrieve messages at their need. The postmen also create contracts among each other to handle the backup of messages and ensure that message is always available at the end user clients' request, i.e. backup service.

2. Literature Review

Instant messaging has been an integral part of internet communication. Services like Facebook messenger, Skype, Viber has been very popular among the internet users today. These systems as of now heavily depend on the central servers. Most of the existing systems have shown to have severe security problems with respect to user privacy, message authenticity and eavesdropping. Secure instant messaging systems are limited and often suffer from scalability problems. Over the last few years, there have been only a few platforms to provide decentralized messaging using blockchain, most of which are targeted to cryptocurrency users and are usually for a specific cryptocurrency.

Coinspark [2] is one of such implementations which is used for messaging. CoinSpark uses regular bitcoins for all of its operations. No other tokens or coins are required for CoinSpark transactions. CoinSpark operations are recorded in full on the Bitcoin [3] blockchain, which is decentralized and replicated thousands of times across the Internet. Any server-side functionality can be delivered freely by any entity, and it provides open source versions that anyone can run. Coinspark differs because of its legally enforceable contract which could be designed as a message to be sent to the receiver. Another similar application related blockchain messaging is Blokcom [4] which provides a platform in which each connected element is authenticated and certified; all data exchanged is verified and guaranteed against mutability and falsification; every interaction is traced and verified, automatically and without the need for user confirmation. Moreover, it dissociates from the concept of cryptocurrencies and allows any digital asset to be represented as the item being exchanged.

Blokcom is targeted as a more general sense of message sending which acts more as a remote control system. But when it comes to functional similarity, the one that comes closer to our project is ECHO [5]. Although this application is in its pre alpha release phase, the project goals for this application aims at a blockchain messenger for general public. Other than that, ECHO was proposed as a solution to the tedious process of money transfer in traditional sense. It's problem statement focuses on the fact that most of our favorite chat apps are open, unprotected like a postcard and everybody can read them. Most of our messages are been tracked, analyzed and stored without our knowledge. Cyber fraud, data theft, and blackmailing is a high risk for everybody and most of us do not know how to handle our data.

ECHO is designed to be an app that protects our privacy, encrypt all our voice, video and text messages plus makes money transfer easy again at the same time. ECHO is proposed to give the best messaging experience, make no compromises and a truly private chat with friends and family. Though aimed to be an application for both messaging and money transfers, ECHO focuses more on the latter part and the messaging part is design as an aid.

A more recently released application, BeeChat [6] is a blockchain based messenger and cryptocurrency community. BeeChat can be used to join active private chats, private and public groups, and discussions that serve cryptocurrency enthusiasts as well as the general public at Large. In addition to message communication, the app also features transfer of various cryptocurrencies. BeeChat is developed using proprietary distributed technology with servers implemented around the world. The messenger uses end to

end encryption to secure the content of the messages transferred. Also, as a part of security and privacy for the users, BeeChat deletes the messages immediately after it is delivered and undelivered messages expire after a fixed period of time. Unlike our project, BeeChat doesn't implement contracts between the clients and network nodes for message transfer and storage.

Similarly, another recently released application related to blockchain messaging is Dust. Dust is the first implementation of mercury protocol [7]. Mercury protocol is a Ethereum based protocol which aims to become a standard framework to implement decentralized social media and messaging on Ethereum blockchain. The main principle behind Dust is that it uses a Ethereum token Global Messaging Token (GMT) as a virtual currency to facilitate transfer of messages and reward the involved parties. Dust provides a secure way of transferring message and also incentivizes the users for using the platform. The incentive is in the form of GMT tokens which are given to users who create content, moderate content, invite friends to use Dust, etc. The servers store the 6 messages in their RAM instead of permanent storage. Also, the users can choose to immediately destroy messages after being received. Dust is only the first step to fully implementing mercury protocol. So, at present, Dust doesn't provide support for cryptocurrency transactions.

e-Chat [8] is a similar messenger and a social platform application based on the Ethereum blockchain. It was announced rather recently and is currently in its alpha phase of release. It uses a distributed hash table (DHT) as a distributed network to store user information and send message across different users. The Ethereum blockchain is used for paid information exchange, token transfer and other contracts between users. It also uses IPFS (Interplanetary File System) to store, retrieve and share files of users over the network. e-Chat provides an incentive to the users by making content monetizable as well as paid upvotes on their posts (they call it cryptolikes). In contrast to our project, e-Chat doesn't seem to provide reward for users being a part of the distributed network and relaying messages to other users. Also, as far as their whitepaper goes, there doesn't seem to be any mechanism to compensate the user when a message transmission and storage fails.

ADAMANT [9] Messenger is another newcomer in blockchain messaging. It was announced while our project was underway and it's ICO (Initial Coin Offering). It's a Blockchain-based system for data and message transfers along with an integrated payment system are providing a truly fundamental benefits for allpersonal and business-like communications The messenger is built on top of a new blockchain. The main feature of this blockchain is that it's heavily focused on transaction processing speed. For this it employs Delegated Proof of Stake (DPoS) for generation of new block, which is a compromise between decentralization and speed adopted by many blockchains. Messages are transferred directly through the blockchain. So, there is no need for a distributed message transfer framework.

3. Methodology

3.1 Hashing

Blockchains are dependent on hashing. Hashing is a cryptographic method of converting any kind of data into a string of characters. As well as providing security through encryption, hashing creates a more efficient store of data, as the hash is of a fixed size. Blockchains hash each transaction before bundling them together into blocks. Hash pointers link each block to its predecessor, by holding a hash of the data in the previous block. Because each block links to its predecessor, data in the blockchain is immutable. The hashing function

means that a change in any transaction will produce an entirely different hash, which will alter the hashes of all subsequent blocks. To propagate a change across the blockchain, 51% of the network would have to

agree to it. Hence, the term "51% attack". A cryptographic hashing algorithm must fulfil specific criteria to be effective:

- The same input must always generate the same output. regardless of how many times you put the data through the hashing algorithm, it must consistently produce the same hash with identical characters in the string.
- The input cannot be deduced or calculated using the output. There should be no way to reverse the hashing process to see the original data set.
- Any change in the input must produce entirely different output.
- The hash should be of a fixed number of characters, regardless the size or type of data used as an input.
- Creating the hash should be a fast process that doesn't make heavy use of computing power.

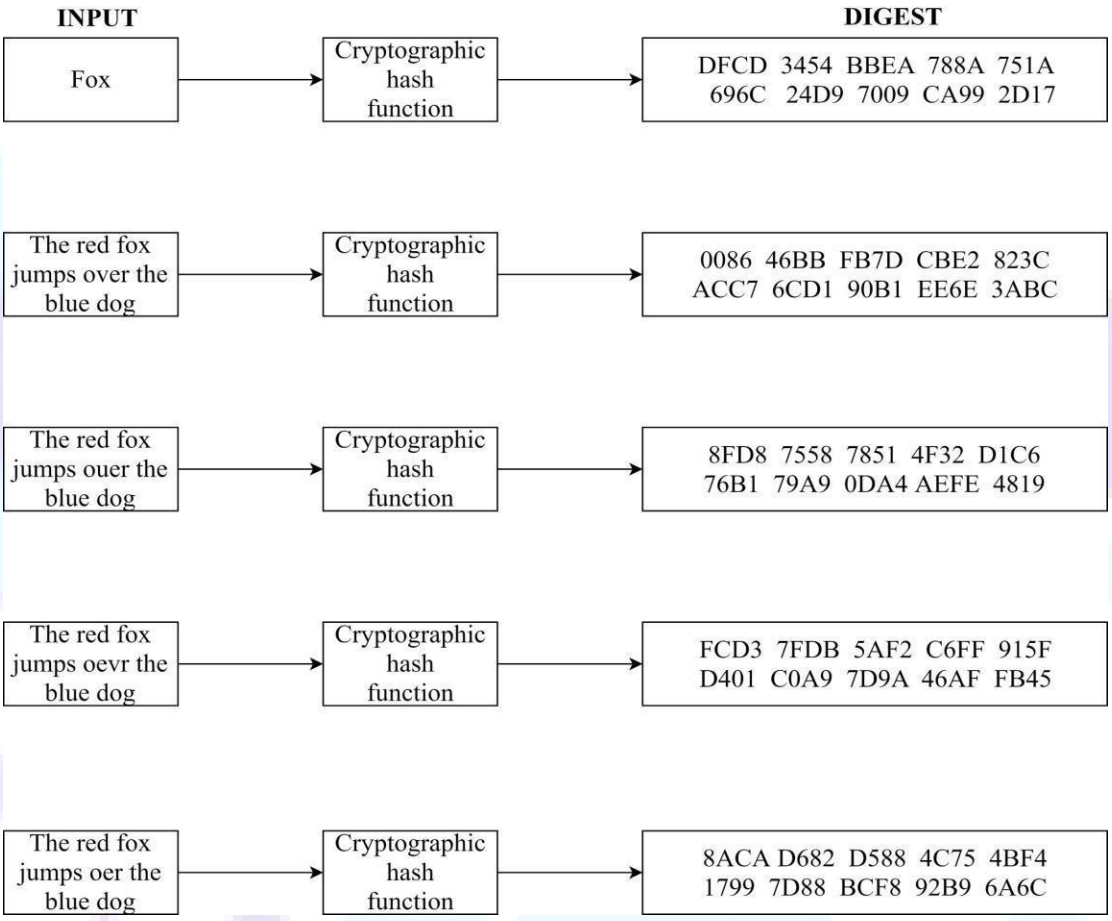

Figure 1: How a hash algorithm generates a hash

3.2 Consensus Algorithm

Blockchain is a distributed decentralized network that provides immutability, privacy, security, and transparency. There is no central authority present to validate and verify the transactions, yet every transaction in the Blockchain is considered to be completely secured and verified. This is possible only because of the presence of the consensus protocol which is a core part of any Blockchain network.

A consensus algorithm is a procedure through which all the peers of the Blockchain network reach a common agreement about the present state of the distributed ledger. In this way, consensus algorithms achieve

reliability in the Blockchain network and establish trust between unknown peers in a distributed computing environment. Essentially, the consensus protocol makes sure that every new block that is added to the Blockchain is the one and only version of the truth that is agreed upon by all the nodes in the Blockchain.

There are various types of consensus algorithm: Proof-of-Work, Proof-of-Stake, Delegated-Proof-of-Stake,

Leased-Proof-of-Stake etc. In our project, we have used Ropsten Test Network as Ether transaction network so, we use Proof-of-Work and Proof of Authority as consensus algorithm. The messages we send uses PoW and PoA is used on the message being validated by the blockchain after paying the required amount of costs involved.

Proof of Work(PoW):

This consensus algorithm is used to select a miner for the next block generation. The central idea behind this algorithm is to solve a complex mathematical puzzle and easily give out a solution. This mathematical puzzle requires a lot of computational power and thus, the node who solves the puzzle as soon as possible gets to mine the next block.

Proof of Authority (PoA):

Proof of authority (PoA) is an algorithm used with blockchains that comparatively delivers fast transactions through a consensus mechanism based on identity as a stake. In PoA-based networks, transactions and blocks are validated by approved accounts, known as validators. Validators run software allowing them to put transactions in blocks. The process is automated and does not require validators to be constantly monitoring their computers. It, however, does require maintaining the computer (the authority node) uncompromised.

4. Results

Decentralized application (Dapps) has been created that consists of a web pages created with React JS. Block chain was used as a data storage destination. Smart Contracts have been deployed using Ropsten Test Network. The messenger app performs wallet operations through the Ethereum client set up in the postman nodes. Handshaking method is used to connect to a network for transactions. Authentication is required for the user on every time a message is to be sent. Supports multiple platforms like both android and web for messaging and messages can be send privately as well. All the transaction history are recorded in blockchain. The deployed contracts and transaction history of the contracts can be viewed through Ethereum block explorer.

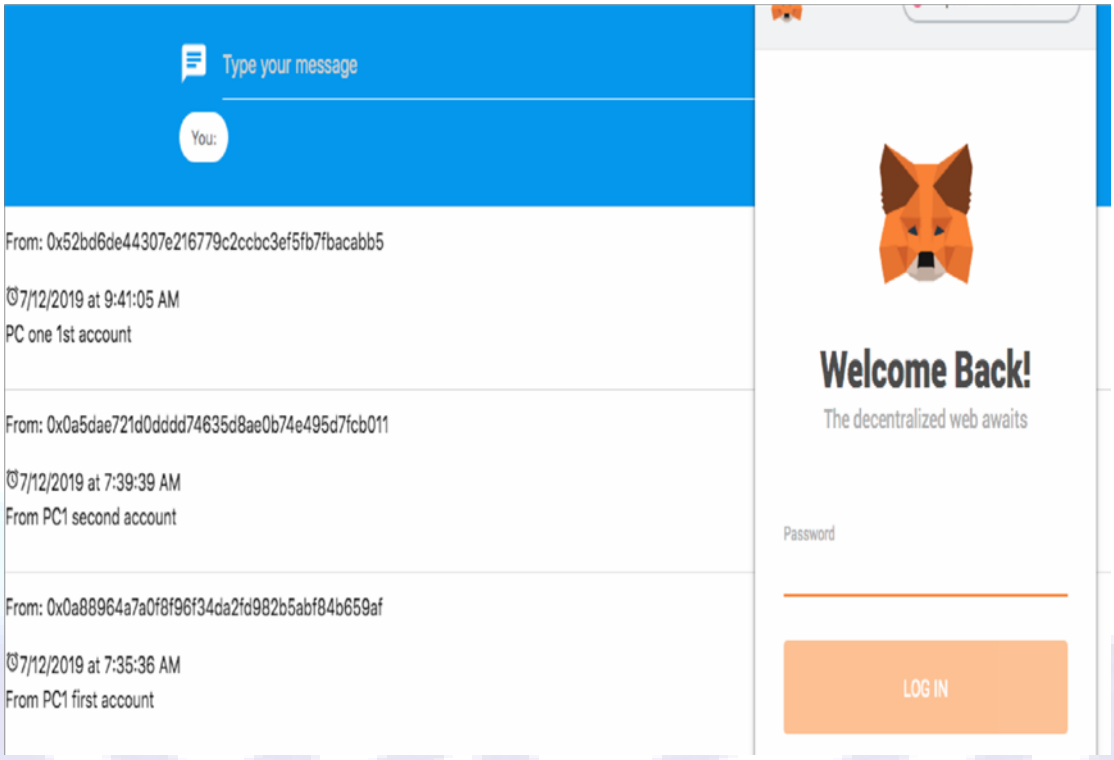

Figure 2: Login Window of Ropsten Test Network

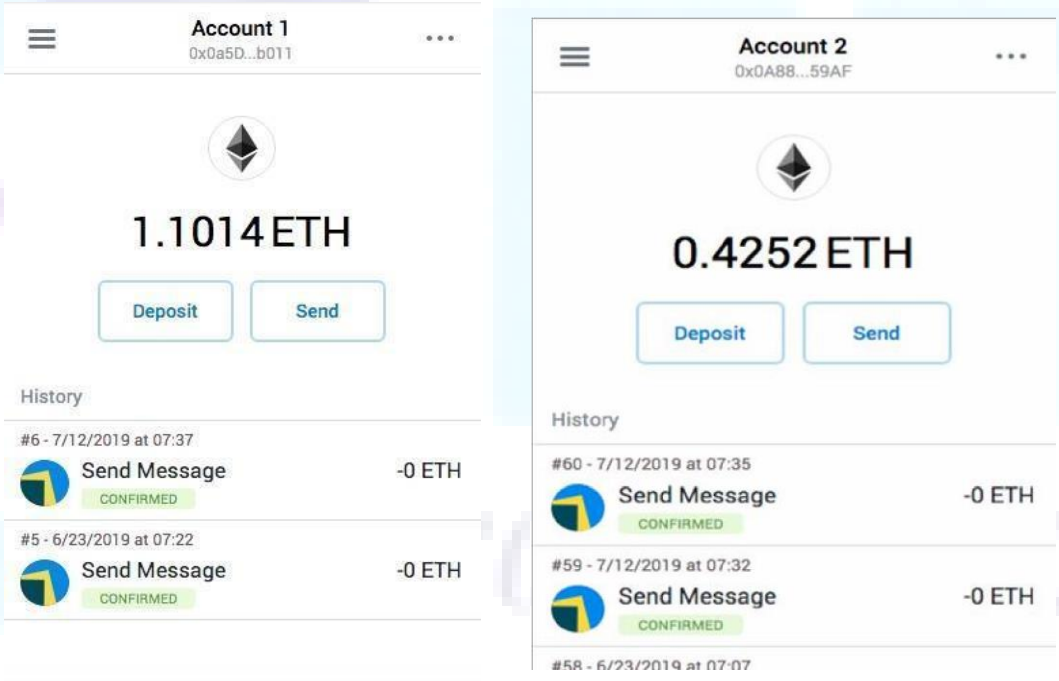

Figure 3: Smart Contract Deployment Process

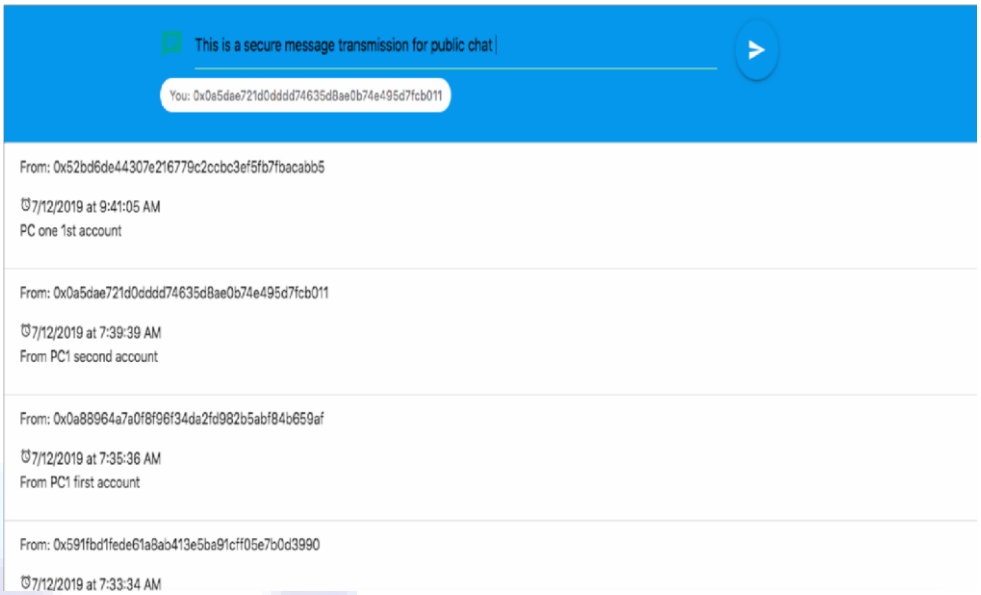

Figure 4: Chat Window for Public Messaging

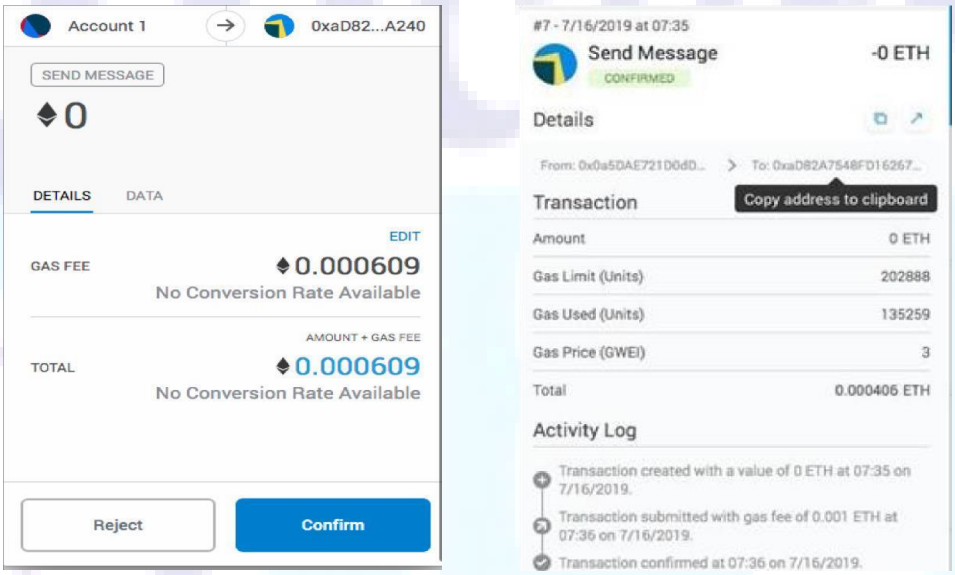

Figure 5: Account Details

5. Conclusion

In this paper, implementation of blockchain technology has been discussed. The paper focuses on to creating an end-to-end encrypted messenger system based on blockchain technologies in on decentralized network. to satisfy the security and privacy needs of the end users. Also block chain technology was integrated to support token transactions and delivery of messages. In the context of Nepal, most people are nowadays being self-aware about their security and privacy of personal data. We are trading usability for privacy and security. And every conversation, interaction or opinion is being recorded for eternity which is a dangerous development. Also with an ever-faster growing world, people will discover new demands and passions for more privacy and security. They are hungry for a new decentralized messenger that cannot be censored, and is very hard to hack. Thanks to modern Block chain and IPFS technologies the block chain messenger will live to encrypt and decentralize all chat messages and wallets to protect all the users. As the system is heavily

encrypted as well as decentralized it can provide secure, efficient and private messenger app which will overcome the inherent flaws of the existing applications. Because of its features, it can be used for military communication, intra-organization communication, banking as well.

References

[1] P. Maymounkov and D. Mazieres, "Kademlia: A Peer-to-peer Information System Based on the XOR Metric", 2002

[2] Coinspark wallet, Coinspark.org, November 2017. [Online]. Available: http://coinspark.org/developers/. [Accessed: Mar. 14, 2019]

[3] S. Nakamoto, "Bitcoin Whitepaper", Bitcoin.org, 2009. [Online]. Available: http://bitcoin.org/bitcoin.pdf. [Accessed: Mar. 14, 2019]

[4] "Blockcom - blockchain messaging platform", Reply.com, November 2017. [Online]. Available:

[5] http://www.reply.com/en/content/blokcom. [Accessed: Mar. 14, 2019]

[6] C. Hering, "Home - Echo Industries", Echo Industries, November 2017. [Online]. Available: https://my-echo.com/. [Accessed: Mar. 14, 2019]

[7] Beeplabs, "Beechat app", Beechat.io, 2017. [Online]. Available: https://beechat.io. [Accessed: Mar. 14, 2019]

[8] Radical App International, "Mercury Protocol whitepaper", 2017. [Online].

[9] Available:https://www.mercuryprotocol.com/wpcontent/uploads/2018/08/Mercury_Protocol_whitepaper.pdf. [Accessed: Mar. 14, 2019]

[10] "e-Chat Whitepaper", Investors.echat.io, 2017. [Online]. Available: https://investors.echat.io/static/doc-pdf/en/eChat_Whitepaper.pdf. [Accessed: Mar. 14, 2019]

[11] ADAMANT TECH LABS LP, "Adamant Whitepaper", 2017. [Online]. Available: https://adamant.im/whitepaper/adamant-whitepaper-en.pdf. [Accessed: Mar. 14, 2019]

[12] B. Awerbuch and C. Scheideler, "Towards a scalable and robust DHT", 2006.

[13] V. Buterin, "Ethereum Whitepaper", ethereum/wilki, 2015. [Online]. Available: https://github.com/ethereum/wiki/wiki/White-Paper. [Accessed: Mar. 14, 2019]

Design and Fabrication of Circular Microstrip Patch Antenna Arrays

Prashanna Sharma Paneru[1], Srijana Aryal[1], R.K. Maharjan[2]

[1]*Electronics and Communication Engineering, ACEM, Kupondole, Lalitpur, Nepal*
[2]*Pulchowk Campus, IOE, Nepal*

prashannapaneru@gmail.com[1], *aryalsrijana11@gmail.com*[1]
rkmahajn@gmai.com[2]

Abstract

Considering the development in the field of telecommunication, design of micro-strip antenna arrays are implemented. Micro-strip patch antenna is the commonly used antenna in mobile sets owing to its advantage of better directivity and inexpensive to manufacture. The return loss and gain characteristics are further improved by making an array. The circular antenna and its arrays have been designed in electromagnetic simulation software HFSS, where the number of elements, spacing and feeding currents have been optimized. This paper discusses and compares the circular micro strip patch antenna (both simulated and fabricated) that resonates at the proximity of GSM band (800 MHz). Same approaches can be used for fabricating other types of antennas.

Keywords**:** *Micro-strip, GSM band, arrays, return loss, gain*

1. Introduction

Antennas play an important role in any wireless system. According to the IEEE standard definition, an antenna is defined as "a means for radiating or receiving radio waves". Patch antenna is a narrowband, wide-beam antenna that is fabricated by etching the copper patch in a dielectric substrate [1] – [3]. These types of antennas are employed in high frequency regime, as their dimensions are directly related to the wavelength factor. Patch antenna arrays are widely used because it increases the radiated power and provide high directional beam which avoids power loss in other directions [4] – [5]. Basically, the arrays are used to improve the radiation pattern. Arrays increase the directivity of the antenna and provide electronic steering. The antenna may be of various shapes: rectangular, circular and so on [4].

It is mostly in high demand in radio sets of mobile phones. This is comparatively inexpensive and easy to fabricate. This paper discusses on the design parameters of an optimized micro strip patch antenna that resonates at a single band. A GSM band of 800 MHz is chosen in the design. We have gone through different designs of circular antenna arrays. Note that antennas can also be simulated using other numerical techniques such as finite-difference time-domain (FDTD) [6]–[7]. However, in this paper, a commercial electromagnetic software, HFSS that is based on finite element method (FEM) is used.

2. Geometry of the Design

The micro strip patch antenna has the radiating element (Copper patch) above the dielectric. FR4 dielectric material of electrical permittivity 4.4 is chosen. The height of this dielectric layer represented as 'h' is

selected as 1.6 mm. This dielectric layer is mounted on a ground plane of height Mt = 0.1 mm.

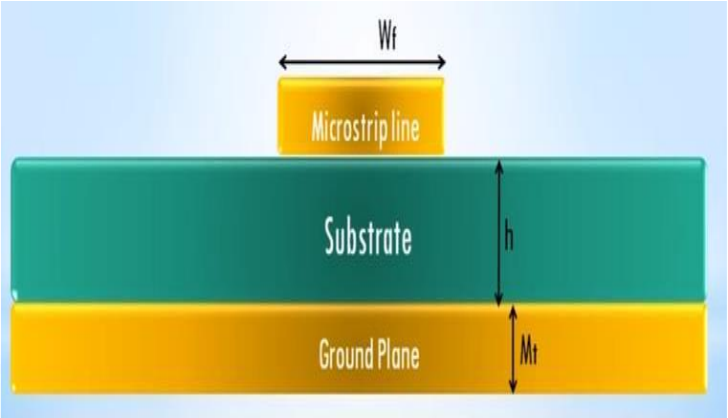

Figure. 1: Side view of Micro strip patch antenna

3. Design and Simulation Results

The microstrip patch antenna has a radiating element (Copper patch) above the dielectric. FR4 dielectric material of electrical permittivity($\epsilon_r = 4.4$) is used as a substrate. Its height 'h' is 1.6 mm. It is mounted on a ground plane of height 0.1 mm. The circular structure is designed in the HFSS software using various tools and elements. To calculate the radius of the patch the following formula is used:

$$a = \frac{F}{\left\{1+\frac{2h}{\pi\epsilon F}\left[ln\left(\frac{\pi F}{2h}\right)+1.7726\right]\right\}^{1/2}} \quad (1)$$

$$\text{Where, } F = \frac{8.791*10^9}{f_r\sqrt{\epsilon}} \quad (2)$$

&a = radius

Table 1: Dimension of different arrays before and after optimization

Parameter	Normal array		Disc-like array		Patterned array	
	Initially (mm)	After optimization (mm)	Initially (mm)	After optimization (mm)	Initially (mm)	After optimization (mm)
Outer radius	49.2	49.326	49.2	49.326	49.2	47.4
Feed width	3.01	2.8	3.01	2.8	3.01	2.9
Width of 100-ohm line	0.7	1	0.7	1	0.7	1
Feed length	23	23	23	23	23	23
Length of 100-ohm line	23	23	23	23	23	23

The figure 1 compares the return loss (S_{11} parameter) of a simple array before and after optimization. The return loss is reduced to -50 dB from -20 dB at 800 MHz. Similarly, the return loss is reduced to -30 dB for a patterned array, and the figure is not shown here due to space constraint. This refers that a very negligible amount of power is reflected from the transmission line at the desired frequency operation. Figure 2 is the radiation pattern of the simple array. It is directional along z axis with back and side lobes. The peak gain value of the simple circular patch antenna array is 16.42dB.

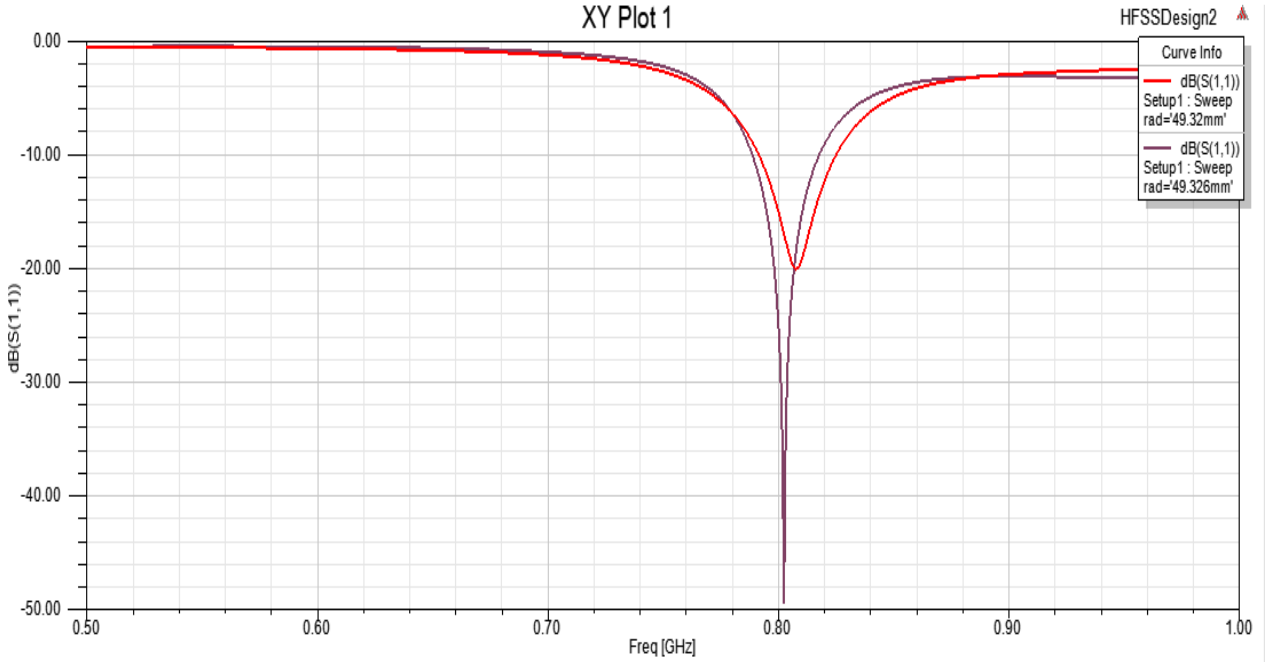

Figure 2: Return loss of simple array before and after optimization

Figure 3: 3D radiation pattern of a simple array antenna

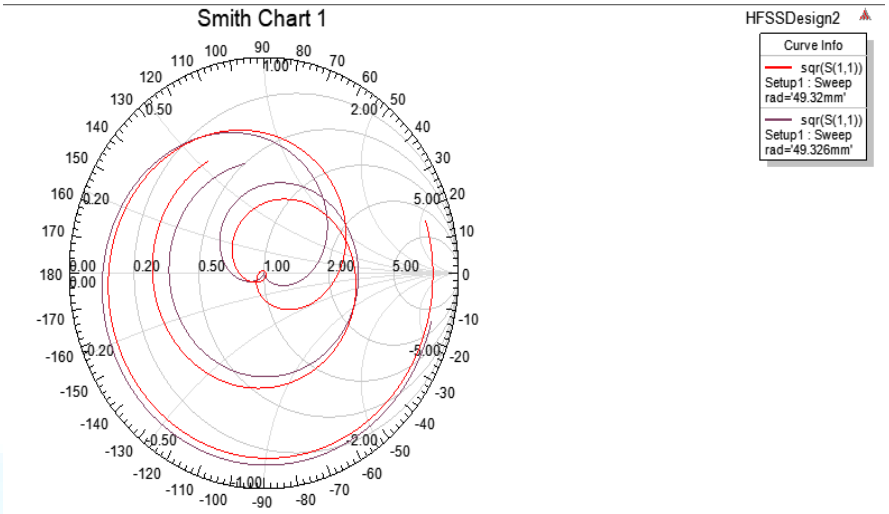

Figure 4: Smith Chart of Simple Array

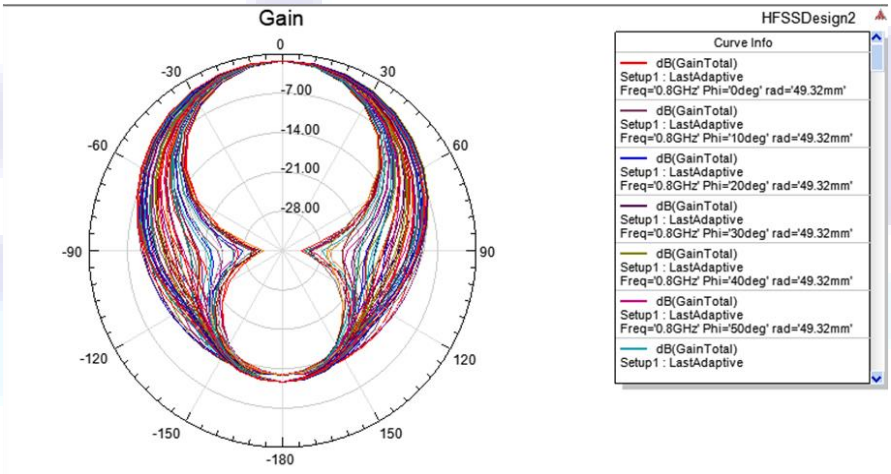

Figure 5: Gain of Simple Array

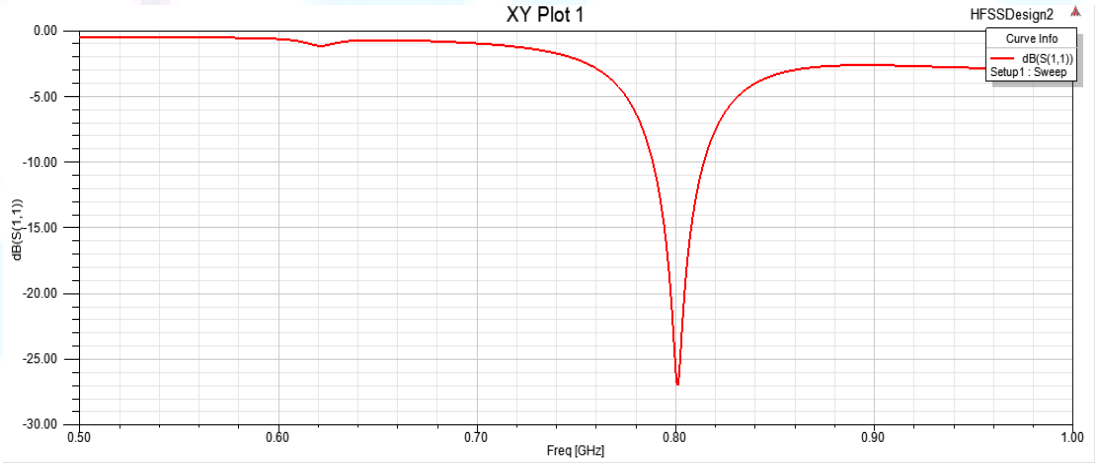

Figure 6: Return Loss (S_{11}) of Disc-like Array

The return loss of the disc like array is reduced to around -27 dB with optimization i.e. shown in the Fig.6.

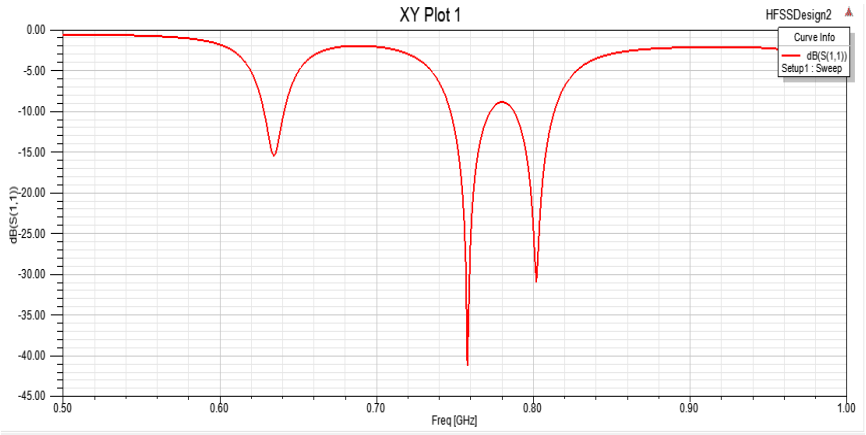

Figure 7: Return Loss(S_{11}) of Patterned Array

The return loss of the disc like array is reduced to around -32 dB at our desired frequency 800 MHz with optimization i.e. shown in the Fig.9. It is operating at triple bands with return loss of -16 dB (at 630 MHz) and -42 dB (at 760 MHz).

4. Fabrication Results

Figure 8: Fabricated simple array, disc-like array and patterned array

All the designs of antenna are fabricated in the FR4 substrate layer with the connector as shown in figure 3. These fabricated antennas are connected with the HP 8720D model network analyzer for measuring different parameters like return loss, SWR etc. The following results are obtained:

- -12.45dB return loss, SWR of 1.68 in a simple array antenna.
- -15.38dB return loss, SWR of 1.43 in a disc-like array antenna.
- -10.1dB return loss, SWR of 1.9 in a patterned array antenna.

As these antennas are manually fabricated, the resonating frequency of fabricated antenna is obtained slightly higher than the simulated result.

Figure 9: Measurement of Return Loss (S_{11}) in network analyzer

5. Conclusion

Antenna plays a significant role in the field of wireless communications. Also, in addition to communication, it is applicable in various other fields which include telemedicine, radar, GPS and many more.

The microstrip patch antenna arrays are successfully designed in both software and hardware. While designing in HFSS software, the dimension of antennas is optimized too for better performance. After the antennas are manually fabricated, their performance is measured using network analyzer. Due to ageing of apparatus, and additional parasitic capacitance of cables, the operating frequency is slightly shifted from the designed parameters. Out of all the arrays, the disc like array has the best return loss with around -15.38 dB at the frequency of operation. Furthermore, the maximum gain of 16.42 dB was obtained. These performances are expected to improve when these antennas are fabricated in a fabrication foundry.

References

[1] A.De, C. K (2016). Design and Performance Analysis of Micro strip Patch Array Antennas with different configurations. International Journal of Future Generation Communication and Networking.

[2] B.J.Kwaha, O. I (2011). The Circular Microstrip Patch Antenna-Design and Implementation.

[3] Goyal, G. K. (2014). A Review- Microstrip Patch Antenna Design.

[4] R. K. Maharjan, N. Y. Kim (2013). Introduction to Microstrip Filter Design and Analysis.

[5] Rao, P. R. (2017). Design and Analysis of High Gain Circular Patch Antenna Arrays for 2.4 GHz applications. *IJIRSET*, 8.

[6] S. Pokhrel, V. Shankar and J. J. Simpson, "3-D FDTD Modeling of Electromagnetic Wave Propagation in Magnetized Plasma Requiring Singular Updates to the Current Density Equation," in *IEEE Transactions on Antennas and Propagation*, vol. 66, no. 9, pp. 4772-4781, Sept. 2018.

[7] S. Pokhrel, M. Rodriguez, A. Samimi, G. Heber and J. J. Simpson, "Parallel I/O for 3-D Global FDTD Earth–Ionosphere Waveguide Models at Resolutions on the Order of ~1 km and Higher Using HDF5," in *IEEE Transactions on Antennas and Propagation*, vol. 66, no. 7, pp. 3548-3555, July 2018.

VANET Analysis for Different Propagation Model on Real Traffic Scenario Using SUMO and NS3

K.K. Jha[1]

[1]*Metrological Forecasting Division, Department of Hydrology & Metrology, Ministry of Population and Environment, Nepal*

krishna.k.jhaa@gmail.com

Abstract

Vehicular ad hoc network (VANET) is a promising Intelligent Transportation System (ITS) technology, which enables vehicles to communicate with each other and roadside station, where nodes involve themselves as servers and/or clients to exchange and share information. VANET have some unique characteristics like high dynamic topology, frequent disconnections and restricted topology. The study of this study field is still simulation based, because of infeasible to use real vehicle in large scenario. The radio propagation model used in wireless has significant role on the performance of VANET. This paper studies performance of different radio propagation model like TwoRayGround, Rayleigh and Nakagami with 802.11p MAC protocol on VANET. The real traffic scenario mobility file has been generated using SUMO and the network simulation has been performed using NS-3. Packet delivery ratio and Throughput are used as parameter of the performance evaluation. Nakagami radio propagation model performs better than other two aforementioned methods.

Keywords: *VANET; SUMO; NS-3; ITS*

1. Introduction

Vehicular ad hoc network (VANET) is a promising Intelligent Transportation System (ITS) technology, which enables vehicles to communicate with each other and roadside station. Both vehicle-to-vehicle (V2V) and vehicle-to-road-side-unit (V2R) communications are supported in VANETs to efficiently collect/report traffic updates from/to vehicles as well as road side units (RSUs). In VANET communication the vehicle acts as transceiver. It can support critical vehicular safety applications such as emergency warning, collision avoidance, road condition broadcast, and lane changing assistance [1]. The collected real-time traffic information can be utilized for freeway-traffic-flow managements, individualized vehicle path planning, and vehicle localization. VANET utilizes multiple ad-hoc networking technologies such as WiFi IEEE 802.11 b/g, WiMAX IEEE 802.16, Bluetooth etc. In most of the related works assume that the incorporated VANETs have sufficiently small delivery delay for real-time information collection. Actually, as VANETs rely on short-range multi-hop communications, the end-to-end transmission delay can be non-neglectable in some scenarios. Therefore, evaluations should be conducted to study how the end-to-end transmission performance of vehicular communications impacts on the performance of path planning in different scenarios and how to design the transmission mechanisms to reduce the delay when delay is not neglectable. The VANET architecture is shown in fig. 1.

Recently, VANETs experience rapid development due to above mentioned application, as well as emerging

self-driving car technologies. An IEEE dedicated short range communication (DSRC) standard [2], also known as IEEE 802.11p, has been initialized to specify Media Access Control (MAC) protocols and Physical Layer (PHY) for VANETs. Continuous mobility is a key feature of VANETs, which results in rapid topology changes. Also, the physical channel condition and radio propagation model has great role on performance of VAENT in this dynamic topology. My previous work [3] study the role of different routing protocol to efficiently route the packets in this dynamic scenario of VANET.

This paper is focused to study the effect of various radio propagation model on the performance of VANET in real traffic scenario. The real traffic scenario is generated by SUMO and simulation is done on NS3.

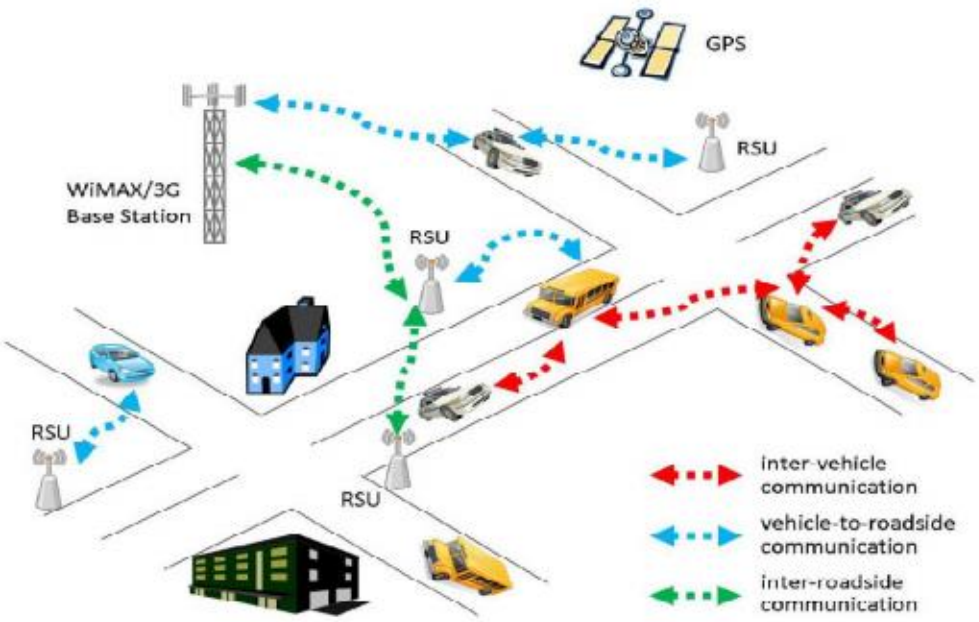

Figure 6: VANET Structure

2. Literature Review

In the area of vehicular communications, there has been a plethora of research work. The IEEE has specified 802.11p [4] as the MAC and PHY standard for data exchange between high-speed vehicles and between vehicles and roadside infrastructures in the licensed ITS band of 5.9 GHz (5.85–5.925 GHz). At MAC layer, data are transmitted using broadcast, which is a subset of the IEEE 802.11 standard distributed coordination function (DCF). As a result, most existing VANET Markov models are extensions from the general DCF models. [5] Proposed a Markov model for the throughput of the enhanced distributed channel access (EDCA) mechanism in the IEEE 802.11p MAC sublayer under saturated traffic conditions.

Mr. Rafi U Zamam [6] studied & compared the performance of DSDV, AODV and DSR routing protocols for ad hoc networks using NS-2 simulations. Vahid Garousi [7] studied an analysis of network traffic in ad-hoc networks based on the DSDV protocol with an emphasis on mobility and communication patterns of the nodes. In this paper, he observed that simulations measured the ability of DSDV routing protocol to react to multi-hop ad-hoc network topology changes in terms of scene size, mobile nodes movement, number of connections among nodes, and also the amount of data each mobile node transmits.

Imran Khan and others [8] has analyzed the AODV and OLSR routing protocols performances in highly fading scenario using Nakagami propagation model. A research study focused on the limitations of Two Ray

Ground propagation model. This study doesn't stress the details of mobility and propagation models utility.

Mobility simulators i.e. MOVE, SUMO can be used to move the vehicle nodes on highway roads as in generally the case in a VANET – either based on measured or generated traffic traces [9].

Christoph Sommer and Falko Dressler [10] in his study have well defined the historical evolution of mobility models in VANET.

3. Related Theory

a. WAVE

WAVE is an overall system architecture for vehicular communications. The standards for specifying WAVE include a set of extensions to the IEEE 802.11 standard, found in IEEE Std 802.11p -2010, and the IEEE 1609 standard set, consisting of four documents: resource manager: IEEE 1609.1, security services: IEEE 1609.2, network and transport layer services: IEEE 1609.3, and multi -channel coordination: IEEE 1609.4. Additionally, SAE standard J2735 describes a Dedicated Short Range Communications (DSRC) application message set that allows applications to transmit information using WAVE.

The WAVE protocols are designed for the 5.850-5.925 GHz band in the United States (US), known as Intelligent Transportation Systems Radio Service (ITSRS). This 75 MHz band is divided into one central Control Channel (CCH) and six Service Channels (SCHs). An overview of the WAVE protocol families is illustrated in fig.2. The IEEE 802.11p standard [11] defines the physical (PHY) and Medium Access Control (MAC) layers based on earlier standards for Wireless LANs. The IEEE 802.11p uses the Enhanced Distributed Channel Access (EDCA) MAC sub-layer protocol designed based on that of the IEEE 802.11e with some modifications, while the physical layer is OFDM (Orthogonal Frequency Division Modulation) as used in IEEE 802.11a.

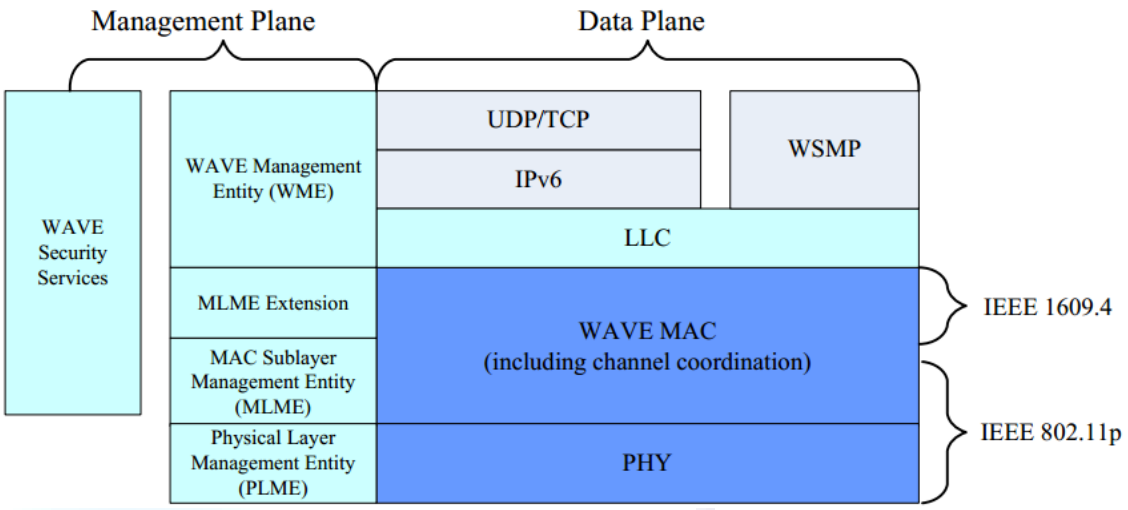

Figure 7: The WAVE Protocol Unit

In the U.S., the IEEE1609 WAVE (Wireless Access in Vehicular Environments) protocol stack builds on IEEE 802.11p WLAN operating on seven reserved channels in the 5.9 GHz frequency band. The WAVE protocol stack is designed to provide multi-channel operation (even for vehicles equipped with only a single radio), security, and lightweight application layer protocols. Within the IEEE Communication Society, there is a Technical Subcommittee on Vehicular Networks & Telematics Applications (VNTA). The charter of this committee is to actively promote technical activities in the field of vehicular networks, V2V, V2R and V2I

communications, standards, communications-enabled road and vehicle safety, real-time traffic monitoring, intersection management technologies, future telematics applications, and ITS-based services.

b. Channel Condition at PHY Layer

The channel condition at PHY layer has great influence on throughput and data loss. The different models used for propagation of signal has varying effect on data loss and throughput. Radio propagation is the behavior of radio waves when they are transmitted, or propagated from one point on the Earth to another, or into various parts of the atmosphere. Like light waves, radio waves are affected by the phenomena of reflection, refraction, diffraction, absorption, polarization and scattering [12].

The fig. 3 represents the radio propagation models and the evolution of it's from free space to Nakagami radio propagation. This paper analyzes three propagation model i.e. TwoRayground, Rayleigh and Nakagami. These three models are chosen because the first one TwoRayground is the simplest propagation model to analyze the signal propagation through space, which consider only the line of sight and ground reflected wave. However, the other two are chosen because they consider not only the ground reflected wave but also the fading due to multipath reflection from building, toll structure and other reflected structure in urban area which seems practical in scenario like VANET. Where the fading is due to multipath and reflection from different reflection structure. The Nakagami is the general propagation model where the fading parameter can be controlled according to distance, whereas the Rayleigh model uses the same fading parameter throughout the distance. The Rayleigh model is a special case of Nakagami model.

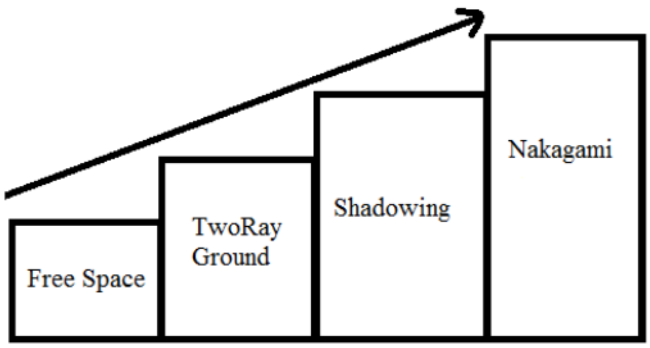

Figure 8: Radio Propagation Model Evolution for VANET

i. *TwoRayGround Radio Propagation*

This radio propagation model is highly preferred in the research of MANET. TwoRayGround radio propagation model is also used for protocols performance in VANET scenario. This is a more realistic than the Free-Space model when we consider a ground reflected propagation path between transmitter and receiver.

The received power at distance d is predicted by:

$$\text{Pr} = \frac{P_t G_t G_r h_t^2 h_r^2}{d^4 L} \qquad (1)$$

In the equation h_t and h_r are the heights of the transmitter and receiver antennas respectively and L denotes the system loss.

ii. *Nakagami Propagation Model*

Nakagami is a mathematical general modeling of a radio channel with fading. Nakagami distribution is defined by the following probability density function:

$$f(x) = \frac{2m^m x^{2m-1}}{\Gamma(m)\Omega^m} exp\left[\frac{-mx^2}{\Omega}\right], x \geq 0, \Omega > 0, m \geq 1/2 \quad \text{.....(2)}$$

The corresponding pdf (probability density function) of power (square of the signal amplitude) at the given distance can be obtained by a change of variables and is given by a gamma distribution of the following form:

$$p(x) = \left(\frac{m}{\Omega}\right)^m \frac{x^{m-1}}{\Gamma(m)} exp\left[\frac{-mx}{\Omega}\right], x \geq 0 \quad \text{.....(3)}$$

Ω is the expected value of the distribution and can be interpreted as the average received power and m is the shape or fading parameter. The values of the parameters m and Ω are functions of distance. So, the Nakagami model is defined by two functions: Ω (d) and m (d).

The Nakagami model is a general model, the Rayleigh distribution is a special case of Nakagami distribution where m (d) = 1 (for every d).

iii. *Rayleigh Fading/Propagation Model*

Rayleigh fading is the name given to the form of fading that is often experienced in an environment where there is a large number of reflections present. The Rayleigh fading model uses a statistical approach to analyze the propagation, and can be used in a number of environments.

Rayleigh distribution is defined by the following probability density function:

$$f(x) = \frac{2x}{\Gamma(m)\Omega^m} exp\left[\frac{-x^2}{\Omega}\right], x \geq 0 \quad \text{..... (4)}$$

4. Methodology

In this paper, the VANET analysis for real time traffic goes through two steps:

i) Real Traffic Mobility Generation using traffic simulator
ii) Network Simulation using network simulator

a. Traffic Simulator

Traffic simulation is Mathematical modelling of transportation systems which is used for the application of computer software in order to help and provide a better way to effectively plan, design and operate transformation systems.

i. *Simulation of Urban Mobility*

Simulation of Urban Mobility (SUMO) is an open source traffic simulation package including net import and demand modelling components. SUMO helps to investigate several research topics e.g. route choice and traffic light algorithm or simulating vehicular communication. Therefore, the framework is used in different projects to simulate automatic driving or traffic management strategies.

Here the SUMO is used to generate real traffic on 4- way intersection junction to create real time traffic.

Steps Generating Real Time Traffic on 4-way intersection Junction

The fig. 4 shows the steps involved in creating the real-time traffic on 4-way intersection Junction. First a node file is created with a given number of nodes having node ID, position, type and other attributes. This node in real field represents the junction of the road network. The edge file is also created along with node file. The edge file joins the node, which has a unique ID, source node to destination node, type and other attributes. After that another file called connection file is defined, which describe how a node's incoming and outgoing edges are connected. We can specify connections on the edge level or you can declare in in detail which incoming lane shall be connected to which outgoing lanes. All together these three files are used to convert into network file with "netconvert command".

Traffic demand and route data is defined together with vehicle type data in a file with the extension name.rou.xml. And then sumo configuration file is written, which takes input as route file and network file and generate the trace file which is later used to convert into ns2mobility trace file using traceExporter.py command of sumo.

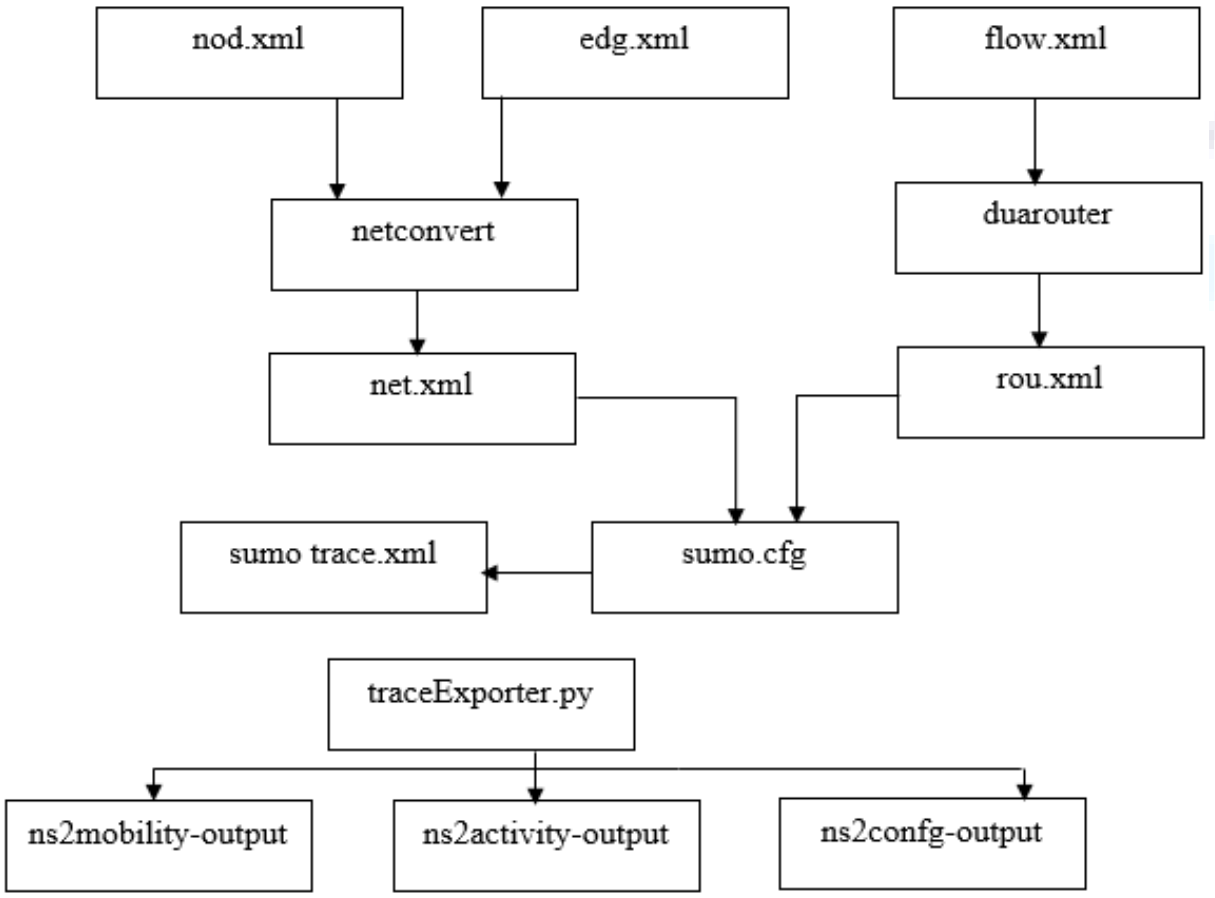

Figure 9: Steps involve in Generating Real Traffic Mobility

b. Network Simulator

A network simulator consists of a wide range of networking technologies and protocols and help users to build complex networks from basic b uilding blocks like clusters of nodes and links.

i. NS3

NS-3 is a discrete-event network simulator and a free software which succeeds popular network simulator NS-2, licensed under the GNU GPLv2 license and is publicly available for research, development and use [9]. The goal of the NS-3 project is to develop a preferred, open simulation environment for networking research. NS-3 is available for Linux, Mac OS and MS Windows using Cygwin.

A simple NS3 script can be written in either C++ or Python language. NS-3 is built on both-C++ and Python bindings. Here C++ scripts is used in simulation. Here different propagation module and wave as well as 802.11p modules have used for the performance analysis of VANET.

5. Simulation

The fig. 5 shows the real-time traffic on 4-way intersection Junction create for VANET analysis.

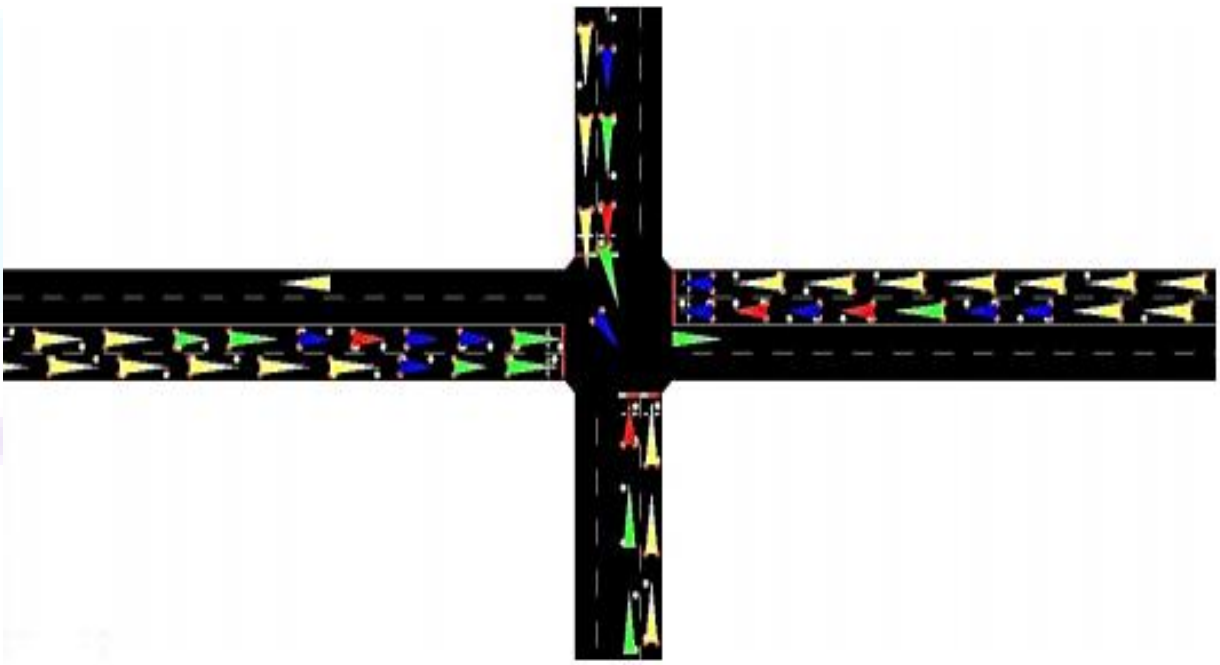

Figure 10: 4-way Junction Traffic Simulation

The VANET network is simulated under various propagation model using the above generated mobility file. The fig. 6 shows the animation of simulation of VANET.

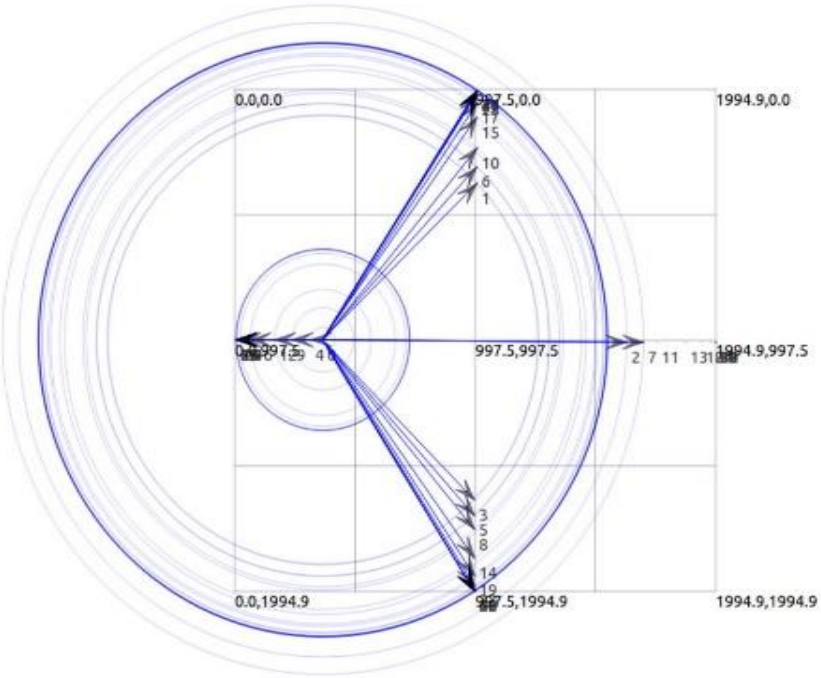

Figure 11. Packet delivery in VANET

The simulation parameter used for VANET simulation and traffic simulation is given in Table 1.

Table 1: The simulation parameter used of VANET simulation and traffic simulation

MAC/Phy Layer Parameter	**Value**
Area	2KM * 2KM
Propagation Model	Two Ray, Rayleigh, Nakagami
MAC Protocol	802.11P
Basic Safety Packet Size	200B
Rate	6Mbps
Application Routing Packet Size	64B
Application Rate	2.048Kbps
Transmit Power (dBm)	20
Carrier Frequency f_0	5.9GHz
Antenna Height above z	1.5
Antenna gains of transmitter and receiver	1
Vehicle No.	120
Vehicle Type	CAR
Car-following Model	Krauβ-model
Sigma (Driver imperfection 0-1)	0.5
Lane Max Speed in Km/hr	70,40
Car Maximum Speed	170,140,110

6. Result and Discussion

Different propagation model for VANET are compared on the basis of packet delivery ratio and throughput

by simulation in real traffic environment. The packet delivery ratio and throughput along with the delay in packet transmission are most widely used parameter in VANET analysis. However here only two PDR and throughput are chosen for analysis purpose, here the focus is not given to delay in packet transmission. The packet delivery ratio gives the idea of how many packets are successfully received out of transmitted packets. And the throughput gives the idea of time rate of successfully received packets in the network. So these two parameters analyze the performance of VANET.

Packet Delivery Ratio= Total Packet Received/Total Packet Sent

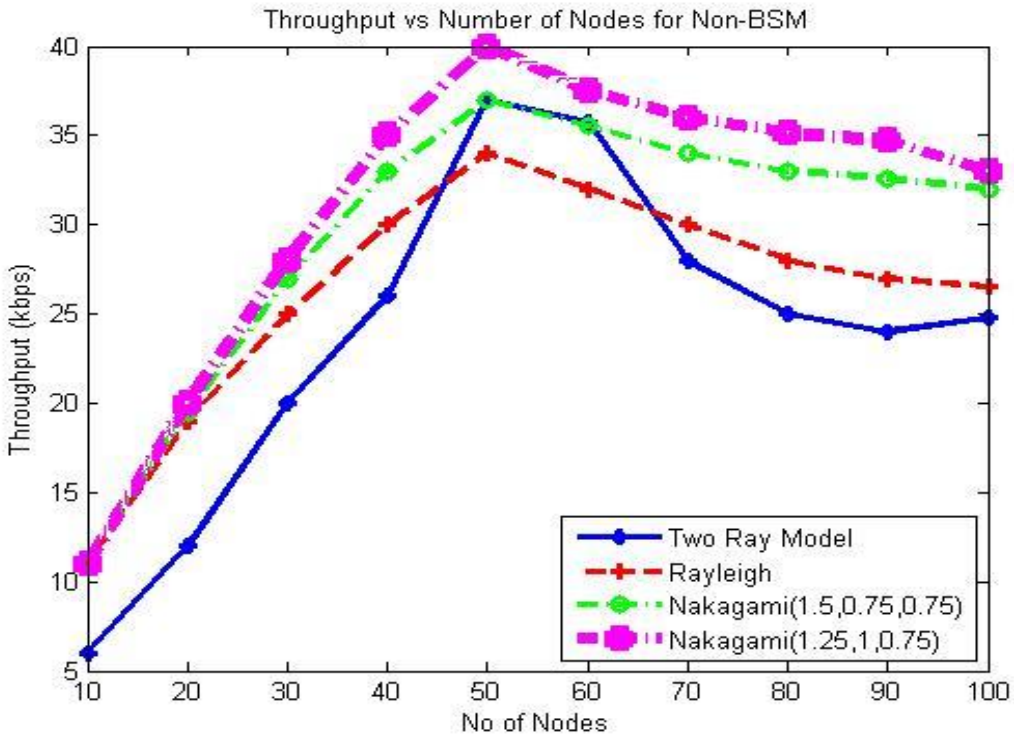

Figure 12: Throughput Vs No. of Nodes for Non-BSM packets

The fig.7 shows the variation of throughput vs number of nodes for different propagation model. It is found that the Nakagami model perform better than other two. Because the Nakagami model is the general model and it consider all the possibilities for signal fading, which is more realistic in VANET scenario. The Nakagami model can also be configured according to our requirement. Here the two cases of Nakagami model are used. Rayleigh model is a special case of Nakagami mode. The TwoRayGround propagation model does not perform well because it considers only line of sight and multi path component by single ground reflected wave.

The fig. 8 shows the variation of throughput vs number of nodes for BSM packets for 200m safety ranges. The Nakagami model performs better than other two methods. The throughput increases rapidly initially in all cases up to 60 number of nodes and then it starts to increase gradually. Initially there is less number of vehicle in the fixed simulation area so the successful reception of BSM packets is maximum but as the number of vehicle starts to increases the channel congestion and interference level also increases due to which the throughput rate of increment becomes slow.

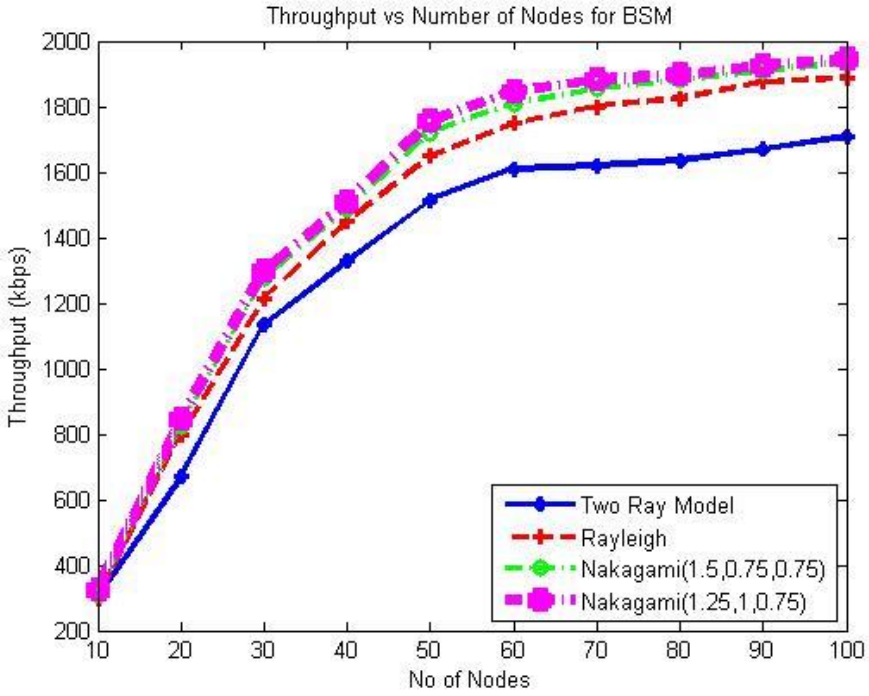

Figure 13. Throughput vs No. of Nodes for BSM packets

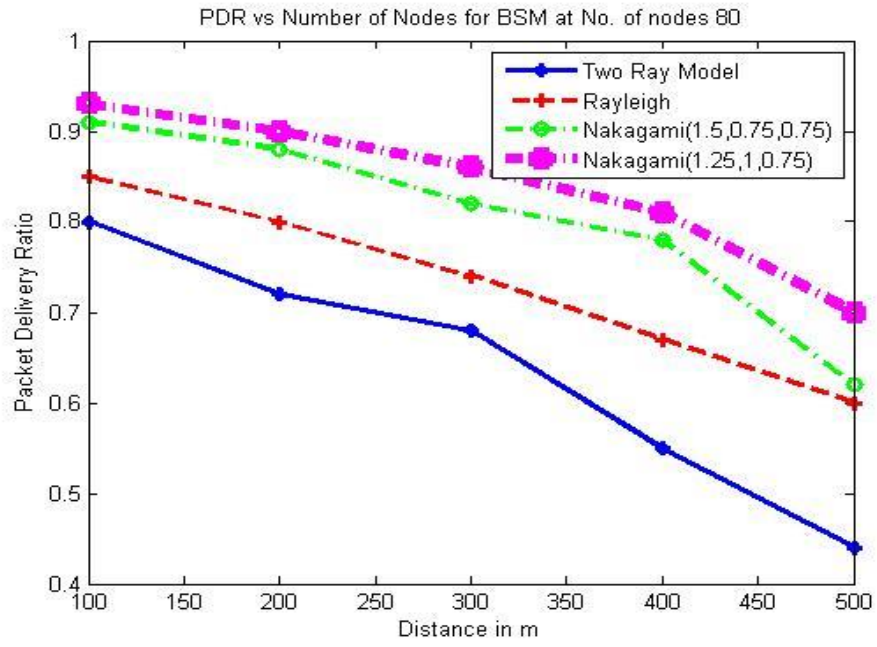

Figure 14. PDR vs Number of Nodes for BSM at No. of Nodes 80

The fig. 9 shows the variation of packet delivery ratio vs distance for BSM packets at 80 number of nodes. The packet delivery ratio decreases as the distance increases. The performance of Nakagami model is better than others.

7. Conclusion and Future Works

This paper compares the performance of different propagation model based VANET on real traffic environment generated by SUMO on the basis of throughput and packet delivery ratio. It has been found that the performance of VANET is better in the case of Nakagami model. The Rayleigh model is a special case of

Nakagami model.

It is concluded that the Nakagami model is more realistic and suitable radio propagation model for dynamic structure and multi hop based communication network like VANET.

The performance of VANET is not only affected by propagation model, the MAC layer has also great effect on its performance. The VANET performance can also be improved by using cluster based communication. So, In the future the analysis can be carried out on cluster based VANET along with the MAC layer.

References

[1] Huixian Wang et al., "*VANET Modelling and Clustering Design Under Practical Traffic, Channel and Mobility Conditions*", IEEE Transactions on Communication, March 2015

[2] Amendment 6: "Wireless Access in Vehicular Environment (Part 11: Wireless LAN medium access control (MAC) and physical layer (PHY) speci-fications)", IEEE Std 802.11p TM-2010, Jun. 17, 2010.

[3] D.S.Baral, K.K.Jha," VANET Analysis for Real Time Traffic of Nepal Using SUMO and NS3 under different protocol", IOE Graduate Conference, December 2015
http://vehicularcommunication.blogspot.com/ 27 September, 2015

[4] H. Su and X. Zhang, "*Clustering-based multichannel MAC protocols for QoS provisionings over vehicular Ad Hoc networks*", IEEE Trans. Veh. Technol., vol. 56, no. 6, pp. 3309–3323, Nov. 2007.

[5] Mr. Rafi U Zamam "*An Efficient DSDV Routing Protocol for Wireless Mobile Ad Hoc Networks and its Performance Comparison*", http://www.computer.org/portal/web/csdl/doi/10.1109/EMS.208.11" /2 October 2, 2016

[6] Vahid Garousi, "*Simulating Network traffic in Multi-hop Wireless Ad Hoc Networks based on DSDV (Destination Sequenced Distance Vector) protocol using NS (Network Simulator) Package*", University of Waterloo, fall 2001.

[7] Khan, I. Qayyum, A. Center of Res. in Networks & Telecom (CoReNeT), M.A. Jinnah Univ., Islamabad, Pakistan, "*Performance evaluation of AODV and OLSR in highly fading vehicular ad hoc network environments*" appears in Multitopic Conference, INMIC 2009, IEEE 13th, International Issue, 14-15 Dec. 2009 On page(s): 1 – 5

[8] V. Naumov, R. Baumann, and T. Gross, "*An evaluation of inter-vehicle ad hoc networks based on realistic vehicular traces*," in MobiHoc '06: Proceedings of the 7th ACM international symposium on Mobile ad hoc networking and computing. New York, NY, USA: ACM, 2006, pp. 108-119.

[9] Sommer, C.; Dressler, F.; Univ. of Erlangen Nuremberg, Erlangen, "*Progressing Towards Realistic Mobility Models in VANET Simulations*" appears in: Communications Magazine, IEEE Issue Date: November 2008, Volume: 46 Issue:11 On page(s): 132 – 137

[10] "*IEEE standard for information technology–telecommunications and information exchange between systems–local and metropolitan area networks–specific requirements part 11: Wireless lan medium access control (mac) and physical layer (phy) specifications amendment 6: Wireless access in vehicular environments*," IEEE, pp. 1–51, 2010

[11] Pranav Kumar Singh, Kapang Lego "*Comparative Study of Radio Propagation and Mobility Models in Vehicular Adhoc Network*", International Journal of Computer Application, 2011.

Part V: Construction Field and Building Techniques

A Critical Analysis of the Most Significant Causes of Skilled Workers' Low Performance in Nepalese Construction Industry

Arvind Neupane[1], Jibendra Mishra[2]

[1]*ACEM & LEC alumnus*
[2]*Project Manager, Trade Route Improvement Project, DOR, Butwal*

Abstract

Skilled workers' performance is one of the crucial aspects of labor productivity that requires proper attention for effective projects delivery in the construction industry. The level of skilled workers' low performance has been seen to be a major factor which contributes toward inefficient construction projects productivity. Therefore, the objective of this research is to identify the most significant causes of low-skilled workers' performance in construction projects in the Nepal. The objective was achieved through a structured quantitative method of questionnaire distributed to 43 respondents that comprise of active stakeholders in the Nepalese construction industry. 43 responses representing 100% were retrieved. The data were analyzed using descriptive statistics and MS-Excel 2007. The finding shows that; low wages of skilled workers, delay in payment of skilled workers' wages, delay in supply of materials and equipment to site, lack of incentive scheme programs for skilled workers & shortage of plants and equipment on site were the most significant causes of low-skilled workers' performance in the Nepalese construction industry. The research findings indicate the need for stakeholders in the Nepalese construction industry to provide incentives and motivate skilled workers, provision of materials and equipment on time, increase the wages as time progresses, make timely payments to the workers and prevent the shortage of plants and equipment on site in order improve low-skilled workers' performance in Nepalese construction industry towards optimal performance.

Keywords: *project performance; skilled workers; construction industry*

1. Introduction

Construction industry in many developing countries are greatly concerned with low level of skilled workers' productivity due to economic, social, physical and psychological related factors influencing the performance of the skilled workers. Low productivity of skilled workers' is one of the most serious tasks facing the construction industry especially in developing countries such as Malaysia, Indonesia, Singapore, Hong Kong, and other states in South East Asia. In today's global economic, skilled workers' productivity is becoming more intense than ever due to the low level of quality performances of the skilled workers in the construction industries in most developing countries. M. Arshad and Ab Malik assert that, productivity improvement can be achieved when construction workers with high skills and knowledge, together with sound

physical and mental health perform tasks with efficiency and effectiveness. In most countries, the cost of operatives comprises 30 % to 50 % of the overall projects' cost, and thus, it is regarded as a true reflection of the efficiency of the operation.

2. Methodology

The methodology of the study was based on cross-sectional quantitative research design. Available data from the department of roads and DUDBC was used to locate various road and building projects inside Rupandehi. From literature review, twenty-three causes of low performance were identified. Five scale importance indices of Likert's scale (5 to 1-point scale: strongly agree=5, agree=4, neutral=3, disagree=2, strongly disagree =1) was used to get perception of the participants. Field survey and unstructured interview with concerned Project Managers, Project Engineers, Site Engineers and Site Supervisors was done.

The process of developing questionnaire finished with a pilot survey, which was used to modify and eliminate a number of variables until the final questionnaire was designed. Experts on the subject were consulted, to ensure that the questions were properly phrased, and the suitability of the questionnaire was tested on a sample of six respondents (one project manager, four engineers and a sub-engineer) working on different building and road construction projects outside Rupandehi district, to ensure a suitable coverage of the domain of each construct.

43 questionnaires were distributed to the participants (project/contract managers, project engineers, site engineers, sub-engineers and supervisors) who were directly monitoring the performance of the skilled workers and who were dealing with low-performance issues. All 47 of the questionnaires were received and analyzed. The primary data sources were structured questionnaires. The secondary data sources were various published and unpublished reports, articles, thesis and related literature for review literature of this study.

3. Data Analysis

This chapter deals with the analysis and interpretation of the data that has been gathered to meet the objectives of this study. The descriptive and analytical study of data has been done to show the association of dependent and independent variables. For this, the questionnaires were distributed to the key stakeholders: project managers, project engineers, site engineers and site supervisors of different building and road construction projects in Rupandehi district. The total questionnaires distributed were collected and all responses were kept for analysis and interpretation.

The analysis of data is grouped into three major segments:

a) Demographic distribution/analysis of the respondents.
b) Distribution and analysis of responses for each of the listed variables/causes
c) Ranking of the listed causes by their mean score and analysis of the most significant of the causes.

The collected data were analyzed in MS-Excel 2007. In this part simple descriptive analysis and interpretation of data is presented. Simple descriptive analysis includes distribution analysis of different independent as well as dependent variables in the form of percentage and frequencies.

4. Findings

Following tables (Findings Part: I) show demographic distribution of participants:

Table 1: Distribution of respondents' positions in Organization

Position	Frequency	Percentage
Project Manager	7	16.27
Project Engineer	8	18.6
Site Engineer	10	23.25
Site Supervisor	18	41.86
Total	43	100

Table 2: Distribution of respondents' working experience

Work experience	Frequency	Percentage
1-3 years	12	28
4-6 years	13	30
7-9 years	11	26
10 years and above	7	16
Total	43	100

Table 3: Distribution of respondents' role in the Organization

Parameters	Frequency	Percentage
Planning programme of works	7	16
Coordinating financial aspects	3	7
Monitoring subcontractors	5	12
Daily operations of field work	7	16
Technical adviser	3	7
Supervision of construction projects	18	42
Total	43	100

Table 4: Distribution of respondents' Age group

Age Group	Number	Percent
Less than 25 yrs.	9	21
25-40 yrs.	27	63
40-55 yrs.	7	16
More than 55 yrs.	0	0

Table 5: Distribution of respondents' Qualification

Qualification	Number	Percent
Masters	10	23
Bachelors	15	35
Diploma	18	42
Total	43	100

The below table (Analysis Part II :) shows distribution and analysis of responses for each of the common existing causes of skilled workers' low performance:

Table 6: Distribution of responses for each of the common existing causes of skilled workers' Low performance

S.N.	Variables	Frequency of Scores					Mean Scores
		1	2	3	4	5	
1.	Low wages of skilled workers			8	20	15	4.16
2.	Delay in payment of skilled workers' wages		3	13	9	18	3.98
3.	Delay in supply of materials and equipment to site	1	3	10	15	14	3.88

4.	Lack of incentive scheme programmes for skilled workers	1	6	7	14	15	3.84
5.	Shortage of plants and equipment on site	2	5	10	14	12	3.67
6.	Excessive rework by skilled workers due to construction errors	2	4	13	12	12	3.65

S.N.	Variables	Frequency of the scores					Mean score
		1	2	3	4	5	
7.	Outdated machines for operation on site	2	8	10	11	12	3.53
8.	Plants malfunction and maintenance on site	2	9	9	11	12	3.51
9.	Unfavorable weather conditions	2	7	13	10	11	3.49
10.	Vulnerability to safety and health care services on site	7	6	4	12	14	3.47
11.	Lack of standard salary scales for skilled workers	4	7	10	10	12	3.44
12.	Lack of opportunity to observe public holidays for skilled workers	3	6	14	10	10	3.42
13.	Ineffective vocational training programmes for skilled workers	5	6	9	13	10	3.40
14.	Lack of free medical facilities for skilled workers	5	5	12	13	8	3.33

5. Evaluation of the Causes/Factors of Low Performance

This section of the research focuses on the mean ranking analyzed on the objective that is 'the most significant causes of low-skilled workers' performance in construction projects in Nepal'. The data analyzed from the survey conducted was evaluated to determine its significance using the average mean index scale adopted by A. Abdullah as shown in table below:

Table 7: Average mean index scale

Average index	Range
1.00 ≤ Average Index < 1.50	Not Significant
1.50 ≤ Average Index < 2.50	Slightly Significant
2.50 ≤ Average Index < 3.50	Moderately Significant
3.50 ≤ Average Index < 4.50	Most Significant
4.50 ≤ Average Index < 5.00	Extremely Significant

Using Table 6 & Table 7, ranks were assigned to all 23 common causes of low performance in descending order of their significance which is summarized in the Table 8 below:

Table 8: Ranking for causes of low-skilled workers' performance in construction projects in Nepal

S. N	Variables	Mean	Rank
1.	Low wages of skilled workers	4.16	1
2.	Delay in payment of skilled workers' wages	3.98	2
3.	Delay in supply of materials and equipment to site	3.88	3
4.	Lack of incentive scheme programmes for skilled workers	3.84	4
5.	Shortage of plants and equipment on site	3.67	5
6.	Excessive rework by skilled workers due to construction errors	3.65	6
7.	Outdated machines for operation on site	3.53	7

8.	Plants malfunction and maintenance on site	3.51	8
9.	Unfavorable weather conditions	3.49	9
10.	Vulnerability to safety and health care services on site	3.47	10
S. N	Variables	Mean Index	Rank
11.	Lack of standard salary scales for skilled workers	3.44	11
12.	Lack of opportunity to observe public holidays for skilled workers	3.42	12
13.	Ineffective vocational training programmes for skilled workers	3.40	13
14.	Lack of free medical facilities for skilled workers	3.33	14
15.	Lack of issuance of training certificates on completion of training programmes	3.19	15
16.	Lack of free residential accommodations for skilled workers	3.14	16
17.	Lack of gifts during festive periods for skilled workers	2.86	17
18.	Lack of sufficient skill acquisition centers for skilled workers	2.74	18
19.	Overcrowding of skilled workers during project execution	2.70	19
20.	Conflicts among skilled workers on site	2.63	20
21.	Lack of free food vouchers for skilled workers	2.47	21
22.	Change of orders of project execution	2.40	22
23.	Lack of free transportations for skilled workers	2.33	23

6. Analysis of Questionnaire Survey

A detailed questionnaire was prepared and sent to 43 personnel who were working in 10 different road and building projects within Rupandehi district of Nepal by direct meeting, regular mail and also via internet. The questionnaire survey method and their responses rate are shown in Table 9 below.

Table 9: Distribution of questionnaire

Questionnaire sent	Direct Meeting	Via. Online	Total
No. of participants	42	1	43
No. of responses	42	1	43
Response rate	100%	100%	100%

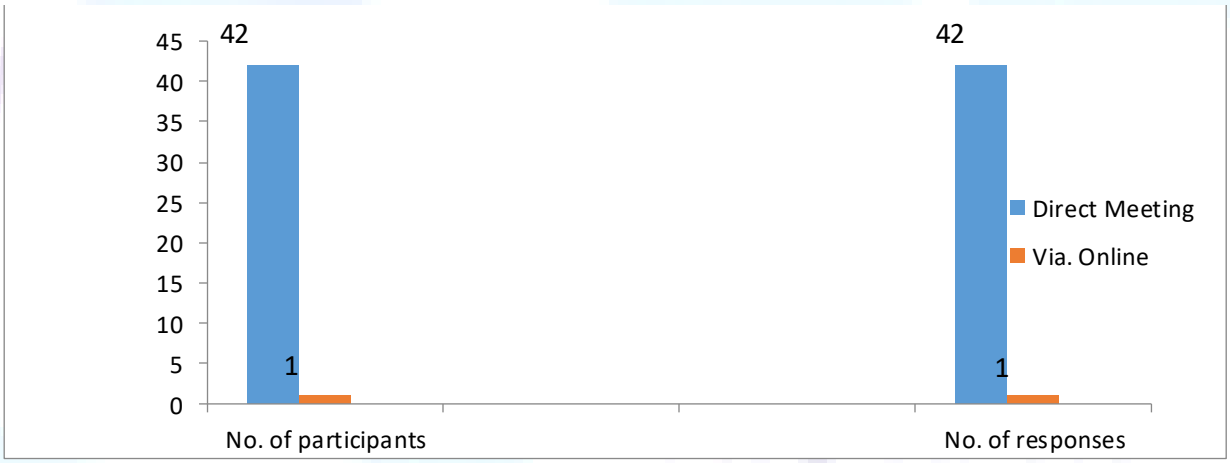

Figure 1: Questionnaire Distribution vs Responses Chart

7. Validity of Research Instrument

Validity refers to the extent to which the instrument really measures what it is supposed to measure (Bastos et al 2003:52). Polit et al. (2004:291-292) refer to four types of validity: face, content, criterion and construct validity. These authors add that although face validity is useful, content, criterion, and construct validity are more important in research instrument. For this, content validity was important. The literature review confirmed content relevance and validity.

Content validity: An instrument has content validity if researchers agree that the instrument is made up of group of items covering all the issues to be measured i.e. that it represents a specific thematic universe. This

is a subjective evaluation, which we consider suitable because these critical factors in the evaluation of the most significant causes of low-skilled workers' performance in construction industry of Nepal have been obtained from a review of the literature and feasibility was tested using a pilot survey. Validity was maintained by the discussions with the research supervisor to identify the core aspects that need to be studied during the research. The researcher used the instrument used by Alhaji Ali Zannah, Aryani Ahmad Latiffi, Abdulazeez Umar Raji, Abdullahi Abba Waziri and Usman Mohammed on the study of the "Causes of low-skilled workers performance in construction projects in Nigeria" which is already a validated research instrument as their paper is officially published online. The research design later on was reconstructed based on the researcher's interest and research objective.

8. Reliability of Research Instrument

Reliability is the level of consistency or accuracy with which the instrument measures the attribute it is intended to measure (Polit et al. 2004:432). Reliability can be measured taking into account the stability of the instrument when the instrument provides the same results in repeated instances; in other words, when an instrument produces the same result in repeated testing (LoBiondo-Wood) & Haber 1998:192).

Tools were developed only after the adequate review of literature and were pre-tested in 10% of the total sample and necessary modifications on tools were made. Questionnaires were made in simple, clear and language based on need. Data were checked for errors and omissions on same day and the consistency of data was maintained. Each filled questionnaire was re-checked so that any under responding can be corrected. The research was conducted in continuous guidance of the research supervisor.

With regard to the reliability of the questionnaire, after submitting it to testing with same individual multiple times, exactly the same results were obtained. Its reliability was thus verified.

9. Ethical Consideration

Ethical considerations are the basic principles established by a discipline or institution so as to guide the researcher when doing research with human beings (Polit et al 2004:431). Ethical considerations are necessary and important when conducting any research in order to protect the human rights of the research subjects (LoBiondo-Wood & Haber 1998:171).

For this study, consensus from the Lumbini Engineering Management and Science College research committee was taken before conducting the research. Similarly, approval from the concerned contractors was taken for the study. First, explanation about the study was given to the respondents before collecting the data and after their consent the data were collected voluntarily. Confidentiality regarding the personal identity was maintained. No omission, manipulation and correction of the actually collected data were done for the researcher's own purpose. For this study, the following ethical considerations were upheld: respect for the person, beneficence, justice, loyalty, truthfulness, and confidentiality.

Respect for the person is related to autonomy and enables the person to choose whether or not to participate in a study. It is also the protection of individuals whose autonomy is altered or diminished thus making them more vulnerable to abuse or harm, such as the elderly, children and patients.

Beneficence aims to safeguard the participant's well-being and prevent deliberate or potential damage.

Justice is the ethical obligation of treating each person correctly and fairly, in other words, to accord each one, in an equal (impartial) manner, onus (obligation) and benefit.

Loyalty involves trust between researcher and participant.
Truthfulness is the obligation to tell the whole truth about the possibility of risks, real and potential damage (possible; virtual) and any other occurrence during or after participating in the study.
Confidentiality refers to researchers' obligation to guarantee the participants' right to anonymity (Secaf 2001:48-49)

10. Eligibility Criteria

Inclusion criteria: Sample comprised of all the personnel who are directly related and concerned with the performance of skilled workers and who themselves are one of them. The selected respondents are the key stakeholders like: project managers, project engineers, site engineers and site supervisors mainly. Only the persons who gave their consent to participate in the study were included

Exclusion criteria: Sample did not comprise of the respondents who do not have anything to do with the low performance of skilled workers and also those who do not monitor their performance in the projects.

11. The Most Significant Causes of Low Performance (output from questionnaire survey)

Based on the revelations of Table 8 and with reference to Table 7, eight causes were found to be the most significant ones accountable for the low performance of skilled workers in the construction industry in Nepal.

Eight of the most significant causes of low performance of skilled workers are: 1) low wages of skilled workers, 2) delay in payment of skilled workers' wages, 3) delay in supply of materials and equipment to site, 4) lack of incentive scheme programmes for skilled workers, 5) shortage of plants and equipment on site, 6) excessive rework by skilled workers due to construction errors, 7) outdated machines for operation on site and 8) Plants malfunction and maintenance on site.

12. Conclusion

A case study comprising 43 respondents that included Project Managers, Project Engineers, Site Engineers and Site Supervisors from 10 different road and building projects inside Rupandehi district aimed at finding the most significant causes of skilled workers' low performance revealed eight causes as the critical ones.

Based on questionnaire survey, low wages of skilled workers with the highest mean index of 4.16 ranked first in the critical list. Seemingly, skilled workers are highly concerned about the monetary value of their work and efforts in the first place, accompanied by timely payments of wages, and on time delivery of materials & equipment, having respective indices of 3.98 & 3.88, in the second and third priorities respectively.

While lack of incentive scheme programs, shortage of plants and equipment on site, excessive rework due to construction errors, outdated machines for operation on site, and plants malfunction & maintenance on site standing next on the significance list makes it apparent that skilled workers are motivated highly by extra motivational factors viz. provision of bonuses and flexible working hours. Similarly, poor management of plants and equipment coupled with redundancy in works due to provision of faulty drawings and instructions are also critically accountable for low productivity of skilled workers.

13. Recommendations

Based on the findings of the research, following recommendations are drawn for optimizing performance

of skilled workers:

However, in light of the preceding conclusions, the following recommendations are offered as possible means of enhancing skilled workers' performance in Nepalese construction industry, particularly in building and road construction projects inside Rupandehi District as it will go a long way in reducing the poor quality of building and road stock being constructed in the area. Contractors in the Nepalese construction industry should take it as a responsibility to provide incentive scheme programmes to skilled workers as such incentive programs increase overall performance of the workers. Incentive scheme programs are often used to reduce turnover, boost morale and loyalty, improve workers' wellness, increase retention, and drive daily performance of skilled workers. Likewise, increasing the wages of the skilled workers as they gain more experience in the organization, paying them on time, making sure that materials and equipment arrive the site on timely manner & providing required number of plants and equipment on site are some major recommendations for the contractors who mainly benefit from the performances of their skilled workers.

References

[1] Abdullah, A., Mohandes, S., Hamid, A., & Singh, B. (2016). *The Practices of Corporate Social Responsibility among Construction Companies in Malaysia*. Research Journal of Applied Sciences, Engineering and Technology, 2(7), 742–755.

[2] Abdulsalam, D., Faki, A. I., & Dardau, A. A. (2012). *Impact Assessment of Incentive Schemes for theSustainable Development of Nigerian Construction Industry*. Journal of Civil Engineering and Architecture, 6(9), 1194–1201.

[3] Adamu, K. J., Dzasu, W. E., Haruna, A., & Balla, S. K. (2011). *Labour productivity constraints in the Nigerian construction industry*. Continental Journal of Environmental Design and Management, 1(2), 9–13.

[4] Adedokun, O. A., Ibironke, O. T., & Olanipekun, A. O. (2013). *Vulnerability of motivation schemes inenhancing site workers productivity for construction industry's sustainability in Nigeria.* International Journal of Sustainable Construction Engineering and Technology, *4(1), 21–30*

[5] Adewale, P. O., Siyanbola, A. B., & Siyanbola, S. O. (2014). *Building craftsmanship skill developmentand Nigeria's vision 20: 2020: Imperatives and daunting challenges.* International Journal of Vocational and Technical Education, 6(4), 36–42.

[6] Aibinu, A. A., & Jagboro, G. O. (2002). *The effects of construction delays on project delivery in Nigerian construction industry.* International Journal of Project Management, 20(8), 593–559.

[7] Aina, O. O., & Adesanya, D. A. (2015). *Factors affecting performance of incentive schemes in theconstruction industry in Nigeria*. Civil and Environmental Research, 8(7), 81-89.

[8] Aiyetan, A. O., & Olotuah, A. O. (2006). *Impact of motivation on workers' productivity in the Nigerian construction industry*. In D. Boyd (Ed.), Proceedings 22nd Annual ARCOM Conference, 4–6 September 2006, Birmingham (UK), Association of Researchers in Construction Management (pp. 239–248).

[9] Akinsiku, O. E., & Akinsulire, A. (2012). *Stakeholders' perception of the causes and effects of construction delays on project delivery*. Journal of Construction Engineering and Project Management, 2(4), 25–31.

[10] Alhaji Ali Zannah 1, Aryani Ahmad Latiffi 2, Abdulazeez Umar Raji 3, Abdullahi Abba Waziri 4, Usman Mohammed 4. *Causes of Low-Skilled Workers' Performance in Construction Projects.*

[11] Alinaitwe, H., Mwakali, J., & Hansson, B. (2006). *Factors Affecting Productivity of Building Craftsmen A Case of Uganda.* In Proceedings from the International Conference on Advances in Engineering and Technology *(*pp. 277–284).

[12] Ameh, O. J., & Shokumbi, B. B. (2013). *Effectiveness of non-financial motivational scheme on construction workers output in Nigeria*. Ethiopian Journal of Environmental Studies and Management, 6(3), 263-72.

[13] Arshad, M. N., & Ab Malik, Z. (2015). *Quality of human capital and labour productivity: A Case ofMalaysia.* International Journal of Economics, Management and Accounting, 23(1), 37–55.

[14] Attar, A. A., Gupta, A. K., & Desai, D. B. (2012). *A study of various factors affecting labourproductivity and methods to improve it.* IOSR Journal of Mechanical and Civil Engineering, 1(3), 11-14.

[15] Baral Santosh. *http://santoshbaral.blogspot.com/2009/12/nepalese-construction-industry.html*

[16] Bernardin, H. J., Kane, J. S., & Wiatrowski, M. (1995). *Performance appraisal*. In N. Brewer & C. Wilson (Eds.), *Psychology and Policing* (pp. 257–289). Hillsdale: Lawrence Erlbaum Associates.

[17] Bernstein HM (2007). *Measuring Productivity in Construction: Improving Business Performance*. Dodge Sweets Architectural Record ENR Regional Publications.

[18] Bheemaiah, K., & Smith, M. J. (2015, June 2). *Inequality, Technology and Job Polarization of the Youth Labour Market in Europe*

[19] Bilau, A. A., Ajagbe, A. M., Kigbu, H. H., & Sholanke, A. B. (2015). *Review of shortage of skilledcraftsmen in small and medium construction firms in Nigeria.*. Journal of Environment and Earth Science, 5(15), 5–12.

[20] Brockman, J. (2012, December). *The Cost of Interpersonal Conflicts in Construction.*

[21] Chandra, H. P. (2015). *Initial investigation for potential motivators to achieve sustainable construction safety and health.* Procedia Engineering, 125, 103–108.

[22] Cox, R. F., Issa, R. R., & Frey, A. (2006). *Proposed Subcontractor-Based Employee Motivational Model.* Journal of Construction Engineering and Management, 132(2), 152–163.

[23] Danso, H. (2014). *Poor Workmanship and Lack of Plant/Equipment Problems in the ConstructionIndustry in Kumasi, Ghana.* International Journal of Management Research, 2(3), 60–70.

[24] Davenport, T. H. (2008). *Thinking for a living: how to get better performances and results fromknowledge workers.* Boston: Harvard Business Press.

[25] Doloi, H., Sawhney, A., Iyer, K. C., & Rentala, S. (2012). *Analysing factors affecting delays in Indian construction projects.* International Journal of Project Management, 30(4), 479–489.

[26] Enshassi, A., Mohamed, S., Mustafa, Z. A., & Mayer, P. E. (2007). *Factors affecting labour productivityin building projects in the Gaza Strip*. Journal of Civil Engineering and Management, 13(4), 245–254

[27] Funso, A., Sammy, L., & Gerryshom, M. (2016). *Application of Motivation in Nigeria Construction Industry: Factor Analysis Approach.* International Journal of Economics and Finance, 8(5), 271–276.

[28] Garcés-Mascareñas, B. (2015). *Revisiting bordering practices: Irregular migration, borders, and citizenship in Malaysia.* International Political Sociology, 9(2), 128–142.

[29] Ghoddousi, P., Poorafshar, O., Chileshe, N., & Hosseini, M. R. (2015). *Labour productivity in Iranian construction projects: Perceptions of chief executive officers*. International Journal of Productivity and Performance Management, 64(6), 811–830.

[30] Griggs, T. L., Eby, L. T., Maupin, C. K., Conley, K. M., Williamson, R. L., Griek, O. H., & Clauson, M. G. (2016). *Who Are These Workers, Anyway?* Industrial and Organizational Psychology

[31] Hershcovis, M. S., Barling, J. (2010). *Towards a multi-foci approach to workplace aggression: A meta-analytic review of outcomes from different perpetrators*. Journal of Organizational Behavior, 31(1), 24–44.

[32] Hickson, B. G., & Ellis, L. A. (2014). *Factors affecting construction labour productivity in Trinidadand Tobago*. The Journal of the Association of Professional Engineers of Trinidad and Tobago, 42(1), 4–11.

[33] Hughes, P., & Ferrett, E. (2016). *Introduction to Health and Safety in Construction: for the NEBOSH National Certificate in Construction Health and Safety* (5th ed.). Abingdon; New York: Routledge.

[34] Husseini, A. A. (1992). *The importance of manpower training and management to the construction industry*. In Proceedings of National Seminar on Effective Contract Management in the Construction Industry

[35] Hyder, M. B. (2016). *Vulnerability, sustainable livelihoods and workers' rights: a case study ofconstruction workers in Dhaka, Bangladesh* (Master's thesis).

[36] Ibrahim, M. (2013). *Contractors perspective toward factors affecting labour productivity in building construction.* Engineering, Construction and Architectural Management, 20(5), 446-60.

[37] Ikediashi, D. I., Ogunlana, S. O., Awodele, O. A., & Okwuashi, O. (2012). *An evaluation of personneltraining policies of construction companies in Nigeria.* Journal of Human Ecology, 40(3), 229–238.

[38] Jarkas, A. M., & Radosavljevic, M. (2013). *Motivational factors impacting the productivity of construction master craftsmen in Kuwait.* Journal of Management in Engineering, 29(4), 446-454.

[39] Joe Hannsen, *https://top7business.com/?expert=Joe_Hannsen*

[40] Kamar, K. A., Azman, M. N.,& Nawi, M. N. (2014). IBS Survey 2010: *Drivers, Barriers and the CriticalSuccess Factors in Adopting Industrialized Building System (IBS) Construction by G7Contractors in Malaysia*. Journal of Engineering Science & Technology, 9(5), 490–501.

[41] Kaming, P. (1997). *Factors influencing craftsmen's productivity in Indonesia*. International Journal of Project Management, 15(1), 21-30.

[42] Kazaz, A., Manisali, E., & Ulubeyli, S. (2008). *Effect of basic motivational factors on construction workforce productivity in Turkey*. Journal of Civil Engineering and Management, 14(2), 95–106.

[43] Kuroshi, P. A., Lawal, M. (2014). *Study of internal factors affecting labour productivity in mediumsized construction firms in Nigeria*. International Journal of Education and Research, 2(12), 83–92.

[44] Liepmann, K. (1960). *Apprenticeship: An Enquiry into Its Adequacy under Modern Conditions*. London: Routledge.

[45] Ling, Y. Y., & Tan, F. (2015). *Selection of site supervisors to optimize construction project outcomes*. *Structural Survey, 33*(4/5), 407-422.

[46] Lowe G (1987). *The Measurement of Productivity in the Construction Industry*. Construction Management and Economics, 5, pp. 101-113.

[47] Modular Building Institute. (2010). *Improving efficiency and productivity with modular construction*.

[48] Moselhi, O., Assem, I., & El-Rayes, K. (2005). *Change orders impact on labour productivity*. Journal of Construction Engineering and Management, 131(3), 354–359.

[49] Motwani J, Kumar A, and Novakoski M (1995). *Measuring Construction Productivity: A Practical Approach.* Work Study, 44(8), p. 18-20.

[50] Mr. A.A. Attar, Prof. A.K. Gupta, Prof. D.B. Desai. *A Study of Various Factors Affecting Labour Productivity and Methods to Improve It.*

[51] Naoum, S. G. (2016). *Factors influencing labor productivity on construction sites: A state-of-the-art literature review and a survey*. International Journal of Productivity and Performance Management, *65*(3), 401-421.

[52] Odesola, I. A, Otali, M., & Ikediashi, D. I. (2013). *Effects of project-related factors on construction labour productivity in Bayelsa State of Nigeria*. Ethiopian Journal of Environmental Studies and Management, 6(2), 817–819.

[53] Odesola, I. A. (2015). *Assessment of Management-Related Factors Affecting Construction LabourProductivity in Cross River State of Nigeria*. Covenant Journal of Research in the Built Environment, *3*(2), 13–29.

[54] Odia, L. O, & Omofonmwan, S. I. (2007). *Educational system in Nigeria problems and prospects*. Journal of Social Sciences, 14(1), 81–86.

[55] Offei–Nyako, K., Osei–Tutu, E., Fugar, F. D., & Adinyira, E. (2013). *Skilled artisanal availability in theGhanaian construction industry*. Covenant Journal of Research in the Built Environment, 1(1), 1–9.

[56] Ogochukwu, O. C. (2014). *Evaluatingthe Impact of Construction Crafts' Skills Acquisition and Critical Knowledge Development on Project Performance in Nigeria* (Doctoral thesis). Okafor, N. (2010). *Funding the Rehabilitation of Universities*. The Alumnus Special Millennium Education Journal, 1, 55–56.

[57] Olateju, B. (1992). *Enhancing the contract management capabilities of the indigenous contractors*. In Proceedings of National Seminar on Effective Contract Management in the Construction Industry, Ikeja, August 22–23, 1991 (pp. 132–143). Lagos: Nigerian Institute of Building.

[58] Olatunji, O. A, Aje, O. I, Odugboye, F. (2007). *Evaluating health and safety performance of Nigerianconstruction site*.

[59] Olubodun, O. (1985). *Low productivity of the Nigerian construction workers*. InReport No. Unpublished Seminar Paper, Building Department, OAU, Ile-Ife.

[60] Oni, C. S. (2007). *Globalization and Its Implication for Vocational Education in Nigeria*. Essays in Education, *21*(1), 30.

[61] Oseghale, B. O, Abiola-Falemu, J. O., & Oseghale, G. E. (2015). *An Evaluation of Skilled Labourshortage in selected construction firms in Edo state, Nigeria*. American Journal of Engineering Research, 1(4), 156–167.

[62] Parida, R., Sarkar, S., & Ray, P. (2016). *Selection of Alternate Work Systems to Improve OccupationalHealth of Indian Construction Workers: A Design of Experiment-Based Approach*. In P. Mandal &J. Vong (Eds.), Smart Technologies for Smart Nations (pp. 155–173). Singapore: Springer Singapore.

[63] Randolph Thomas, William F. Maloney, R. Malcolm, W. Horner, Gray R. Smith, Vir K. Handa, Steve R. Sanders. *Modeling construction labor productivity Journal of Construction Engineering and Management,* ASCE, 116 (4) (1990), pp. 705-726

[64] Salisu, J. B., Chinyio, E., & Suresh, S. (2015). *The impact of compensation on the job satisfaction ofpublic sector construction workers of jigawa state of Nigeria*. The Business & Management Review, 6(4), 282–296

[65] Schwarzkopf, W. (2004). *Calculating lost labour productivity in construction claims* (2nd ed.). Maryland: Frederick Aspen Publisher.

[66] Sheebe, J. (2016). *A study on the impact of training programs of Central Board for Workers Educationon the quality of work life of the organized, unorganized and rural labour in Kerala*.

[67] Sherekar. V., & Tatikonda, M. (2016). *Impact of Factor Affecting on Labour Productivity inConstruction Projects by AHP Method*. International Journal of Engineering Science and Computing, 6(6), 6771–6775.

[68] Sinha, P. (2015). *Towards higher maintenance effectiveness: Integrating maintenance management with reliability engineering*. International Journal of Quality & Reliability Management, *32*(7), 754–762.

[69] Sweet, S., & Meiksins, P. (2017). *Changing contours of work: Jobs and opportunities in the new economy* (3rd ed.)

[70] Uchitelle, L. (2009, June 23). *Despite Recession, High Demand for Skilled Labor*. The New York Times.

[71] Wong, J. M., Ng, S. T, & Chan, A. P. (2010). *Strategic planning for the sustainable development of the construction industry in Hong Kong*. Habitat International, 34(2), 256–263.

[72] Yerramreddy, V. A. (2014). *Schedule Quality: Delay Analysis Perspective* (Doctoral dissertation).

[73] Zhang, L, & Huo, X. (2015). *The impact of interpersonal conflict on construction project performance*: A moderated mediation study from China. International Journal of Conflict Management, *26*(4), 479–498.

[74] Zou, P. X., Zhang, G., & Wang, J. (2007). *Understanding the key risks in construction projects in China*. International Journal of Project Management, *25*(6), 601–614.

Effective Utilization of Plastic Wastes in Asphalt Concrete

Rup Bahadur Rawal[1,2], I. M. Amatya[2], Anil Marsani[2]

[1]*Central Laboratory, Departmetn of Roads, Government of Nepal*
[2] *Department of Civil Engineering, Institute of Engineering, Tribhuvan University Pulchowk, Lalitpur, Nepal*

Abstract

This research was carried out to see the performance of waste plastic as binder with bitumen for asphalt concrete road. The study also aimed to find out the Marshall stability value with addition of different percentage of plastic and compare this values with the standard values of other relevant parameters like flow value, density, percentage air voids, VMA, VFB. The main aim of this research was to focus on improvement of Marshall Stability value by addition of partial amount of waste plastic to hot aggregate, before preparing Asphalt Concrete. Plastic waste, consisting of carrying bags, cup and other utilized plastic are separated from municipal solid waste. The plastic wastes (LDPE) were cleaned and were cut into 2.36 mm to 4.75 mm. The sample aggregate was heated to temperature of 160°C–170°C and plastic was effectively coated over the aggregate and then mixed with bitumen to make the Plastic Modifies Asphalt Concrete. Then the optimum binder content was determined with no plastic. Then plastic mixed samples were prepared for 0%, 5%, 10%, 15%, 20% and 25% percentage of plastic content with respect to optimum bitumen content and then Marshall Stability tests were carried out. On the basis of the experimental results obtained, it was found that Asphalt concrete prepared with plastic waste showed higher Marshall Stability value suggesting higher load carrying capacity and better properties compared to the Asphalt Concrete without plastic mix. Hence, the plastic waste can be disposed off judiciously by incorporating it in bituminous mixes.

Keywords: *Waste Plastic; Bitumen; Marshall Stability; Asphalt Concrete; Modified Asphalt Concrete; Flow value; Density.*

1. Background

Plastic is non-biodegradable and hence possesses a big challenge to waste management in metropolitan areas. Plastic garbage has exacerbated environmental problems in urban Nepal. Studies show that about 16 percent of urban waste in Nepal is comprised of plastic materials. In 2012 the daily plastic garbage production was about 2.7 tons. This is because these days nearly every household uses large amount of 'use and throw' plastic materials like polythene bags, bottles and plastic wrappers. (Vikash Raj Satyal, My Republica, Friday, 17 August 2018). As per the Nepal Plastic Manufacturers´ Association (NPMA), Kathmandu valley alone uses around 4,700,000 to 4,800,000 plastic bags daily. Researchers claim humans have produced 9.1 billion tons of plastic and much of it ends up in nature causing harm to both living beings and the environment. (The Kathmandu post, 5 June 2018). With a population of about 2.5 million (including the districts of Kathmandu, Lalitpur and Bhaktapur) the Kathmandu Valley produces 523 tonnes of waste per day out of which 12% is estimated to be plastic. Due to the lack of awareness and a dysfunctional waste management system some of the plastic and polythene bags are thrown into or dumped on the banks of the rivers and rivulets that run through the valley and finally end up in the Bagmati River considered Nepal's holiest river but is heavily

polluted.

2. Literature Review

The deteriorating quality of roads is another area of concern as the present roads are not able to withstand the increasing traffic and also are less resistant to adverse weather conditions. The waste plastic material is shredded into small pieces and is made to stick to heated aggregate to form a thin layer of plastic over the aggregate particles. Here the plastic can be used as a modifier for aggregates (plastic coated aggregates). The results showed improved properties for PCA when compared to normal aggregates. (Bhageerathy *et. al.*, 2014). The coating of plastics reduces the porosity, absorption of moisture and improves soundness. The polymer coated aggregate bitumen mix forms better material for flexible pavement construction as the mix shows higher Marshall Stability value and suitable Marshall Coefficient. Hence the use of waste plastics for flexible pavement is one of the best methods for easy disposal of waste plastics. (Dr. R. Vasudevan 2007). Use of plastic along with the bitumen in construction of roads not only increases its life and smoothness but also makes it economically sound and environment friendly. Mohd et al (2017) investigated the use of modified bitumen with the addition of processed waste plastic of about 5%–10% by weight of bitumen helps in substantially improving the Marshall stability, fatigue, life strength, and other required properties of bituminous concrete mix, which improves the durability and pavement performance with marginal saving in bitumen usage. The process is environment friendly.

3. Methodology

Plastic Modified Concrete was prepared first followed by laboratory tests for Marshall Stability. The detailed procedure is explained below.

Field Studies of Plastic wastes

Field studies were made at two different transfer stations (Teku and Balkhu) and the local municipality offices were visited during this study. During the field studies, the plastic wastes in the MSW were classified and their proportion was identified. The result of table 1 shows that the amount of plastic waste in Kathmandu Valley was found to be 12.1 %. The different categories of Plastics like PET 20.806%, HDPE 9.768, PVC 1.810%, LDPE 59.642%, PP 5.658%, PS 0.781%& Others 1.457 % respectively are shown in Figure 1.

Table1: Field study of Plastic waste

Waste / Station	Total Waste Kg	Plastic Waste Kg	Percentage of Plastic Waste	Remarks
Teku Transfer Station	43.2	5.01	11.60	
Balkhu Segregation Station	126.05	15.85	12.60	

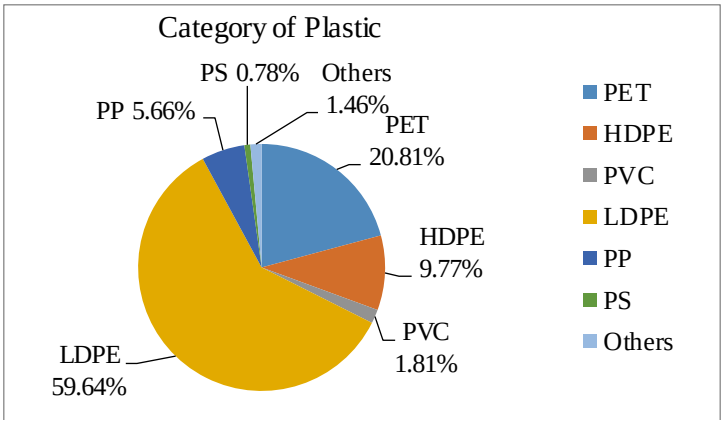

Figure 1: Different Category of Plastics

Particle size distribution of all aggregates (Combine grading)

The particle size distribution for individual of 20 mm down, 16 mm down, 10 mm down and wash grading of stone dust was found to be within the limit of standard specification. The combine grading curve shows the smooth distribution of all size of aggregates with respect to particular sieve size as shown in figure 2.

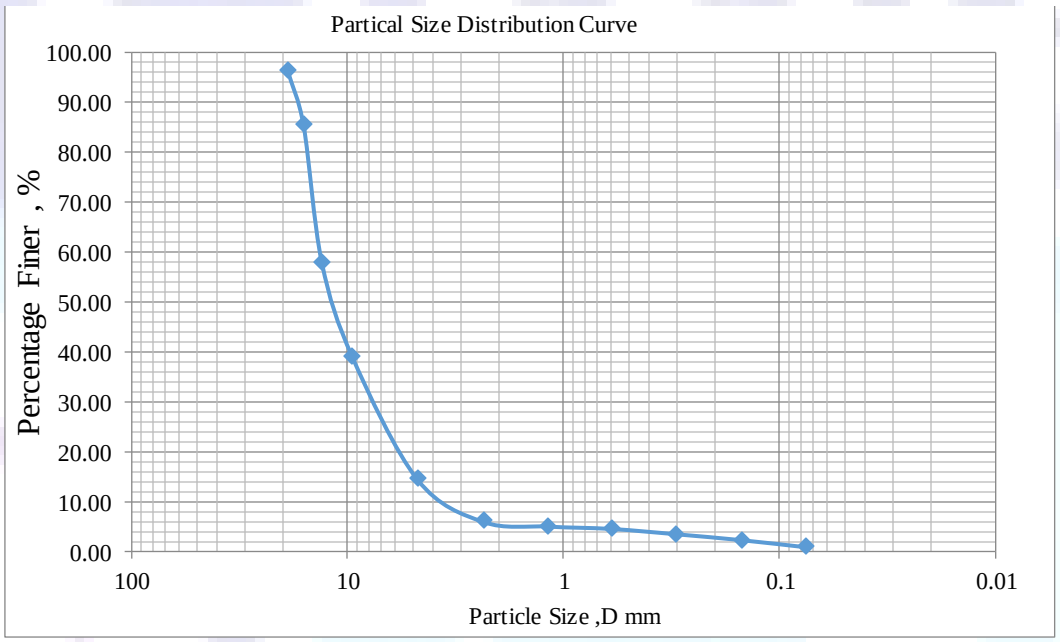

Figure 2: Sieve Analysis Result of 20 mm down all aggregates (Combine Grading)

Bitumen and bitumen conformation test

The bitumen was viscosity grade paving bitumen complying with the Indian Standard. Specification IS: 73. VG 10 Indian bitumen used in road construction of flexible pavement was used.

Preparation of Plastic-Coated Aggregate (PCA)

The plastic wastes were coated on aggregate. The basic process involved in preparation of plastic-coated aggregate are

1. Collection of waste plastic

- The plastic wastes from municipal transfer station were collected.
- Plastic wastes collected from various sources were separated from other wastes.
- Maximum thickness of plastic waste was 60 microns.

2. Cleaning and shredding of waste plastic

- The waste plastics was shredded or cut into small piece (2.36mm – 4.75mm)
- The different types of plastic wastes were mixed together.

3. Mixing of shredded waste plastic with aggregate
- The aggregate was heated to 160-170°C.
- The shredded plastic waste was added in proportion.
- Plastic Coated aggregate was prepared.

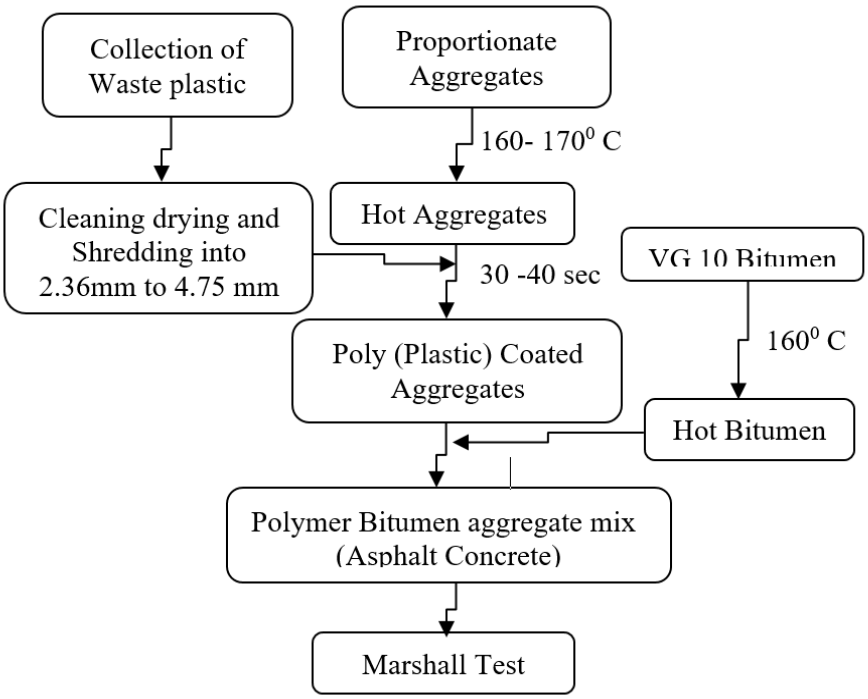

Figure 3: Methodology flow chart for Plastic modified bituminous mix (Dry Process)

Requirement for Asphalt Concrete

Asphalt concrete is the mixture of binder, coarse and fine aggregate and mineral filler. The bitumen content required were determined following the Marshall Mix design Procedure contained in Asphalt Institute Manual MS-2.

Table 2: Requirements of Asphalt Concrete mix (SS)

Sn	Asphalt Concrete	Wearing course For VG Bitumen)	Test Method
Properties	75 blows each face of specimen		
1	Minimum stability (kN at 60 oC) (KN)	Min 8 (for Heavy traffic)	AASHTO T245
2	Marshall Flow Value (mm)	2-4	AASHTO T245
3	Marshall Quotient (Stability/Flow)	2-5	MS-2 & ASTM
4	% Air Voids	2-5	
5	% Voids Filled with Bitumen (VFB)	65-75	
7	Compression/Immersion Ratio	>0.75	

The above values of table 2 are referred from the standard specification and this value was used as a reference and limiting values in design and calculation of different Marshall Parameters.

Preparation of specimen and Test

The 1200 g of aggregates and filler put together was heated to a temperature of 160-170°C. Bitumen was heated to a temperature of 160°C with the first trial percentage of bitumen (say 4.5% by weight of the mineral aggregates). Then the heated aggregates and bitumen are thoroughly mixed at a temperature of 160 - 170°C. The mix was placed in a preheated mould and compacted by a hammer having a weight of 4.5 kg and a free fall of 45.7 cm giving 75 blows on either side at a temperature of 160°C to prepare the laboratory specimens of compacted thickness 63.5+/-3 mm. In this research, the compaction of all the samples are performed using seventy-five blows of the Marshall hammer on either side of the sample. The height of the samples was measured and specimens are immersed in a water bath at 60°C for 35±5 minutes. Samples were removed from the water bath and placed immediately in the Marshall loading head. The load was applied to the specimen at a deformation rate of 50.8 mm/minute. Stability was measured as the maximum load sustained by the sample before failure. Flow was the deformation at the maximum load. The stability values were then adjusted with respect to the sample height. For the proposed design mix gradation, three specimens were prepared for each bitumen contents within the range of 4.5 – 6.5 % at increments of 0.5 percent for the finding of optimum Bitumen Content.

The waste plastics content as 2.5 %, 5%, 7.5%, 10%, 12.5%, 15%, 17.5%, 20% and 25% by weight of Optimum bitumen Content. The procedure adopted for the preparation of Marshall Specimen was the same as used in control mixtures, except, the Plastic pieces were added in heated aggregate prior to mixing them with heated bitumen (dry blending method). The average values of stability, flow, bulk specific gravity, obtained above were plotted separately against the bitumen content and a smooth curve drawn through the plotted values. The optimum bitumen content (OBC) for the mixture was determined at first before plastic mixed.

4. Discussion and Data Analysis

The results of the Laboratory experiment of the Marshall Stability test for Plastic Modified Asphalt Concrete Mix are presented.

Marshall Job Mix Design

Table 3 shows the aggregate grading for Asphalt Concrete mix based on job mix method. The percentage of aggregates and stone dust passing through the sieves were within the specification limit.

Table 3: Combine aggregate grading and Job mix design

Design as per SS-2073						
Job mix method(option)						
Sieve size(mm)	20 down%	16 down%	10 Down %	Dust %	Specification Limit	
19	99.32	100	100	100		
13.2	41.05	57.93	100	100	90	100
9.5	17.31	37.37	97.28	100	59	79
4.750	4.16	10.47	35.76	84.75	52	72
2.360	3.77	2.00	18.74	71.33	35	55
1.180	3.63	0.73	14.96	52.96	28	44
0.600	3.51	0.56	13.74	40.75	20	34
0.300	2.27	0.41	12.37	29.09	15	27

0.150	0.76	0.27	10.20	24.29	10	20
0.075	0.15	0.09	2.61	19.08	5	13
					2	8
Sive size(mm)	22	22	24	32	100	
	(%)	(%)	(%)	(%)	Total	
19.000	21.85	22	24	32	99.9	ok
13.200	9.03	12.745	24	32	77.8	ok
9.500	3.81	8.221	23.347	32	67.4	ok
4.750	0.92	2.303	8.582	27.12	38.9	ok
2.360	0.83	0.440	4.498	22.8256	28.6	ok
1.180	0.80	0.1606	3.590	16.9472	21.5	ok
0.600	0.77	0.1232	3.298	13.04	17.2	ok
0.300	0.50	0.0902	2.969	9.3088	12.9	ok
0.150	0.17	0.0594	2.448	7.7728	10.4	ok
0.075	0.03	0.0198	0.626	6.1056	6.8	ok

The outcomes of the Table 3 shows that the different size of aggregates of nominal size 20mm down was adjust as 22%, 16 mm down was adjust as 22%, 10mm down was adjust as 24% and stone dust was adjust as 32% by weight passing from respective sieve size for the design within the limit of standard specification. The graph 4 is the percentage passing by weight was plotted corresponding to sieve size shows that the design line in between maximum and minimum limiting value which is within the boundary gives design is acceptable.

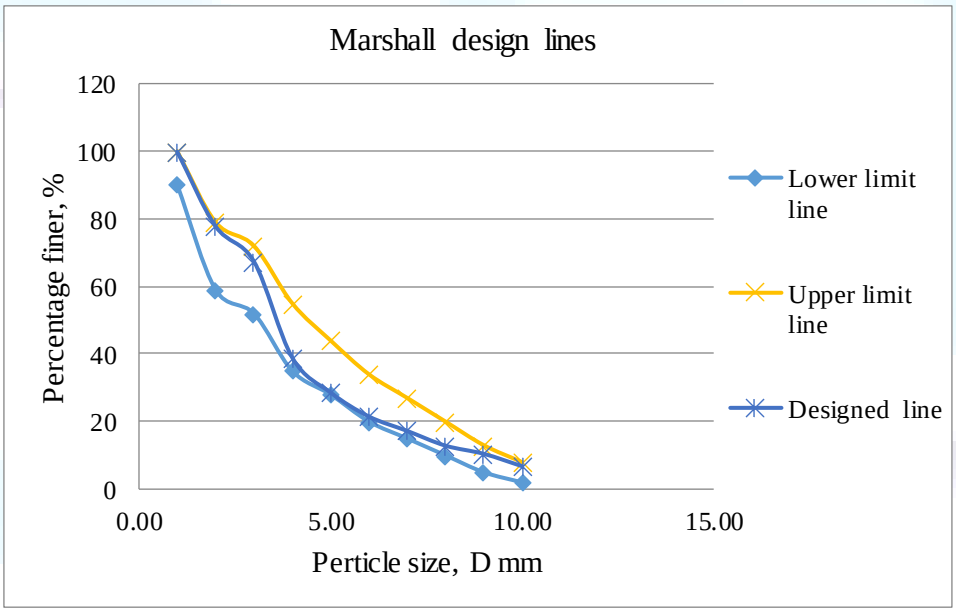

Figure 4: Asphalt Mix Design line showing limiting maximum and minimum limit

Bitumen Optimization

The results of table 4 shows that the optimum bitumen content for the Marshall Mix design with respect to maximum stability value, Maximum density, average percentage air voids within the standard flow value was found to be 5.5 %. At this bitumen content the Marshall Stability value was found to be 11.41 KN which also presented in graph shown in figure 5.

Table 4: Marshall Test result and calculated parameters

Bitumen Content %	Stability KN	Flow value mm	Air Voids %	Density gm/cc	VMA %	VFB %
4.5	10.16	1.68	4.49	2.42	15.15	70.39
5	10.26	2.21	3.57	2.42	15.45	76.85
5.5	11.41	2.74	2.47	2.43	15.58	84.17
6	8.67	3.03	1.65	2.43	15.96	89.69
6.5	7.49	3.45	0.96	2.43	16.45	94.19

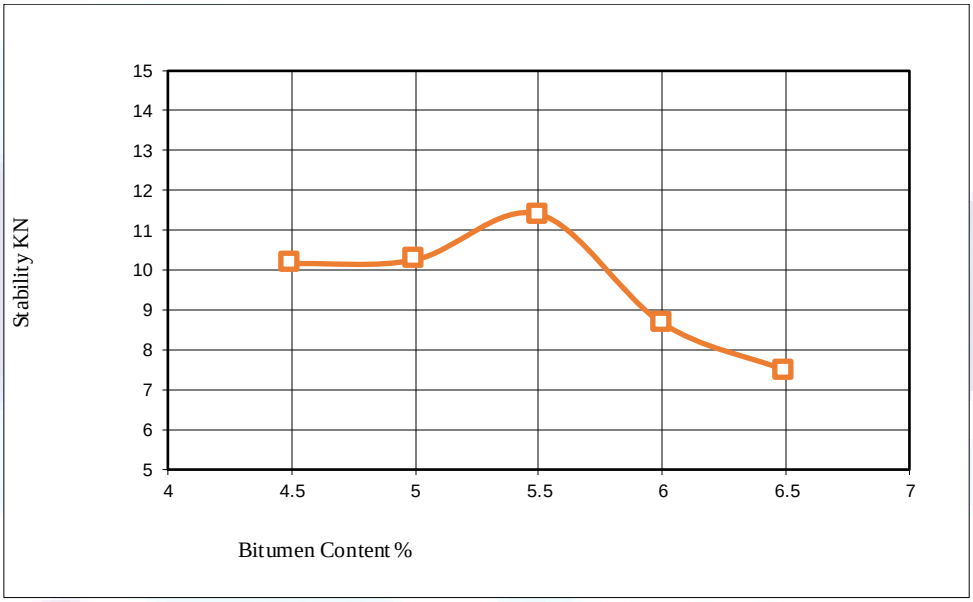

Figure 5: Stability-Bitumen

Optimum Plastic for Plastic Modified Asphalt Concrete Mix

The optimum Plastic content for the Plastic modified Marshall Mix design was found to be range at 16%. At this bitumen content the Highest Marshall Stability value was found to be 15.4 KN which is 25.9 % higher strength than the Marshall Stability value without plastic adding. The values of other parameters were within a limit of standard specification and the improved values were obtained as shown table 5 and combine presentation of this value as shown in figure 6.

Table 5: Marshall Test result and calculated parameters

Plastic Content %	Stability KN	Flow value mm	Air Voids %	Density gm/cc	VMA %	VFB %
0	11.41	1.68	2.45	2.43	15.56	84.28
5	12.57	2.41	2.61	2.43	15.73	83.44
10	14.10	2.74	2.80	2.43	15.93	82.45
15	15.36	3.03	3.95	2.41	16.96	76.69
20	15.18	3.45	4.77	2.40	17.70	73.04
25	12.94	3.45	5.66	2.38	18.51	69.40

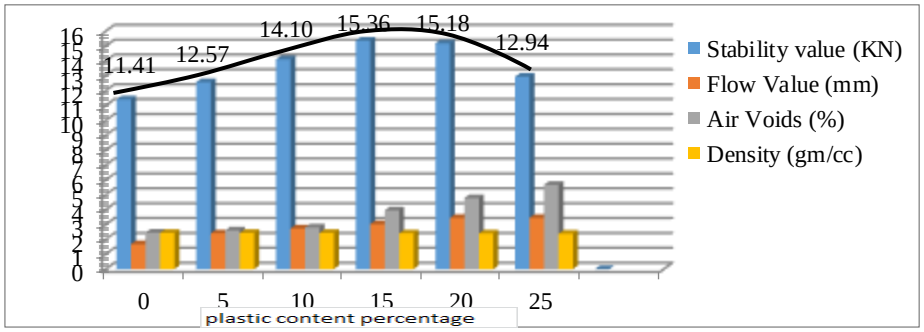

Figure 6: Marshall Test result for different percentage of Plastic Content

Combine presentation of Marshall Stability value without plastic adding as shown in figure 6.

Table 6: Marshall Test result for Plastic Modified Asphalt Specimen

The result of different values for different percentage of Plastics at 5.5 % Optimum Bitumen Content

% Bitumen (Optimum)	% Plastic with respect to bitumen	% Plastic With respect to aggregates	Sp.Gr. Of 20 mm aggregate	Sp.Gr. Of 16 mm aggregate	Sp.Gr. Of 10 mm aggregate	Sp.Gr.of filler	Sp. Gr.of agg.mix	% agg. Mix	Density .of comp.Mix gm/cc	Max Sp.Gr	% Air voids	% VMA	% VFB	Sp.Gr.of bitumen	Sp.Gr.of LDPE Plastics	Remarks
5.5	0	0	2.714	2.708	2.724	2.733	2.719	94.5	2.430	2.490	2.445	15.6	84.3	1.019	0.930	
5.5	5	0.275	2.714	2.708	2.724	2.733	2.719	94.23	2.432	2.497	2.605	15.7	83.4	1.019	0.930	
5.5	10	0.55	2.714	2.708	2.724	2.733	2.719	93.95	2.433	2.503	2.795	15.9	82.4	1.019	0.930	
5.5	15	0.825	2.714	2.708	2.724	2.733	2.719	93.68	2.410	2.509	3.954	17.0	76.7	1.019	0.930	
5.5	20	1.1	2.714	2.708	2.724	2.733	2.719	93.4	2.396	2.516	4.773	17.7	73.0	1.019	0.930	
5.5	25	1.375	2.714	2.708	2.724	2.733	2.719	93.13	2.379	2.522	5.663	18.5	69.4	1.019	0.930	

The discussion about value obtained in table 6 and graph plotted of respective parameters with percentage adding of plastic as following.

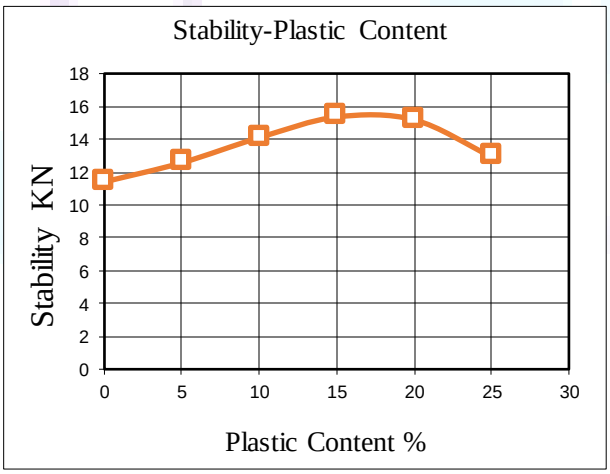

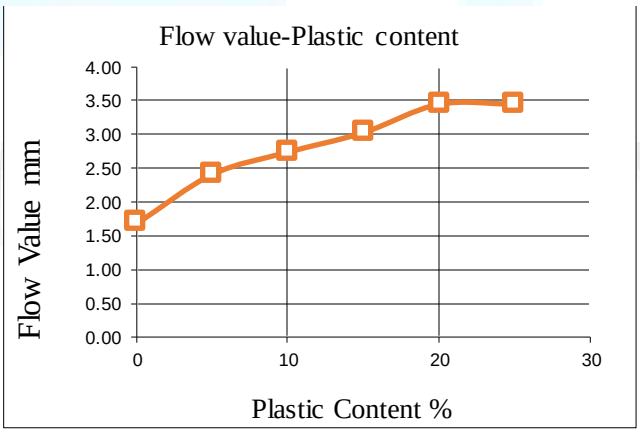

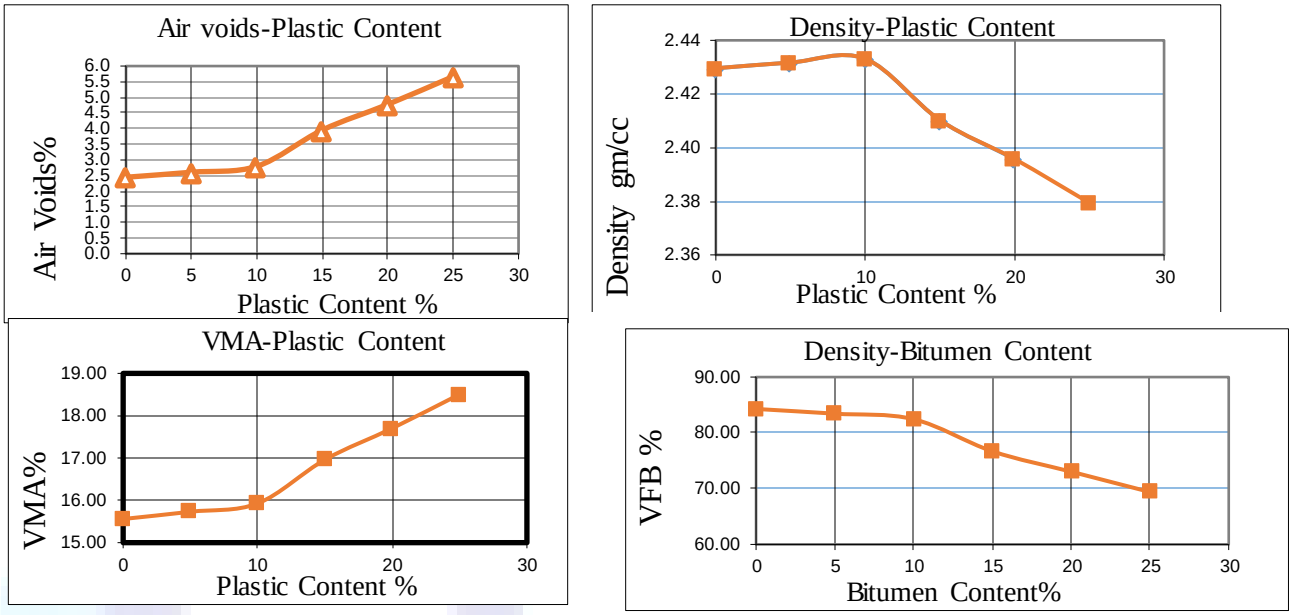

Figure 7: Marshall Parameters with different percentage of plastic content.

The Marshall Stability Value increase with increase in plastic content up to some limit. The Marshall Stability test value with 0 % plastic content is 11.41 KN at optimum bitumen content. Then in 5 %, 10 % 15 % plastic content there is increase in Marshall Value. After that at 20 % slightly decrease in stability value and at 25 % of plastic content here was sudden decrease in stability value with high flow value and sudden disturbance on other design parameter seen after calculation. The Stability load value, flow value and calculated other parameter are almost constant and within the best limit of standard specification of road and bridge at 10 % plastic and 15 % plastic content. Hence from the graph plotted as figure 7 the best value for Marshall Stability considering maximum stability within the range of other parameters was found to be 15.4 KN shows that the optimum percentage of plastic content is 16 %. It is clearly seen from that plastic modified Asphalt Concrete show the higher Marshall stability value, Higher density within the best limit of others parameters which can be withstand to heavy traffic load more efficiently than the Plane asphalt concrete. Hence the plastic modified Asphalt Concrete is best used for the road construction with effective and Eco friend utilization of waste plastics.

5. Findings and Conclusion

The present research work was aimed to find the Marshall Stability Value for Plastic modified Asphalt Concrete.

Based on result, following conclusion have been made

- The Marshall Stability value for the plastic modified mix Asphalt concrete was found to be very much higher than the normal bituminous asphalt concrete.
- The Maximum Stability value was found to be 15.4 KN which was obtained at 16 % plastic content by weight of optimum bitumen of 5.5 % considering all relevant parameters.
- The Marshall Stability value of plastic modified Asphalt concrete was found to be 25.90 % more than that for the normal bituminous Asphalt concrete which indicates an increase in load carrying capacity.

6. Recommendations

The works which requires further study are recommended as

1. The property of plastic modified bitumen could be studied.
2. The time dependent property of plastic modified Asphalt Concrete could be studied.
3. The bitumen optimization by waste plastic content required in preparation of plastic modified Asphalt Concrete could be studied.
4. Comparison of properties of plastic coated Asphalt Concrete mix and bitumen coated Asphalt concrete mix could be studied.
5. The study of effect of plastic modifier on the property of asphalt concrete could be studied.

References

[1] Asian Development Bank (ADB), 2013, "Solid Waste Management in Nepal", pp. 31 – 50.

[2] Ramananda Mishra, 2017, "Utilization of Plastic Wastes to Improve the Properties of Aggregate in Road Construction", Degree Thesis, pp. 11-25

[3] Anil Prasad Banskota, 2015, "Effective Management of Plastic Wastes and other solid waste in Nepal", Degree Thesis, pp. 6 - 10.

[4] Bhageerathy, K. P, Anu, P., Manju, V. S, and Raji A. K, 2014, "Use of Biomedical Plastic Waste in Bituminous Road Construction", *International Journal of Engineering and Advanced Technology (IJEAT),* vol. 3(6), pp. 89 - 92

[5] Desai, R.N., Vora, N.A., and Dave, H.K., 2013, "Use of Plastic in Bituminous Concrete Mixes", *PARIPEX - Indian Journal of Research*, vol. 2(4), pp. 176-180

[6] Material Testing Procedure, 2015, "Quality Control handbook for rural road construction and maintenance (Volume II)", pp. 79 – 115.

[6] Standard Specifications For Road and Bridge Works, Government of Nepal, Ministry of Physical Infrastructure and Transport Department of Roads, 2073 BS (New).

[7] MS-2 Asphalt Mix Design Methods, Assistant Professor Dr. Abdulhaq Hadi Abedali, Head of Highway and Transportation Department, Faculty of Engineering ;Mustansiriyh University.

[8] Ahmed Trimbakwala, Plastic Roads Use of Waste Plastic in Road Construction, *International Journal of Scientific and Research Publications, Volume 7, Issue 4, April 2017*, Department of Civil Engineering, K. K. Wagh Polytechnic, Nashik

[9] Yash Menaria1, Rupal Sankhla2, " Use of Waste Plastic in Flexible Pavements-Green Roads", Open Journal of Civil Engineering, 2015, 5, 299-311

[10] Mohanty, M., 2013, "A study on use of waste polythene in bituminous paving mixes", M. Tech. Thesis, Department of Civil engineering, National Institute of Technology, Rourkela.

[11] Practical Action, 2008, "Best Practice on Solid Waste Management Of Nepalese Cities.", pp. 4-45.

[12] Rokade, S., 2012, "Use of Plastic waste and waste Rubber tyres in Flexible Highway Pavement." *International Conference on Future Environment and Energy*, Vol 28, pp. 105–108.

[13] Rajasekaran, S., Vasudevan, R., Paulraj, S., 2013, "Reuse of Waste Plastic Coated Aggregates-Bitumen Mix Composite for Road Application- Green Method", *American Journal of Engineering Research*, Vol. 2, Issue II, PP 1-13

[14] Subedi, K.S., 2015, "Plastic Bag Ban Still a Burning Issue." https://thehimalyantimes.com/environment/plastic-bag-ban-still-a-burning-issue.

Experimental Study on the Effect of Rice Husk Ash and Marble Dust on Strength Development of Cement Concrete

Sharon Maharjan[1], Shishir Parajuli[2], Suman Neupane[3], Sunita Adhikari[4]

[1,2,3,4] *Undergraduate Student, Department of Civil Engineering, Advanced College of Engineering and Management, Kupondole, Lalitpur, Nepal*

Abstract

This paper presents the study of concrete mix design using rice husk ash and marble powder where rice husk ash was used as a partial replacement for cement and marble dust was used as a partial replacement for sand. Compressive strength test was conducted on RHA-MD concrete mix to evaluate the strength development of cement concrete. Analysis of strength was done by varying percentage of rice husk ash and marble dust from 5 to 20%. Three sets of analysis were done: using marble dust only, using rice husk ash only and using both of them together and compressive strength of the concrete was studied. The partial replacement of Rice husk ash and Marble dust slurries, gives best compressive strength at 15% replacement on all sets of analysis.

Keywords: *Rice husk ash, Marble dust, Agro-dust, Compressive strength.*

1. Introduction

Concrete is an essential building material which is widely used in the construction of infrastructure such as buildings, bridges, highways, dams, and many other facilities. Concrete's versatility, durability, sustainability, and economy have made it the world's most widely used construction material. The quality of concrete is judged largely on the strength of that concrete. Strength is usually the basis for acceptance or rejection of the concrete in the structure.

Very recently, few replacements for the materials used in concrete has been found through some researches. This research is also oriented in increasing strength of concrete by replacing some part of cement and sand in concrete by introducing new materials in construction: Rice husk ash and marble dust.

Rice husk is generated from the rice processing industries as a major agricultural by product in many parts of the world especially in developing countries. Nepal, being an agricultural country also produce tons of paddy. After incineration only about 20% of rice husk is transformed to RHA. It is usually dumped into water streams or as landfills causing environmental pollution. RHA is an active pozzolana that improve strength as they are smaller than the cement particles, and can pack in between the cement particles and provide a finer pore structure. RHA has two roles in concrete manufacture, as a substitute for Portland cement, reducing the cost of concrete in the production of low cost building blocks, and as an admixture in the production of high strength concrete.

Similarly, marble is also a most used material during the construction of buildings. Disposal of the waste materials of the marble industry, consisting of very fine powders, is one of the environmental problems worldwide today. Now-a-days the cost of material is increasing so if we use the waste material in the production of the mortar so we decrease the price and usage of marble dust in concrete can increase strength of concrete and solve the wastage issue.

2. Objectives

- This project aims in reusing RHA (an Agro-waste) in cement concrete.
- This project aims to reuse Marble Dust in cement concrete.
- This project also aims to evaluate the strength of structural concrete by using RHA(Rice Husk Ash) and MD.
-

3. Project Concept

We have used materials like cement, sand, coarse aggregates, and fine aggregates to make around 350 cubes in this project. The concept of this project is to partially replace cement with rice husk ash and sand with marble dust to study the effect of such replacements on the strength development of concrete.

4. Literature Review

BabooRai, Khan Naushad (2011) studied the influence of marble powder in cement concrete mix. In this paper the effect of use of marble powder and granules has been studied by partially replacing with mortar and concrete constituents. And check the different properties like relative workability and compressive and flexure strengths. By partial replacing the constitution it reveals that increased waste powder or waste marble granules ratio result in increased workability and compressive strengths of the mortar and concrete.

Demirel (2010) has investigated, the effect of using waste marble dust as a final material on the mechanical properties of the concrete. For this purpose, different series of concrete mixtures were prepared by replacing the fine sand with waste marble dust. He found following conclusion. Unit weight of the concrete increased as a result of the fact that certain properties of WMD had been added to the concrete as very fine aggregate substitutes. This is an expected outcome due to the high specific gravity of WMD and also filler effect of marble dust because it has finer particles than fine aggregate. Compressive strength of the concrete has increase with percentage of marble dust additions at all curing ages.

Karim et al. (2012) has discussed rice husk ash (RHA) is used as supplementary cementing material in mortar and concrete and has demonstrated significant influence in improving the mechanical and durability properties of mortar and concrete.Iit can be concluded that RHA could be used as supplementary cementing material up to a certain level of replacement (about 20-30% of binder) without sacrificing strength of concrete. Proper consumption of these RHA contributes in solving environmental pollution and production of cost-effective concrete; it can also play a vital role for the production of sustainable concrete. It participates to produce denser and durable concrete with a particular level (about 20-30%) of replacement.

Kartini & Mahmud (2006) reported on the ―Improvement on Mechanical Properties of Rice Husk Ash Concrete with Super plasticizer‖. Without super plasticizer RHA concrete attained lower compressive strength than that of the control due to the higher amount of water for similar workability. RHA concrete improves the durability of concrete. It is concluded from the paper that by adding super plasticizer to the RHA mixes, higher replacement levels are possible. Concrete containing up to 30%RHA can attain strength of 30 N/mm^2 at 28 days.

Komal Patidar (2015) investigated the effects of partially replacing cement with Rice Husk Ash and sand with marble dust. It is concluded that partially replacing cement and sand with Rice Husk Ash and marble dust increased the compressive strength of concrete. Replacement upto 30% each of sand and cement was done in this research.

Maurice & Godwin (2012) investigated the effects of partially replacing OPC with RHA. It is

concluded that Adding RHA to concrete resulted in increased water demand, increase in workability and enhanced strength compared to the control sample. This results show that an addition of RHA from 5 -10% will increase the strength.

5. Theoretical Concept

Materials used:

Cement- Cement used was obtained from local market of Nepal. The cement used is OPC of 53 grades. The fineness value of cement was found to be 1.667%, Initial setting time 47 minutes and Final setting time 385 minutes. The compressive strength at 3, 7 and 28 days was found to be 29.174 MPa, 40.9336 MPa and 54.6188 MPa respectively. All the results were verified with the requirement as per IS 12269:2013.
Sand- Obtained from river banks and beds, this construction sand was medium coarse to coarse.
Rice Husk Ash- Obtained from local rice mill of Nepal. The color of RHA was grey.
Marble Dust- Obtained from marble industry inside Kathmandu valley, which was very fine powdery texture, white color and odorless.
Aggregate- The coarse aggregate used had fineness modulus of 6.14028, Water absorption 0.361, oven dried bulk specific gravity of 2.842, Saturated Surface Dry Bulk Specific Gravity of 2.853 and apparent specific gravity of 2.872. All the results were in accordance with the requirement of IS 383-1970 and BS 812-2.

6. Concrete Mix Design

General:

Nominal maximum size of aggregate: 20 mm, Shape of CA: Angular, Specific gravity of cement: 3.15, Specific gravity of FA: 2.65, Specific gravity of CA: 2.7, Type of exposure: Mild, Zone III sand.

Table 2: Mix ratio

Grade of Concrete	Mixing ratio of Cement:FA:CA:Water (From mix design calculation)
M20	1: 1.543 : 3.446 : 0.491
M25	1: 1.283 : 3.028 : 0.434
M30	1: 1.087 : 2.679 : 0.388

7. Mix Proportioning

In this experiment, concrete cubes were prepared first for virgin concrete then partial replacement of cement was done using 5%, 10%, 15% and 20% RHA. After that partial replacement of sand was done using 5%, 10%, 15% and 20% MD. Finally both sand and cement was replaced at the same time on varying percentage of 5%, 10%, 15% and 20% by MD and RHA respectively.

8. Results and Discussions

DATA ANALYSIS

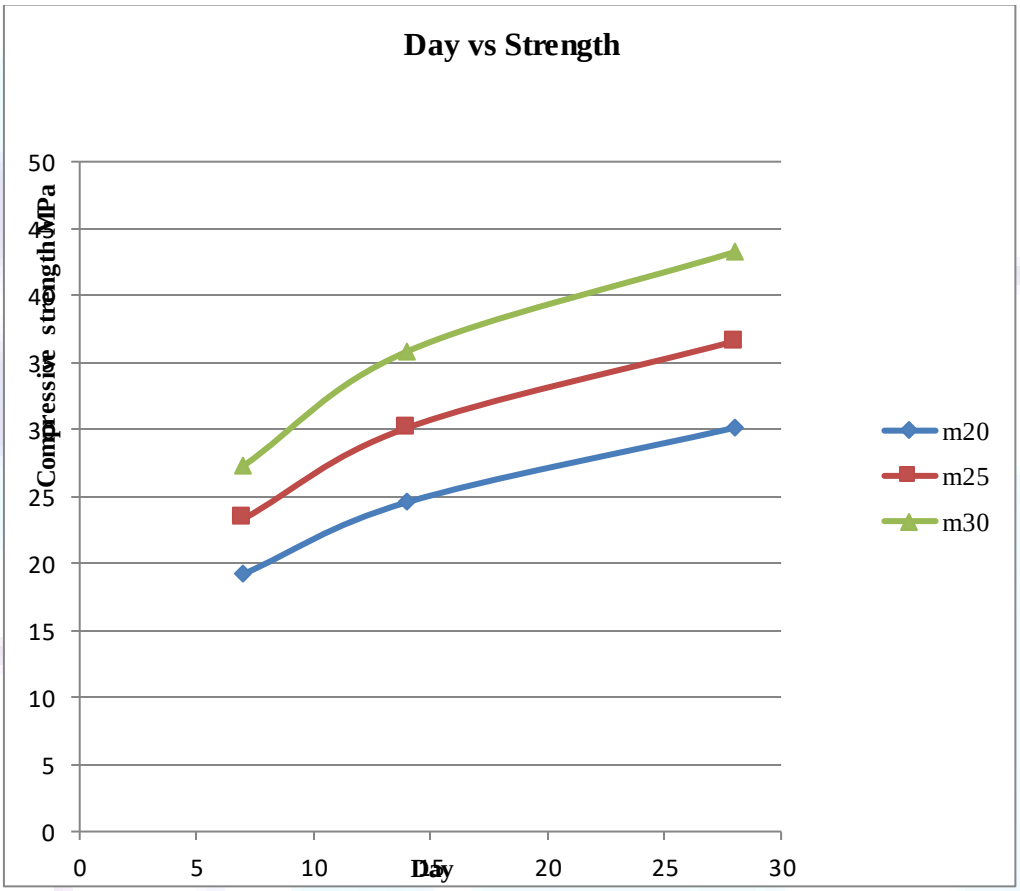

Figure 1: Compressive strength of virgin concrete

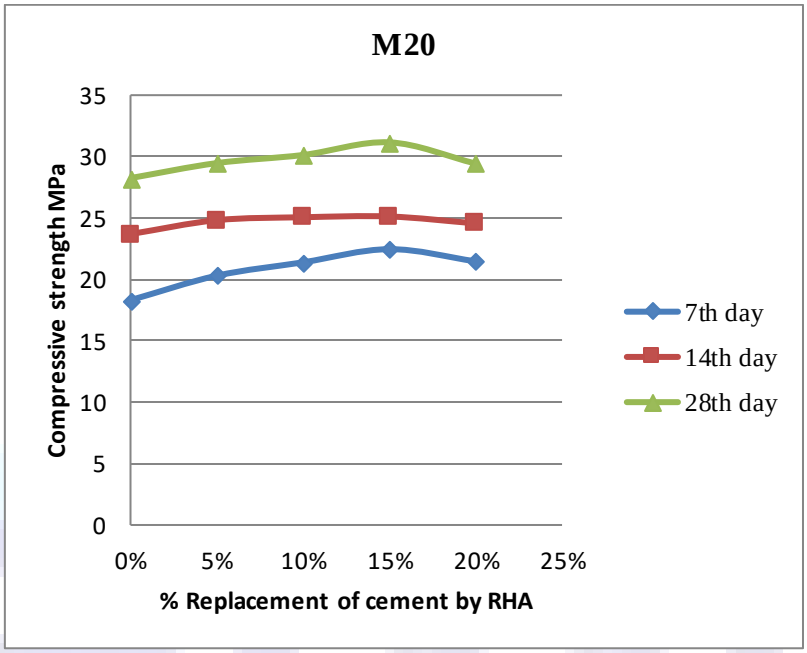

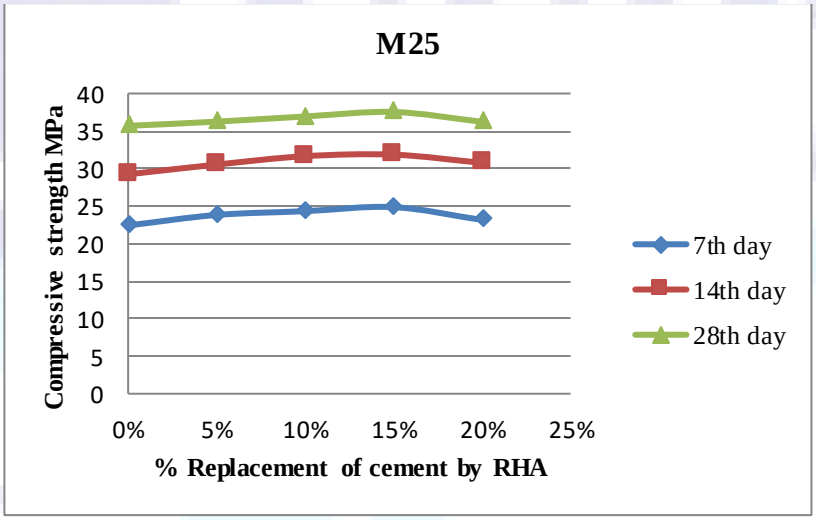

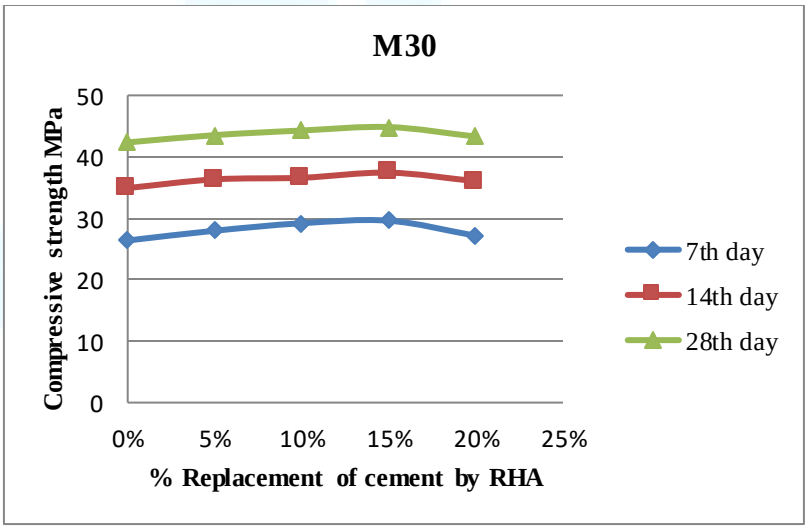

Figure 2: Compressive strength of concrete after replacement of cement by RHA

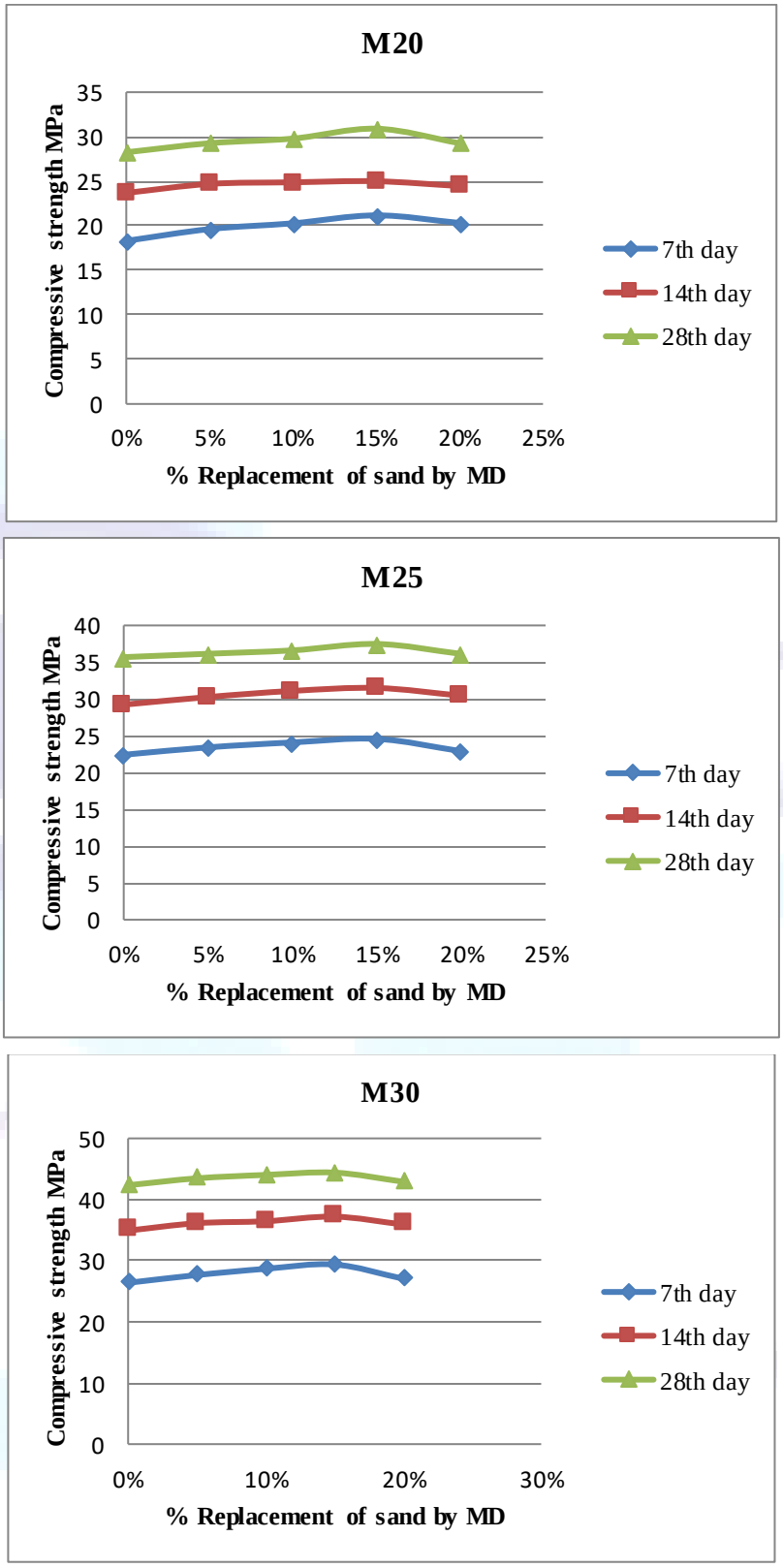

Figure 3: Compressive strength of concrete after replacement of sand by MD

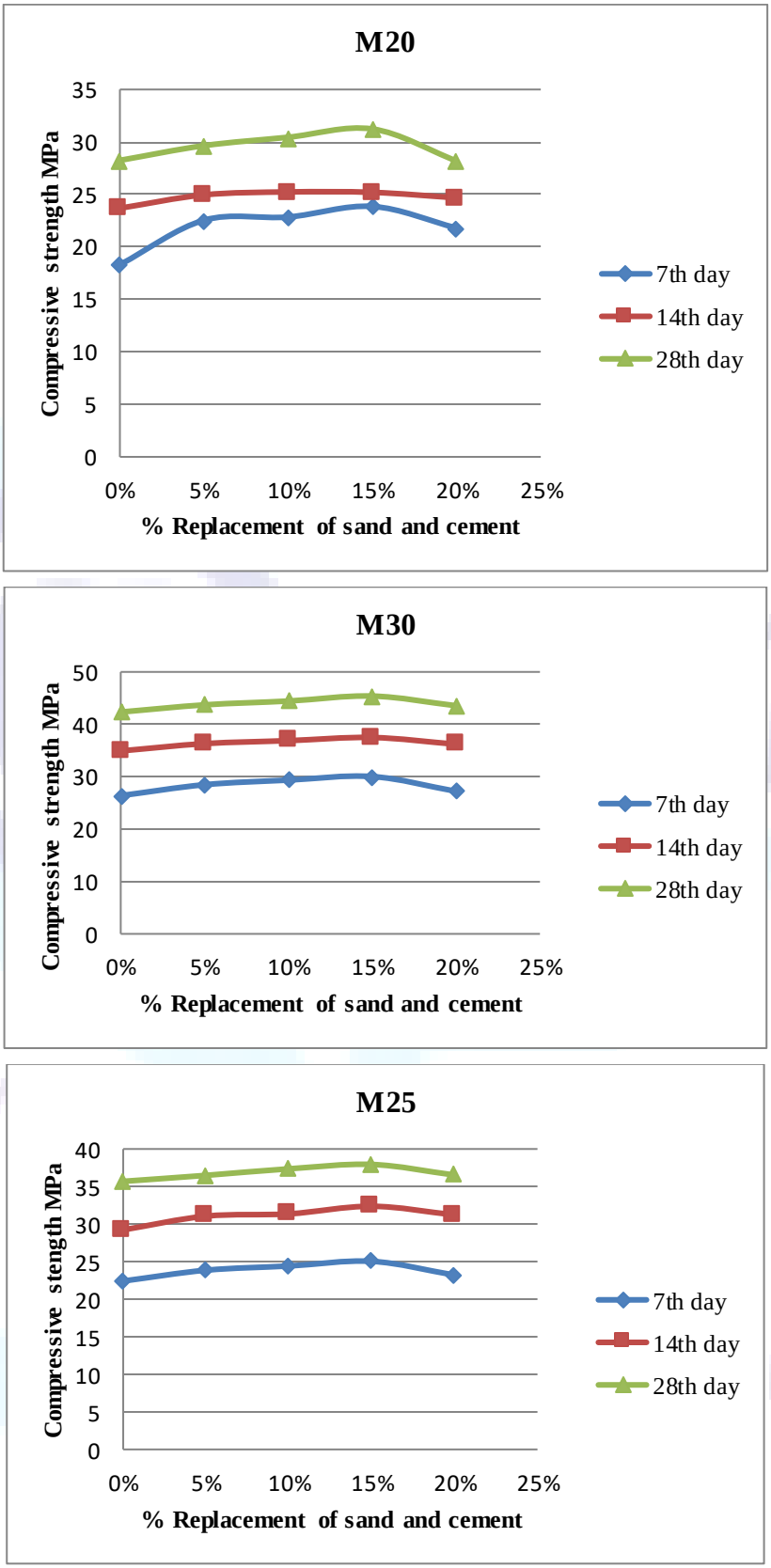

Figure 4: Compressive strength of concrete after replacement of cement and sand by RHA and MD respectively

Increment Analysis

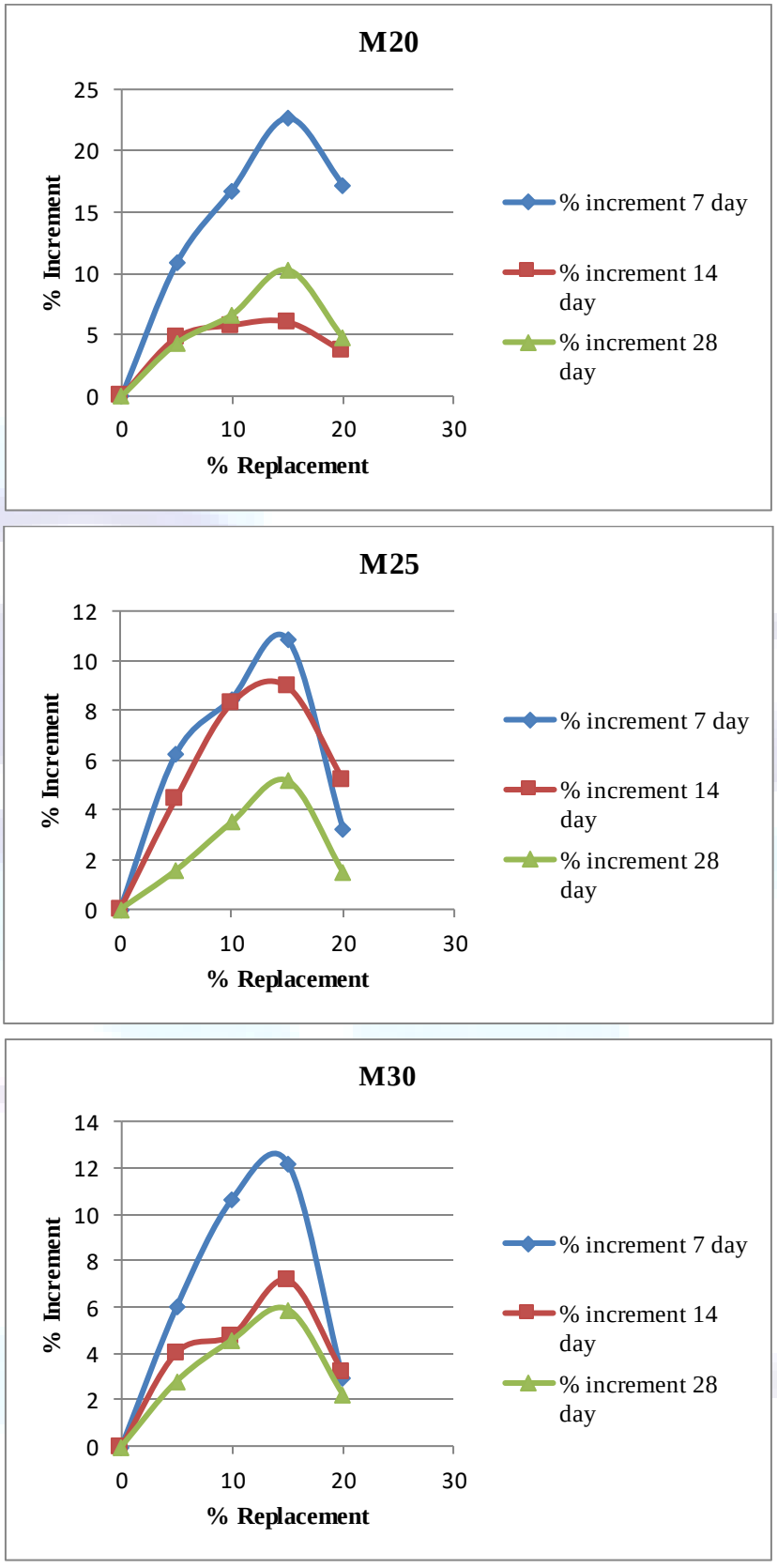

Figure 5: Replacement of cement by RHA

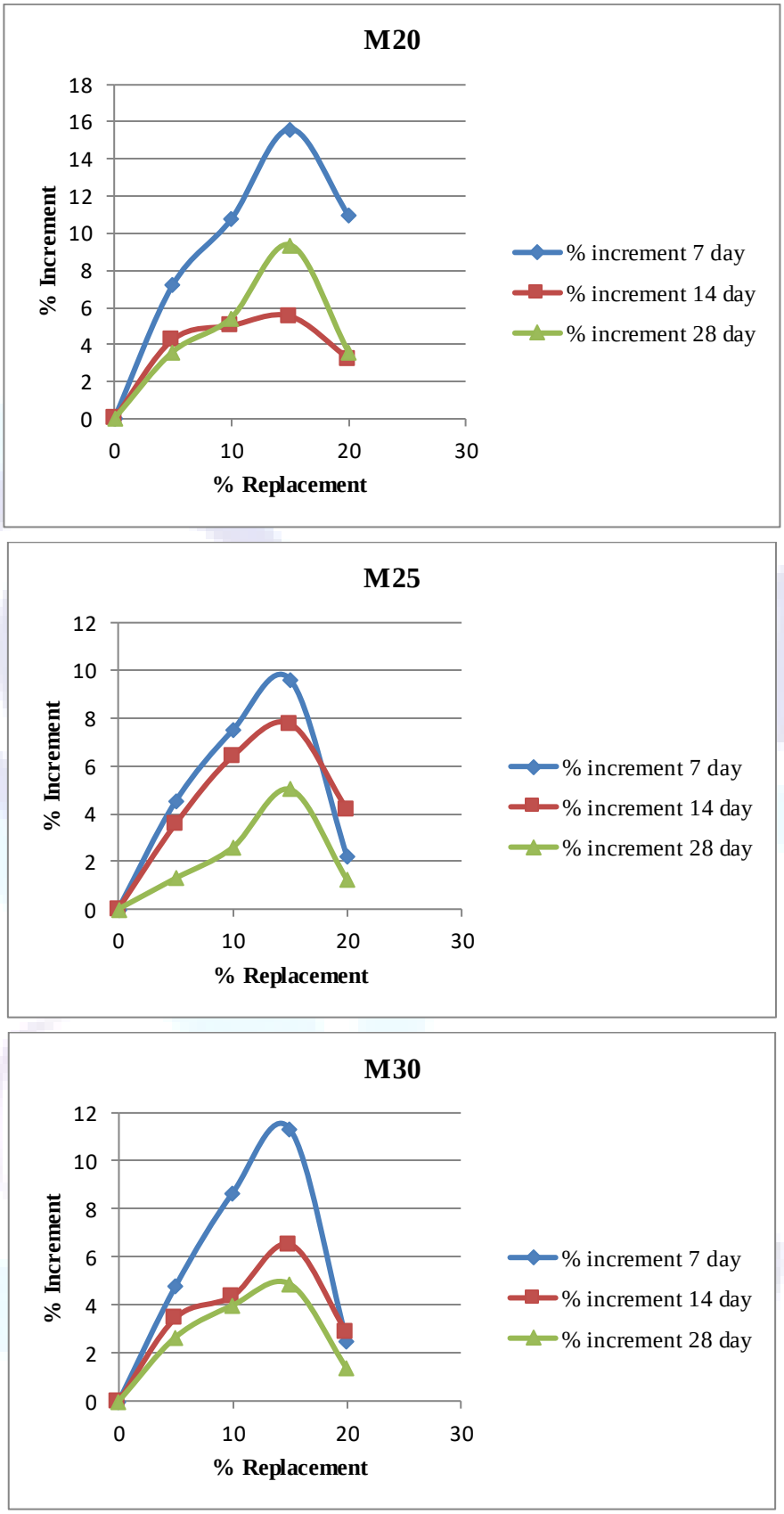

Figure 6: Replacement of sand by MD

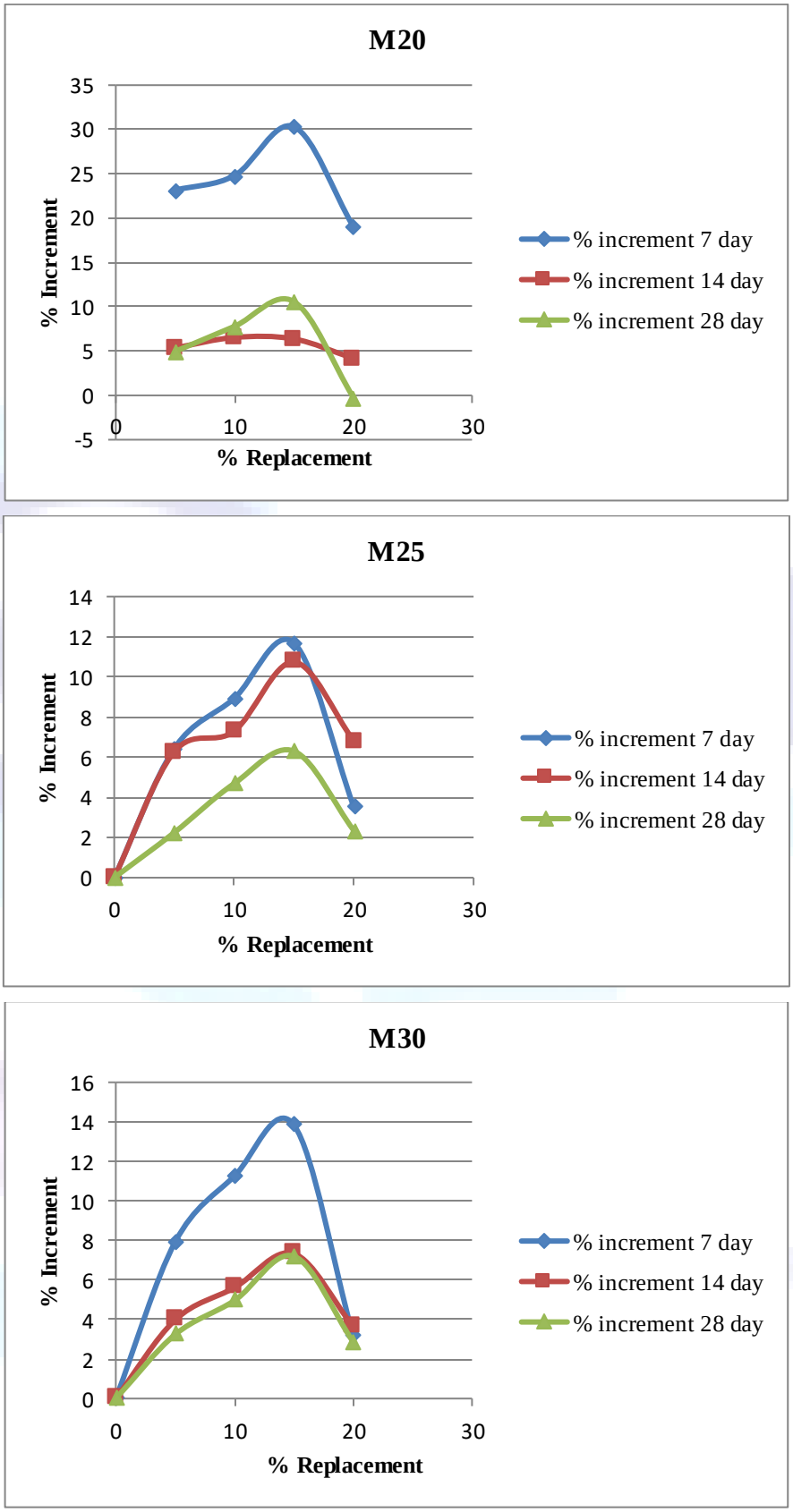

Figure 7: Replacement of cement and sand by RHA and MD respectively

9. Conclusion

On the basis of the results obtained from the laboratory performance evaluation the following conclusions were drawn:

1. Compressive strength of the concrete has increased with increasing percentages of Rice Husk Ash and Marble Dust at all curing ages. The highest Compressive strength has been demonstrated by replacement of 10% to 15% of Marble Dust and Rice Husk Ash. Strength decreased at the replacement of 20%.
2. The increase in compressive strength was found to be of from 4% to 11% for different grades namely M20, M25 and M30 at the age of 28 days and strength increment of around 25% was also found for the curing age of 7 and 14 days.
3. Strength of concrete increased in all the combinations: Replacement of sand with marble dust only, replacement of cement with Rice Husk Ash only and replacement of sand and cement with marble dust and rice husk ash respectively. But, the best result was found for the replacement of sand and cement with marble dust and rice husk ash respectively.
4. The best result for all the combinations was found at the replacement of 15%.
5. For the replacement of cement with 15% RHA, the strength increment from virgin concrete was found to 10.3% for M20 mix, 5.18% for M25 mix and 5.9% for M30 mix.
6. For the replacement of sand with 15% marble dust, the strength increment from virgin concrete was found to be 9.38% for M20 mix, 5.02% for M25 mix and 4.87% for M30 mix.
7. For the replacement of cement with RHA and sand with MD, the strength increment from virgin concrete was found to be 10.58% for M20 mix, 6.3% for M25 mix and 7.2% for M30 mix.

8. Scope for Future Work

The following tests are essential and included in the future scope of the work.

1. Mortar making property test
   - Bond strength
   -Water Rententivity test
2. Durability test
   -Water permeability test
   -Sulphate resistance test
   -Carbonation test
   -Leaching test
   -Effect of different curing condition.
3. Flexural Strength Test
4. Tension Test

Acknowledgement

It gives us immense pleasure to express our deepest sense of gratitude and sincere thanks to our highly respected and esteemed guide Er. Siddharth Shankar, supervisor of this project, for his valuable guidance, encouragement and help for carrying out this work. We would like to express our sincere thanks to Associate Professor Er. Laxmi Bhakta Maharjan (Head of Department, Department of Civil Engineering, Advanced College of Engineering and Management), for giving us this opportunity to undertake this project. We are also grateful to Er. Rajesh Khadka (Former Head of Department, Department of Civil Engineering, Advanced College of Engineering and Management) for his motivation and guidance to undertake this project.

References

[1] Baboo Rai , Khan Naushad H , Abhishek Kr , Tabin Rushad S , Duggal S.K, Volume 1, No 4, 2011, Influence of Marble powder/granules in Concrete mix" Bui D D, Hu J and Stroeven P 2005 Particle size effect on the strength of rice husk ash blended gap-graded portland cement concrete Cement & Concrete Composites 27 pp 357–366

[2] Demirel, Bahar, 2010. "The effect of the using waste marble dust as fine sand on the mechanical properties of the concrete". Department of Construction, Faculty of Technical Education, Firat University, Elazig, 23119, Turkey.

[3] Farah. A., Badorul, Bakar,B. H., Johari, M.A., and Jaya, R.P. (2011). Properties of concrete block containing rice husk ash subjected to girha. IJRRAS 8(1):57-64.

[4] Gemma Rodriguez de Sensale 2006 Strength development of concrete with rice husk ash Cement & Concrete Composites 28 pp 158-160

[5] Hanifi Binici1, Hasan Kaplan and Salih Yilmaz (August, 2007). "Influence of marble and limestone dusts as additives on some mechanical properties of concrete".

[6] IS: 2386 .1963. (Part I) Methods of test for aggregate for concrete, Indian Standards.

[7] IS: 10262 .1982. Recommended Guidelines for concrete mix design, Indian Standards.

[8] IS: 12269 .1987. Specification for 53 grading ordinary Portland cement, Indian

[9] IS: 383. Specification for coarse and fine aggregates from natural sources for concrete. Bureau of Indian Standards; 2002.

[10] Maurice and Godwin (2012) "Compressive strength of concrete with rice husk ash as partial replacement of ordinary Portland cement". Department of Civil Engineering, Rivers State University of Science and Technology Port Harcourt, Nigeria.

[11] Patidar and Sheknawant, 2015. Effect on the properties of concrete and mortar with partial replacement of cement to RHA and sand to MD slurry. MPUAT, Udaipus.

[12] shirule p et al. (2012) —partial replacement of cement with marble dust powder. Department of civil engineering, ssbts coet ,bambhori, jalgaon maharashtra.

[13] SP 23.1982. Indian standards handbook on concrete mixes, Indian Standards.

[14] Tashima M M, Carlos A R da Silva, Jorge Akasaki L and Michele Beniti B 2004 Proc. Conf. (Brazil) The possibility of adding the rice husk ash to the Concrete.

Proportional Use of Aggregates from Demolished Concrete

Indu Gyawali[1], Dhiraj Shrestha[1], Manoj Koirala[1], Meena Ghimire[1], Bharat Mandal[2]

[1]*Department of Civil Engineering, Advanced College of Engineering and Management, T.U.*
[2]*Lecturer, Department of Civil Engineering, Pulchowk Campus, T.U.*

Abstract

*To have a valid reason and data based result to assure public about reuse of aggregates from demolished concrete, research on "**Proportional use of aggregates from demolished concrete**" was done. Initially examining recycled aggregates, if they are viable to be used in constructional field through experiments like sieve analysis, water absorption, aggregates crushing and weight density tests. To fix the amount of RA (recycled aggregates) with VA (virgin aggregates) in different batches and proportion, compression and splitting test to samples prepared was obligatory and hence performed in an accordance to "IS 2386". A best proportion which resulted to corresponding mix's characteristics strength came out to be mix of 30 to 50% of RA with corresponding percentage of VA. With some assumptions regarding temperature and batches of mix, having in considerations to limitations like limited number of tests, a single mix design and limitations of time, the result obtained might enclose some sorts of discrepancy in compression and tension stresses shown by UTM. The research performed was totally for academic purpose and not for any marketing circumstances.*

Keywords: *concrete demolition, mix design, sample preparation, curing, crushing and splitting test, sample comparison to standards.*

1. Introduction

1.1 Background

Crushed concrete is available nowadays in large quantities, which results from the demolition of old structures and waste concrete from new structures. A report presented in 1999 to the European Commission estimated the amount of construction waste (non-recycled) to be 130 million t / year [1]. A decrease in the compressive strength was generally observed in all concretes in which the natural coarse aggregate was replaced with recycled aggregate prepared by the crushing of old concrete. The mechanical properties of the concrete decreased with the increase in the proportion of aggregate replaced. RILEM Technical Committee 121-DRG (1994) recommended that only 20% of the natural aggregate can be replaced with recycled coarse aggregate in the preparation of new concrete of all strength classes, and limited the concrete classes when 100% recycled construction waste is used [2].

1.2 Need of Study

The concrete industry makes up approximately 30% of the total market for aggregates and it is estimated that 165 million tones are used annually in concrete [3]. As the population is increased and there is increase in urban development, recycling the waste construction materials becomes important. These recycled materials are used in our concrete in the form of aggregate. As recycled aggregate are easy to obtain and its cost is cheaper, this can be used in the replacement of natural aggregate [2]. It possesses many advantages including low energy requirement, utilization under different environmental conditions. The manufacture process of recycled aggregate is a relatively simple as it involves breaking, removing, crushing existing concrete in to a

material with a specified size. Generally, the cost of recycled aggregate may be 15 to 30% lower than natural aggregate [2].

In Nepal, especially in Kathmandu valley, after the earthquake of April 25, 2015 (Baisakh 12, 2072 B.S) several houses were destroyed and demolished. The majority of solid wastes were found to be concrete pieces. Due to lack of disposal sites, tons of concrete pieces were dumped at Tudikhel, Nepal and outside the Kathmandu Valley consuming huge amount of money only for the dumping of the waste concrete. In such case, the necessity of utilization of recycled aggregate is accounted.

2. Literature Review

In the context of Nepal production of concrete is expensive and in the other hand disposal of demolished concrete is being an issue due to place of disposal. The concept of reusing the concrete has nowadays struck in many minds and people have started making lots of ideas regarding effective and usable disposal of demolished concrete in areas like road sub grade, retaining walls and many other fields. But is the structural use of demolished concrete possible?? Or are the aggregates from demolished concrete usable??

The idea of **"Proportional use of aggregates from demolished concrete"** is generated from all these circumstances. To find an optimum limit of use of (RA) recycled aggregate with virgin aggregate(VA), the research is made to contribute a value in certain percentage which can be beneficial in making proper mix for recycled concrete as a complete structural element. ACI Committee 555, Removal and Reuse of Hardened Concrete, ACI 555R-01, ACI Committee 555 Report, American Concrete Institute, Farmington Hills, Michigan, 2001, says proportional use of RA with VA is possible for concrete production with same natural strength. In American context, the report signifies the use of 30% of RA in proportion to VA [7]. In American circumstances like temperature, aggregate constituents, grade of mix made for sample, curing method adopted and admixtures used moreover report does not accomplish of tests on RA if they are feasible from every aspect of concrete production. **"Research on proportional use of aggregates from demolished concrete"** accomplish of tests on RA, comparisons of test results to standards, compressive strength test of sample in many proportions, splitting test of best proportion obtained, test on certain replacement of sand and RA with stone dust, findings of application areas.

Concrete compressive stress depends upon the quality of RCA for all load phases. Increasing the quantity of coarse RCA up to 100% will increase the concrete compressive stress up to 25% [8]. Shrinkage of concrete depend upon the amount of recycled concrete aggregate., concrete with more than 50% of recycled CA has significantly more shrinkage compared to NA increased shrinkage is the result of attached mortar and cement paste in the RCA grain [8].

The use of 100% RCA is possible to produce concrete with acceptable quality. The concrete produced with RCA has generally 80% to 90% of the strength of a comparable NCA concrete [9]. The use of fine RCA in a new concrete mix requires careful examination, as the recycled fines further reduce the strength of concrete. In general, 10% to 20% replacement of virgin sand by recycled fines is acceptable [9].

Observing all results by different researchers and having a brief look to their assumptions and different conditions of test procedures, "**Research on proportional use of aggregates from demolished concrete** "was carried out regarding the use of RCA considering material properties, climatic conditions, degree of workability, weathering on built up concretes and quality of material available in context of Nepal.

3. Methodology

3.1 Sample aggregate extraction

Cubes and cylinders made by students in earlier batch for their subject point of view and demolished concrete found in open areas were used as a sample aggregates. Basically just to demolish the hard and concrete in bigger geometry Universal Testing Machine (UTM) was used; to get the pieces of aggregates and aggregates in portable form manually hammering was done. In real field crushers can be used to get aggregates in usable form.

3.2 Sample aggregate test

3.2.1 *Sieve analysis [I]:*

Use of different sieves as standardized by the IS code and passing the aggregates through them and thus collect different sized particles left over different sieves.

- Apparatus used:

i. A set of IS Sieves of sizes: 63mm, 40mm, 25mm, 20mm, 16mm, 12.5mm, 10mm,4.75mm, 2.36mm.
ii. Balance or scale with an accuracy to measure 0.1 percent of the weight of the test sample.

The sample for sieving should be prepared from the larger sample either by quartering or by means of a sample divider.

- Procedure:

i. The test sample is dried to a constant weight at a temperature of 110 + 5°C and weighed. The sample is sieved by using a set of IS Sieves.
ii. On completion of sieving, the material on each sieve is weighed.
iii. Cumulative weight passing through each sieve is calculated as a percentage of the total sample weight.
iv. Fineness modulus is obtained by adding cumulative percentage of aggregates retained on each sieve and dividing the sum by 100.

3.2.2 *Aggregate crushing value test [II]:*

- *Equipment and apparatus used:*

Steel Cylinder, Sieves (12.5mm, 10mm), Cylindrical metal measure, Tamping Rod, Balance (0-10kg), Oven (300^0C), Compression testing Machine (2000KN)

- *Procedure:*

i. The cylindrical steel cup filled with 3 equal layers of aggregate, each layer tamped to 25 strokes by the rounded end of tamping rod
ii. The net weight of aggregate in the cylindrical steel cup is determined to the nearest gram (W_A) and this weight of aggregate is used for the duplicate test on the same material.
iii. The surface is leveled and the plunger is inserted so that it rests horizontally on the surface. The whole assembly is then placed between the platens of testing machine and loaded at a uniform rate so as to reach a load of 40 tons in 10 minutes.
iv. The load is then released and all aggregate is removed from the cup and sieved on 2.36 mm. IS sieve until no further significant amount passes in one minute. The fraction passing the sieve is weighed to an accuracy of 0.1 g (W_B).

3.2.3 *Water absorption test [III]:*

For Aggregate Larger than 10 mm

- *Apparatus required:*

Balance, Oven, A wire basket, watertight container, dry soft absorbent cloths and tray.

- *Test Procedure:*

i. The washed sample shall be placed in the wire basket and immersed in distilled water at a temperature between 22°C and 32°C. Immediately after immersion, the entrapped air shall be removed from the sample allowing it to drop 25 times at the rate of about one drop per second. The basket and aggregate shall remain completely immersed during the operation and for a period of 24 ±1/2 hours afterwards.
ii. The basket and the sample shall then be jolted and weighed in water at a temperature of 22 to 32°C (weight A1).
iii. The basket and the aggregate shall then be removed from the water and allowed to drain for a few minutes, after which the, aggregate shall be gently emptied from the basket on to one of the dry clothes, and the empty basket shall be returned to the water, jolted 25 times and weighed in water (weight A2).
iv. The aggregate shall be dried with the cloth, transferring it to the second dry cloth and a gentle current of unheated air may be used to accelerate the drying of difficult aggregates. The aggregate shall then be weighed (weight B).
v. The aggregate shall then be placed in the oven in the shallow tray, at a temperature of 100 to 110°C and maintained at this temperature for 24 ± l/2 hours. It shall then be removed from the oven, cooled in the airtight container and weighed (weight C).

3.2.4 *Weight density test [III]:*

- *Apparatus required:*

  Cylinder (15cm diameter×30cm height), Tamping rod

- *Procedure:*

i. First the weight of empty cylinder should be taken
ii. The demolished aggregate shall then to be placed on an empty cylinder.
iii. The cylindrical steel cup is filled with 3 equal layers of aggregate and each layer is tamped 25 strokes by the rounded end of tamping rod and the surplus aggregate struck off, using the tamping rod as a straight edge.
iv. Then the weight of cylinder with the aggregates shall be taken

As per IS 383 -1970 weight density of aggregate should lie between 1400 to 1600 kg/m^3

3.3 Mix design (M20) [IV]:

Concrete mix design is the process of finding the proportions of concrete mix in terms of ratios of cement, sand and coarse aggregates. For e.g., a concrete mix of proportions 1:2:4 means that cement, fine and coarse aggregate are in the ratio 1:2:4 or the mix contains one part of cement, two parts of fine aggregate and four parts of coarse aggregate. The concrete mix design proportions are either by volume or by mass. The water-cement ratio is usually expressed in mass

- *Procedure:*

i. Determine the mean target strength f_t from the specified characteristic compressive strength at 28-day f_{ck} and the level of quality control.

$f_t = f_{ck} + 1.65\ S$

Where S is the standard deviation obtained from the Table of approximate contents given after the design mix.

ii. Obtain the water cement ratio for the desired mean target using the empirical relationship between compressive strength and water cement ratio so chosen is checked against the limiting water cement ratio. The water cement ratio so chosen is checked against the limiting water cement ratio for the requirements of durability given in table and adopts the lower of the two values.

iii. Estimate the amount of entrapped air for maximum nominal size of the aggregate from the table.
iv. Select the water content, for the required workability and maximum size of aggregates (for aggregates in saturated surface dry condition) from table.
v. Determine the percentage of fine aggregate in total aggregate by absolute volume from table for the concrete using crushed coarse aggregate.
vi. Adjust the values of water content and percentage of sand as provided in the table for any difference in workability, water cement ratio, grading of fine aggregate and for rounded aggregate the values are given in table.
vii. Calculate the cement content from the water-cement ratio and the final water content as arrived after adjustment. Check the cement against the minimum cement content from the requirements of the durability, and greater of the two values is adopted.
viii. From the quantities of water and cement per unit volume of concrete and the percentage of sand already determined in steps 6 and 7 above, calculate the content of coarse and fine aggregates per unit volume of concrete from the following relations.

$$V = \left[W + \frac{C}{S_c} + \frac{1}{p}\frac{f_a}{S_{fa}} \right] \times \frac{1}{1000}$$

$$V = \left[W + \frac{C}{S_c} + \frac{1}{1-p}\frac{C_a}{S_{ca}} \right] \times \frac{1}{1000}$$

3.4 Curing

All batches of cubes and cylinder made were cured for 7 days and 28 days respectively. To each mixes of nine proportions, three samples were made and submerged curing was done on a cylindrical vessel of height one and a half meter and diameter of half meter.

4. Test of sample aggregates

4.1 Sieve analysis:

Different sieves as standardized by the IS code is used and then aggregates are passed through them.

Sieve size(mm)	Weight of empty sieve (Kg)	Cumulative %retained									
		Batch 1	Batch 2	Batch 3	Batch 4	Batch 5	Batch 6	Batch 7	Batch 8	Batch 9	Batch 10
63	0.385	0	0	0	0	0	0	0	0	0	0
40	0.370	0	0	1.2	0	0.6	1.0	1.2	1.2	0.8	1.24
25	0.385	39.6	48.2	45.2	60.6	39.4	44.6	44.8	44.4	44.32	44.84
20	0.365	71.2	70	69.2	79.4	68.4	69.4	70	69.6	69.92	70.04
16	0.390	97.8	94.8	94.0	96.8	95.4	93.4	93.6	93.4	93.16	94.44
10	0.345	99.8	99.8	99.8	99.6	99.6	99.6	99.64	99.6	99.6	99.64
4.75	0.405	99.8	99.8	99.8	99.8	99.8	99.8	99.8	99.8	99.8	99.8
2.36	0.370	99.8	99.8	99.8	99.8	99.8	99.8	99.8	99.8	99.8	99.8

Pan	0.340	100	100	100	100	100	100	100	100	100	100
Fineness Modulus= $\frac{Sum\ of\ cumulative\%retained}{100}$		6.08	6.12	6.094	6.36	6.03	6.076	6.0884	6.078	6.074	6.097

Table 4. 1: Data for particle size distribution for various batches

Average data:

Sieve size (mm)	Weight of empty sieve (Kg)	Weight of sieve with retained aggregate(kg)	Weight of retained aggregate(kg)	%Retained	Cumulative %retained	%Passing
63	0.385	0.385	0	0	0.00%	100%
40	0.037	0.037	0	0	0.00%	100%
25	0.385	1.375	0.99	39.60%	48.20%	51.80%
20	0.365	1.155	0.79	31.60%	70.00%	30%
16	0.39	1.055	0.67	26.60%	94.80%	5.20%
10	0.345	0.395	0.05	2%	99.80%	0.20%
4.75	0.405	0.405	0.00	0.00%	99.80%	0.20%
2.36	0.37	0.37	0.00	0.00%	99.80%	0.20%
pan	0.34	0.345	0.005	0.20%	0.00%	

Average fineness Modulus=$\frac{6.08+6.124+6.094+6.36+6.03+6.076+6.0884+6.078+6.074+6.097}{10}$

= 6.1102

4.2 Water absorption test:

Notation:

A= Weight of saturated aggregates in water= A_1-A_2

A_1= Weight of bucket + wire basket + aggregates

A_2= Weight of bucket + wire basket

B= Weight of saturated surface dried aggregates in air

C= Weight of oven dried aggregate

Water absorption = $\frac{B-C}{C}$* 100

=100*0.0199

=1.19%

4.3 Aggregates crushing value test:

Aggregates crushing value test is done to find out the limit of resistance to impact of raw aggregate while performing experiment or working in field with reference to experimental value.

Notation:

B= Weight of fraction passing appropriate sieve

A= Weight of surface dried sample

Aggregate crushing value=$\frac{B}{A}$*100%

=$\frac{0.58}{2.685} * 100\%$

=21.6%

4.4 Weight density test:

Weight density test is done to find out the dry density of aggregates, aggregates taken in a mould of known dimension with proper compaction followed by application of simple formula:

$\frac{mass}{volume}$,

Notation:

D= Diameter of cylinder in (cm) = 15

H= Height of cylinder in (cm) = 30

W_1= Weight of empty cylinder =7.405 kg

W_2= Weight of cylinder with aggregates = 14.925 kg

Volume of empty vessel (cylinder) =V = $\frac{\pi D^2}{4} * H$

$=\frac{\pi * 0.15^2 * 0.3}{4}$

$=5.301 * 10^{-3} m^3$

Weight of aggregates (W) = W_2- W_1

= 14.925-7.405

=7.52 Kg

Weight density of aggregates = $\frac{W}{V}$

$=\frac{7.52}{5.301 * 10^{-3}}$

= 1418.48 Kg/m^3

4.5 Crushing Test of Cube

Nine different mixes was made for making compression test in different proportions as mentioned below:

i. 100% old aggregate
ii. 60% old aggregate + 40% new aggregate
iii. 50% old aggregate + 50% new aggregate
iv. 40% old aggregate + 60% new aggregate
v. 30% old aggregate + 70% new aggregate
vi. 10% stone dust + 90% sand + 100% old aggregate
vii. 10% stone dust + 100% sand + 90% old aggregate
viii. 20% stone dust + 100% sand + 80% old aggregate
ix. 100% new aggregate

Use of stone dust was for making check if workability gets affected and does the cementation get influenced with use of it.

To have crushing test done UTM is used with an application of gradually increasing load unless significant crack is observed.

Table 4.2: Actual Data for compressive load for various mix proportions

mix proportion	Cube Test For 7 Days Curing		
	Load (KN)		
	specimen 1	specimen 2	specimen 3
100% old aggregate	209.3	212.6	216.9
60% old agg. + 40% new agg.	196.3	199.5	202
50% old agg. + 50% new agg.	316.1	314	312
40% old agg. + 60% new agg.	260.4	263.2	267.5
30% old agg. + 70% new agg.	271.2	274.8	279
10% stone dust + 90% sand + 100% old aggregate	298.2	301.7	305.9
10% stone dust + 100% sand + 90% old aggregate	236.4	239.8	243.2
20% stone dust + 100% sand + 80% old aggregate	287.2	288.3	288.8
100% new aggregate	287.2	288.3	288.8

mix proportion	Cube Test For 28 Days Curing		
	Load (KN)		
	specimen 1	specimen 2	specimen 3
100% old aggregate	360	362.5	363.3
60% old agg. + 40% new agg.	278.7	279.4	277.6
50% old agg. + 50% new agg.	465.3	467.3	472.2
40% old agg. + 60% new agg.	343.8	344.2	345.9
30% old agg. + 70% new agg.	456.9	453.3	451.2
10% stone dust + 90% sand + 100% old aggregate	364.48	364.9	365.4
10% stone dust + 100% sand + 90% old aggregate	356.5	357.9	358.7
20% stone dust + 100% sand + 80% old aggregate	369.4	371.6	372.5
100% new aggregate	360.2	391.4	423.2

4.6 Splitting Test of Cylinder

To get information regarding tensile behavior of concrete, splitting test of a sample made in a cylinder of dimension 30 cm height and 15 cm diameter was done on UTM by a progressively increasing load.

Table 4.3: Data for tensile load for various mix proportions.

mix proportion	Load (KN)					
	Splitting Test For 7 Days Curing			Splitting Test For 28 Days Curing		
	specimen 1	specimen 2	specimen 3	specimen 1	specimen 2	specimen 3
60% old agg. + 40% new agg.	77.7	78.9	79.5	108.7	110.5	111.3
20% stone dust + 100% sand + 80% old aggregate	91.35	92.4	94.8	128.3	129.4	1321.7

5. Result:

5.1 Eye examination of sample aggregate:

Properties	Description
Shape and size	Angular and well graded
Texture	Rough surface
Porosity	Fairly porous

5.2 Sample aggregate:

5.2.1 Sieve analysis:

From the test the average fineness modulus is found to be 6.1102%.

- Gradation curve: From the gradation curve as shown below, the aggregate is found to be **well graded** as the curve is **S-shaped**.

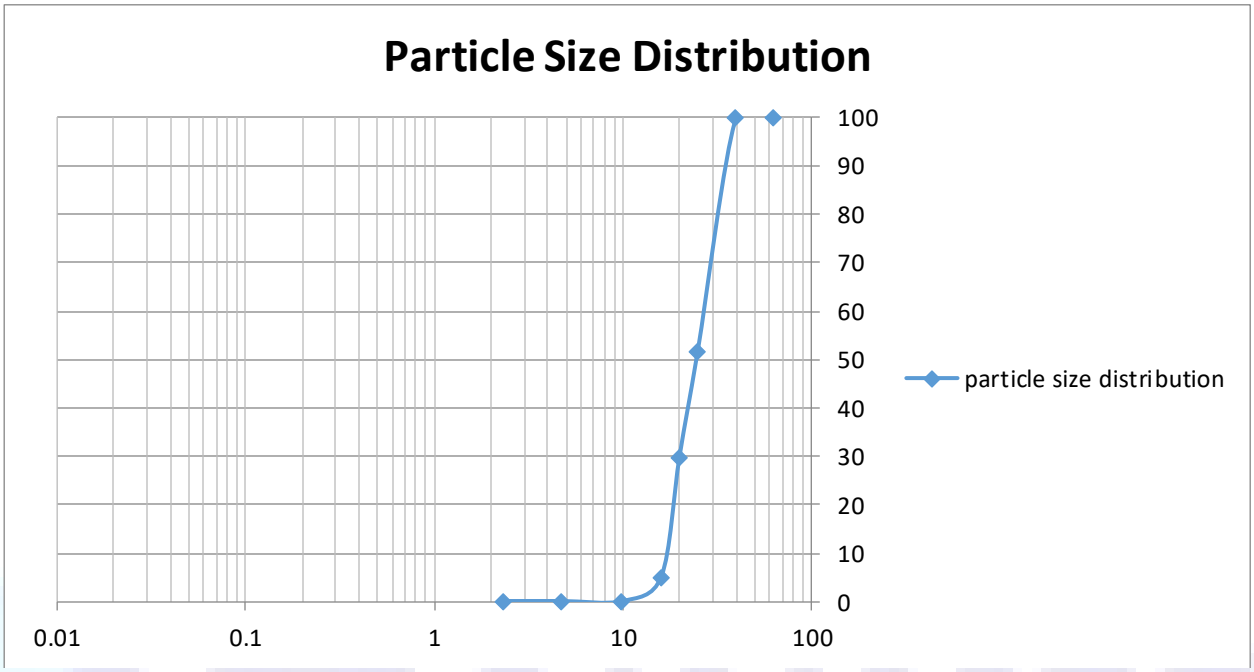

Figure 5.1: Gradation Curve

5.3 Crushing test of Cube:

The average crushing value and the corresponding compressive strength of the cube for different mix proportion for 7 days and 28 days curing are as shown in the following tables:

Table 5.1: Average compressive strength for 7 days and 28 days curing, with consideration of correction suggested by calibration report.

)S.N	Description	Average Load (KN)		CompressiveStress (N/mm^2)	
		7 days curing	28 days curing	7 days curing	28 days curing
1	100% old aggregate	359.9	508.9	15.73	22.43
2	60% old aggregate + 40% new aggregate	346.4	425.6	15.13	18.73
3	50% old aggregate + 50% new aggregate	461.1	615.3	20.23	27.13
4	40% old aggregate + 60% new aggregate	410.7	591.6	18.03	26.03

5	30% old aggregate + 70% new aggregate	422	600.8	18.53	26.53
6	10% stone dust + 90% sand + 100% old aggregate	448.9	511.9	19.73	22.53
7	10% stone dust + 100% sand + 90% old aggregate	386.8	504.8	16.93	22.23
8	20% stone dust + 100% sand + 80% old aggregate	412.4	519.2	18.13	22.83
9	100% new aggregate	435.3	538.5	19.13	23.73

- Bar chart for compressive strength of cube for various mix proportion:

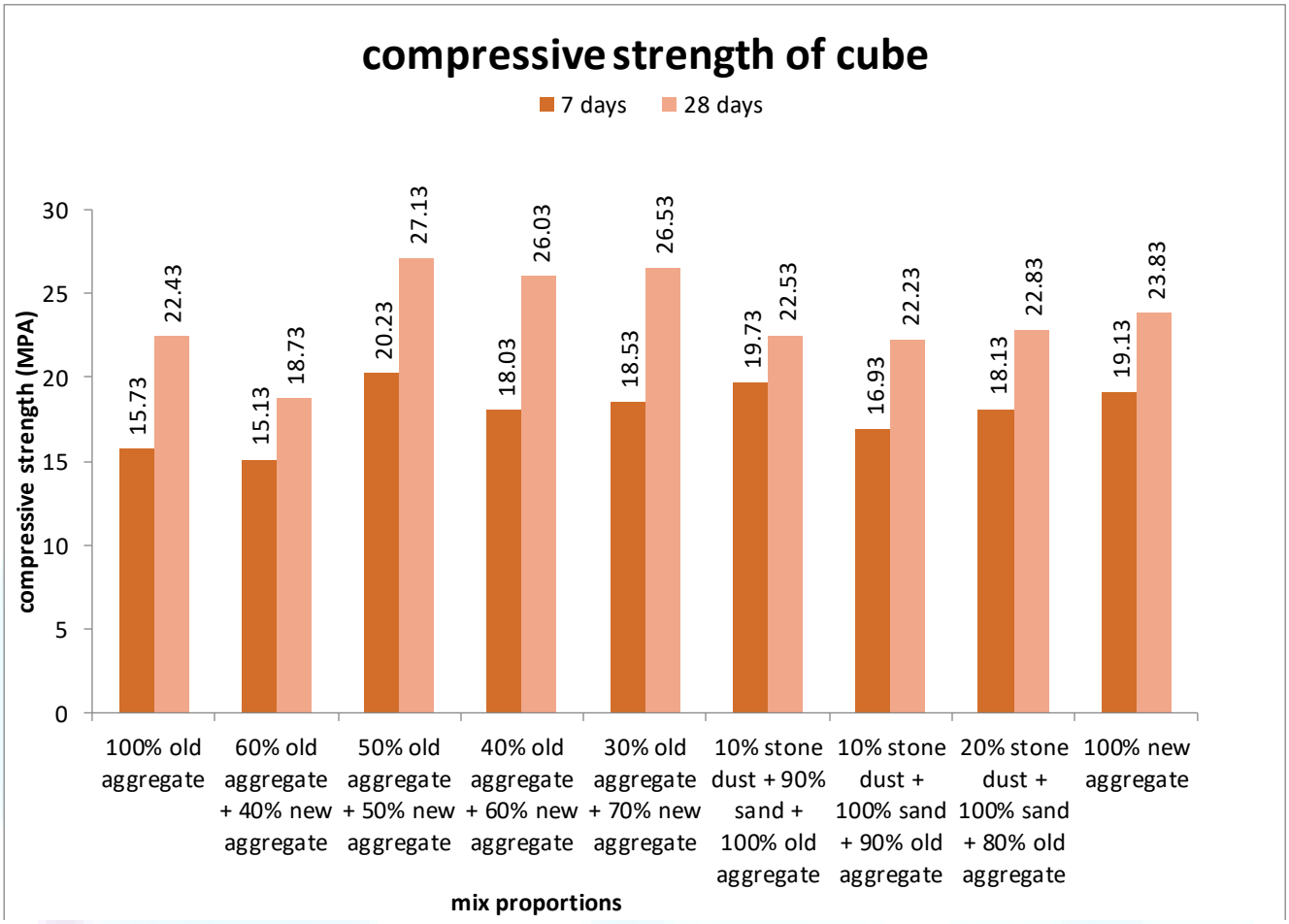

Figure 5.2: Bar chart showing compressive strength for various mix proportion

5.4 Splitting Test of Cylinder:

The average tensile load and the corresponding tensile strength of the cylinder for different mix proportion for 7 days and 28 days curing are as shown in the following tables:

- For 7 days curing:

Table 5.2: Average tensile strength for 7 days and 28 days curing

S.N	Description	Average load (KN)	Tensile Stress(N/mm^2)
1	60% old aggregate + 40% new aggregate	78.7	1.7
2	20% stone dust + 100% sand + 80% old aggregate	92.8	2.1

- For 28 days curing:

S.N	Description	Average Load (KN)	Tensile Stress (N/mm^2)
1	60% old aggregate + 40% new aggregate	110.25	2.5
2	20% stone dust + 100% sand + 80% old aggregate	130.05	2.9

5.5 Comparison to standards:

5.5.1 *Sieve analysis [V]:*

According to IS 383-1970, the Fineness Modulus should be 5.5% to 8%. From the experiment, the Fineness Modulus is found to be 6.112% which lies between 5.5% and 8%. Hence the aggregate is appropriate for construction.

5.5.2 *Crushing value test [V]:*

According to IS 383-1970, the aggregate crushing value should be less than 45%. From the test, the aggregate crushing value is found to be 21.60%. Hence the aggregate is appropriate for construction.

5.5.3 Water absorption test [V,VI]:

According to BS 812-2, the water absorption value should be less than 3%. From the test, the water absorption value is found to be 1.19%. Hence the aggregate is appropriate for construction.

5.5.4 *Weight density test [V]:*

According to IS 383-1970, the weight density of the aggregate should lie between 1400 to 1600 kg/m^3. From the test, the weight density of the aggregate is found to be 1418.48 kg/m^3. Hence the aggregate is appropriate for construction.

5.5.5 *Crushing strength of cube [IV]:*

The ultimate crushing strength of cube for 50% old aggregate plus 50% new aggregate mix proportion is found to be 292.7 KN or 1300.741 N/mm^2.

6. Conclusion and recommendation

Feasibility to use:

Aggregates from demolished concrete are reusable to any constructional field, as suggested by the experiment result.30%-50% RA in a mix with VA provides an appropriate strength as characteristics strength of mix. With the procedures specified by IS code and in a comparison to values specified for aggregates in constructional concrete a summary can be made "proportional use of aggregates from demolished concrete is possible"

Every value obtained from experiments of aggregates remains in range and criteria specified by IS 456-2000. Observed characteristics strength in compression does meets the limit and definition of characteristic strength that not more than five percent of sample's F_{ck} falls below 20 mpa. Results of splitting test as in general is 10% to 15% of $F_{ck.}$ Result obtained for splitting test of cylinders in UTM applying load in longitudinal axis can be summed as 10% of F_{ck}. An appropriate enough to make sure the use of such concrete in tested proportion

is feasible to be used.

Cost effectiveness:

Generally, cost of recycled aggregates may be 15 to 30% lower than NA [2],
Lower importance structures like:

- Bank protections
- Backfill
- Base course in pavements

Where 100% RCA can be used without considering strength factor as strength of 100% RCA is also significantly sound.For RCC works 30%-50% replacement of NA with RCA makes structures economic and strong.

Application area:

With considerations to strength and economy following are the areas where RCA can be used either in suitable proportion recommended or with100% replacement of NA.

- With 30-50% replacement of NA in high importance RCC structures.
- As building blocks.
- Road pavement construction.
- Drainage construction.
- Backfill in pipe zone along trenches.

References

[I] IS 2386 PART I-1963
[II] IS 2386 PART III-1963
[III] IS 2386 PART IV-1963
[IV] IS 456 -2000
[V] IS 383-1970
[VI] BS 812-2
[1] Symonds Group Ltd, 46967 Final Report, February 1999
[2] RILEM Technical Committee 121-DRG (1994)
[3] PQ STAFFS, 2016 Aggregate production statistics, may 29, 2017
[4] Puthussery JV, Kumar R, Garg A.WasteManag. 2017 Feb; 60:270-276. Epub 2016 Jun 25.
[5] Marinković S, Radonjanin V, Malešev M, IgnjatovićI.WasteManag. 2010 Nov; 30(11):2255-64.
[6] American Concrete Institute, ACI 555R-01, ACI Committee 555 Report, Farmington Hills, Michigan, 2001
[7] Mirjana Malesev, TrgDositejaObradovica 6, Serbia
[8] Recycling of Demolished Concrete and Masonry; Hansen, T.C., Ed.; Taylor and Francis: Oxfordshire, UK, 1992
[9] Fisher, C.; Werge, M. EU as a Recycling Society; ETC/SCP Working Paper 2/2009.

Seismic Vulnerability Assessment and Comparative Study of Steel and RC Structure by Developing Fragility Curve

Roshan Thapa[1], Sanjay Bhadel[1], Rosan Shrestha[1], Rhythm Thapa[1], Roshan K.C.[1], Arun poudel[2]

[1]*BE civil Engineering, Advanced college of Engineering and Management, TU.*
[2]*Lecturer, Department of Civil Engineering, IOE, Pulchowk Campus, T.U.*

Abstract

Selection of kind of structures to use in the areas with significant seismic activities is one of the serious challenges faced by any designer Engineer. Development of fragility curve provides an opportunity for designers to select a structure that will have the least fragility. This project is carried out to assess the seismic vulnerability of four types of structural system as defined by HAZUS namely RC frame, steel frame, steel braced frame and steel frame with cast in-place concrete shear wall of various heights confirming to low-rise, mid-rise and high-rise building by developing the seismic fragility curve, so as to determine which structural system shows the better performance during seismic activities. Linear dynamic analyses of low –rise (three storey), mid-rise (six storey), and high-rise (nine storey) building of all structural system considered are carried out using SAP 2000 V19. HAZUS methodology has been employed and the results are compared. The definition of damage states is based on the descriptions provided by HAZUS, which gives the limit states and the associated inter storey drift limits for structures.

Among the structures taken under consideration, the RC frame structure shows the highest probability of damage. Also the fragility curve shows the similar nature for low-rise and mid-rise building while it shows different nature for high-rise building.

Keywords: *seismic vulnerability; fragility curve; linear Dynamic Analysis; HAZUS methodology.*

1. Introduction

Earthquakes are no more a matter of surprise for mountainous country Nepal with several numbers of active faults (Nakata, 1989). The damages to the building equally have histories associated with it. Nepal has always lost its precious heritages after every strong ground motion. It has been seen that a number of high magnitude earthquakes have taken place in context of Nepal and there is equal probability of recurrence of such devastating earthquake in the future as well. Thus structures need more attention regarding seismic safety and hence Seismic Vulnerability Assessment should be practiced in structures to be constructed in Nepal.

1.1 Fragility curve

Fragility curve is a statistical tool representing the probability of exceeding a given damage state (or performance) as a function of an engineering demand parameter that represents the ground motion (preferably spectral displacement at a given frequency). Fragility curves give information on how the probability of structural damage increases with increasing peak ground acceleration. They are resumed to follow a lognormal distribution. Literature reviews show that utilization of fragility curves began with nuclear facilities because the damage to these structures can be so devastating, these structures are considered extremely important.

Fragility curves were first designed for nuclear power plants in 1980.Fragility curves were discussed based on three types of structures, namely, steel, reinforced concrete, and timber. Most studies covered

steel and reinforced concrete structures. However, less research has been conducted on timber structure.

Fragility function provides the probability of exceeding a prescribed level of damage for a wide range of ground motion intensity. The levels of damages are categorized into four states i.e. slight damage, moderate damage, extensive damage and complete damage. These damage states are numerically interpreted as a function of yield displacement (dy) and ultimate displacement (du) capacity whose values are suggested by HAZUS-MH MR3.

HAZUS (Hazard US) is a well-known loss estimation methodology that defines five damage states, none, slight, moderate, extensive, and complete, using physical (qualitative) descriptions of damage to building elements. The HAZUS methodology has been applied to various seismic hazard assessment studies by adapting capacity and fragility curves for structures in specific regions.

According to HAZUS- MH MR3, the probability of being in or exceeding a given damage state is modeled as a cumulative lognormal distribution. For structural damage, given the spectral displacement demand, Sd, the probability of being in or exceeding some damage state ds, is modeled as:

$$P[ds|Sd] = \emptyset\left[\frac{1}{\beta ds} ln\left(\frac{Sd}{\bar{S}d,ds}\right)\right]$$

Where:

$\bar{S}d, ds$ is the median value of spectral displacement at which the building reaches the threshold of the damage, ds

βds is the standard deviation of the natural logarithm of spectral displacement of damage state, ds, and

$\emptyset$ is the standard normal cumulative distribution function.

According to 5.4.4 section of HAZUS-MH-MR3, the total variability of each equivalent PGA structural damage state, ($SPGA$) is modeled by the combination of following two contributors to damage variability:

Uncertainty in the damage-state threshold of the structural system ($SPGA$) = 0.4 for all building types and damage states

Variability in response due to the spatial variability of ground motion demand ((V) = 0.5 for long period spectral response).

The two contributors to damage state variability are assumed to be log normally distributed, independent random variables and the total variability is simply the square root-sum-of-the-squares combination of individual terms i.e. $\beta(SPGA) = 0.64$.

The four damage states (ds) used as the capacity of the building in terms of yield displacement (dy) and ultimate displacement (du) as suggested by Giovianazzi and Lagomarsino 2006 after conducting a pushover analysis are:

For slight damage capacity = 0.7dy

Moderate damage capacity = 1.5dy

Extensive damage capacity = 0.5 (dy+du)

Complete damage capacity = du

Where,

Yield displacement= dy

Ultimate displacement =du

These four numerical values, used as the capacity of the building for a prescribed level of damage represents the median value of spectral displacement ($\bar{S}d, ds$) at which the building reaches the threshold of the damage, ds.

2. Literature review

In Nepal, numbers of researches have been carried out to study the seismic vulnerability of building. Past researches indicate that the methodologies used were linear static and dynamic methods. However, recent trend of research shows the use of macro seismic as well as mechanical methods as done by, Srijana Gurung Shrestha 2013 and Saroo Shrestha 2014.

Federal Emergency Management Agency ((FEMA-154, 2002)) prepared a hand book to conduct Rapid Visual Screening of Buildings in 1988 to evaluate the buildings in California. Revisions have been made in this handbook after obtaining new data on the performance of the buildings in earthquakes. Rapid Visual Screening method has been used by Prem Nath Maskey(2012), and Srijana Gurung Shrestha (2013) in their researches.

FEMA 154 method was used to determine the vulnerability of the buildings. The buildings also were analyzed using FEM technique in SAP 2000 to obtain fragility curves for different damage states.

Srijana Shrestha Gurung, 2013 conducted Rapid Visual Screening (RVS) method and additionally developed fragility curves to assess the vulnerability for five typical building models located at Jhatapol, Patan. She found that the results of fragility analysis are different from that of RVS methodology of assessing vulnerability.

Sharoo Shrestha, 2014 also conducted the seismic vulnerability of a historic timber masonry monumental building in Nepal. She studied the seismic vulnerability assessment of SaatTalle Durbar (Seven-storey Palace) of Nuwakot following the guidelines of HAZUS-MH-MR3 for the estimation of displacement capacity during different damage states. The seismic demand, on the other hand, had been determined from linear Time History analysis. Finally, structural vulnerability of the building was expressed in terms of fragility curves.

Bibek Sigdel (2015) developed fragility curve for three different historical building located in Kathmandu. Similarly, Bhabuk Raj Aryal (2015) also developed fragility curve for the bridge piers of different geometry.

Similarly, Arun Poudel (2016) developed fragility curve for the Calculation of PGA at specific site for RCC buildings during Gorkha earthquake dated 25th April 2015. All of them followed the Hazus-MH-MR3 and FEMA 154 extensively in their work.

These researches which were done recently indicate the reliability of researchers on fragility curve.

3. Methodology

3.1 Selection of model buildings

The educational building of typical floor plan as shown below with plinth area 512.824 sq.m and storey height of 3 m each was selected for study. Following four structural systems namely concrete moment frame, steel moment frame, steel braced frame and steel frame with cast-in-place concrete shear wall were considered for study. Each of them were further classified on the basis of classification suggested by FEMA-178 which is shown in table 1.

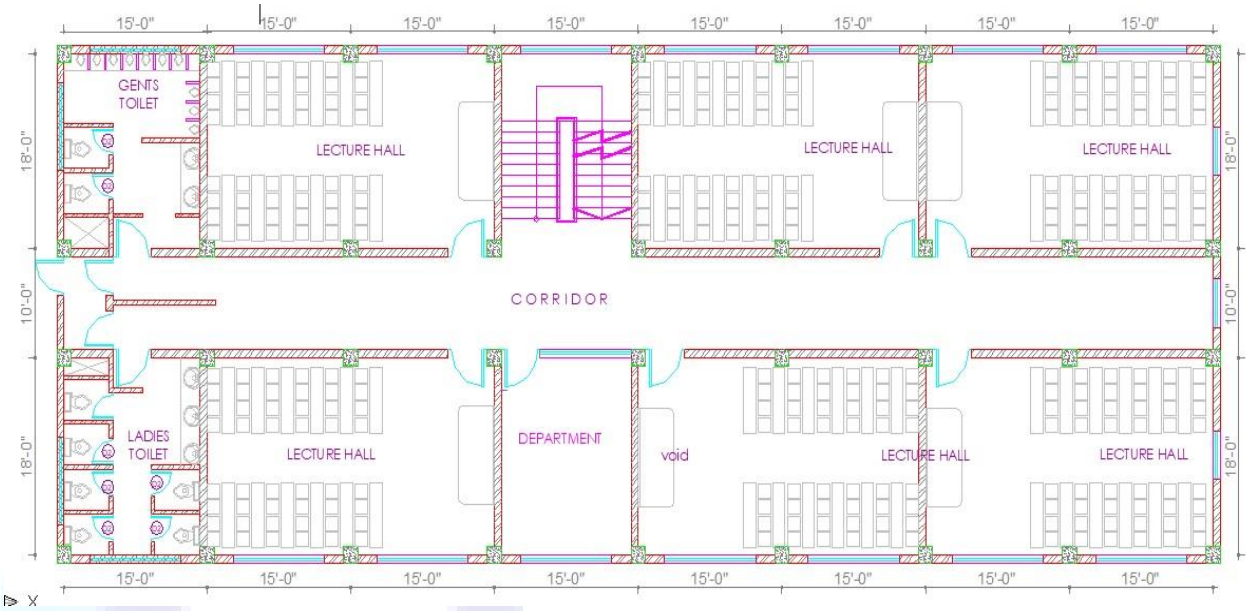

Figure 1: Typical floor plan of the building

Table 1: Model Building types taken under study

Label	Description	Height	
		Name	Stories
S1L S1M S1H	Steel moment frame	Low-rise Mid-rise High-rise	3 6 9
S2L S2M S2H	Steel braced frame	Low-rise Mid-rise High-rise	3 6 9
S4L S4M S4H	eel Frame with Cast-in-Place Concrete Shear Walls	Low-rise Mid-rise High-rise	3 6 9
C1L C1M C1H	oncrete Moment Frame	Low-rise Mid-rise High-rise	3 6 9

3.2 Building modeling

All the twelve buildings considered under study were modeled using SAP 2000 V19. Beam and Column elements were modeled as two node beam element while slab was modeled as shell element. The end connections of beam are modeled as rigid connection. The structural members were optimized for each model building types. Table 2 shows the section properties of all structural members for each model building types.

Table 2: Section properties of structural components

ilding Type	ction Properties				
	am Size	lumn Size(mm*mm)	b Thickness	gle Section	ear Wall Thickness
L	*12"	0*300			
M	*12"	0*400			
H	"*18"	0*450			
L	MB250	ilt up section ISMC300)			
M	MB250	ilt up section ISMC300)			
H	MB300	ilt up section ISMC400)			
L	MB250	ilt up section ISMC300)		A80*80*8	
M	MB250	ilt up section ISMC300)		A100*100*10	
H	MB300	ilt up section ISMC400)		A110*110*11	
1	MB250	ilt up section ISMC300)			
M	MB250	ilt up section ISMC300)			
H	MB300	ilt up section ISMC400)			

3.3 Selection of Accelerogram

The actual ground motion data of Gorkha earthquake dated April 25th, 2015 was obtained from Nepal seismological centre, Lainchaur. The graphical representation of the accelerogram is shown below:

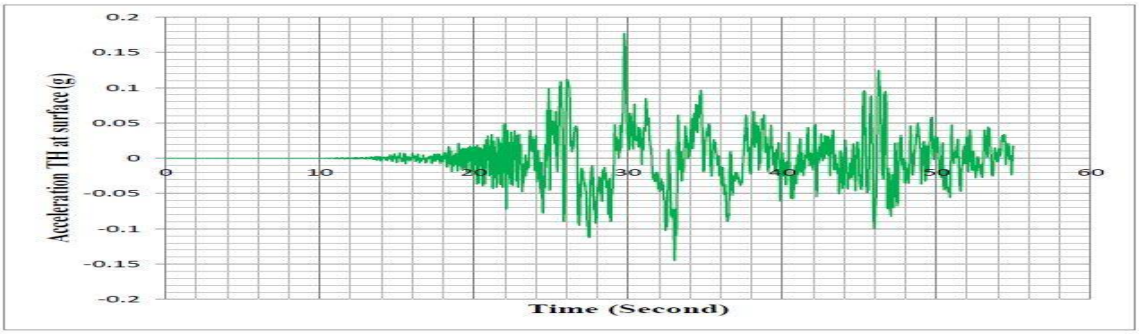

Figure 2: Accelerogram of Gorkha earthquake

3.4 Linear Time History Analysis

Linear time history analysis was performed to determine the dynamic response of the structure. According to the CSI Analysis Reference manual, two types of linear time history analysis methods are available i.e. Modal Time-History Analysis and Direct Integration Time-History Analysis. For the rigid structures modeled in SAP 2000 the Direct Integration Time-History Analysis method was followed. The damping associated with the analysis was used as mass and stiffness proportional damping whose values as suggested by Clough and Penzien.

3.5 Abstraction of required data from HAZUS MH-MR3 manual

The definition of damage states is based on the descriptions provided by HAZUS. The values for the yield and the ultimate displacements are taken from table 5.7 (a) from HAZUS which is as shown in table below: -

Table 3: Values for the yield and the ultimate displacements as per HAZUS MH-MR3

Building type	Yield capacity point	Ultimate capacity point
	D_y(in.)	D_u(in.)
C1L	0.39	9.39
C1M	1.15	18.44
C1H	2.01	24.13
S1L	0.61	14.67
S1M	1.78	28.4
S1H	4.66	55.88
S2L	0.63	10.02
S2M	2.43	25.88
S2H	7.75	61.97
S4L	0.38	6.91
S4M	1.09	13.1
S4H	3.49	31.37

The four damage states (ds) used as the capacity of the building in terms of yield displacement (dy) and ultimate displacement (du) as suggested by Giovianazzi and Lagomarsino 2006 after conducting a pushover analysis are:

For slight damage capacity = 0.7dy
Moderate damage capacity = 1.5dy
Extensive damage capacity = 0.5 (dy +du)

Complete damage capacity = du

Table 4: Top capacity displacement of different building under study

Building Type	Top capacity displacement (mm)			
	Slight	**Moderate**	**Extensive**	**Complete**
C1L	6.9342	14.859	124.206	238.506
C1M	20.447	43.815	248.793	468.376
C1H	35.737	76.581	331.978	612.902
S1L	10.845	23.241	194.056	372.618
S1M	31.648	67.818	383.286	721.360
S1H	82.854	177.546	768.858	1419.352
S2L	11.201	24.003	135.255	254.508
S2M	43.205	92.583	359.537	657.352
S2H	137.795	295.275	885.444	1574.038
S4L	6.756	14.478	92.583	175.514
S4M	19.380	41.529	180.213	332.740
S4H	62.052	132.969	442.722	796.798

4. Observation and Results

After analyzing the structure roof displacement vs. time is obtained as output of the time history analysis for all the model building considered under study.

Case 1: 3 storey RC building

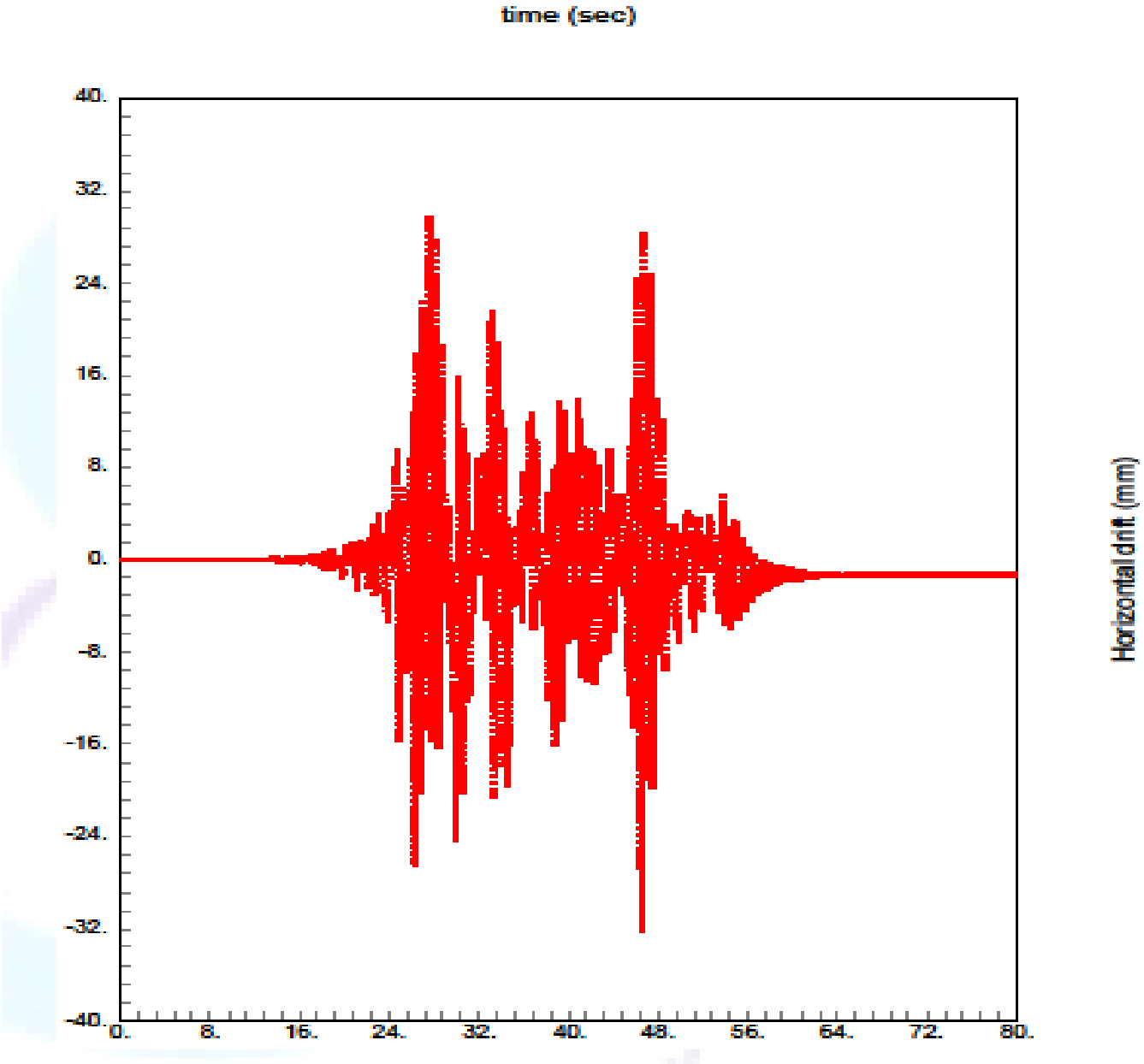

Figure 4: Displacement vs time graph for 3 Storey RC Building

Table 5: Calculation of Probability of Failure for 3 storey RC building

PGA (g)	Top displacement					Probability of failure at damage state (Pf)			
	Demand (mm)	Capacity (mm)							
		Slight	Moderate	Extensive	complete	Slight	Moderate	Extensive	Complete
0.000	0.000	6.934	14.859	124.206	238.506	0.000	0.000	0.000	0.000
0.050	9.130	6.934	14.859	124.206	238.506	0.666	0.223	0.000	0.000
0.100	18.260	6.934	14.859	124.206	238.506	0.935	0.626	0.001	0.000
0.150	27.390	6.934	14.859	124.206	238.506	0.984	0.830	0.009	0.000
0.177	**32.320**	6.934	14.859	124.206	238.506	**0.992**	**0.888**	**0.018**	**0.001**
0.200	36.520	6.934	14.859	124.206	238.506	0.995	0.920	0.028	0.002
0.250	45.650	6.934	14.859	124.206	238.506	0.998	0.960	0.059	0.005
0.300	54.780	6.934	14.859	124.206	238.506	0.999	0.979	0.100	0.011
0.350	63.910	6.934	14.859	124.206	238.506	1.000	0.989	0.150	0.020
0.400	73.040	6.934	14.859	124.206	238.506	1.000	0.994	0.203	0.032
0.450	82.169	6.934	14.859	124.206	238.506	1.000	0.996	0.259	0.048
0.500	91.299	6.934	14.859	124.206	238.506	1.000	0.998	0.315	0.067
0.550	100.429	6.934	14.859	124.206	238.506	1.000	0.999	0.370	0.088
0.600	109.559	6.934	14.859	124.206	238.506	1.000	0.999	0.422	0.112
0.650	118.689	6.934	14.859	124.206	238.506	1.000	0.999	0.472	0.138
0.700	127.819	6.934	14.859	124.206	238.506	1.000	1.000	0.518	0.165
0.750	136.949	6.934	14.859	124.206	238.506	1.000	1.000	0.561	0.193
0.800	146.079	6.934	14.859	124.206	238.506	1.000	1.000	0.600	0.222
0.850	155.209	6.934	14.859	124.206	238.506	1.000	1.000	0.636	0.251
0.900	164.339	6.934	14.859	124.206	238.506	1.000	1.000	0.669	0.280
0.950	173.469	6.934	14.859	124.206	238.506	1.000	1.000	0.699	0.309
1.000	182.599	6.934	14.859	124.206	238.506	1.000	1.000	0.726	0.338

Results in terms of displacement: -
Height of the displacement observation node = 9m

Earthquake	P.G.A(g)	Max. Displacement of node(mm)
Gorkha	0.177	32.32

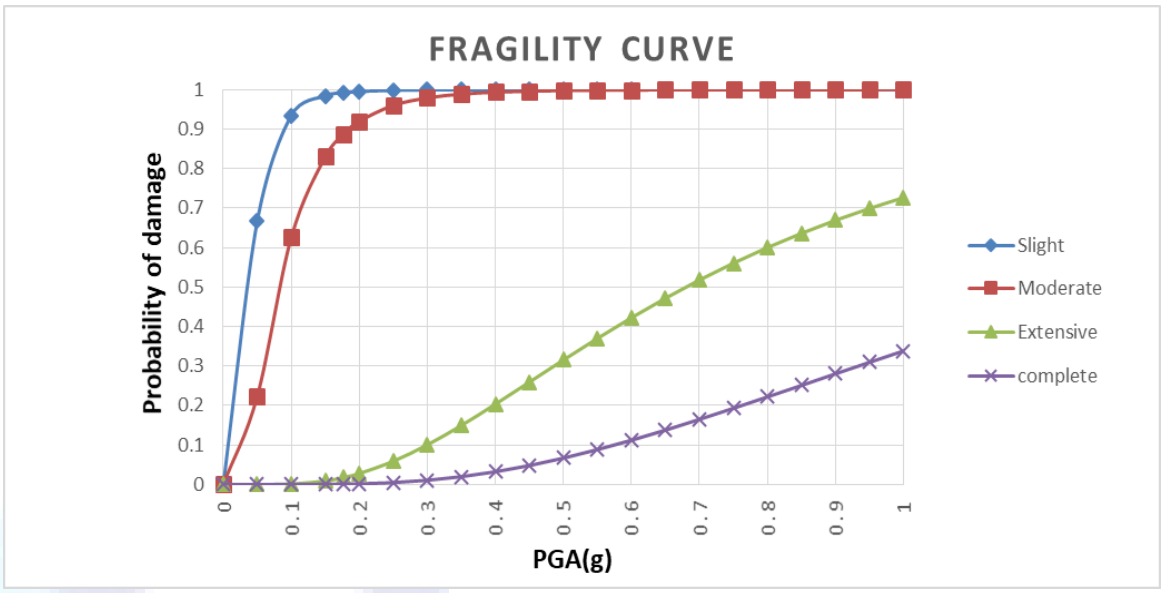

Figure 5: Fragility curve for 3 storey RC Building

Similar procedure was followed to generate the fragility curve for all model buildings which are as shown below.

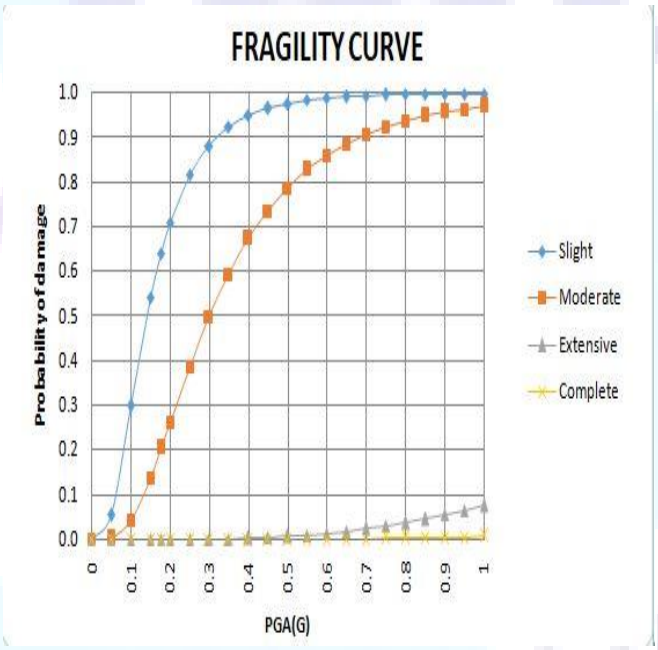

Figure 6: Fragility curve for 3 storey RC Building

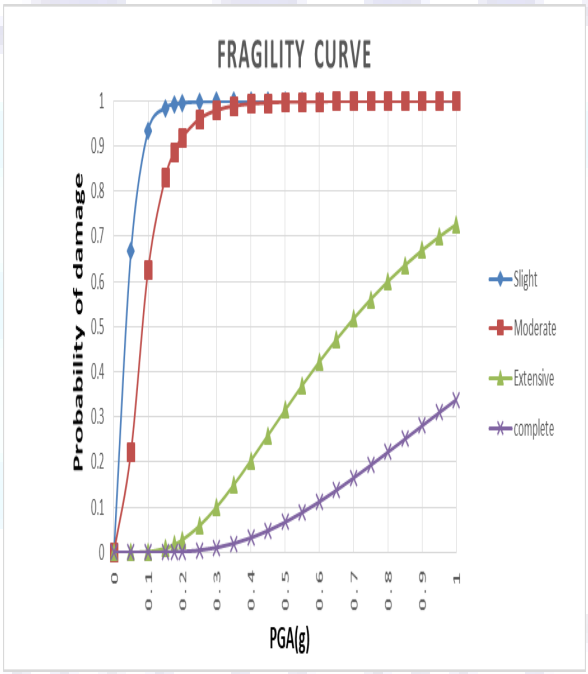

Figure 7: Fragility curve for 3 storey steel moment frame Building

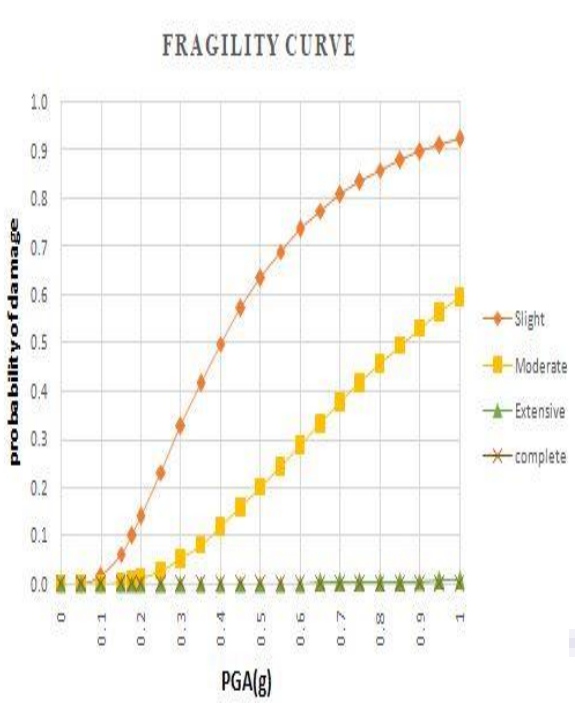

Figure 8: Fragility curve for 3 storey steel braced frame Building

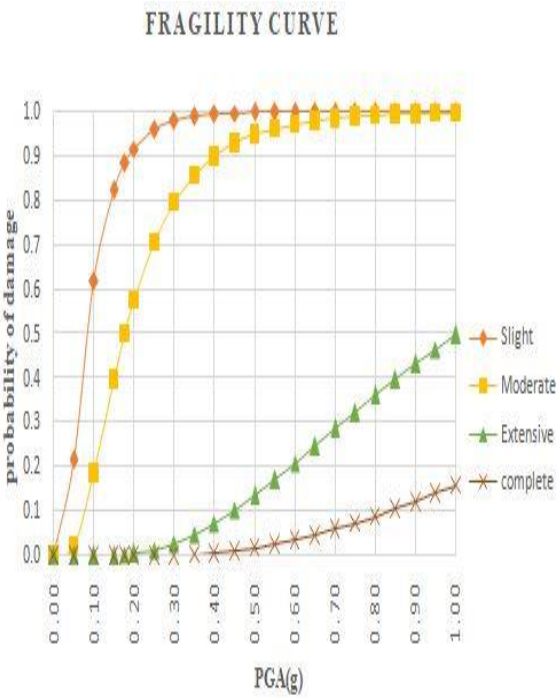

Figure 10. Fragility curve for 6 storey RC Building

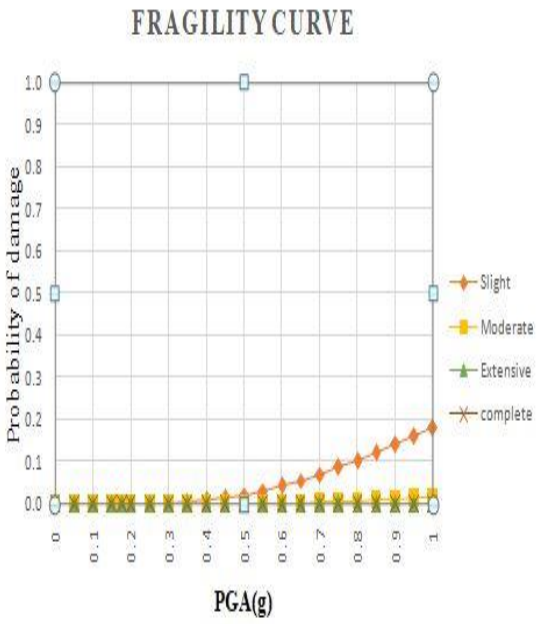

Figure 9: Fragility curve for 3 storey steel frame building with cast-in-place concrete shear wall Building

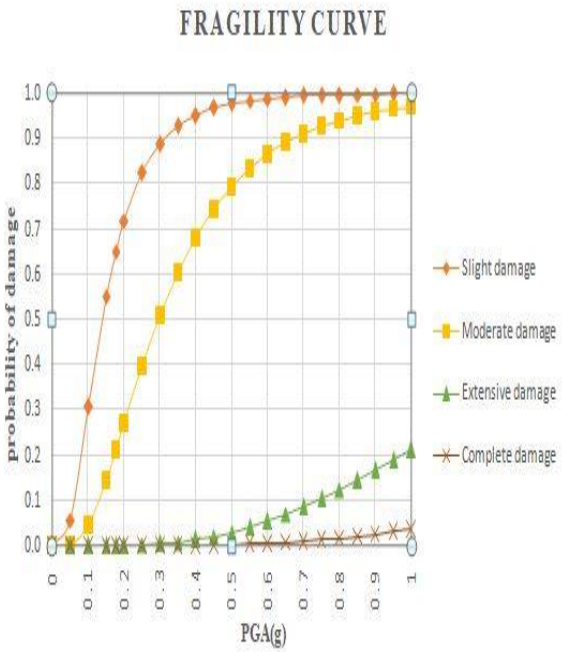

Figure11. Fragility curve for 6 storey steel moment frame Building

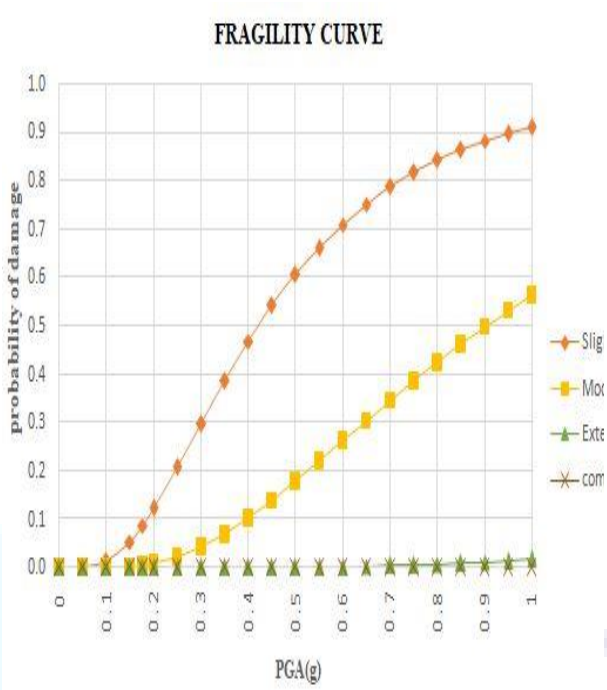

Figure 12. Fragility curve for 6 storey steel frame building with cast-in-place concrete shear wall

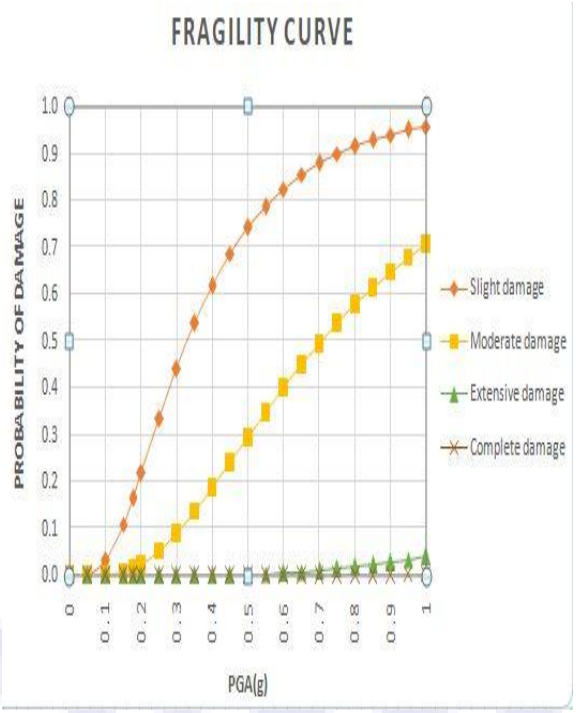

Figure 14. Fragility curve for 9 storey steel moment frame Building

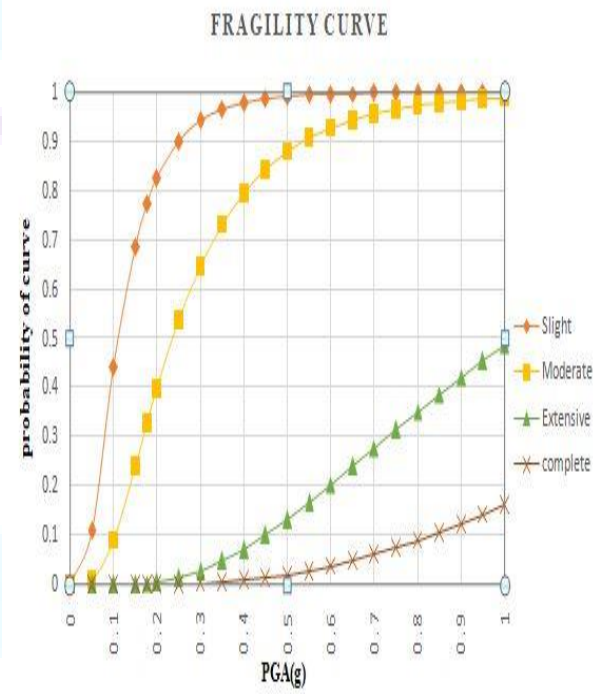

Figure 13. Fragility curve for 9 storey RC Building

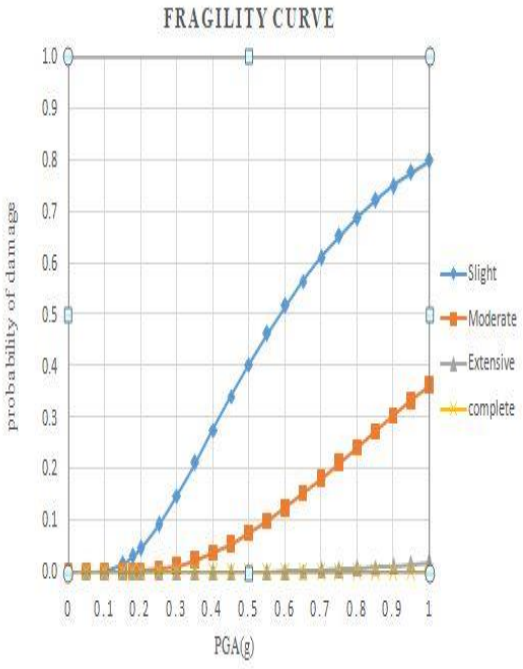

Figure 15. Fragility curve for 9 storey steel braced frame Building

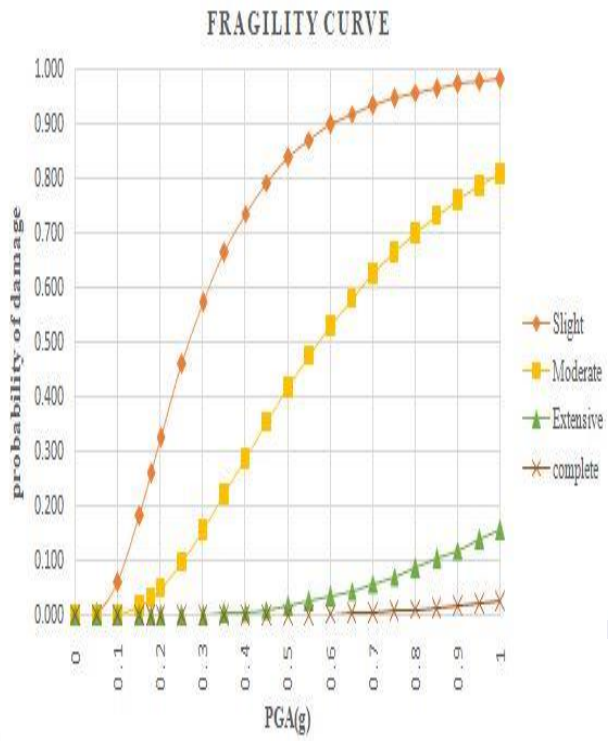

Figure 16. Fragility curve for 9 storey steel frame building with cast-in-place concrete shear wall

5. Comparative study

Case 1: Three storey Buildings

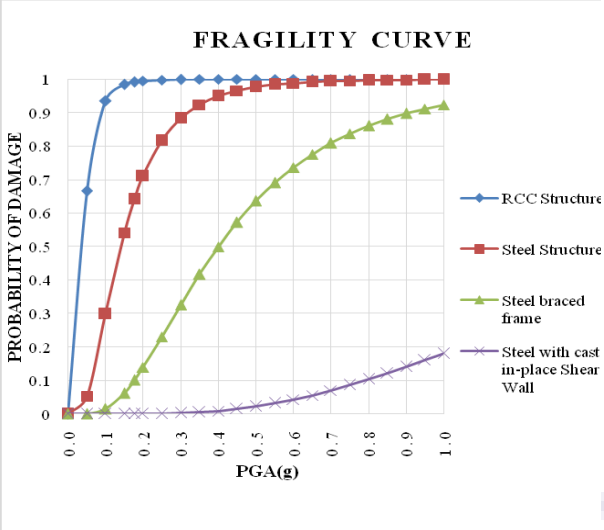

Figure 17. Fragility curve for different 3 storey buildings for slight damage state

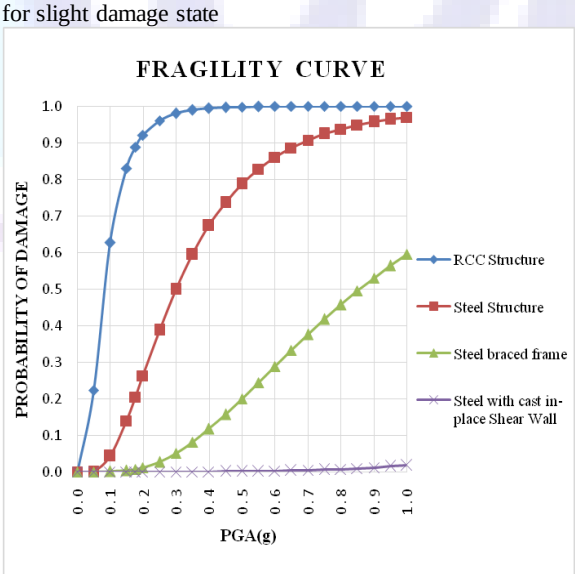

Figure 18. Fragility curve for different 3 storey buildings for moderate damage state

The fragility curve for 3 storey RC frame, steel moment frame, steel braced frame and steel frame with cast- in place concrete shear wall buildings are plotted and compared for slight, moderate, extensive and complete damage state as shown in Fig: 17-20. These figures indicate that the fragility of RC frame is highest among all other structural system.

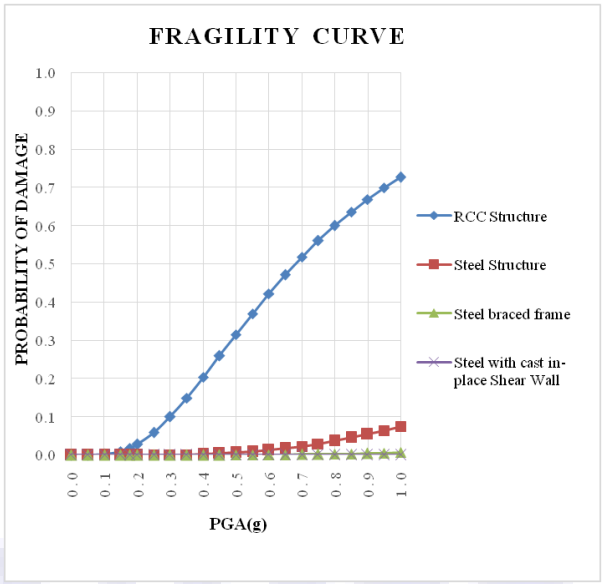

Figure 19. Fragility curve for different 3 storey buildings for extensive damage state

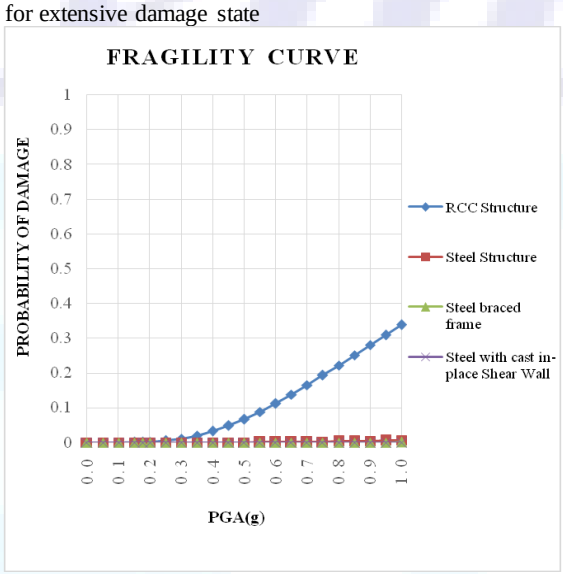

Figure 20. *Fragility curve for different 3 storey buildings for complete damage state*

The probability of damage decreases gradually from RC frame, steel frame, steel braced frame to the steel frame with cast-in place concrete shear wall respectively. These figures also show that for extensive and complete damage state the curves nearly overlap to each other for higher PGA value except for RC frame.

Case 2: Six storey Buildings

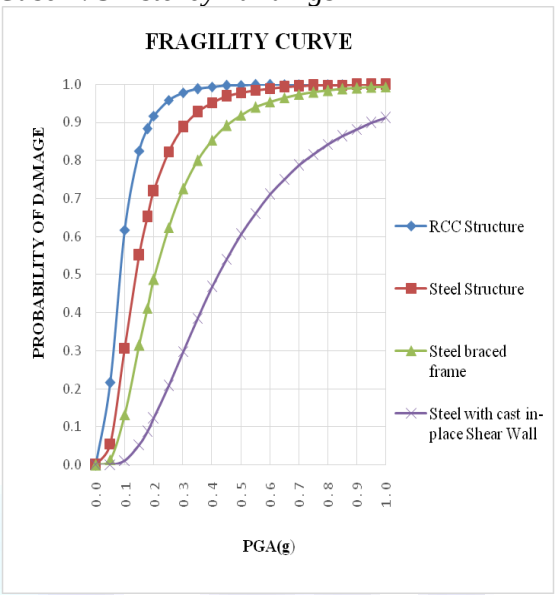

Figure 21. Fragility curve for different 6 storey buildings for slight damage state

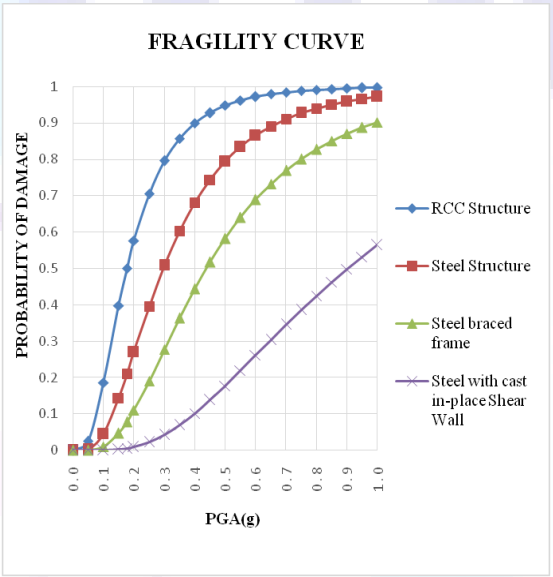

Figure 22. Fragility curve for different 6 storey buildings for moderate damage state

The fragility curve for 6 storey RC frame, steel moment frame, steel braced frame and steel frame with cast- in place concrete shear wall buildings are plotted and compared for slight, moderate, extensive and complete damage state as shown in Fig: 21-24. These Fig. shows the similar nature to that of three storey buildings.

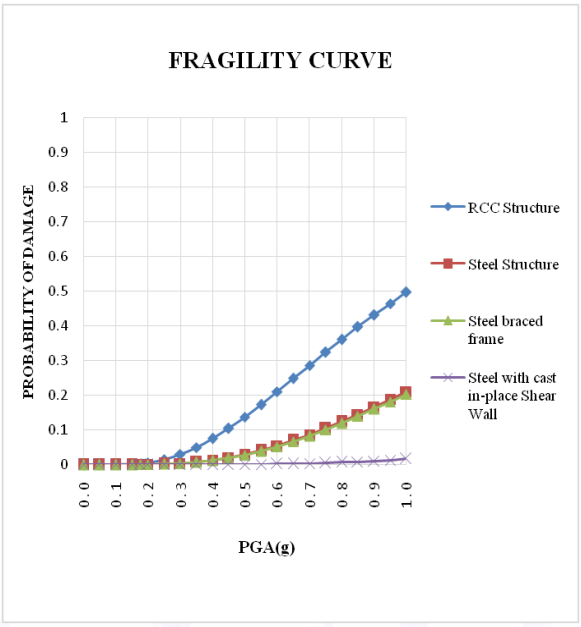

Figure 23. Fragility curve for different 6 storey buildings for extensive damage state

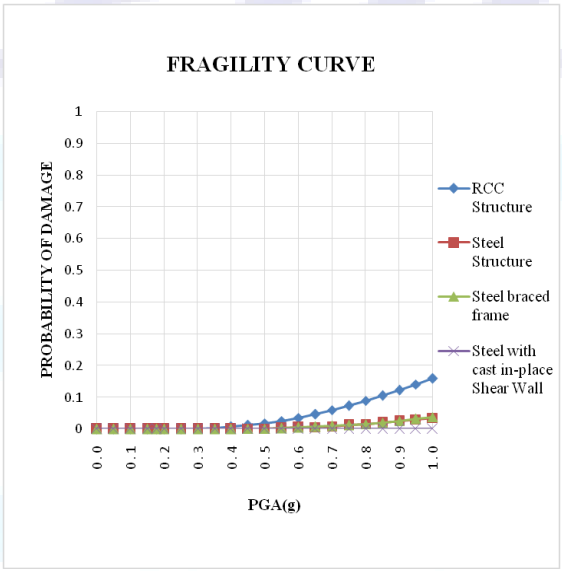

Figure 24. Fragility curve for different 6 storey buildings for complete damage state

Case 3: Nine storey Buildings

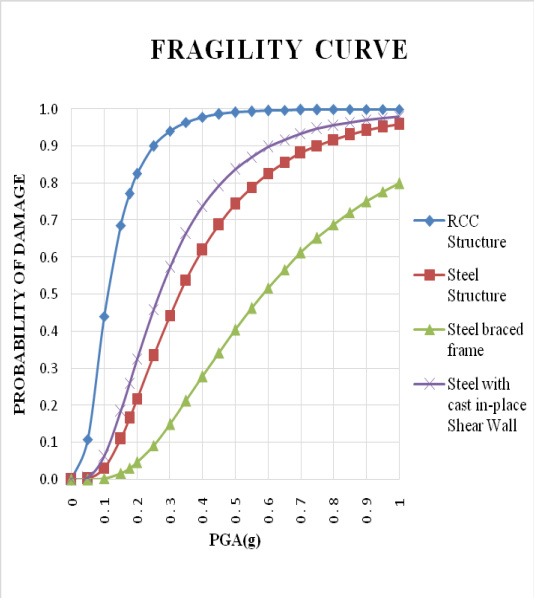

Figure 25. Fragility curve for different 9 storey buildings for slight damage state

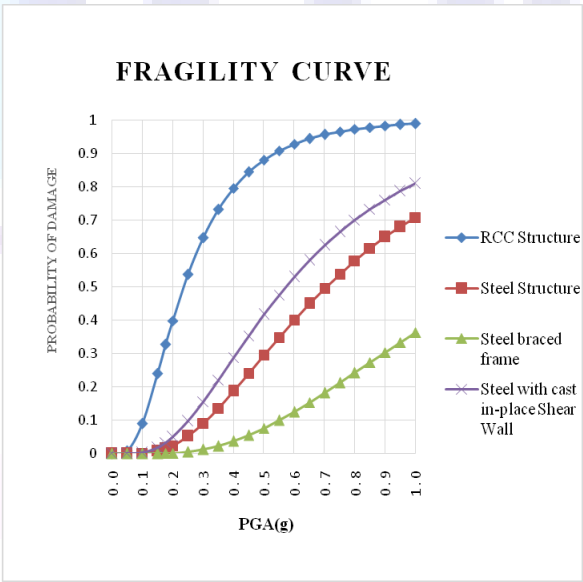

Figure 26. Fragility curve for different 9 storey buildings for moderate damage

The fragility curve for 9 storey RC frame, steel moment frame, steel braced frame and steel frame with cast- in place concrete shear wall buildings are plotted and compared for slight, moderate, extensive and complete damage state as shown in Fig: 25-25. These Fig. exhibits the different nature to that of three-

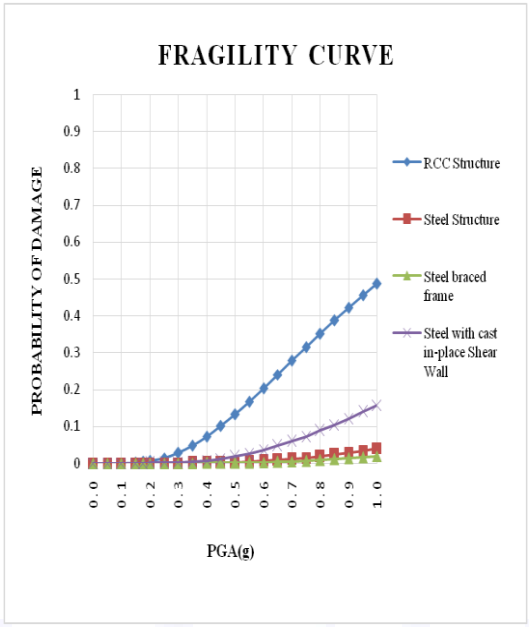

Figure 27. Fragility curve for different 9 storey buildings for extensive damage

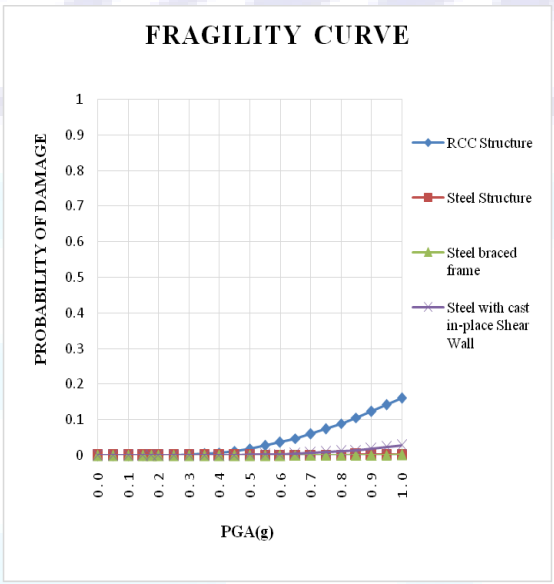

Figure 28. Fragility curve for different 9 storey buildings for complete damage

storey and six storey buildings. The RC frame structure shows the highest probability of damage among all structure as in previous case but the steel frame with cast-in place concrete shear wall shows more vulnerability than the steel moment frame in while the steel braced frame show least vulnerability among the considered structures.

6. Conclusion

This project assesses the seismic vulnerability of RC frame, steel frame, steel braced frame and steel frame with cast in-place concrete shear wall of various heights confirming to low-rise, mid-rise and high-rise building by developing the seismic fragility curve. HAZUS methodology have been employed, and the results were compared. The main conclusions are as follows:

1. The slope of the fragility curve is larger at lower PGA and vice versa.
2. Increase in PGA leads to increase in fragility of the structure.
3. In case of low-rise (3 storey) and mid-rise (6 storey) buildings, the fragility curve showed similar nature while it exhibited different nature in case of high-rise building (9 storey).
4. The probability of damage gradually decreases from RC frame, Steel frame, Steel braced frame to Steel frame with cast in place concrete shear wall respectively in low-rise and mid-rise building while the probability of damage decreases from RC frame, Steel frame with cast in place concrete shear wall, Steel frame to Steel braced frame in high-rise building.

7. Limitation of the study

1. The research relies on several assumptions in calculation of yield displacement and ultimate displacement. In this project ultimate displacement and yield displacement is obtained from the values given from HAZUS- MH MR3 in order to determine actual yield and ultimate displacement we have to carry out nonlinear analysis.
2. The effect of environmental factors, time and temperature on material properties and inaccuracies in construction has not been considered in the analysis.
3. As nonlinear direct integration nonlinear time history analysis took quite longer time around 11, 12 hours for one run of analysis, linear analysis has been adopted to determine the demand displacement due to time limit of project.
4. They should not be considered reliable for prediction of damage to a specific facility without confirmation by a seismic/structural engineering expert.

References

[1] HAZUS-MH-MR3, *"Multi-hazards Loss Estimation Methodology: Technical Manual"*, Federal Emergency Management Agency , Washington D.C., (2003).

[2] Giovinazzi, S.L., "Macroseismic and Mechanical models for the Vulnerability and Damage assessment of Current Buildings", Springer Science+Business Media B.V., (2006).

[3] Paudel, A., *"Calculation of PGA at specific site by development of fragility curve for RCC Buildings"*, Institute of Engineering, Tribhuwan University, (2016).

[4] Iman Mansouri et.al*," Assessment of seismic vulnerability of steel and RC moment building using HAZUS and statistical methodologies*", Discrete dynamics in nature and societies, volume 2017, Article ID 2698932, 16 pages
https://doi.org/10.1155/2017/2698932

[5] Gurung Shrestha, S., *"Seismic Vulnerability Analysis of Traditional Brick Masonry Buildings"*, Institute of Engineering, Tribhuwan University, (2013).

[6] Lagomarsino, S.G., *"A Macroseismic Method for the Vulnerability Assessment of Buildings"*, Vancouver, B.C. Canada, (2004).

[7] Tremayne, B.A., *"Time History Analysis as a Method of Implementing Performance Based Design",* Auckland, New Zealand, (2005).

[8] FEMA-154., *"Rapid Visual Screening of Buildings for Potential Seismic Hazards"*, National Institute of Building Science.Redwood City ,California, (2002).

[9] Kramer, S.L., " *Geotechnical Earthquake Engineering ",* . Upper Saddle River.N.J. , Prentice Hall, (1996).

[10] Nakata, T., "Active *Faults of the Himalayas of India and Nepal",* Special Paper, Geological Society of America, (1989).

Suitability of Polyethylene Terephthalate Fibers as a Partial Substitute of Aggregates in the Footpath Concrete

Sanjit Kumar Sah[1], Iswar Man Amatya[2], Kamal Bahadur Thapa[2]

[1]*MSc in Environmental Engineering, Pulchowk Campus, T.U.*
[2]*Assoc. Prof., Department of Civil Engineering, Pulchowk Campus, T.U.*

[1]*shahsanjit11@gmail.com*, [2]*iswar@ioe.edu.np, kamal.thapa@ioe.edu.np*

Abstract

This paper deals with finding an optimized proportion of polyethylene terephthalate (PET) fibers as a partial substitute of mineral aggregate in footpath concrete without compromising its strength parameters. The aim of this investigation program is to utilize the huge bulk of PET waste into footpath concrete in the volumetric proportions of 0, 0.5, 1, 1.5, 2, 2.5 and 3% and find the optimum fiber content that ensures minimum compressive strength of M20 concrete. The optimized fiber content was further checked for flexure strength and split tensile strength. Obtained experimental results showed a gradual decrease in compressive strength with the increasing PET fiber content. Similarly, the optimized fiber mixed concrete showed better flexure strength and split tensile strength than that of plain concrete. However further research and analysis were recommended to understand more physical properties of fiber mixed concrete.

Keywords: *Polyethylene terephthalate fiber; Footpath concrete; plastic waste; Fiber mixed concrete; Department of Road.*

1. Background

With the modernization and change in living style, use of PET bottle is quite common in daily life. Its portability, affordability, compatibility, strength and attractiveness have made its use as the very common liquid carrier. On the one hand, PET bottles have eased our daily life activities while on the other hand; they have imposed much more problems on the environment. People have conceived PET bottles as a use and throw commodity and never hesitate to throw out their used PET bottles as waste in dust bin or even at roadside or other public places.

The PET association of Nepal states that 20,000 tons of PET are used for bottles each year in Nepal. That's nearly a billion bottles. Estimates suggest that 400 thousand PET water bottles are thrown away each day in Kathmandu alone. It is estimated that 85% of these end up as waste, most going to Sisdole landfill site in nearby Nuwakot district (Britton, 2017). Therefore, to ensure a sustainable use of waste PET, its use as filler in footpath concrete is suggested. The main objective of this research is to find the optimum percentage of fiber content that ensures the minimum strength characteristics of footpath concrete in accordance with the Department of Road, Nepal.

2. Methodology

A field study was conducted at the Balkhu waste segregation center. Municipal solid wastes collected from different parts of the city were segregated here for further recycle and disposal. The field study was conducted to quantify the proportions of plastic waste which is described below.

2.1 Field Study of Plastic Wastes

Random waste bags were selected from different vehicles and the contained plastic wastes were segregated according to their type. Their proportions were analyzed on the basis of their weight which showed that 12.49% of total waste was plastic waste. The proportions of different types of plastics are shown in Figure 2.1.

The PET fiber mixed concrete was optimized on the basis of compressive strength test for the different fiber content of 0.5, 1.0, 1.5, 2.0, 2.5 and 3.0% by volume. The other different materials required for making PET fiber mixed concrete are described below.

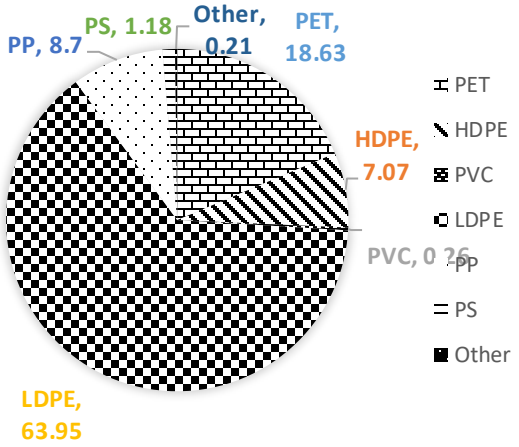

Figure 2.1: Segregated plastic proportion in Balkhu collection center

2.2 Materials

Cement:

The cement used was 53 grade Ordinary Portland cement (OPC) with fineness of cement 6.35%.

Fine aggregate:

Good quality quarry sand was used after washing which confirm the grading of IS 383-1970.

Coarse aggregate:

Crusher run angular coarse aggregates of 20 mm down size were used whose grading confirms to that of IS 383-1970. The Los Angeles Abrasion Value (LAA), Aggregate Crushing Value (ACV) and Aggregate Impact Value (AIV) are 26.60%, 21.43% and 13.44% respectively.

PET fibers:

PET fibers obtained from waste PET water bottles have been used in this research work. Fibers of 35 mm length and 1 mm width are cut from waste PET bottles and the bulk density of PET fiber is 75 kg/m^3.

2.3 Mix Design

Nominal mix design for M20 concrete, i.e., 1:1.5:3 proportion of cement, sand and coarse aggregate respectively was adopted. The water-cement ratio provided was 0.5 to ensure sufficient workability. The batching process involved volumetric batching.

2.4 Concrete Mixing, Casting and Curing

The specified ingredients of concrete were collected in the lab and mixed in volumetric proportion in mixing machine till a homogenous mixture was obtained. Mixes with different PET fiber content were mixed separately and their respective slump value were measured. This concrete was then ready to be casted into moulds.

Moulds of size 150mm* 150mm* 150mm were used for compressive strength test. For flexure strength test, moulds of size 150mm* 150mm* 750mm were used. Similarly, cylindrical moulds of 100mm diameter and 200mm length were used for split tensile test. Curing was done after 24 hours of casting in a tank full of clean and fresh water.

2.5 Concrete Strength Testing

Compressive strength test of concrete:

Compressive strength test of concrete was tested for 7- and 28-days compressive strength as per IS 516-1959. Three samples of each percentage of PET fiber content were tested and their average were analyzed.

Flexure strength test of concrete:

Flexure strength test of concrete was tested for 28 days strength as per IS 516-1959. Three samples of each percentage of PET fiber content were tested and their average were analyzed.

Split tensile strength test of concrete:

Split tensile strength test of concrete was tested for 28 days strength as per IS 5816-1999. Three samples of each percentage of PET fiber content were tested and their average were analyzed.

3. Discussions and Data Analysis

According to the specification of Department of Road (DOR), Nepal (2001), the footpath concrete should be of grade M20 with 20mm down aggregates. To confirm the specification of DOR, compressive strength tests were done on concrete. At the same time, the optimized PET mixed concrete was further checked for flexure strength and split tensile strength and compared with that of plain concrete. The lab results are shown below.

Figure 3.1 shows that the workability of concrete decreases as the PET fiber content increases. This might be because the fibers bridge over the voids that provide strength to the green concrete against free flow and hence reduce the slump value.

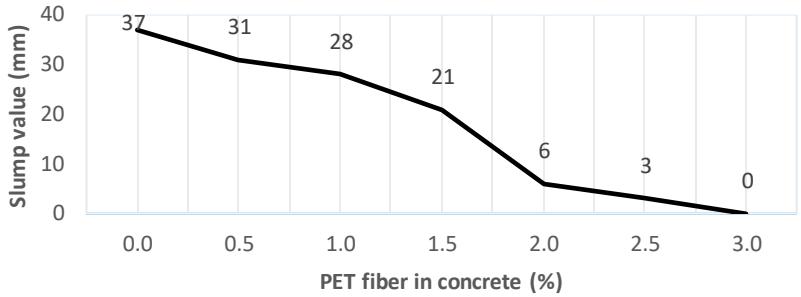

Figure 3.1: Workability test for different percent of PET fiber

The crushing strength for the M20 concrete in 7 days is expected to be 65% of the specified characteristic compressive strength, i.e., 13 N/mm2. Thus, the minimum crushing load is expected to be 292.5 KN (Mohod, 2015). From Figure 3.2, it can be observed that concrete with PET fiber content upto 2% confirms the minimum strength requirement and other do not possess sufficient strength. Similarly, 28 days strength of test cubes should be equal to specified characteristic strength of concrete. Since we have casted M20 co ncrete, the crushing strength should be equal to 20 N/mm2, i.e., the average crushing load should be minimum 450 KN. From Figure 3.3, it can be observed that concrete with PET fiber content up to 1.5% confirms the minimum strength requirement and other do not possess sufficient strength. This might be because the PET fibers being smooth textured lack sufficient slip resistance in the concrete which in return reduces the direct compressive strength of the concrete. Hence, PET fiber content of 1.5% is considered as the optimized fiber content for the concrete.

Again, the concrete with 1.5% PET fiber content is checked for 28 days flexure strength and split tensile strength whose outcomes are shown below.

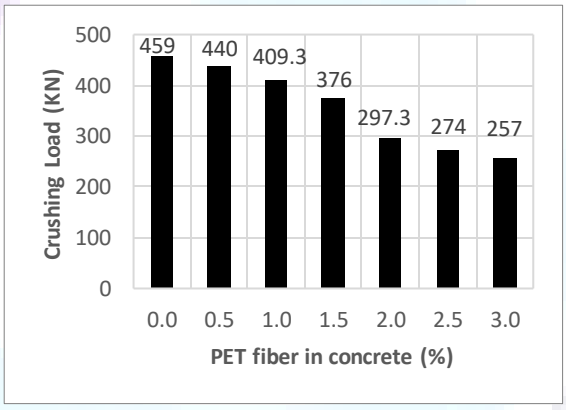

Figure 3.2: Crushing strength of 28 days' cubes

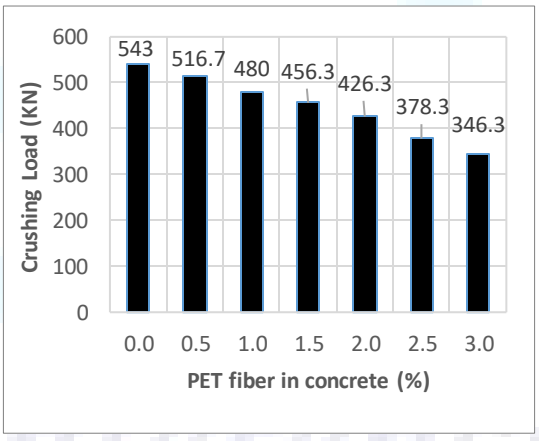

Figure 3.3: Crushing strength of 28 days' cubes

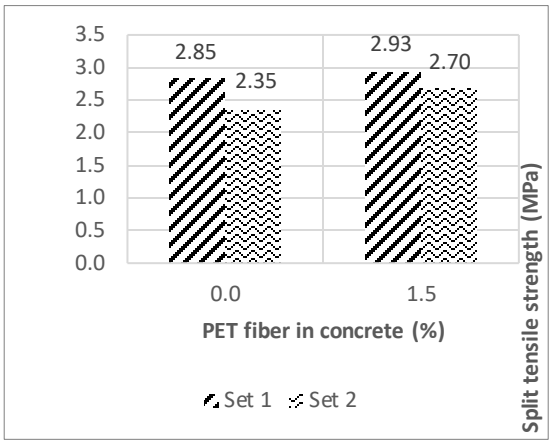

Figure 3.4: Average 28 days split tensile strength of PET mixed concrete

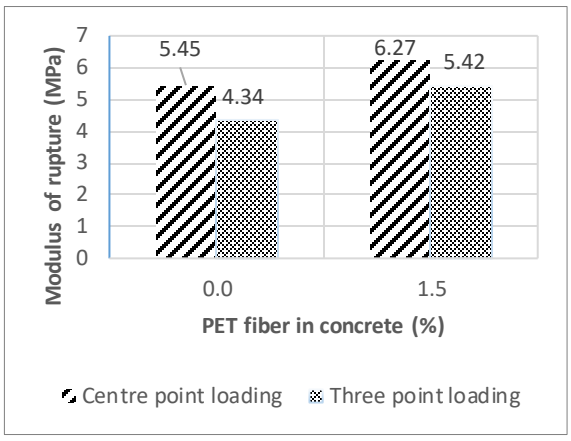

Figure 3.5: Average 28 days' flexure strength of PET mixed concrete

From Figure 3.4 and 3.5, it can be clearly observed that the flexure strength and split tensile strength of PET fiber mixed concrete is better than that of the plain concrete. This might be because the PET fibers being fibrous material, bridge over the cracks developed during the process of flexure and tension cracking and provide further resisting strength before the complete failure.

4. Findings and Conclusion

4.1 Findings

1. We have collected the data about the prevalent plastic wastes in day to day waste of the Kathmandu valley which shows that out of total solid wastes, 12.49% were plastic wastes whose 18.63% were PET wastes. This implies that PET wastes are among the major problems for the solid waste management.
2. From the result of this research, we found that the use of PET fiber in the fresh concrete decreases its workability. From the results of the standard slump test, it was concluded that the increasing percentage volume of PET fiber added into the concrete shows the decreased workability in nonlinear pattern. Higher percentage volume of PET fiber made the concrete significantly stiff and difficult to compact. However, the bleeding and segregation in the fresh concrete mixture was reduced.
3. It was also observed that the compressive strength of cube specimens decreased with increased PET fiber percentage volume. However, compressive strength of concrete with fiber dosage up to 1.5%, showed the minimum strength requirement. So, the maximum permissible percentage of fiber content found from research is found out to be 1.5%.
4. In splitting tensile strength test, we found that tensile strength was improved for 1.5% of fiber dosage than that of the concrete without fiber content.
5. In flexure strength test, we found that flexure strength was improved for 1.5% of fiber dosage than that of the concrete without fiber content. Hence, it may be concluded that the optimum value of fiber content is 1.5% for ensuring compressive strength, tensile strength and flexural strength in M20 concrete.

4.2 Conclusion

As per the current specification prescribed by the DOR, MoPIT, Nepal, the footpath concrete must be M20 concrete with 20mm down aggregates. From the experimental analysis conducted, it is clear that in spite of being a weak filler in the concrete compared to that of the mineral aggregates, the addition of PET fiber up to 1.5% volumetric proportion have ensured the compressive strength of M20 concrete and the flexure strength and tensile strength of the concrete are also improved compared to that of the plain concrete. Hence, the suitability of PET fibers as a partial substitute of aggregates in the footpath concrete is justified for 1.5% PET fiber content.

Recommendations

Although the objective of my research is justified, further research is suggested to analyze the wholesome utility of PET fibers in concrete so that we can overcome the practical constraints and the use of PET fiber mixed concrete can be ensured in day to day life. Further recommendations are listed below:

- The effect of varying dimension of PET fiber on the strength and workability of the concrete needs to be analyzed.
- The use of plasticizer in the concrete which improves the workability may lead to better strength of the concrete. Taking this in consideration, further researches may be conducted.
- The significance of PET fibers in concrete inferior to M20 concrete could be analyzed.
- The use of PET fibers in combination with steel fibers could give more favorable results. Their optimized proportion for use may be a more useful field of research.

References

[1] Aciu, C., Adriana, D., Varvara, I., Manea, D.L., Orban, Y.A., & Babota F. (2018). Recycling of plastic waste materials in the composition of ecological mortars. *Procedia Manufacturing*, 22, 274-279.

[2] Anand, P. (2016). Use of synthetic fibres in concrete flooring and plastering. Retrived from https://civildigital.com/use-of-synthetic-fibres-in-concrete-flooring-and-plastering-advantages

[3] Britton, B. (2017), Plastic Nepal- adventures in polymers. Retrived from https://medium.com/@ben.britton/plastic-nepal-adventures-in-polymers.

[4] DOR, MoPIT, GON, (2001). Standard specifications for road and bridge works. Retrived from https://dor.gov.np/home/publication/standard-specification-of-roads-and-bridges

[5] Himalayan Climate Initiative (2014). A study on waste PET bottles. Retrived from http://www.himalayanclimate.org/images/projectMultipleSubPage/GaHteA Study on Waste PET Botlles.pdf

[6] IS 383 (1970). Specification for coarse and fine aggregates from natural sources for concrete. Bureau of Indian Standards, New Delhi.

[7] IS 516 (1959). Method of Test for Strength of Concrete. Bureau of Indian Standards, New Delhi.

[8] Islam, G.M.S., & Gupta, S.D. (2016). Evaluating plastic shrinkage and permeability of polypropylene fiber reinforced concrete. International Journal of Sustainable Built Environment, 5, 345–354.

[9] Mohod, M.V. (2015). Performance of polypropylene fiber reinforced concrete. IOSR Journal of Mechanical and Civil Engineering, 12(1), 28-36.

[10] Portland Cement Association (PCA), (2018). How concrete is made. Retrived from http://www.cement.org/cement-concrete-applications/how-concrete-is-made.

[11] Rao, K.S., Kumar, S.R., & Narayana, A.L. (2013). Comparision of performance of standard concrete and fiber reinforced standard concrete exposed to elevated temperatures. American Journal of Engineering Research (AJER), 2(3), 20-26.

[12] Saito, N. (2013). Solid waste management in Nepal. Retrived from https://www.adb.org/sites/default/files/publication/30366/solid-waste-management-nepal.pdf

[13] Satyal, V.R. (2016). Plastic thinking. Retrived from https://myrepublica.nagariknetwork.com/news/plastic-thinking.

[14] The Construction specifier (2018). Specifying steel fibers for concrete floors. Retrived from https://www.constructionspecifier.com/specifying-steel-fibers-for-concrete-floors.

[15] The constructor (2018). Civil engineering construction. Retrived from https://theconstructor.org/

[16] Thomas, G.P. (2012). Recycling of polyethylene terephthalate. Retrived from https://www.azocleantech.com/article.aspx?ArticleID=254

[17] Winner, N., & Zebua, S.B. (2017). The influence of pet plastic waste gradations as coarse aggregate towards compressive strength of light concrete. Procedia Engineering, 171, 614-619.

Part VI: Soil Mechanics and Irrigation

Deep Tube-Well Irrigation: A Case Study of Bardiya District

Suresh Ayer[1], Sunil Jang Rai[1], Shreejesh Poudel[1], Sunil Giri[1], Utsab Pathak[1], Dr. Yogendra Mishra[2]

[1]*Advanced College of Engineering and Management, Kupondole, Lalitpur, Nepal*
[2]*Ministry of Energy Water Resources and Irrigation*

[1] suresh.ayeren@gmail.com, raijung109@gmail.com, Iamshreejesh@gmail.com, sunilgiri967@gmail.com, erupats@gmail.com, [2] mailto:ymeshra@gmail.com

Abstract

In Nepal, sources of irrigation are rainfall, surface water and groundwater. How much water is coming from rainfall and how much water should be covered by irrigation is difficult to predict as rainfall varies greatly from season to season. This report depicts the trend analysis of climatic and rainfall data of past 20 to 33 years in southern part of Bardiya district, Nepal. Based on the graphical interpretation, we observed an increasing trend in maximum and minimum temperature, humidity & rainfall and the decreasing trend in wind speed and sunshine hours. A model study is carried out to optimize the abstraction of groundwater in order to meet the greater demand for irrigation. The study is divided into two phases. Firstly, it involves the determination of CWR using CROPWAT8.0 software. The maximum irrigation requirement obtained is 0.69litres/s/ha in the month of July. Secondly, it involves the design of deep tube-well that consist 275 numbers of uniformly distributed DTWs having depth of 75m, strainer diameter 0.248m and yielding 0.083m3/s each, that is required within a total of 11,000ha area to fulfill the irrigation need of variety of crops throughout the year.

Keywords: *Irrigation, trend analysis, CWR, irrigation requirement, DTWs, strainer.*

1. Introduction

Irrigation in simple words refers to the supply of water to the land or crops to help the plants for their proper growth. Agriculture in Nepal is central to the economy of this country. Nearly 76% percent of the population depends on agriculture in some way. In the economic year 2018/19, agriculture accounted for 27.59% of Nepal's GDP (1). But there is not enough production to support the population. There is a chronic issue of child malnutrition and an estimated 47% percent of Nepal's children are affected by stunting (2).

Nepal is the country of diverse topography. There are three major climatic regions in Nepal known as terai, hill region and mountainous region, with each providing unique crops. More than 76% potential irrigable land area lies in terai region of our country. In hills where more head is available there are less agricultural fields and in plains where more agricultural fields are available there is less head. Thus, topography and fragile geology creates more challenges to the development of surface irrigation projects. Also the rainfall pattern is

highly variable in respect of time and place (3). Due to these reasons the actual potential of the country in agricultural field is not fully achieved. Government has made efforts to improve the production of agriculture in Nepal but has had minimal success. Nepal has vast water resources, but its terrain allows cultivation of only 17.9% of its total land area (2,641,000 ha). Of the total cultivable area only 1,766,000 ha is suitable for irrigation. In the year 2018, the actually irrigated land area was 1,433,287 ha. Among this, 813,067 ha through surface water irrigation, 443,365 ha through groundwater irrigation and 167,925 ha through traditional FMIS (4).

The history of irrigation in Nepal before 1922 were all developed, operated and maintained by farmers called Farmer Managed Irrigation System (FMIS). From 1922 to 1957, Government made little effort to develop irrigation infrastructures in Nepal. However, irrigation development has high priority since 1957, the milestone of the beginning of periodic plan in Nepal. The government investment in irrigation development, especially in the large scale irrigation systems in the Terai increased tremendously from 1970 onwards. At present scenario, irrigation policy 2004 is in practice. Similarly, Irrigation Master Plan 1990, Agriculture Perspective plan 1995, Water Resources Strategy 2002 and National Water Plan 2005 are other few documents which guide irrigation development in Nepal. Some of the large scale canal irrigation projects for the development of irrigation schemes are: Sikta Irrigation Project, Babai Irrigation Project, Bagmati Irrigation Project, Mahakali Irrigation Project (Phase III), Rani Jamara Kularia Irrigation Project, Bheri Babai Diversion Multipurpose Project, Sunkoshi Marin Diversion Multipurpose Project etc. Similarly, the major completed deep and shallow tube-well irrigation projects of Nepal are: Kailali-Kanchanpur Tube-well Irrigation Project (7,056ha), Bhairahawa Lumbni GW Project (Rupandehi-20,309ha), Sagarmatha Integrated Rural Development Project (Siraha, Saptari & Udayapur-14,510ha), Seti Integrated Rural Development Project (Kailali-1,100ha), Community Shallow Tube-well Irrigation Project (Sunsari, Siraha, Saptari, Sarlahi, Rautahat-4,855ha), Narayani Irrigation Sector Project (Bara & Parsa-2,800ha), etc (3).

Groundwater is available in most parts of the country, but the amount and depth vary from place to place. In the Terai, the upper unconfined aquifer (50–60 m) has been considered as good productive shallow zones and most of groundwater production is limited to upper 250 m. Recharge in the Terai is estimated to be 8800 MCM/year. At present, only about 22% of the available dynamic groundwater recharge in terai is being utilized. GW resources have not been accurately investigated yet in the hills and mountains region. The annual groundwater reserve in these regions is estimated to be at least 1,713 MCM. Groundwater from both deep and shallow aquifers is suitable for irrigation without any treatment, but for drinking and industrial uses, treatment is necessary [(5), (6)].

A tube well is a type of water well in which a long, 100-200 millimeter-wide, stainless steel tube or pipe is bored into an underground aquifer. The lower end is fitted with a strainer and a pump lifts water for irrigation. The required depth of the well depends on the depth of the water table (7). The discharge in a general open well is just limited to 3 to 6 liters/s. The mechanical pumping of water from the open wells of small discharges is not economical. So in order to obtain large discharge mechanically, tube-well, which is a long pipe or a tube, is bored deep into the ground. Deep tube-wells are as deep as 70 to 300m, and tap more than one aquifer. The general average yield from the standard DTWs is ranges from 40 to 45litres/s (8). There exists about more than 70,000 deep and shallow tube-wells in our country and every year the number is increasing (9). Shallow tube-wells are those having depth 20 to 70m and tapping only one aquifer. Such wells may yield as high as 15 to 20litres/s, if located at proper places. Each STW can irrigate about 8 hectares. Obviously, a tube well cannot be constructed everywhere and requires some geographical conditions favoring its installation. Well irrigation is widely practiced in those areas where sufficient sweet groundwater is available (8).

Our studies have been so prepared that it can address the same problem of irrigation which is insufficient for agriculture in Bardiya district. The main objective of this report is to enable the utilization of large amount of ground water reserve in Bardiya district, for the irrigation purpose using one of the fast growing technologies like Deep tube-well. This report particularly describes about the ground water condition and CWR of proposed area; and the design of deep tube-well. We believe that, this project can benefit the whole group of the farmers in the area who are mainly dependent in agriculture for their livelihood. By increasing the potential of agriculture in the area employment opportunities can highly be increased. This can reduce the seasonal migration to some extent.

2. Study Area and Data

2.1 Study Area

Bardiya district, one of the seventy-seven districts of Nepal, is part of Province No. 5 of Nepal. Gulariya is the districts headquarter of Bardiya. It has occupied 202,500 ha area and lies in the west of Banke district, south of Surkhet district, east of Kailali district and to the south lies, Uttar Pradesh, India. It is located at Latitude 28˚ 17′ to 28˚ 39′ North and Longitude 81˚ 3′ to 83˚ 41′ East. It has maximum altitude 1279 meters at Chepang Gaun and minimum altitude 138 meters. Its climate consists of mainly lower tropical temperature. The maximum temperature recorded here is 40 ºC and minimum temperature is recorded as 4 ºC. Its average annual rainfall is 1900 mm with fluctuating pattern. (10). In Bardiya, there are eight municipalities, out of which six are urban municipalities and two are rural municipalities. The population of the district is counted to be 423,656 (11). Our study area belongs to the municipal area of Madhuwan and gulariya municipality of Bardiya district. Babai River is in the eastern part of this area. People in bazar areas are dependent on business while others are in agriculture and Baideshik rojgar; few are in jobs sector (12).

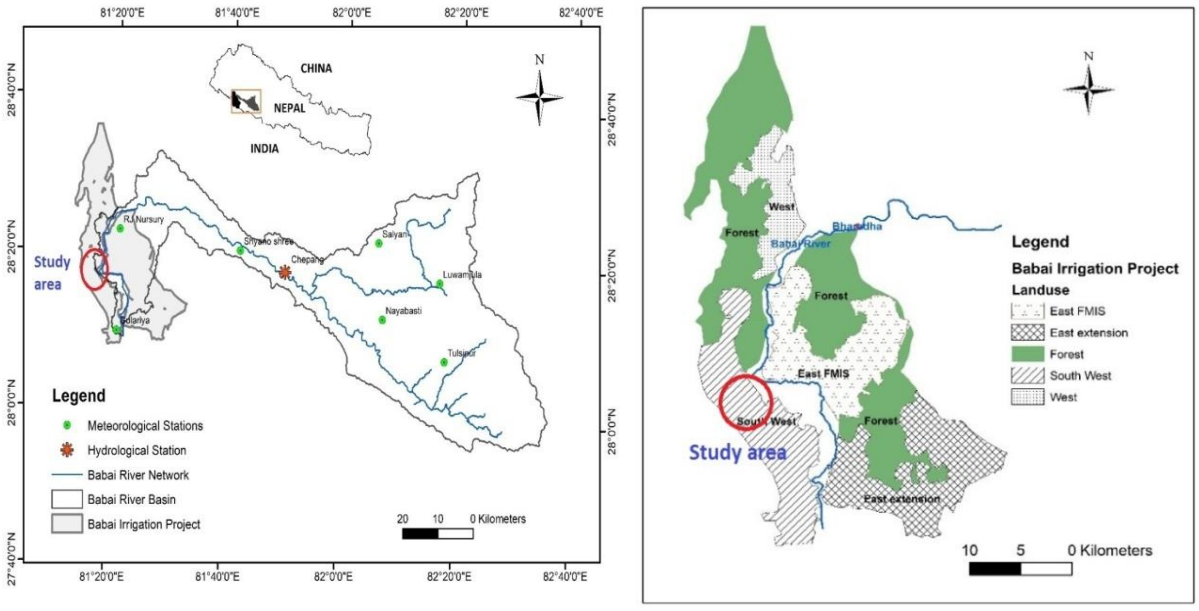

(a) (b)

Figure 1. (a) Geographical profile including Hydro-meteorological stations of Bardiya
(b) Land distribution and natural resources of Bardiya (Source: DOI)

2.2 Data Analysis

Data related to the study of Earth's atmosphere and the variations in temperature and moisture patterns that produce different weather conditions are termed as meteorological data. Several institutes and agencies may keep climatic records such as DHM or nearby Agricultural Research Stations. The maximum and minimum temperature, rainfall and humidity data are measured in Rani Jaruwa Nursery, which is about 15 km north-east from our study area. Similarly, the wind speed & sunshine hours are measured in Nepalgunj airport which is about 45 km south-east from the study area. In this study, different climatic and rainfall data of past 20 to 33 years, recorded in the nearest stations [Figure 1(a)] were acquired from the Department of Hydrology and Meteorology (DHM) whereas cropping pattern and soil type data were obtained from DOI and DOA [Table 1].

Table1. Type & frequency of data, its sources and the time duration

SN	Description	Frequency	Source	Vintage
1	Temperature	Daily (T-max/T-min)	DHM	1986-2013
2	Humidity	Morning & Evening	DHM	1981-2011
3	Wind speed	Daily	DHM	1981-2013
4	Sunshine	Hours	DHM	1991-2010
5	Rainfall data	Daily	DHM	1984-2015
6	Cropping pattern	Current	DOI & DOA	
7	Soil type	Current	DOI & DOA	
8	Lithological data		Survey	

Climatic and rainfall data

Maximum and minimum temperature, humidity, wind speed and rainfall data provided by the source were daily recorded and the sunshine data were recorded in number of hours of a day [Table 1]. Missing data were fulfilled by interpolation and were processed to obtain monthly average maximum and minimum temperature, humidity, wind speed, sunshine hours and the monthly cumulative rainfall [Table 2].

Table 2. Different climatic and rainfall data after processing

S.N	Temperature		Rainfall (mm)	Humidity (%)	Wind speed (Km/day)	Sunshine (Hours)
	T.max	T.min				
1.	31.2˚	18.3˚	1278.2	75	59	7.4

Cropping pattern

The total cultivable land of our study area is 11,000 ha. The collected information on planting and harvest dates should be systematically arranged in a cropping pattern. The major crop grown in Bardiya is rice followed by wheat, maize and vegetables respectively. Rice is grown in the month of July to November in the area of 9900ha out of total cultivable area 11000ha, in a year. While rice is grown, no other crops are simultaneously grown. [Table 3] shows the cropping pattern of different crops in the study area. The net area sown by different crops in a year is 16,830 ha, therefore the cropping intensity of that field is found to be 1.5.

Table 3. cropping pattern in yearly basis for different crops within the study area

Crop	Area (Ha)	Jan	Feb	Mar	Apr	May	Jun	Jul	Aug	Sep	Oct	Nov	Dec
Rice	9900												
Wheat	3960												
Vegetables	770												
Maize	2200												
Total	16830	Cropping intensity											1.5

Soil data

Information from the soil surveys carried out in our project site shows distinct soil categories. The soil logging at the southern part of Bardiya district shows clayey soil at the surface up to 3m depth. It also consists of different layers below the surface clay [Table 4].

Table 4. Soil logging data in the study area

Soil logging at Bardiya (Southern Part)	
Soil Type	Depth in (m)
Surface clay	0 to 3 m
Coarse sand	3 to 10
Clay	10 to 15
Medium sand	15 to 18
Clay with sand stone	18 to 30
Very fine sand	30 to 44
Clay with kankar	44 to 59
Coarse sand	59 to 75
Clay with sand stone	Below 75m

The soil survey should also collect data on total available soil moisture, maximum infiltration rate, maximum rooting depth and initial soil moisture depletion for dry crops. However, for rice crop, the additional soil data are required such as, drainable porosity, critical depletion for puddle cracking, water availability at planting and maximum water depth [Table 5].

Table 5. Detail soil data for dry and wet crops

Soil survey parameters		Data
Data for non-rice (dry) crop	Total Available soil moisture (FC-WP)	140 mm/meter
	Maximum rain infiltration rate	30 mm/day
	Maximum rooting depth	900 cm
	Initial soil moisture depletion (as % TAM)	0 %
Additional data for rice (wet) crop	Drainable porosity	15%
	Critical depletion for puddle cracking	0.20 fraction
	Water availability at planting	15 (% depl.)
	Maximum water depth	150 mm

3. Methodology

This study is based on the secondary data. All these data and information are collected from previous reports, related literature reviews, institutes and agencies such as department of hydrology and meteorology, department of irrigation and nearby agricultural research stations. The meteorological data are used to calculate evapotranspiration. The methods for calculating ET from meteorological data require various climatological and physical parameters such as atmospheric pressure, latent heat of vaporization, psychometric constant, air temperature, air humidity, solar radiation, wind speed, sunshine hours etc. The Reference Evapotranspiration (ET_o) represents the potential evaporation of a well-watered grass crop. The water needs of other crops are directly linked to this climatic parameter. Although several methods exist to determine ET_o, the Penman-Monteith Method has been recommended as the appropriate combination method to determine ET_o (13).

The collected data and information are further processed through CROPWAT 8.0 software to obtain the desired outputs. CROPWAT is a decision support tool developed by the Land and Water Development Division of FAO. CROPWAT 8.0 for windows is a computer program which is used to calculate; i) Reference evapotranspiration, ii) Crop water requirement, iii) Crop irrigation requirements and to develop; i) Irrigation schedules under various management conditions and ii) Scheme water supply.

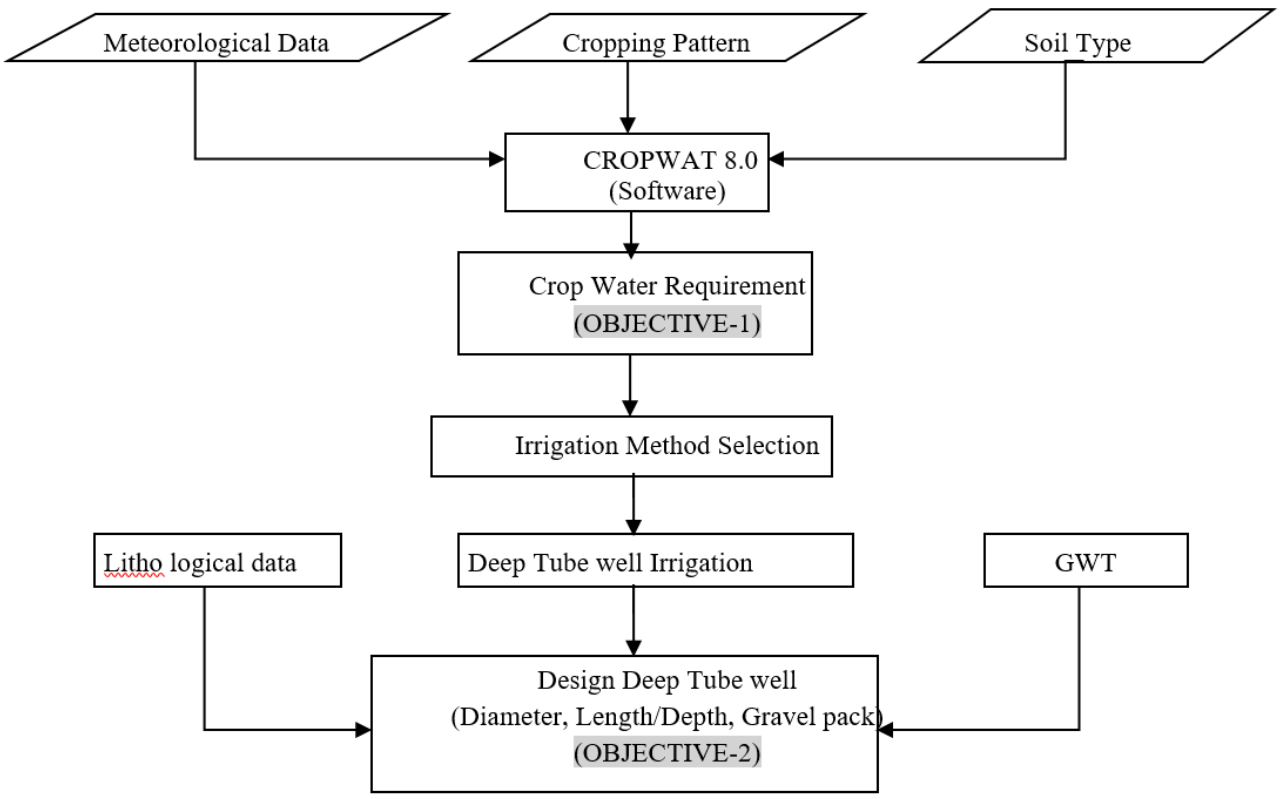

Figure 2. Methodology of deep tube well Irrigation

CROPWAT 8.0 can also be used to evaluate farmer's irrigation practices and to estimate crop performance under both rained and irrigated conditions. The water balance method is used for calculation of irrigation schedules in CROPWAT 8.0, which means that the incoming and outgoing water flows from the soil profile are monitored[(13)(14)].

CROPWAT 8.0 Data Inputs	
Parameters	**Description**
Climate/ ET_o	The calculation of reference evapotranspiration is carried out from the monthly climatic data, according to the FAO adopted Penman-Monteith approach. This module involves: • Basic information on the climatic station, country name, station name, altitude, latitude and longitude. • Monthly climatic data on means of max and min temperature, relative humidity, sunshine hours and wind speed.
Rainfall	Monthly cumulative rainfall
Crop	Kc , Crop description, max. Rooting depth, % area covered by the plant
Soil	Initial soil moisture condition & available soil moisture
Crop pattern	Irrigation scheduling criteria
CROPWAT 8.0 Data Outputs	
• Reference evapotranspiration • Crop water requirement • Crop irrigation requirements • Actual crop evapotranspiration • Soil moisture deficit • Estimated yield reduction due to crop stress • Irrigation scheduling (13)	

Design Methodology

The gravel pack is usually designed on the basis of pack aquifer ratio (PA ratio).

$$\text{i.e. PA ratio} = \frac{D50\ of the gravel}{D50\ of the aquifer}$$

According to the Central Board of Irrigation and Power (1967), for Indian condition: PA ratio should be between (a) 9 and 12.5 for uniform aquifers having $C_u \leq 2.0$, (b) 12 and 15.5 for graded aquifers having $C_u > 2.0$.

In practice, the slot size varies from the values as low as 0.2 mm to as large as 5mm. In market, two sizes i.e. 1.6mm & 3.2mm slots are generally available. Finally, the minimum length of the screen can be designed by using the equation:

$$h = \frac{Q}{A_o * V_e} \text{ ---------- (I)}$$

Where, Q = Design discharge of the tube well; A_o = Area of the screen openings per meter length of the screen (= π.d.p); d = Diameter of pilot hole, p = Percentage of openings (usually varies between 15 to 20 % of screen area); V_e = Optimum safe entrance velocity of the given aquifer.

We have the general rules for screen length in confined aquifers. At least 0.3m aquifer depth at top as well as at bottom of the aquifer should be left unscreened to safeguard against the error in the placement of the screen during installation (8).

4. Result and Discussion

This research project is aimed at the analysis and evaluation of crop water requirement, cropping pattern, cropping intensity, ground water condition and the design of deep tube-well to fulfill the irrigation demand of the proposed area. The process includes the analysis of climatic data such as temperature, humidity, sunshine hours, wind speed and the rainfall data of past years.

4.1 Analysis part:

- *Graphical Interpretations*

1) Temperature

The line graph [figure 3 (a), (b)]shows the trend of yearly average maximum and minimum temperature of each month in the years from 1986 to 2013 respectively. We can see that the maximum temperature is rising from the month January to May and is decreasing from May to December. Also from the graph it is seen that both the maximum and minimum temperatures are in increasing trends. Similarly, the line graph [figure 3 (c), (d)] shows the variation of monthly average maximum and minimum temperatures are in increasing trend in the years.

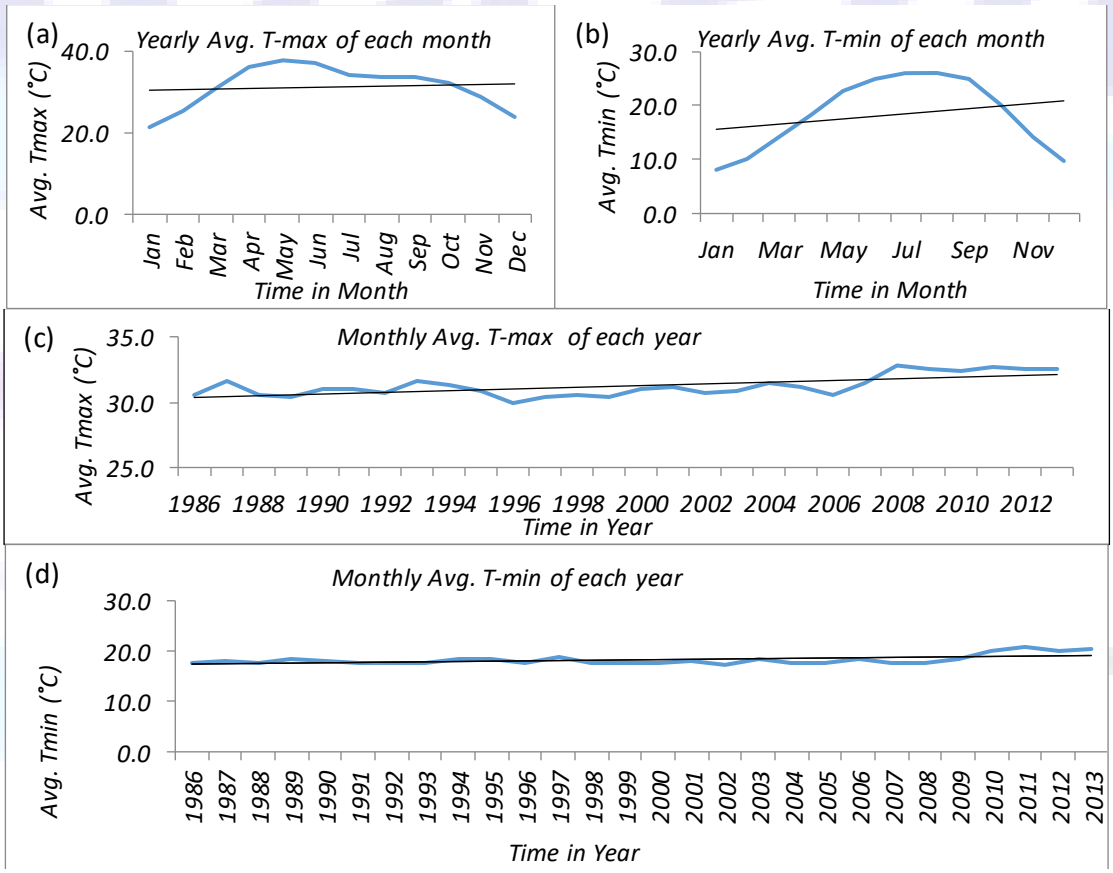

Figure 3. Yearly averages (a) T-max, (b) T-min; of each month (1986-2013); Monthly average (c) T-max, (d) T-min; of each year from (1986-2013) in ˚C

2) *Humidity*

The bar chart [Figure 4 (a), (b), (c)], illustrates comparison of the average humidity of different patterns ranging from (1981-2011). Here the trend in the years shows that the humidity is increasing. Too high humidity results in soft growth of crop, nutrient deficit, root disease etc. and too low humidity leads to wilting of crop, smaller leaf size, leaf curl etc. (15). Hence humidity is one of the most important climatic parameter that should be considered in CWR calculations.

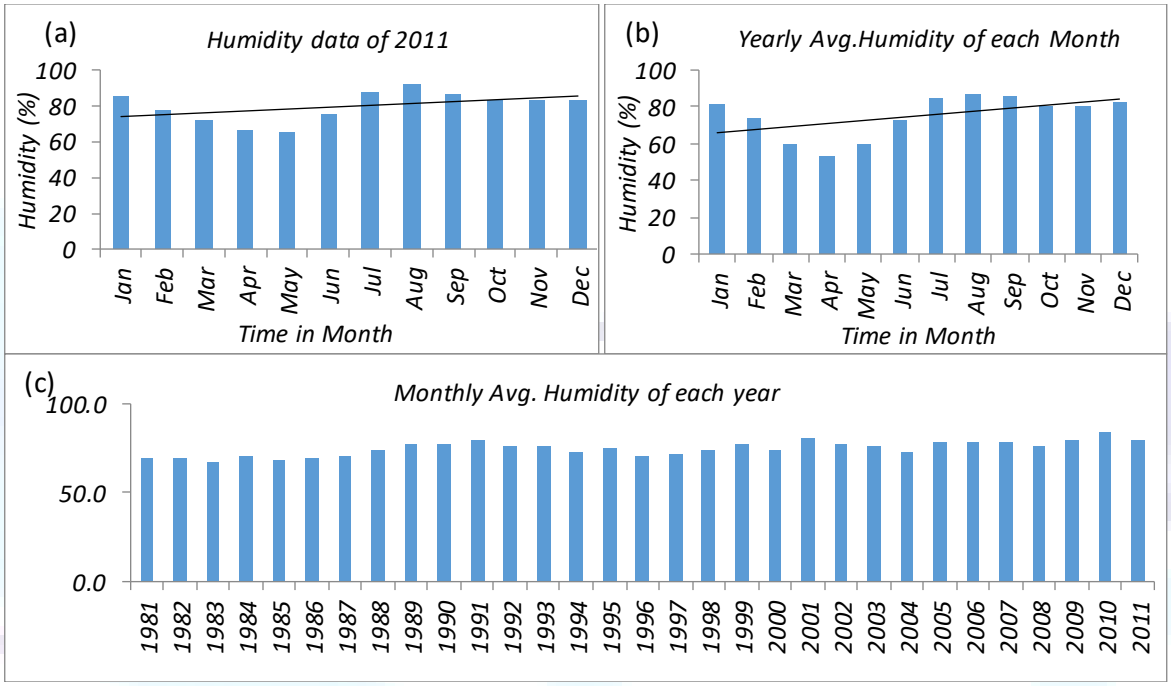

Figure 4. (a) Average humidity of each month in 2011, (b) Yearly avg. humidity of each month, (c) Monthly average humidity of each year; from (1981-2011) in %

3) *Wind speed*

[Figure 5 (a), (b), (c)], illustrates comparison of the average wind speed of different patterns ranging from (1981-2013).

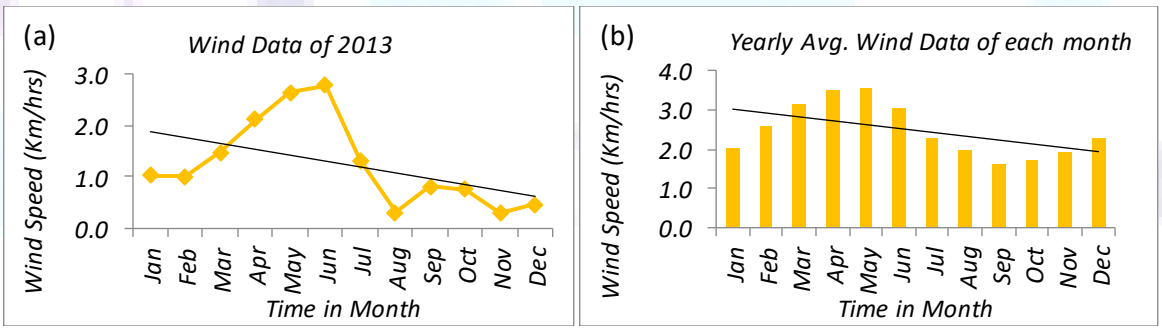

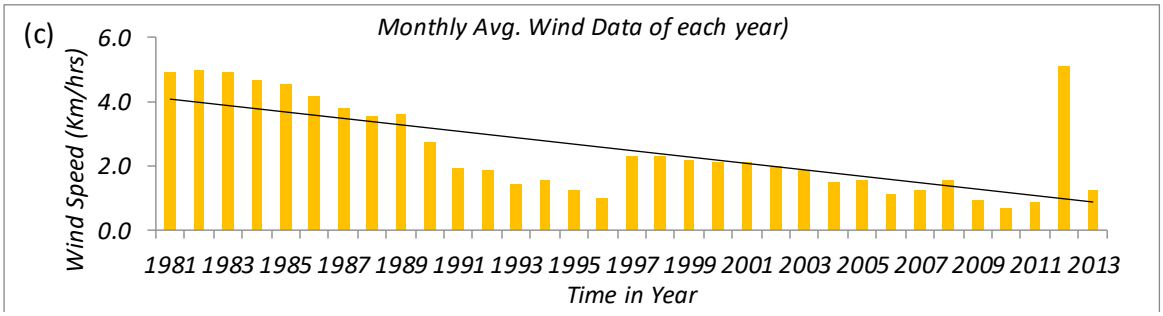

Figure 5. (a) Average wind speed of each month in 2013, (b) Yearly average wind speed of each Months, (c) Monthly average wind speed of each year; from (1981-2013), in km/hrs

4) Sunshine hours

The bar chart [figure 6 (a), (b), (c)], illustrates comparison of the average sunshine hours of different patterns ranging from (1991-2010).

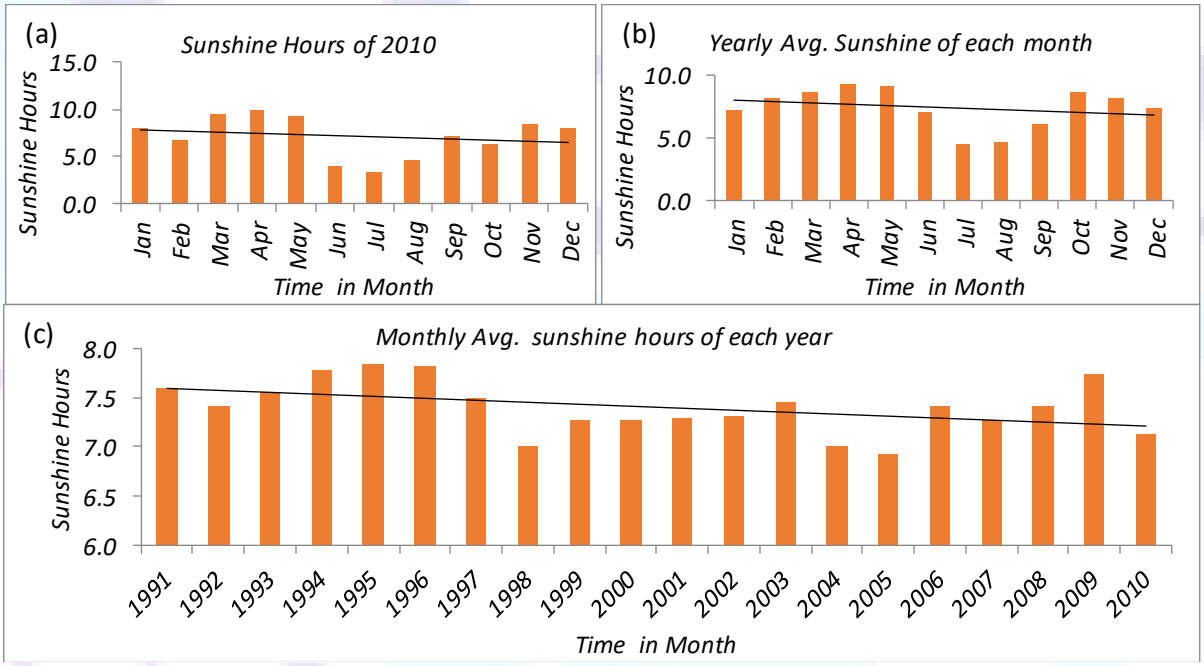

Figure 6. (a) Average sunshine hours of each month in 2010 (b) Yearly average sunshine hours of Each month, (c) Monthly average sunshine hours of each year; from (1991-2010)

5) Rainfall

We observed an annual change in rainfall for each month. The bar chart [figure 7 (a), (b), (c), (d)], illustrates comparison of the cumulative rainfall of different patterns ranging from (1984-2015). Here the graphical interpretation shows a linearly increasing trend under each scenario. Frequently, it is seen that cumulative rainfall in the month of June, July & August is Maximum and it is minimum in the month of November, December and January. It can be concluded that the monsoon or the summer season has the highest rainfall whereas it is least in the winter season.

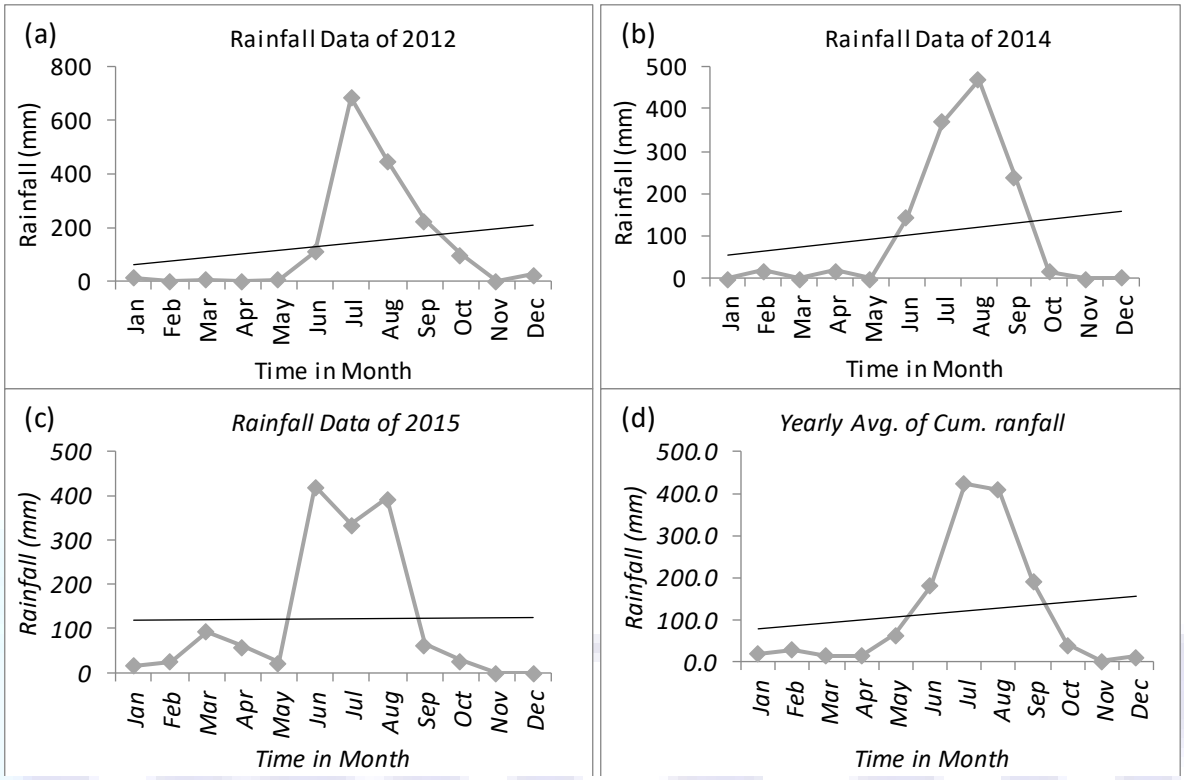

Figure 7. Cumulative rainfall of each month in the year (a) 2012 (b) 2014 (c) 2015; (d) Yearly average of Cumulative rainfall of each month from the year (1984-2015); in mm

➢ *Determination of CWR*

The CWRs are calculated by using CROPWAT 8.0 software. Data on Climate/ET_o, Rainfall, Crop and Soil are required for determining CWR. The CWR calculations include the irrigation water requirement of the crop on a decadal basis and over the total growing season, as the difference between the crop evapotranspiration under standard conditions (ET_o) and the Effective rainfall [Table 6].

Table 6. Results of CWR calculation for different crops in our study area

S.N	Crop	Plant Date	Harvest Date	Area %	Actual crop vapo-transpiration (ET_o) (mm/dec)	Effective Rainfall (mm)	Irrigation Requirement (mm)
1	Vegetables	01-Dec	28-Feb	7	165.9	53.7	112.2
2	Maize	01-Mar	28-Jun	20	486.1	191.7	321.9
3	Wheat	01-Dec	30-Mar	36	214.9	66.6	148.0
4	Rice	01-Jul	28-Nov	90	538.1	482.8	352.8

➢ *Scheme Water Requirement*

Finally, the irrigation supply to any irrigation scheme or canal command area can be calculated by adding up the requirements of each cropped area. Any changes in cropping pattern can be conveniently calculated by modifying area size of the different crops. From the Scheme module we obtained irrigation water requirement of each month for the actual area. Among IWR of different months, we adopted the maximum value and designed the system of irrigation using that value, so that CWR of the driest year can also be reached. The maximum value of irrigation water requirement was found to be 0.69 l/s/ha [figure 8], in the month of July.

ETo station: Rani Jaruwa | Rain station: Rani Jaruwa | Cropping pattern: Cropping Pattern

	Jan	Feb	Mar	Apr	May	Jun	Jul	Aug	Sep	Oct	Nov	Dec
Precipitation deficit												
1. Project_Rice	0.0	0.0	0.0	0.0	0.0	0.0	184.5	0.0	8.2	84.9	75.3	0.0
2. Project_WheatSpr	25.1	50.1	60.4	0.0	0.0	0.0	0.0	0.0	0.0	0.0	0.0	6.5
3. Project_Vegetables	35.7	41.8	0.0	0.0	0.0	0.0	0.0	0.0	0.0	0.0	0.0	31.1
4. Project_Maize	0.0	0.0	27.8	122.3	139.1	14.4	0.0	0.0	0.0	0.0	0.0	0.0
Net scheme irr.req.												
in mm/day	0.4	0.7	0.9	0.8	0.9	0.1	5.4	0.0	0.2	2.5	2.3	0.1
in mm/month	11.5	21.0	27.3	24.5	27.8	2.9	166.0	0.0	7.4	76.4	67.7	4.5
in l/s/h	0.04	0.09	0.10	0.09	0.10	0.01	0.62	0.00	0.03	0.29	0.26	0.02
Irrigated area	43.0	43.0	56.0	20.0	20.0	20.0	90.0	0.0	90.0	90.0	90.0	43.0
(% of total area)												
Irr.req. for actual area	0.10	0.20	0.18	0.47	0.52	0.06	0.69	0.00	0.03	0.32	0.29	0.04
(l/s/h)												

Figure 8. Scheme water requirement results

- *Irrigation method selection*

Surface (canal) irrigation & ground water (tube-well) irrigation are two important method of irrigation. The major difference between them is based on the source of water, cost of construction and operation, conveyance system, efficiency and distribution of water to the field. Due to higher elevation, the command area of our site is isolated from the canal irrigation provided by Bheri-Babai diversion multipurpose project. Hence we have adopted deep tube well irrigation (DTWs) to fulfill the irrigation requirements of this field.

4.2 Design Part

- *Gravel pack and slot size design*

As per IS:8110-1976 we adopted the thickness of gravel pack equal to 15cm and the slot size of 3.2mm wide & 10cm long, keeping minimum thickness between two slots equal to 3mm. The slots are so designed that they are distributed in a group of 3 or 4, and arranged in order that the slots of one group are not in line with those in adjacent row, so as to maintain the adequate strength in the well pipe. A thicker gravel pack does not materially increase the well yield, nor will it reduce the possibility of sand pumping. Too thick a gravel pack, instead of giving any advantages, may make the final development of the well more difficult (8).

- *Design of DTWs (Discharge, length, diameter and numbers of DTWs)*

From the available soil logging data at southern part of Bardiya district, the required discharge of 0.083m3/s per well was available after drilling 4th layer of aquifer. For this project, we need 275 deep tube-wells in the total cultivable land of 11,000 hectors. The actual screened length of well was 36.6m within the total depth of 75m having well diameter of 0.248m. The DTWs are always installed on the irrigated area in specific spacing so as to make uniform distribution of water on the field. After studying various soil logging data and field conditions, we recommended the screen type gravel pack slotted pipe deep tube-well.

5. Conclusion

In this report we studied and analyzed various data and information from different articles, books, irrigation manuals, literature reviews, irrigation and agricultural institutions etc. We examined the climatic and rainfall data of past (20 to 33) years recorded in the local stations. From the graphical interpretations, we found that temperature, rainfall and humidity are in increasing trend and sunshine hours and wind speed are in decreasing

trends. In Bardiya, rice is found to be the majorly grown crop followed by wheat, maize and vegetables respectively and the cropping intensity is 1.5. From the analysis the irrigation water requirement is found to be Maximum (i.e.0.69 l/s/ha) in the month of July. From the design and observations of DTWs, it is found that the tube-well irrigation system has fewer components to design and its overall design methodology is simple & less time consuming as compared to the canal irrigation. Therefore, it is concluded that deep tube-well irrigation is one of the best alternative sources, especially in terai of Nepal, where there is large reserve of ground water. Also for the qualitative development of agriculture in our country a large scale canal irrigation system supported and supplemented by tube-wells are needed.

Acknowledgement

We are thankful to Dr. Yogendra Mishra for his guidance and valuable suggestions, Er. Laxmi Bhakta Maharjan and Er. Rajesh Khadka for their support and encouragement. We would also like to acknowledge department of hydrology and meteorology, department of irrigation and department of agriculture Nepal, for providing the data.

References

[1] Nepal, Central Bureau of Statistics. "National Accounts of Nepal 2018/19" (PDF). [Online] May 5, 2019.

[2] Nepal- Overview. [Online] february 4, 2013. https://www.worldbank.org/en/country/nepal/overview.

[3] Jha, Dr. Prem Chandra. *A Text book of Irrigation & Drainage Engineering*. Kathmandu : Heritage , 2074.

[4] Ministry of Energy, Water Resources & Irrigation. *Present status and future plan of energy, water resources and irrigation.* s.l. : Ministry of Energy, Water Resources & Irrigation, GoN, 2018.

[5] *Groundwater Resources of Nepal: An Overview.* Surendra R. Shrestha, Ganesh N. Tripathi. 2018, SpringerLink.

[6] *Uses of Ground Water in Nepal.* Rana, Krishna. 2011.

[7] Tubewell-Wikipedia. [Online] 2019. https://en.wikipedia.org/wiki/Tube_well.

[8] Garg, Santosh Kumar. *Irrigation Engineerng And Hydraulic Structure*. s.l. : Khanna Publishers, 2006.

[9] ADB. Shallow Tubewell Irrigation in Nepal-Impacts of the community ground water irrigation sector project. [Online] https://www.adb.org/sites/default/files/evaluation-document/35900/files/ies-nep-final.pdf.

[10] Ltd., Multiscope Consultancy Pvt. District Climate and Energy Plan for Bardiya District . [Online] 11 2015. http://ddcbardiya.gov.np/wp-content/uploads/2015/11/District-Climate-and-Energy-Plan-Bardiya.pdf.

[11] GoN, Ministry of Fedral Affairs and General Administration. Sthaniya Taha. [Online] 2017. http://103.69.124.141/gis/website/.

[12] Wikimapia. Sanoshree taratal municipality (town). [Online] 2019. http://wikimapia.org/30963761/sanoshree-taratal-municipality-town.

[13] CROPWAT8.0, Example of the use of. Example of the use of CROPWAT8.0. [Online] http://kisi.deu.edu.tr//cem.cetinkaya/sulama/CROPWAT8_0Example.pdf.

[14] Nations, Land & Water- Food and Agriculture Orgnizaton of the United. *Food and Agriculture Orgnizaton of the United Nations*. [Online] 2019.

[15] News, Scott Shelton. 2005. "Sweating High Humidity" Greenhouse Product. [Online]

Effects of Chemical Fertilizer in Zinc Concentration of Paddy Field Soil of Terai Region

Awdhesh Kumar Shah

Department of Civil Engineering (Environmental Engineering), Pulchowk Campus, Lalitpur, Nepal

awdheshkumarshah672@gmail.com

Abstract

The mechanization of fields that are taking place in Terai areas is generating soil with poor structure and lack of nutrients. The application of chemical and compost fertilizer for improving soil properties is becoming a frequent practice, but with the risk of producing a negative impact, because of the presence of heavy metals. In the present study, the influence of zinc sulfate fertilizer application in paddy field soils from the Rajpurtulsi, Yamuna Mai, Rautahat (26.85^0 N, 85.29^0 E) of Terai has evaluated. The area has a lower tropical climate and the main type of soil is calcareous. The study focuses on the change of plant-available Zn content in 8 different disturbed plots with different doses. Same treatments and practices were applied in all 8 plots. The main metal component of the zinc sulfate fertilizer, has been analyzed and established a relationship with soil pH, soil salinity, soil OM (Organic Matter), soil CEC (Cation Exchange Capacity) and compared the extracting capacity. Plant available fractions (extraction with $(NH_4)OAc$-Dithizone, 0.1 N HCl and 65% HNO_3) for Zn have analyzed.

Different doses of zinc sulfate i.e. (0.00-2.37)Kg per Katha is not polluting the soil of paddy field. The concentration of zinc residues in the soil after paddy plant harvesting is in the range of (0.5-0.8) ppm, 0.1N HCl, which is very less in comparison to the pollution level of the soil. Zinc concentration in groundwater is found to be 0.5ppm, in 3 feet below soil of one of the set is 0.9ppm and in straw ash <0.1 ppm by 0.1N HCl. The zinc level in soil with plantation and without the addition of zinc sulfate is 0.5ppm by 0.1N HCl which is less than the initial residues 0.7ppm, 0.1N HCl, before plantation. Hence 0.2ppm zinc is consumed by the paddy plant which can be fulfilled without further addition of zinc sulfate. Dithizone method of zinc extraction is not applicable for Flame AAS. This method is more appropriate for calorimetrically analysis. Availability of zinc for the plant is dependent on other soil property; decrease with increasing pH, increase with the increase of salinity, increase with the increase of OM, increase with the increase of CEC. The increasing rate of OM retards the rate of CEC at higher level hence the availability of zinc decreases at higher level of OM. So, the optimum dose of zinc sulfate fertilizer is 1Kg/Katha.

Keywords**:** *Zinc, Soil, $(NH_4)OAc$-Dithizone(Ammonium Acetate Dithizone), 0.1 N HCl, OM, CEC, Salinity, pH, 65% HNO_3*

1. Introduction

Zinc is essential for the growth in animals, human beings, and plants. It is vital to crop nutrition as required in various enzymatic reactions, metabolic processes, and oxidation-reduction reactions. Zinc occurs naturally in air, water, and soil, but zinc concentrations are rising unnaturally, due to an addition of zinc through human

activities. When the soils of farmland are polluted with zinc, animals will absorb concentrations that are damaging to their health. Water-soluble zinc that is located in soils can contaminate groundwater.

Changes in land use and management can affect soil quality. Terai region, located in the lower tropical climate, south of Nepal, where the main land use is paddy fields for one season, it has experienced changes in the production system because of increased mechanization, which has enabled significant soil movement and alteration of the terrain layers. In many cases this has been carried out without preserving the topsoil, sometimes mixing or burying the surface horizon in deeper layers underneath poorer materials. After a disturbance, and before Paddy plant plantation, the application of organic wastes and chemical fertilizer is becoming a common practice, and it is repeated every half year or one year without additional evaluation of the impact on soil and water pollution. These organic and inorganic materials could improve the physical properties of soil and enrich the soil in nutrients in a readily utilizable inorganic form, but they usually have trace elements, which in moderate doses could be beneficial for the soil but could have a negative effect if they are increased without control (Romos, 2005). Most of the elements applied with these residues are immobilized in soil by chelation with organic matter and adsorption on clay minerals; they are precipitated as insoluble compounds, and in most cases accumulate in the upper soil layers (Yaron *et* al., 1996). Due to the high erosion rates due to flood recorded in the area, some of these elements will also reach surface waters by runoff, adversely affecting the quality of the surface waters. The determination of total content is important in order to follow the impact of agricultural practices. However, the toxicity of metals depends not only on total concentration but also on their mobility and reactivity.

The most common way to analyze the metal mobility is by using extractants. Although much effort is being made to harmonize and standardize analytical methods (Quevauviller *et* al., 1993), at present there is no reference method for determining each fraction. The power of the extracting method depends on the soil characteristics. The amount of extracted metal gives an idea of the quantity of metal which might be depleted by a plant during a growth period. Although these fractions are usually strongly correlated with the total soil concentration, they do not always predict the amount taken up by plants and the equivalence to plant uptake has been questioned, depending on the soil tested and the specific element. Beckett *et* al. (1983) and Williams and McLaren (1982) have warned against equating the extractable soil fraction of an element to the plant-available one.

However, the study is mainly to assess zinc contents in the soil. As fertilizer is an external agent which may influence the soil properties including zinc concentration, it's properties should also be ascertained. Some soil properties like soil pH, soil salinity, organic matter contents, cation exchange capacity etc. should be ascertained for the relationship between zinc concentration and soil properties (Romos, 2005; Romos and Lopez-Acevedo, 2003).

Main objective: to determine the optimum dose of $ZnSO_4.7H_2O$ in order to enhance soils and environmental health

Specific objectives;

- To assess the effect of chemical fertilizer application on zinc levels in paddy field of Terai by determining zinc concentration
- To evaluate the relationship between zinc concentration and soil properties
- To compare different chemical extraction methods to evaluate Zinc bioavailability

2. Literature Review

The chemistry of zinc is dominated by the +2 oxidation state. Zinc deficiency affects about two billion people in the developing world and is associated with many diseases. In children, deficiency causes growth retardation, delayed sexual maturation, infection susceptibility, and diarrhea. Consumption of excess zinc can cause ataxia, lethargy and copper deficiency. Concentrations of zinc as low as 2 ppm adversely affects the amount of oxygen that fish can carry in their blood (Wikipedia, 2018). Soils contaminated with zinc from mining, refining or fertilizing with zinc-bearing sludge can contain several grams of zinc per kilogram of dry soil. Levels of zinc in excess of 500 ppm in soil interfere with the ability of plants to absorb other essential metals, such as iron and manganese (Addae, 2013). Zinc levels of 2000 ppm to 180,000 ppm have been recorded in some soil samples (Addae, 2013). The remainder of the total Zn is fixed in the soil in an insoluble or unexchangeable form and difficult to make available to crop (Hafeez *et* al., 2013). Meanwhile, high pH and high contents of $CaCO_3$, organic matter, clay, and phosphate can fix Zn in the soil and give rise to the reduction of available Zn (Ahmad *et* al., 2012). According to the Food and Agriculture Organization (FAO), about 30% of the cultivable soils of the world contain low levels of plant available Zn. Generally, Zn deficiency is expected in calcareous soils, sandy soils, peat soils, and soils with high phosphorus and silicon. The availability and solubility of Zn decreases while pH increases.

Zinc toxicity is usually caused by interactions in plant uptake of other essential elements like phosphorous and iron. Zinc deficiencies symptoms usually start for most plants species at zinc levels lower than (20-25) ppm (Bolt and Bruggenwert, 1978). Toxicity levels are at about 400 ppm and up (Bolt and Bruggenwert, 1978). Zinc toxicity in animals starts if the Zinc content of the diet exceeds roughly 1,000 ppm (Bolt and Bruggenwert, 1978). Most plants have been severely injured at high Zinc level. The higher toxicity sensitivity of plants as compared to animals serves as an automatic protection agent zinc accumulation in the food chain. The total zinc level in the soil is at normal conditions in the (10-300) ppm range, with (30-50) ppm as a rough average value (Bolt and Bruggenwert, 1978).

Zinc in Environment

Zinc may also increase the acidity of waters. Some fish can accumulate zinc in their bodies when they live in zinc-contaminated waterways (International Zinc Association, 2018). When zinc enters the bodies of these fish it is able to biomagnify up the food chain. Water-soluble zinc that is located in soils can contaminate groundwater. On zinc-rich soils, only a limited number of plants has a chance of survival. Due to the effects upon plants zinc is a serious threat to the productions of famlands. Finally, zinc can interrupt the activity in soils, as it negatively influences the activity of microorganisms and earthworms (International Zinc Association, 2018). The breakdown of organic matter may seriously slow down because of this.

Health Effects of Zinc

Zinc is a trace element that is essential for human health. When people absorb too little zinc, they can experience a loss of appetite, decreased sense of taste and smell, slow wound healing and skin sores. Zinc-shortages can even cause birth defects (International Zinc Association, 2018). Although humans can handle proportionally large concentrations of zinc, too much zinc can still cause eminent health problems, such as stomach cramps, skin irritations, vomiting, nausea, and anemia. Very high levels of zinc can damage the pancreas and disturb the protein metabolism, and cause arteriosclerosis (International Zinc Association, 2018). In the workplace environment, zinc contagion can lead to a flulike condition known as metal fever. Zinc can be a danger to unborn and newborn children (International Zinc Association, 2018). When their mothers have

absorbed large concentrations of zinc the children may be exposed to it through blood or milk of their mothers.

3. Methods & Methodology

a.Field Preparation

The size of the plot was considered 1 m^2. The plantation consists of (6 inc x 6 inc) pattern (Dass *et* al., 2017). Thus, the single plot consists of 43 number of paddy bunch. For seepage control, the plots were laid with a plastic sheet underneath at the depth of 3 feet by removing the upper soils. The boundary of the plots was again protected with the plastic sheet above the ground level up to 1 foot. A strong banking was done around the plot to protect the entry of surface run-off. The total number of the undisturbed plots identified for the study was two; One was without plantation and the second was with plantation and with compost fertilizer application. These were the plots in which soils was disturbed by soils replacement (Ramos, 2005). The total number of the disturbed plots identified for the study was nine. The first one was with plantation and compost fertilizer application. And other eight were with plantation and mineral fertilizer application with varying doses i.e. (0.00Kg, 0.34Kg, 0.68Kg, 1.02Kg, 1.35Kg, 1.69Kg, 2.03Kg, and 2.37Kg) per Katha. These eight plots have mainly used for the analysis. The plot was prepared on 2073/3/25 BS.

Undisturbed,Control, 1m^2 Plot No.-11		Undisturbed, Planted, Compost 700Kg/katha, 1m^2 Plot No.-10	Disturbed, Planted, Compost 700Kg/Katha, 1m^2 Plot No.-9
Disturbed, Planted, Mineral 0.00Kg/Katha, 1m^2 Plot No.-8	Disturbed, ha, Planted, Mineral 0.34Kg/Kat 1m^2 Plot No.-7	Disturbed, Planted, Mineral 0.68Kg/Katha, 1m^2 Plot No.-6	Disturbed, Planted, Mineral 1.02Kg/Katha, 1m^2 Plot No.-5
Disturbed, Planted, Mineral 1.35Kg/Katha, 1m^2 Plot No.-4	Disturbed, ha, Planted, Mineral 1.69Kg/Kat 1m^2 Plot No.-3	Disturbed, Planted, Mineral 2.03Kg/Katha, 1m^2 Plot No.-2	Disturbed, Planted, Mineral 2.37Kg/Katha, 1m^2 Plot No.-1

Figure 3.3: plots Layout

b. Plantation and Harvesting

The technique of rice cultivation included using 10–15-day-old seedlings, with quick and careful transplanting; planting intervals (20 x 20)cm; three weddings, preferably soil-aerating mechanical weeding at 10–12, 22–25 and 40–42 days after transplanting; and inorganic fertilizer was applied for soil nutrient supply and for enhancement of the soil biota (Dass et al., 2017; Uphoff, 2015). Another management intervention is intermittent irrigation and soil drying during the vegetative stage and avoidance of continuous deep flooding that creates hypoxic conditions in the soil. Maintaining mostly aerobic soil conditions together with the other SRI practices induces improvements in rice crops' morphological and physiological characteristics as has been demonstrated by Thakur *et* al. (2009) and Subramaniam *et* al. (2013). The plantation was done on 2073/3/25

BS. General description of field work is tabulated in Table 3.4.

Table 3.2: General Description of Field works

Total No. of plots considered in the research	11
Total No. of plots considered for analysis	8
Total No. of plots considered for surface data	3
Size of each plot considered in the research	1 m2
No. of paddy crop bunch for each plot	35-40
No. of weeds for each bunch	3-4
Spacing of each bunch	6 Inc. X 6 Inc.
Name of Paddy crop	14-42 Dhan
Field prepared and planted date	2073/3/25 BS
Dose of DAP(Phosphorus) fertilizer application in plot No. from 1 to 8	13gm(i.e. 4.4Kg/Katha) Reco. dose(3-5)Kg/Katha
Dose of Urea(Nitrogen) fertilizer application in plot No. from 1 to 8	13gm(i.e.4.4Kg/Katha) Reco. dose (3-5)Kg/Katha
Dose of Potas(Potassium) fertilizer application in plot No. from 1 to 8	3gm(i.e.1.02Kg/Katha) Reco. dose (1-2)Kg/Katha
Dose of compost fertilizer application in plot No. 9 and 10	2 Kg (i.e. 700Kg/Katha)
Date of fertilizer application	2073/4/15 BS
Date of harvesting the crop	2073/6/7 BS
Date of soil sample taken from the plot	2073/6/8 BS
Average quantity of grain collected from each plot (Maximum in plot 2,3,4 and gradually decrease on both sides outward)	250gm

c. Sample Collection

One soil sample was collected from each plot of a fairly uniform gradient. For composite soil sample collection, a small amount of surface soil was collected up to a depth of 15cm from at least 5 welldistributed spots in the plot. The soils are mixed well and taken ½ Kg of representative soil in a labeled cotton bag of size 20cm x 10cm to the laboratory (Superintending Engineer & Director Irrigation Research and Development, 2009; Gelderman and Mallarino, 2012; Haluschak, 2006).

Soil samples taken for laboratory analysis labeled and are shown in Table 3.5.

Table 3.3: Labels of Soil Samples

Plot No.	Label of sample (No.)	Quantity of fertilizer	Fertilizer
1	1	7gm	Zinc sulfate
2	2	6gm	Zin csulfate
3	3	5gm	Zin csulfate
4	4	4gm	Zin csulfate
5	5	3gm	Zin csulfate
6	6	2gm	Zinc sulfate
7	7	1gm	Zinc sulfate
8	8	0gm	Zinc sulfate
9	9	2Kg, Disturbed	compost
10	10	2Kg, Undisturbed	compost

11	11	Control plot	Bare Plot

d. Sample Preparation

The soil sample was dried in open air. Dried soils were crushed with a wooden pestle on wooden or heavy porcelain mortar. While crushing, avoided the crushing of pebbles, roots and rock pieces. The crushed soil samples were screened through 2 mm sieve and 250 gm sample is kept in a plastic container for analysis. For micronutrient analysis, the sieve used was of the size of 0.5 mm. For each sample test, the representative soil sample is prepared by sampling method (Superintending Engineer & Director Irrigation Research and Development, 2009; Gelderman and Mallarino, 2012; Haluschak, 2006).

e. Soil Property Analysis

Some specific soil properties such soil pH, soil salinity, soil organic matter content, soil cation exchange capacity were measured. Here the pH test by the potentiometric method has followed with the help of pH meter as the procedure explained by Hendershot and Lalande, (2006) and Haluschak (2006). The same soil sample used for the determination of soil pH was used for salinity determination. Here the method followed for salinity test by conductivity meter suggested by Whitney, (2012). For organic matter content, the volumetric method has followed i.e. the Walkley-Black method as suggested by Combs and Nathan, (2012), and Haluschak (2006). The followed CEC test was done by Ammonium acetate method with the help of another reagent as explained by (Ciesielski et al., 1997; Chapman, 1965; Haluschak, 2006).

f. Extraction procedures

Three simple extraction methods, in parallel to the determination of total metal were performed in order to evaluate the plant availability of metal. NH_4OAc (pH4.8), 0.1 N HCl and 65%HNO_3 were used in the extractions. The Zn extracted by dithizone-ammonium acetate shows a significant relationship with plant uptake whereas the values for other extractants except for NH_4OAc (pH4.8) did not approach the level of significance. The dithizone method is conveniently applicable only to estimate of amounts of 0.001 to 0.1 mg of zinc or other metal (Hibbard, 1937). The 0.1 N HCl test has been used quite successfully throughout the North Central Region and is presently used in Michigan, Ohio, and Wisconsin. 0.1N HCl method followed here is the procedure developed at the University of Missouri. The most aggressive extraction procedures using a mixture of concentrated acids reflect the total concentration of inorganic elements. Other extraction procedures (like diluted acids, EDTA, and /or NH4OAc) only partly extract metals from soil. Usually, NH_4OAc reflect mobilizable metals which can be used and metabolized by plants (Bajo et al., 1991: Gupta, 1991). All chemicals used for the preparation of extraction solutions were of analytical-reagent grade of high quality. The solutions were prepared by dissolving the compound using deionised water and adjusting the suitable pH with the acids. All measurements of the element were obtained by flame AAS.

g. Statistical analysis

Three extraction producers were compared through regression analysis for zinc element. The study compares Dithozone method, 0.1N HCl method, 65% HNO_3 method extraction of paddy field soil. All 8 aliquots (plot No. 1 to plot No. 8) were analyzed by flame atomic absorption spectrometry method (AAS). Analysis showed that Dithozone method is not applicable for AAS. Dithozone method use CCl_4 chemical for purification. CCl_4 is a fire extinguisher so flame of AAS goes off when the aliquot of dithizone inserted in the machine. Other two methods are only partially effective for zinc trace element in soil. The extraction with

diluted HNO_3 was incomplete, as large amounts of siliceous material remained undigested than the 0.1N HCl method. So here zinc concentration data obtained from 0.1N HCl for further discussion and to establish a relationship with other soil property are used. Linear relations between soil properties and zinc concentration were established.

4. Results and discussion

a. Surface Data Analysis and Discussion

The bare plot (plot No. 11) is the control plot; without the tillage, without disturbance, and without fertilization. Zinc residues in the plot is 0.7ppm by 0.1N HCl and 0.02ppm by 65%HNO_3. The higher data, 0.7ppm is very less than pollution level i.e. 400ppm (Bolt and Bruggenwert, 1978). So the bare plot had very trace amount of zinc. The bare plot zinc concentration i.e. 0.7ppm reduced to 0.5ppm after harvesting the crop. The compost fertilizer applied plots are analyzed by 65%HNO_3, considering plant available zinc. Plant available zinc in the disturbed plot is higher than the undisturbed one. Tillage and aeration help for zinc availability for the plant. Zinc concentration of deep soil (at the level of the plastic sheet below ground surface) is 0.9ppm by 0.1N HCl due to frequent percolation nature of chemical fertilizer. This is a threat to groundwater pollution. At present zinc concentration in groundwater of the vicinity was 0.5ppm by 0.1N HCl which is not hazardous for animal and plant. Paddy straw ash contains <0.1ppm, 0.1N HCl zinc which is very less. Surface data are shown in Table 4.1.

Table 4.1: Surface Data of the Study

Sample No.	Quantity of Fertilizer per $1m^2$ before plantation	Fertilizer Type	After Harvesting the Plant	
			Concentration of Zinc by HCl (0.1 N), ppm	Concentration of Zinc by HNO_3 (65%), ppm
8	0gm, Disturbed	Zinc sulfate	0.5	<0.01
9	2Kg,Disturbed	Compost	Not Tested	0.1
10	2Kg, Undisturbed	Compost	Not Tested	<0.01
11	Control Plot	-	0.7	0.02
GW	-	-	0.5	Not Tested
deep soil of plot No. 4	-	-	0.9	Not Tested
Straw Ash	-	-	<0.1	Not Tested

b. Zinc Levels in Soil after Harvesting

Normal soil should contain (30-50) ppm zinc concentration (Bolt and Bruggenwert, 1978). Zinc deficiencies occur for a plant if zinc concentration in the soil is below (20-25) ppm and toxicity start above 400 ppm (Bolt and Bruggenwert, 1978). Here all the samples are at the deficiencies level. The maximum dose of zinc sulfate i.e. 7gm is not causing any soil pollution. The dose of compost fertilizer also not causing any soil pollution. Zinc concentration of control plot is found at the deficiencies level for the plant. The deep soil zinc concentration is at the highest of all. This is because of the seepage or leaching characteristics of chemical fertilizer and is also on the safe side of pollution. But this process is increasing the possibility of groundwater

pollution. Paddy straw contains very less amount of zinc which seems to be negligible. Zinc concentration of the groundwater (GW) is the same as the surface soil. The dose of compost fertilizer is also not causing any soil pollution.

Table 4.2: zinc extraction by 0.1N HCl and 65% HNO_3

Sample No.	Quantity of Fertilizer per 1m2 before Plantation	Fertilizer Type	After Harvesting the Plant	
			Concentration of Zinc by 0.1N HCl, (ppm)	Concentration of Zinc by 65%HNO3 (ppm)
1	7gm	Zinc sulfate	0.7	0.39
2	6gm	Zinc sulfate	0.7	0.21
3	5gm	Zinc sulfate	0.7	0.19
4	4gm	Zinc sulfate	0.6	0.27
5	3gm	Zinc sulfate	0.8	<0.01
6	2gm	Zinc sulfate	0.6	0.32
7	1gm	Zinc sulfate	0.5	<0.01
8	0gm	Zinc sulfate	0.5	<0.01

By both extraction methods, as the dose of fertilizer is increasing, zinc residues in the soil is increasing.The inclination of the HNO_3 extraction method is approximately same as the HCl extraction method. The trend for zinc concentration in the soil is shown in Figure 4.2. The highest dose of zinc sulfate i.e. 7 gm per $1m^2$ leaves 0.64ppm 0.1N HCl zinc residues in the soil which is not harmful against environmental health. Similarly, minimum dose i.e. 0.0 gm zinc sulfate per 1 m^2 leaves 0.53ppm by 0.1N HCl extraction method, this is also not harmful against environmental health. Variation of chemical fertilizer is from 0.00Kg/Katha to 2.37Kg/Katha and the variation of zinc residues in the soil after harvesting is from 0.53ppm to 0.64ppm by 0.1N HCl. So the recommended dose of zinc sulfate i.e. 1Kg/Katha does not cause any environmental pollution.

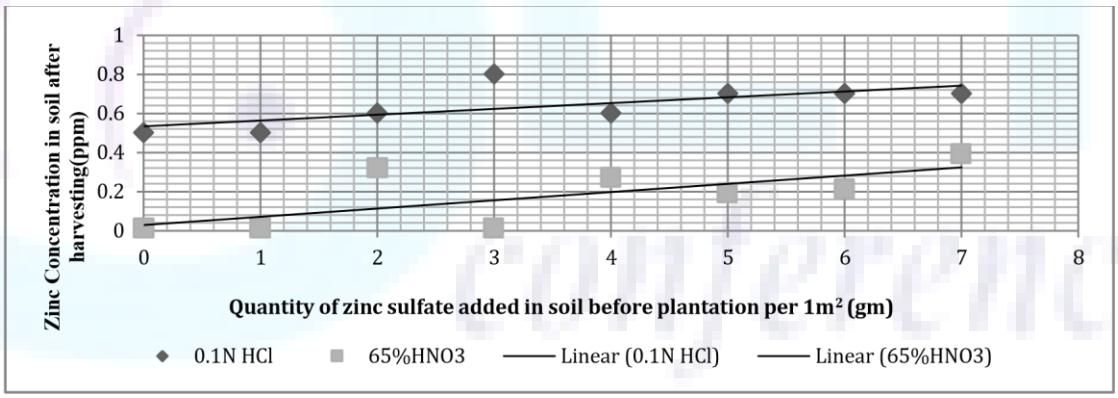

Figure 4.1: Variation of zinc residues with varying dose of zinc sulfateate

Figure 4.2 shows increasing order of zinc residues in soil after paddy plant harvest as the dose of the zinc sulfate increasing. The straight lines of both curve approximately straight. So the extracting power of 0.1N HCl is higher than 65%HNO_3 by 0.5ppm.

c. Soil characteristics

Table 4.3: Different soil properties after harvesting

Sample No.	pH	EC (mV)	OM (%)	CEC (M.Eq/100 gm)
1	6.0	52	2.47	23.0
2	6.0	51	2.53	24.9
3	6.0	52	1.97	19.6
4	6.0	46	2.11	23.8
5	6.1	43	1.94	21.9
6	6.2	40	1.83	24.5
7	6.3	35	1.68	20.3
8	6.3	60	1.83	22.0

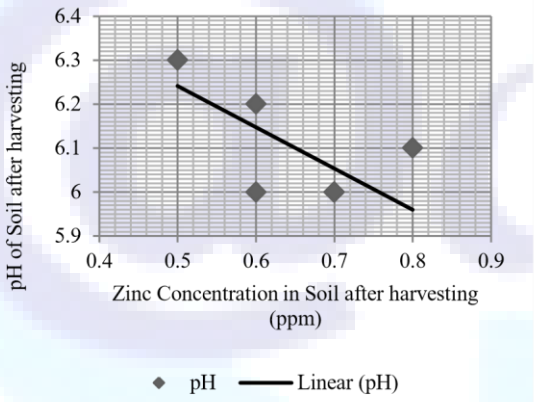

Figure 4.2: Variation of pH with varying concentration of zinc in soil

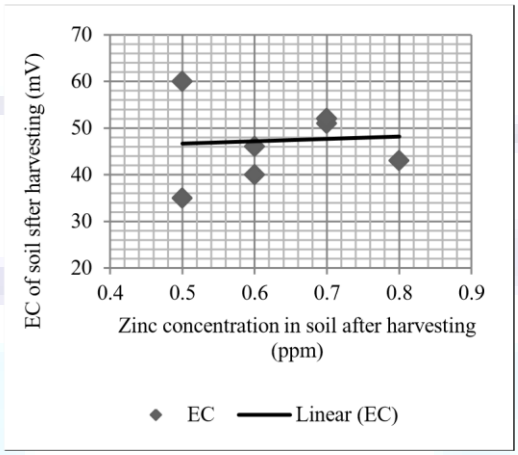

Figure 4.3: Variation of salinity with varying concentration of zinc in soil

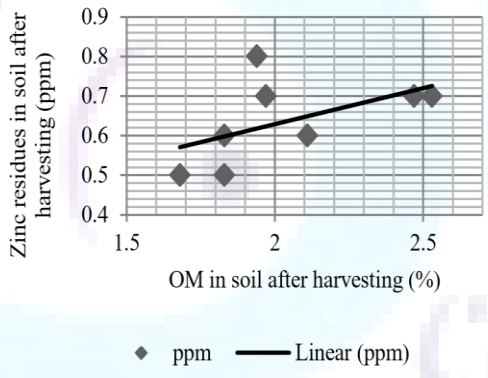

Figure 4.4: Variation of OM with varying concentration of zinc in soil

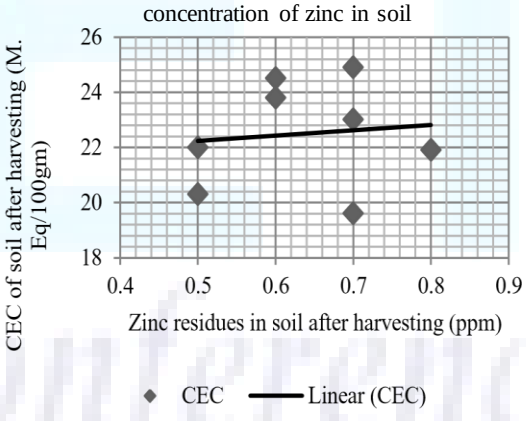

Figure 4.5: Variation of CEC with varying concentration of zinc in soil

Figure 4.2 shows the soil is becoming more acidic as the Zn concentration is increasing. Many soil chemical and biological reactions are controlled by the pH of the soil and soil solution in equilibrium with the soil particle surfaces. Zinc availability is highly dependent on pH. When the pH is above 6, the availability of Zn is usually very low. The availability of Zn in alkaline soils is reduced due to lower solubility of the soil Zn. The concentration of Zn in the soil solution decreases from (6.5 µg/g) with an increase from pH 5 to pH 8

(Hafeez, 2013). Thus it is more probable that Zn deficiency will occur in alkaline rather than acidic soils. In the case of soils characterized by high contents of hydroxyl (OH^-) ions, it is difficult to get a crop response even to applied Zn. The lower availability of Zn under alkaline conditions is attributed to the precipitation of Zn as $ZnOH_2$ or $ZnCO_3$. The higher carbonate contents in alkaline soils also absorb Zn and hold it in an unchangeable form. The movement of Zn in limed soils is considerably lower than in acidic soils so that absorption of Zn by the crop may be low. All these factors contribute to the low availability of Zn at high pH values. Thus, the pH of soil gives an indication of the degree of availability of many soil nutrients and the favorability of soil conditions to microbial activity (Hafeez, 2013).

More often, salinity is not measured directly, but is instead derived from the conductivity measurement Electrical Conductivity (EC). In present test results variation of salinity is not much encountered according to the variation of zinc concentration. Here salinity is slightly seems increasing as the concentration increases. The trend of salinity is shown in Figure 4.3. Soil salinity is a form of land degradation in which salts accumulate in the soil profile to an extent that plant growth or infrastructure are negatively affected. Soil salinity reduces plant growth by a combination of (i) reducing the osmotic potential of the soil solution which limits water uptake by the plant, (ii) specific ion toxicity from ions such as sodium (Hardie and Doyle, 2012). Effects of soil salinity are manifested in loss of stand, reduced plant growth, reduced yields, and in severe cases, crop failure. Salinity limits water uptake by plants by reducing the osmotic potential making it more difficult for the plant to extract water. Salinity may also cause specific-ion toxicity or upset the nutritional balance of plants. In addition, the salt composition of the soil water influences the composition of cations on the exchange complex of soil particles, which influences soil permeability and tilth (Dennis, 2014). The straight curve is approximately horizontal. So the optimum dose of zincsulphate should be 1Kg/katha for good condition of soil salinity.

Figure 4.4 shows that the OM increases as the concentration of zinc in soil increases. Low organic matter contents in soils give rise to Zn deficiency as it is observed that available Zn increases with an increase in organic matter in the soil. The most stable organic compounds in the soil are humic substances such as humic and fulvic acids. Both of these substances contain a relatively large number of functional groups (OH, COOH) which have a great affinity for metal ions such as Zn^{2+}. Fulvic acids mainly form chelates with Zn over a wide pH range and increase the solubility and mobility of Zn (Hafeez, 2013). Simple organic compounds such as amino acids, hydroxy acids and also phosphoric acids are effective in complexing Zn, thus increasing its mobility and solubility in soils. An increase in the organic matter contents of a soil increase its Zn availability; however, if the organic matter content in soil is too high, like in peat and muck soils, this can also contribute to Zn deficiency due to the binding of Zn on solid state humic substances. So the recommended dose of zinc sulfate, 1Kg/Katha, is good as the optimum dose for paddy plant as Zn availability may increase or decrease by increasing OM depending upon the soil type.

Figure 4.5 shows that the CEC increases as the concentration of zinc in soil increases. Low CEC in soils gives rise to Zn deficiency as it is observed that available Zn increases with increase in CEC in the soil. The cations held on the surface of soil minerals and within the crystal framework of some minerals species and those which are part of certain organic compounds can be reversibly replaced by those salt solutions and acids. Soil with high organic matter content, and soils with containing appreciable kaolin, halloysite or other 1:1 type clay minerals, it will often give somewhat lower values for exchange capacity. Macronutrient cations such as Ca, Mg and K inhibit the absorption of Zn by plants from solution. Zinc concentrations progressively decreased with increasing Ca concentrations in solutions. The macronutrient cat ions K, NH4 and Mg all inhibited the rate of Zn absorption strongly from solutions of low Ca concentrations; with increasing Ca concentrations, the inhibitory effects weakened and in the case of two ions (K, Mg) tested at sufficiently high Ca concentration

(Hafeez, 2013). Here zinc availability is increasing as the CEC is increasing also zinc availability is increasing as the organic matter increasing. And with high organic matter low exchange capacity. So the recommended dose of zinc sulfate, 1Kg/Katha, is good as the optimum dose for paddy plant as CEC be at the optimum level.

5. Conclusions

Different doses of zinc sulfate i.e. (0.00 to 2.37)Kg per Katha is not polluting the soil of paddy field. The concentration of zinc residues in the soil after paddy harvesting is in the range of (0.5 to 0.8)ppm by 0.1N HCl which is very less in comparison to pollution level. Also, it can be concluded, the initial residues, before plantation, of zinc in the soil is 0.7ppm by 0.1N HCl is at non pollution level. In literature, normal soil contains zinc residues (30-50)ppm and deficiencies occur below (20-25)ppm. The higher dose leaves very fewer zinc residues in the soil. The 3 feet deep soil of one of the set's zinc concentration is analyzed to be 0.9ppm by 0.1N HCl which is comparatively high. This confirms the loss of zinc is mostly by seepage. We can say the zinc required by the paddy plant is fulfilled without further fertilizer addition. Availability of zinc for the plant is dependent on other soil property; decrease with increasing pH, increase with the increase of salinity, increase with the increase of OM, increase with the increase of CEC. The increasing rate of OM retards the rate of CEC at higher level hence the availability of zinc decrease at higher level of OM. So the optimum dose of zinc sulfate fertilizer is 1Kg/Katha.

Acknowledgement

I would first like to thank my thesis supervisor Dr. Ram Kumar Sharma, Prof. of the Department of Applied Science, Pulchowk Campus, Institute of Engineering, Tribhuvan University; Prof. Mr. Iswar Man Amatya, Coordinator of Environmental Engineering Program. I would also like to thank the experts who were involved in the validation survey for this research project: Dr. Rosa Ranjit, Senior Scientific Officer, NAST; Mrs. Prabha Karmacharya, Senior Lab. Officer, Environmental laboratory, Pulchowk Campus; Mr. Prakash Dhakal, Research Assistant, NAST. A special thanks go to my teammate Mr. Sumit Chandra Mallik. Finally, I must express my very profound gratitude to my parents and to my friends for providing me with unfailing support and continuous encouragement throughout my years of study and through the process of researching and writing this thesis. This accomplishment would not have been possible without them. Thank you.

References

[1] Addae, E. 2013, 'An Assessment of Heavy Metal Contamination in Soils and Vegetation- A Case Study of Korle Lagoon Reclamation Site', *Institute for Environmental and Sanitation Studies (IESS), University of Ghana, Legon*, pp 14-17.

[2] AhmAd, W., WAtts, m.J., ImtIAz, m., Ahmed, I., Zia, m.h. 2012, 'Zinc deficiency in soils, crops and humans' Agrochimica, Vol. LVI - N., pp 1-3.

[3] Bajo, S., Tobler, L., Wyttenbach, A. 1991, 'Concentration profiles of total and extractable As, Br, Co, Fe, K, Sb, Sc, V, Zn in forest soil' In: Farmer JG (ed.), *International Conference, Heavy Metals in the Environment, Vol. 1. Edinburg: CEP consultans Ltd*. pp185-8.

[4] Beckett, P.H.T., Warr, E., Davis, R.D. 1983, 'Cu and Zn in soils treated with sewage-sludge: their 'extractability' to reagents compared with their 'availability' to plants' Plant and Soil:70., pp3–4.

[5] Bolt, G. H. and Bruggenwert, M.G.M. 1978, 'Pollution of Soil', 2nd (ed), *Soil Chemistry A Basic Element*, Elsevier Scientific Publishing Company Amstrdam-Oxford-New York, pp 236-239.

[6] Chapman, 1965, 'CEC at pH 7 with Ammonium Acetate' In: Donald S. R. and Ketterings, Q.(ed.), *Recommended Methods for Determining Soil Cation Exchange Capacity, Methods for Measuring Cation Exchange Capacity*, pp 77,76, 78, 83.

[7] Ciesielski, H, Sterckeman, T, Santerne, M and Willery, Jp, 1997, 'A comparison between three methods for the determination of cation exchange capacity and exchangeable cations in soils' Agronomie, EDP Sciences, 1997, 17 (1), pp.11, 15.

[8] Combs, S. M. and Nathan, M. V. 2012, 'Soil Organic Matter' *Recommended Chemical Soil Test Procedures for the North Central Region, Missuri Agricultural Experiement Station SB 1001*,pp 12.1-12.6.

[9] Dass, A., Chandra, S., Uphoff, N., Choudhary, A. K., Bhattacharya, R., Rana, K.S. 2017, 'Agronomic fortification of rice grains with secondary and micronutrients under different crop management and soil moisture regims in the north India Plains' *The International Society of Paddy and Water Environment Engineering and Springer Japan 2017*, Paddy Water Environ:15, pp745758.

[10] Dennis L. C. 2014, 'Salinity Mobilization and Transport from Rangelands: Assessment, Recommendations, and Knowledge Gaps' *United states Department of Agriculture, USA*.

[11] Gelderman, R.H. and Mallarino, A.P. 2012, 'Soil Sample Preparation' *Recommended Chemical Soil Test Procedures for the North Central Region, Missuri Agricultural Experiement Station SB 1001*,pp 1.1-1.2.

[12] Gupta, S.K. 1991, 'Increase in the mobilisable and leachable heavy metals in anthropogenic and artificially contaminated soils' In: Farmer JG, (ed.) *International Conference, Heavy Metals in the Environment, Vol. 1. Edinburg: CEP consultans Ltd*.pp 185-8.

[13] Hafeez, B., Khanif, Y. M., and Saleem, M. 2013, 'Role of Zinc in Plant Nutrition- A Review'*Agriculture Research Institute Tandojam-Pakistan, Department of Land Management, University Putra Malaysia, Malaysia*, American Journal of Experimental Agriculture 3(2): 374391, pp 374-378.

[14] Haluschak, P. 2006, 'Determination of Cation Exchange Capacity and Extraction of Exchangable Cations (Mineral Samples)' *Laboratory Methods of Soil Analysis, Canada-Manitoba Soil Survey*, pp 97-99.

[15] Haluschak, P. 2006, 'Determination of Organic Carbon' *Laboratory Methods of Soil Analysis, Canada-Manitoba Soil Survey*, pp 58-60.

[16] Haluschak, P. 2006, 'Measurement of soil pH' *Laboratory Methods of Soil Analysis, CanadaManitoba Soil Survey*, pp 58-60.

[17] Haluschak, P. 2006, 'Sample Preparation' *Laboratory Methods of Soil Analysis, Canada-Manitoba Soil Survey*, pp 7-8.

[18] Hardie, M. and Doyle, R. 2012, 'Measuring Soil Salinity' *Methods in molecular biology (Clifton, N.J.) 913:415-25*, pp 415-417.

[19] Hendershot, W. H. and Lalande, H. 2006, 'Soil Reaction and Exchangable Acidity' In Soon Y.K. and Hendershot, W. H., *McGill University, Sainte Anne de Bellevue, Quebec, Canada.*

[20] Hibbard, P.L. 1937, ' A Dithizone Method for Measurement of Small Amounts of Zinc' Ind. Eng. Chem. Anal. (Ed.), 1937, 9 (3), DOI: 10.1021/ac50107a009, pp 127

[21] International Zinc Association 2018, 'Zinc in the Environment' https://www.zinc.org/environment/
22. International Zinc Association 2018, 'Zinc in Human Health' https://www.zinc.org/health/
[22] Quevauviller, P., Ure, A.M., Muntau, H., Griepink, B. 1993, 'Improvement of Analytical Measurement within the BCR-Program: Single and Sequential Extractions Procedures Applied to soil and Sediment Analysis' International Journal of Environmental Analytical Chemistry, pp129– 132.

[23] Ramos, M. C. 2005, 'Metals in vineyard soils of the Penede`s area (NE Spain) after compost application' *Department de Medi Ambient I Ciencies del Soil, Universitat de Lleida, Alcalde Roviro Roure 177, Lieida 25198, Spain,* Journal of Environmental Management 78(2006) pp 209215.

[24] Ramos, M. C. and Lopez-Acevedo 2003, 'Metals in vineyard soils of the Penede`s area (NE Spain) after compost application' *Department de Medi Ambient I Ciencies del Soil, Universitat de Lleida, Alcalde Roviro Roure 177, Lieida 25198, Spain*, Advances in Environmental Research: 8 (2004), pp 687-696.

[25] Subramaniam, G., Kumar, R. M., Humayun, P., Srinivas, V., Kumari, B. R., Vijayabharathi, R., Singh, A., Surekha, K., Padmavathi, Ch., Somashekar, N., Rao, P. R., Latha, P. C., Rao, L. V. S., Babu, V. R., Viraktamath, B. C., Goud, V. V., Loganandhan, N., Gujja, B., Rupela, Om. 2013, 'Assessment of different methods of rice (Oryza sativa. L) cultivation affecting growth parameters, soil chemical, biological, and microbiological properties, water saving, and grain yield in rice–rice system' Paddy and Water Environment.

[26] Superintending Engineer and Director 2009, 'Laboratory Testing Procedure for Soil & Water Sample Analysis' *Government of Maharashtra Water Resources Department Directorate of Irrigation Research & Development, Pune*, pp 3,4.

[27] Thakur Ak, , Uphoff, N, Antony E 2009, 'An assessment of physiological effects of system of rice intensification(SRI) practices, in India' *Water Technology Centre for Eastern Region, Bhubaneswar-751023, Orissa, India, and Cornell International Institute for Food, Agriculture and Development, Ithaca, NY 14853, USA,* Experimental Agriculture, pp1,2,3

[28] Uphoff, N. 2015, 'The System of Rice Intensification (SRI) Responses to Frequently Asked Questions' *SRI-Rice, Cornell University,* 1st Edition, Published by Norman Uphoff, SRI-Rice, B75 Mann Library Cornell University, Ithaca, New York 14853, USA, ISBN: 13: 978-1515022053, pp 3-5,8-13,21-26.

[29] Wikipedia 2018, 'Plant Nutrition' https://en.wikipedia.org/wiki/plant_nutrition

[30]Wikipedia 2018, 'Zinc' https://en.wikipedia.org/wiki/zinc

[31] Whitney, D. A. 2006, 'Soil Salinity' *Recommended Chemical Soil Test Procedures for the North Central Region, Missuri Agricultural Experiement Station SB 1001*,pp 13.1-13.2.

[32] Whitney, D. A. 2006, 'Micronutrients: Zinc, Iron, Manganese and Copper' *Recommended Chemical Soil Test Procedures for the North Central Region, Missuri Agricultural Experiement Station SB 1001*,pp 9.2.

[33] Williams, J.G., McLaren, R.G. 1983, 'Effects of dry and moist incubation of soils on the extractability of native and applied soil copper' *Edinburgh School of Agriculture, West Mains Road, Edinburgh EH9 3JG, Scotland,* Plant and Soil 64.pp 215.

[34] Yaron, Bruno, Calvet, Raoul, Prost, Rene 1996, 'Processes and Dynamics' *Soil Pollution*, Springer-Verlag Berlin Heidelberg, ISBN 978-3-540-60927-8.

Part VII: Electrical Engineering

Design and Performance Analysis of PI and PR Controller for Single Phase PWM Inverter

[1]*Hari Pandey*, [2]*Hao Zhenyang*
[1,2]*College of Automation Engineering*

Nanjing University of Aeronautics and Astronautics, Nanjing 210016, China

[1]pandey.hari077@nuaa.edu.cn, [2]zhenyang_hao@nuaa.edu.cn

Abstract

In this manuscript, we designed and analyzed the performance of proportional-integral and *proportional-resonant controller for single-phase PWM inverter containing LCL filter with the linear and non-linear load. The controller is based on inner current and outer voltage-controlled double loop. The multiple feedback loop PI and PR controller for PWM inverter are designed in Sisotool. Simulated result in the MATLAB/SIMULINK shows that PR controller possesses better steady-state error, good disturbance rejection capacity and low THD with both types of loads.*

Keywords*: Inverter, Proportional-integral (PI) controller, Proportional-resonant (PR) controller*

1. Introduction

DC- AC conversion system is incomplete without an inverter. A well-designed inverter must be capable of producing pure and stable sinusoidal output voltage to the load independent its type. This phenomenon is only possible when its closed-loop controller is designed accurately. The precisely designed inverter closed-loop controller must be able to bring back in original stable steady state by rejecting the disturbances caused by different types of load [1].

There are large numbers of methods that have been proposed for the control of inverter in the last few decades[2-4]. Among them, in the voltage control mode, PI and PR controller have better results and used widely[5]. These controllers are designed after the precise mathematical model of the overall system. For overall controller design, inner current and outer voltage control loop must be contemplated during the design for proper voltage regulation and low THD [6].

Output terminals of the inverter are connected with load through the filters which are inevitable to supply the pure ac to the load. In comparison to the LC filter, LCL filter can supply ripple-free current to the load [7]. The quality of the supplied voltage is also dependent on the selection of filter parameters.

In this manuscript inverter current, load current and capacitor voltage are sensed and controlled by the voltage and current controller to generate the duty cycle of the inverter. PI and PR controller parameters for outer voltage and inner current loops along with their bandwidth and phase margin are evaluated, analyzed, and compared to give the final result.

2. Plant Model

Fig. 1 below shows the overall system used in this analysis. For the study, a linear control strategy is used in this design. Due to the non-linear solid-state switch, the system must be linearized at its operating point for the proper design of the control system. In this paper, 5 kW inverter with load resistance R=10.58 Ω is used for linearization at the operating point.

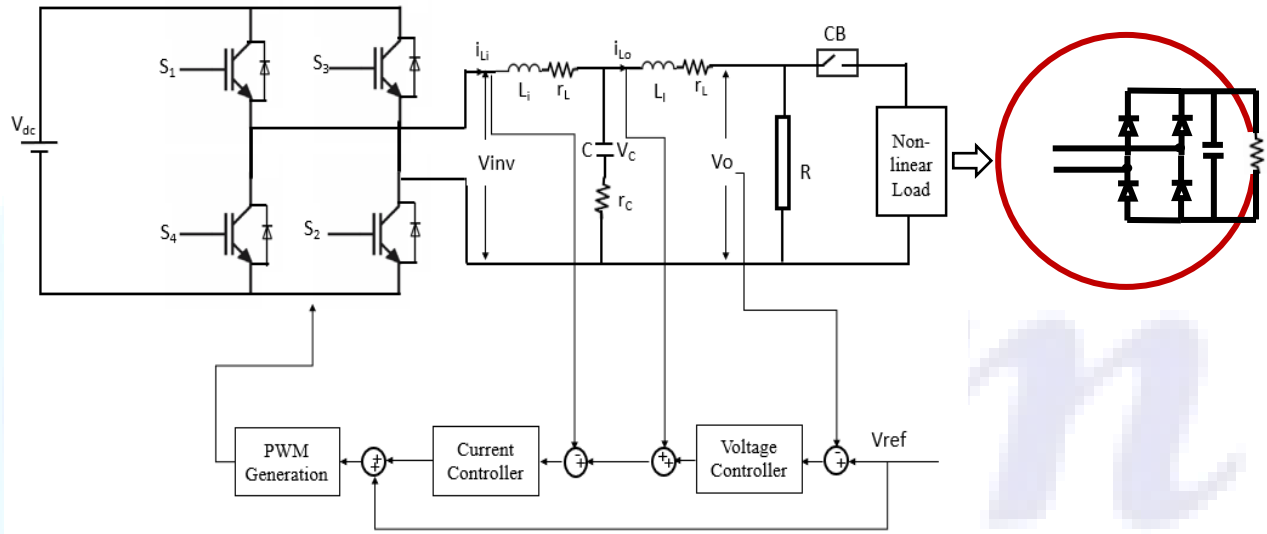

Figure 1: Inverter with LCL filter and control loops

An LCL filter used in the plant modeling can provide effective decoupling with the load as well as it can attenuate the frequency above resonant frequency by 60*dB/decade* [8, 9].

2.1 State-Space Model of the System

As LCL filter is used, the system operates as a third-order continuous-time system. There are three state variables i.e., inverter side inductor current I_i, load side inductor current I_L and capacitor voltage V_c. The state-space model of the system under analysis can be written as:

$$\begin{bmatrix} \dot{I}_i \\ \dot{V}_c \\ \dot{I}_L \end{bmatrix} = \begin{bmatrix} \frac{r_i + r_c}{L_i} & \frac{-1}{L_i} & \frac{r_c}{L_i} \\ \frac{1}{C} & 0 & \frac{-1}{C} \\ \frac{r_c}{L_L} & \frac{-1}{L_L} & \frac{r_L + R + r_c}{L_L} \end{bmatrix} \begin{bmatrix} I_i \\ V_c \\ I_L \end{bmatrix} + \begin{bmatrix} \frac{1}{L_i} \\ 0 \\ 0 \end{bmatrix} [V_{inv}] \quad (1)$$

$$V_0 = [0 \quad 0 \quad R] \begin{bmatrix} I_i \\ V_c \\ I_L \end{bmatrix} \quad (2)$$

2.2 Control loops Analysis

In single-phase inverter shown above, the inverter side filter inductor current acts as an inner loop whereas output voltage/capacitor voltage acts as an outer voltage loop. These loops can be controlled by PI, PR, and Fuzzy controller [10-12]. In this paper, PI and PR, controllers are used to control the current and voltage loop.

2.2.1 *Inner Current loop*

The function of the current control loop is to inject the current to load. Therefore, it should be designed with a higher bandwidth than the voltage controller to track the current accurately [13].

V_{inv} can be expressed as;

$$V_{inv}=(sL_i + r_i)I_i + (sL_L + r_L)I_L + I_L R \quad (3)$$

$$I_L = I_i - I_c \quad (4)$$

$$I_c = \left(\frac{(sL_i+r_i)I_i - V_{inv}}{1+r_c sC}\right) sC \quad (5)$$

$$G_i(s) = \frac{I_i(s)}{V_{inv}(s)} \quad (6)$$

$$G_i(s) = \frac{s^2 L_L C + sC(r_L + r_c + R) + 1}{s^3 C L_L L + s^2 Z_{eqv} + s(L + CR_{eqv}) + R_{se}} \quad (7)$$

Where,

$L = L_L + L_i$

$R_{eqv} = (r_i r_c + r_c r_L + r_i r_L + r_i R + r_c R)$

$R_{se} = r_i + r_L + R$

$Z_{eqv} = C(L_L r_i + L_i(r_L + R) + r_c L$

Since r_i and r_L are very small and can be neglected. So $G_i(s)$ becomes;

$$G_i(s) = \frac{s^2 L_L C + sC(r_c + R) + 1}{s^3 C L_L L + s^2 C(L r_c + L_i R) + s(L + C r_c R) + R} \quad (8)$$

2.2.2 *Outer Voltage loop*

The voltage control loop is required to maintain the power quality supplied by the inverter. THD of supplied voltage should be low under different load conditions because harmonic distortion due to non-linear load may fluctuate the output voltage of the inverter. In case of load variation and disturbances, the voltage control loop should give fast response to recover to a stable state [14]

The Voltage control loop transfer function $G_V(s)$ is given by

$$G_V(s) = \frac{V_o(s)}{V_{inv}(s)} \quad (9)$$

$$G_v(s) = \frac{sL_L + r_L}{s^3 C L_L L + s^2 Z_{eqv} + s(L + CR_{eqv}) + R_{se}} \quad (10)$$

Since r_i and r_L are very small and can be neglected. So $G_V(s)$ becomes;

$$G_v(s) = \frac{sL_L}{s^3 C L_L L + s^2 C(L r_c + L_i R) + s(L + C r_c R) + R} \quad (11)$$

3. Design of Control Systems

Both controllers are designed and tuned to the suitable bandwidth and stability in MATLAB/SIMULINK/*Sisotool*. As mentioned in the above section, the controllers are designed for 10.58Ω linear load, and their performance are evaluated with both linear and non-linear loads. The simulation testing parameters are tabulated below in Table I.

Table 1: 5 kW Inverter Parameters

P_{out}	5 kW
V_{dc}	400V
V_{out}rms	230V
Switching Frequency	15 kHz
Inverter Side Filter Inductor (L_i)	0.542 mH
Load Side Filter Inductor (L_L)	0.3252 mH
Filter Capacitor(C)	15.043 µF
Damping Resistor (r_c)	1.22 Ω
Load	10.58 Ω
Non-linear Load (Diode Rectifier)	R=100 Ω C= 300 µF

3.1 Design of PI Controller

The transfer function of PI controller is:

$$G_{PI}(s) = K_p + \frac{K_i}{s} = K_p\left(\frac{s + \frac{K_i}{K_p}}{s}\right) \quad (12)$$

The value of K_p, K_i, and K_r can be obtained accurately by using *Sisotool* in MATLAB/SIMULINK. Due to the decoupling nature of current loop and voltage loop, control systems are designed separately for each loop. One of the desired specifications of the controller is that the bandwidth of a current controller should be higher than the bandwidth of a voltage controller [15]. The reason behind this requirement is that a current controller has to deal with current harmonics, which are produced due to different kinds of load (linear or non-linear). So, there will be a very fast response towards these disturbances with higher bandwidth.

3.1.1 *Voltage loop PI controller*

The PI controller for voltage loop is designed by using transfer function $G_v(s)$ in (11). The complete TF in addition with PI controller will be;

$$G_V(s) = G_{PI}\frac{sL_L}{s^3CL_LL + s^2C(Lr_c + L_iR) + s(L + Cr_cR) + R} \quad (13)$$

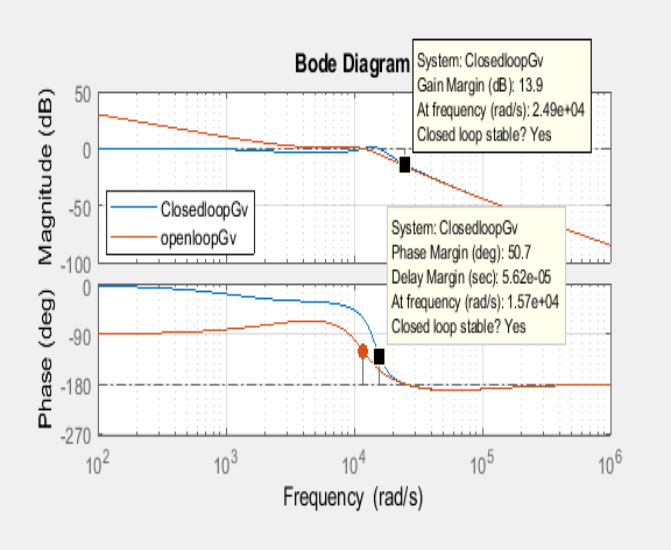

Figure 2: Open and close loop bode for PI voltage controller

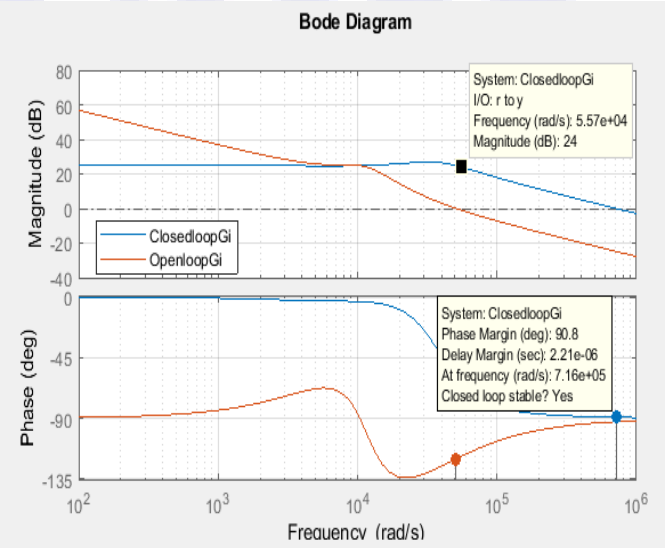

Figure 3: Open and close loop bode for PI current controller

The response of the voltage loop in the frequency domain with compensation for both open and closed-loops can be seen in Fig. 2. After the tuning PI controller, it will have the following gains:

K_p=0.77842

K_i=3129

It is seen from the bode plot that gain margin and phase margin of PI voltage controller are 13.9 dB and 50.7˚respectively, while the bandwidth of the system is 1740 rad/sec in the closed loop.

3.1.2 *Current loop PI controller*

In order to design a current loop PI controller (8) is used. The complete TF with PI controller will be:

$$G_i(s) = G_{PI}\frac{s^2L_LC + sC(r_c + R) + 1}{s^3CL_LL + s^2C(Lr_c + L_iR) + s(L + Cr_cR) + R} \quad (14)$$

The result of the tuned PI current controller is shown in Fig. 3. Controller gains after compensation are as follows:

K_p=22.2

K_i=732468

It is seen that both gain values for the current controller are higher than the voltage controller. The high value of proportional gain for the current controller shows that the current controller possesses the faster response than that of the voltage controller [16]. Similarly, the integral gain is also very high, which shows the strong integral effect on the system. It is stated in [17] that integral gain is directly linked with controller's bandwidth which means, in order to increase the bandwidth of a controller, value of an integral gain needs to be increased. This current controller having bandwidth $5.58*10^4$ rad/sec possesses high gain at the fundamental frequency and both margins (phase and gain) were increased. The bandwidth of the current controller is higher than the voltage controller, which is one of the required specifications.

3.2 Design of PR Controller

The Transfer function of PR controller is given by:

$$G_{PR}(s) = K_p + \frac{2K_r\omega_{PRC}s}{s^2 + 2\omega_{PRC}s + \omega^2} \quad (15)$$

The PR controller is designed at the resonance frequency of ω=314 rad/sec and cut-off frequency ω_{PRC}= 5 rad/sec.

K_p and K_r can be evaluated by using *Sisotool* in MATLAB/SIMULINK.

3.2.1 *Voltage loop PR controller*

To design the PR controller for voltage loop TF of $G_v(s)$ in (11) is used. The complete TF of voltage loop with PR controller can be written as:

$$G_v(s) = G_{PR}\frac{sL_L}{s^3CL_LL + s^2C(Lr_c + L_iR) + s(L + Cr_cR) + R} \quad (16)$$

Fig. 4 shows the frequency response of $G_v(s)$ for both closed and open loops. The tuned PR controller has the following values:

K_p=0.28

K_r=84

The gain margin for voltage loop PR controller is 33.9dB and Phase margin is 120˚, while the bandwidth of the system is 398 rad/sec in closed-loop.

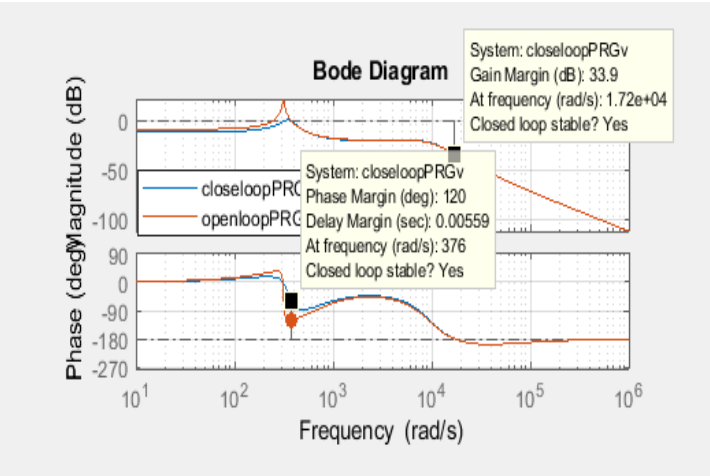

Figure 4: Open and close loop bode for PR voltage controller

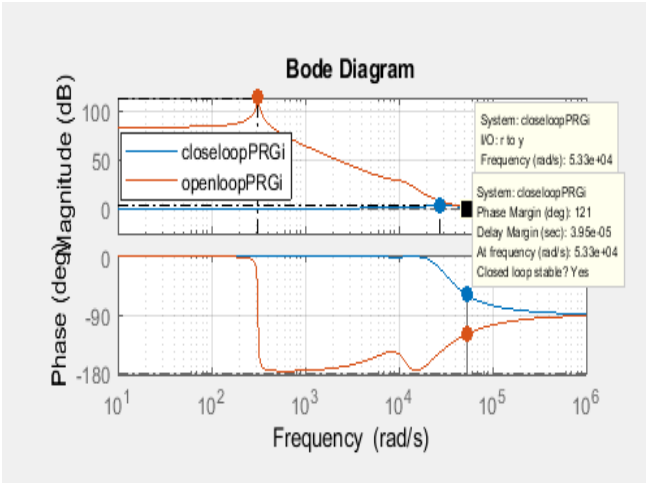

Figure 5: Open and close loop bode for PR current controller

3.2.2 *Current loop PR controller*

PR controller for current loop is designed with (8) and transfer function of the current loop with controller will be:

$$G_i(s) = G_{PR}(s)\frac{s^2L_LC + sC(r_c + R) + 1}{s^3CL_LL + s^2C(Lr_c + L_iR) + s(L + Cr_cR) + R} \qquad (17)$$

The value of K_p and K_R after tuning in the *Sisotool* found as:

K_p=425

K_r=21165

Fig. 5 above shows the open and closed-loop frequency response of the current controller, which has infinite gain margin, i.e., system will be stable for every gain and phase margin of 121 ˚ with a bandwidth of 5.33*10^4 rad/sec.

4. Comparison of Results

In this analysis, both types of controllers are designed for the linear load of 10.58 Ω and performances were evaluated based on margins, the bandwidth of control loops and total harmonic distortion with linear and non-linear load. The non-linear load is connected with CB at t=0.1s to 0.2s. In both control loops, the PR controller has good margins and bandwidth, which ensures the stability under some significant disturbances. The following figures describe the output wave-forms of different controllers with linear and non-linear loads.

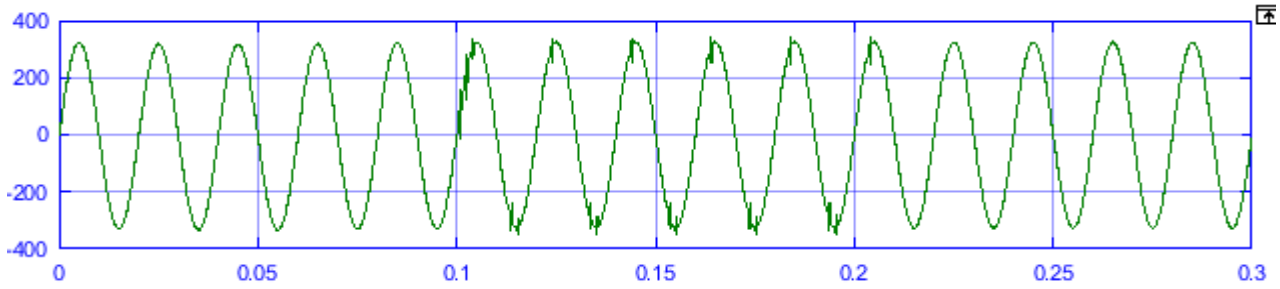

(a)

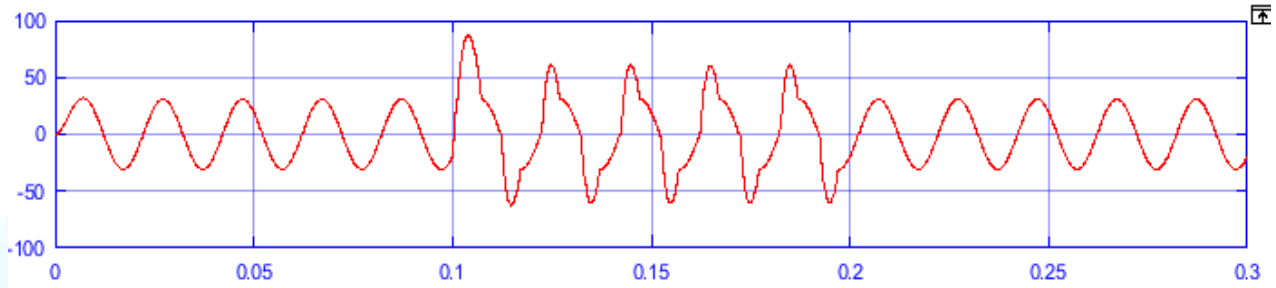

(b)

Figure 6:(a) Voltage, (b) Current wave-form of PI controller

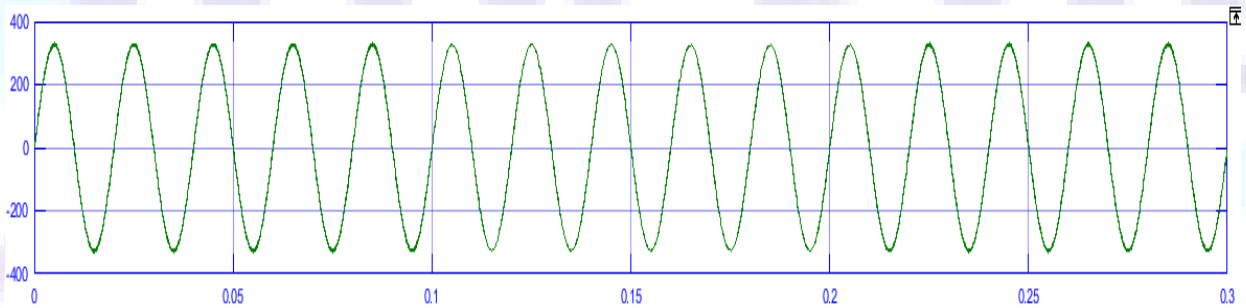

(a)

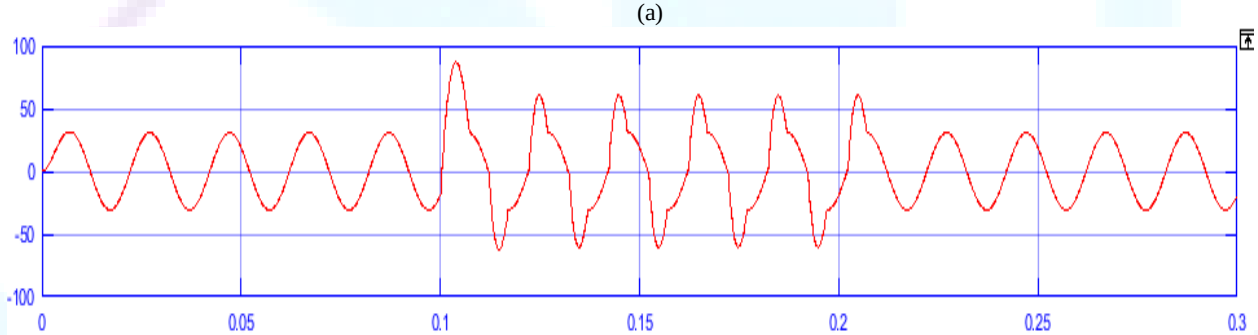

(b)

Figure 7: (a) Voltage, (b) Current wave-form of PR controller

5. Conclusion

The PI and PR controller for single-phase PWM inverter are designed, implemented and compared in this paper. For both types of controller, two loops were considered and used for control action. In order to tune the PI and PR controller gain, *Sisotool* from MATLAB/SIMULINK is used. Results from the simulation of 5 kW inverter with both controllers for linear and non-linear load are shown. Although both the controllers are capable of producing good voltage regulation and fulfilling the IEEE THD limit, PR controller has a better performance against load disturbances, steady-state error and can track reference voltage adequately.

References

[1] Abdel-Rahim, N.M. and J.E. Quaicoe, *Analysis and design of a multiple feedback loop control strategy for single-phase voltage-source UPS inverters.* IEEE Transactions on Power Electronics, 1996. **11**(4): p. 532-541.

[2] Rodríguez, J., et al. *Predictive current control of a voltage source inverter*. in *2004 IEEE 35th Annual Power Electronics Specialists Conference (IEEE Cat. No. 04CH37551)*. 2004. IEEE.

[3] Malesani, L. and P. Tenti, *A novel hysteresis control method for current-controlled voltage-source PWM inverters with constant modulation frequency.* IEEE Transactions on Industry Applications, 1990. **26**(1): p. 88-92.

[4] Zhang, R., et al. *A grid simulator with control of single-phase power converters in DQ rotating frame*. in *2002 IEEE 33rd Annual IEEE Power Electronics Specialists Conference. Proceedings (Cat. No. 02CH37289)*. 2002. IEEE.

[5] Cherati, S., et al. *Design of a current mode PI controller for a single-phase PWM inverter*. in *2011 IEEE Applied Power Electronics Colloquium (IAPEC)*. 2011. IEEE.

[6] Loh, P.C. and D.G. Holmes, *Analysis of multiloop control strategies for LC/CL/LCL-filtered voltage-source and current-source inverters.* IEEE Transactions on Industry Applications, 2005. **41**(2): p. 644-654.

[7] Bao, C., et al., *Step-by-step controller design for LCL-type grid-connected inverter with capacitor–current-feedback active-damping.* IEEE Transactions on Power Electronics, 2013. **29**(3): p. 1239-1253.

[8] Julean, A., *Active damping of LCL filter resonance in grid connected applications.* Aalborg Universitet, Dinamarca, Dissertação de mestrado, 2009.

[9] Lettl, J., J. Bauer, and L. Linhart, *Comparison of different filter types for grid connected inverter.* PIERS Proceedings, Marrakesh, Morocco, 2011.

[1]. Bianconi, E., et al., *Perturb and observe MPPT algorithm with a current controller based on the sliding mode.* International Journal of Electrical Power & Energy Systems, 2013. **44**(1): p. 346-356.

[11] Shen, G., et al., *A new feedback method for PR current control of LCL-filter-based grid-connected inverter.* IEEE Transactions on Industrial Electronics, 2010. **57**(6): p. 2033-2041.

[12] Hilloowala, R.M. and A.M. Sharaf, *A rule-based fuzzy logic controller for a PWM inverter in a stand alone wind energy conversion scheme.* IEEE Transactions on Industry Applications, 1996. **32**(1): p. 57-65.

[13]Liu, F., et al., *Parameter design of a two-current-loop controller used in a grid-connected inverter system with LCL filter.* IEEE Transactions on Industrial Electronics, 2009. **56**(11): p. 4483-4491.

[14] D'Azzo, J.J., Houpis, Constantine H, *Feedback control system analysis and synthesis,*. 1966, N.Y: McGraw-Hil.

[15] Hong, Y., D. Jiyang, and W. Jiaju. *Research on modeling and control of the single-phase inverter system with a nonlinear load*. in *2008 7th World Congress on Intelligent Control and Automation*. 2008.

[16] Mohan, N. and T.M. Undeland, *Power electronics: converters, applications, and design*. 2007: John wiley & sons.

[17] Dash, A., et al., *Analysis of PI and PR controllers for distributed power generation system under unbalanced grid faults*. 2011. 1-6.

Optimal Placement and Sizing of DG in Distribution System Using Genetic Algorithm for Power Loss Minimization

Anil Kumar Panjiyar[1], Abhinav Jha[2]

[1]*Department of Electrical Engineering*
Advanced College of Engineering & Management
[2]*Electrical Engineer Msc Student, Pulchowk Campus*
Lalitpur, Nepal

[1]anil.panjiyar@pcampus.edu.np ,[2] avidavinav@gmail.com

Abstract

Numerous advantages attained by integrating Distributed Generation (DG) in distribution systems. These advantages include decreasing power losses and improving voltage profiles. Such benefits can be achieved and enhanced if DGs are optimally sized and located in the systems.
This project presents a distributed generation (DG) allocation strategy to improve node voltage and power loss of radial distribution systems using genetic algorithm (GA). The objective is to minimize active power losses while keep the voltage profiles in the network within specified limit. In this project, the optimal DG placement and sizing problem is investigated using two approaches. First, the optimization problem is treated as single-objective optimization problem, where the system's active power losses are considered as the objective to be minimized. Secondly, the problem is tackled as a multi-objective one, focusing on total power loss as well as voltage profile of the networks. This approach finds optimal DG active power and optimal OLTC position for tap changing transformer. The simulation study is carried out on a 33 bus radial Distribution System. The results are presented, compared and analyzed in this paper.

Keywords: *Power Systems Stability, Distributed Generation, Genetic Algorithm*

1. Introduction

Globally increasing trends in electric power consumption, congestion in the transmission system, economic and environment concern has led the attention towards small power generation called DG, in distribution system. DG has many advantages such as it increases the power capacity in power system, it reduces the power losses in power system, and it increases the voltage profile of the distribution system as it is in radial nature [1]. DG was previously used as an active power source but today with technological advancement it is available in many forms such as: an active power source of supply (e.g. photovoltaic cell or combined heat and power (CHP), a reactive power source (e.g. synchronous condenser, capacitors or STATCOM), the active and reactive power requirements (e.g. synchronous machines or wind generation). It is projected that around 13% of collective power production is lost as system losses in distribution system [2].

The study reveals that an installation of DG in distribution system significantly reduces the power loss and increase the voltage profile of the system. In order to harness the optimal benefits from DG, it should have proper placement and sizing in the system. Improper placement and sizing will worsen the existing situation. There are many methods that have been used for proper placement and sizing of DG. An analytical method such as 2/3 method has been used for optimal placement and sizing of DG. According

to this method, when the load is balanced then 2/3 size of DG of total incoming generation can be penetrated at 2/3 location of the feeder. However, this method is not suitable for non-uniform loads.

Linear programming method is used for optimal DG placement and to gather maximum amount of energy, considering financial and technical constraints. The probabilistic generation-load model with its all operating condition and probabilities has been accommodated in deterministic model [2]. The optimal placement and sizing of generation units on the distribution network has been continuously studied in order to achieve different aims. The objective can be the minimization of the active losses of the feeder; or the minimization of the total network supply costs, which includes generators operation and losses compensation; or even the best utilization of the available generation capacity. As a contribution to the methodology for DG economic analysis, in this paper it is presented an algorithm for the allocation of generators in distribution networks for loss reduction in distribution network (Loss with DG ≤ Loss without DG). The Genetic Algorithm is used as the optimization technique. The technique satisfies the power balance, bus voltage and system capacity as constraints.

2. Literature Review

Generally, distributed generation means the electric power generation within distributed network to fulfil the rapid energy demand of consumers. However, distributed generation can be defined in a variety of ways.

1) The Electric Power Research Institute (EPRI) defines distributed generation as generation from 'a few kilowatts up to 50 MW' [5].

2) International Energy Agency (IEA) defines distributed generation as generating plant serving a customer onsite or providing support to a distribution network, connected to the grid at distributed level voltages [6].

3) The International Conference on large High Voltage Electric Systems (CIGRE) defines DG as 'smaller than 50- 100 MW' [5].

Although there are variations in definitions, however, the concept is almost same. DG can be treated as small scale power generation to mitigate the consumer energy demand. Distributed Generation can come from a variety of sources and technology. As the technical design of each distribution network is unique, therefore, it cannot be answered what should be the optimum generation capacity or rating of DG [5]. The maximum size or rating of DG which can be connected to a distribution network depends on numerous factors, such as voltage level within the distribution system, power loss profile and other technical, environmental, commercial and regulatory issues. In this paper, we will focus on the technical issues only. As DG offers lots of benefit, the penetration of DG in distribution system is increasing rapidly. Therefore, DG should be allocated in an optimal way to maximize the system efficiency.

In a distribution system power loss varies with numerous factors. Real power losses of a distribution system depend on the resistance of distribution lines, core losses of transformers and motors. As dielectric and rotational losses are so small compared with line losses, therefore, only line losses are considered in this analysis. The complex power S_{ij} from node i to j and S_{ji} from node j to i are

$$Sij = Vi\ I^*ij \quad (1)$$

$$Sji = Vj\ I^*ji \quad (2)$$

Where, V_i and V_j are the voltages at node i and j respectively. The line current I_{ij} which is measured at bus

i in the positive direction of i to j and I_{ji} which is measured at bus j in the positive direction of j to i. Therefore, power loss in any line between node i and j can be written as the algebraic sum of power flows determined from (1) and (2).

$$SLij = Sij + Sji \quad (3)$$

After any converged load flow, power loss in any line can be calculated using (3) and taking the summation of all line losses, total power loss of the network can be calculated using equation (4) where n is the number of lines.

$$Loss = \sum_{k=1}^{n} S\,L\,(k) \quad (4)$$

For any distribution system, placement of any DG unit will change the power loss profile of that system. Actually, in distribution network, power loss curve with the variation of power generation at a particular location is approximately quadratic function because Line Losses $\propto I^2R$ and $I \propto$ considering I is the line current, R is the resistance, and S is the apparent power flowing through the line. Therefore, as the DG size is increased in any location of a power distribution network, the total system losses are reduced to a minimum value. With further increasing of DG, losses again start to increase. This trend of losses with DG size variation is given in Fig. 1 for a test case to demonstrate the sizing and location issues of DG.

Here, for DG size PDG2 we get the minimum power loss which is called optimum DG size for that bus. Actually, the structure of distribution system is such that power should flow from the substation to the consumer end and conductor sizes are also decreased gradually [3]. When a DG is placed in the network, it is desirable that power should be consumed within the distribution network and thus improves power profile. Any size of DG more than the optimum size will create reverse flow of power towards distribution substation. Therefore, excessive power flow through small sized conductors towards

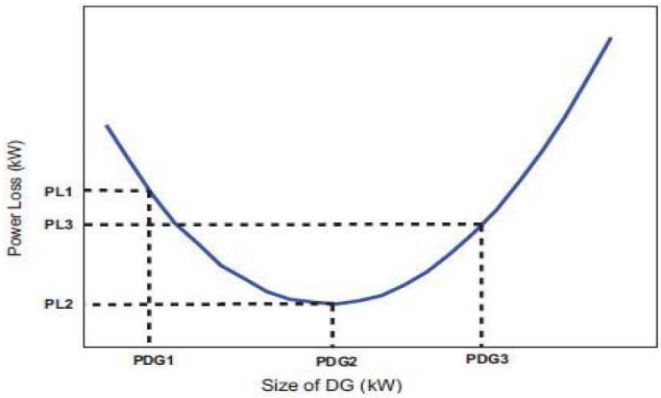

Figure 1: Power loss characteristic of distribution system with DG size variation

the transmission area will increase the power losing distribution network. In the literature, genetic algorithm have been applied to DG placement [10-13].In all these works either sizing or location of DGs are determined by these methods. The DG placement problem has therefore attracted the interest of many research efforts in the last fifteen years [7], since it can provide DSOs, regulators, and policy makers useful input for the derivation of incentives and regulatory measures. The Clonal algorithm is a new population based meta heuristic approach inspired by Clonal principle of immune system of human body. The advantage of this algorithm is that it does not require external parameters such as selection, cross over rate and mutation rate as in case of genetic algorithm and differential evolution and it is hard to determine these parameters in prior.

However, DG placement impacts critically the operation of the distribution network. Inappropriate DG placement may increase system losses and network capital and operating costs. On the contrary, optimal DG placement (ODGP) can improve network performance in terms of voltage profile, reduce flows and system losses, and improve power quality and reliability of supply.

Load Flow of Radial Distribution Networks

A feeder brings power from substation to load points/nodes in radial distribution networks (RDN). Single or multiple radial feeders are used in this planning approach. Basically, the RDN total power losses can be minimized by minimizing the branch power flow or transported electrical power from transmission networks (i.e. some percentage of load are locally meeting by local DG). To determine the total power loss of the network or each feeder branch and the maximum voltage deviation are determined by performing load flow. The Forward/Backward Sweep Load Flow technique is used in this case. The impedance of a feeder branch is computed by the specified resistance and reactance of the conductors used in the branch construction. The Forward/Backward Sweep Load Flow method consist two steps (i) backward sweep and (ii) forward sweep.

Backward sweep: In this step, the load current of each node of a distribution network having *N* number of nodes is determined as:

$$\bar{I}_L(m) = \left\{\frac{P_L(m) - jQ_L(m)}{\bar{V}^*(m)}\right\} \quad (5)$$

$[m = 1,2\ldots\ldots N]$

Where, (m) and $Q_L(m)$ represent the active and reactive power demand at node *m* . Then, the current in each branch of the network is computed

As: $\bar{I}(mn) = \bar{I}(n) + \sum_{m\epsilon\Gamma} \bar{I}_L(m)$ (6)

Where, the set Γ consists of all nodes which are located beyond the node *n*.

***Forward sweep*:** This step is used after the backward sweep so as to determine the voltage at each node of a distribution network as follows:

$$\bar{V}(n) = \bar{V}(m) - \bar{I}(mn)Z(mn) \quad (7)$$

Where, nodes *n* and *m* represent the receiving and sending end nodes, respectively for the branch *mn* and (mn) is the impedance of the branch.

In this work the estimation methodology utilized within the forward/backward load flow is based on (i) equivalent current injections (ECI), (ii) the node-injection to branch current matrix (BIBC) and (iii) the branch-current to nodevoltage matrix (BCBV). The relations between the node current injections and node voltages could be communicated as:

$$[\Delta V] = [BCBV].[BIBC].[I]$$

Genetic Algorithms

Genetic Algorithm is a general-purpose search techniques based on principles inspired from the genetic and evolution mechanisms observed in natural systems and populations of living beings. Their basic principle is the maintenance of a population of solutions to a problem (genotypes) as encoded in formation individuals that evolve in time. Generally, GA comprises three different phases of search:

Phase 1: creating an initial population;

Phase 2: evaluating a fitness function;

Phase 3: producing a new population.

A genetic search starts with a randomly generated initial population within which each individual is evaluated by means of a fitness function. Individual in this and subsequent generations are duplicated or eliminated according to their fitness values. Further generations are created by applying GA operators. This eventually leads to a generation of high performing individuals. There are usually three operators in a typical genetic algorithm : the first is the production operator (elitism) which makes one or more copies of any individual that possess a high fitness value; otherwise, the individual is eliminated from the solution pool; the second operator is the recombination (also known as the 'crossover') operator. This operator selects two individuals within the generation and a crossover site and carries out a swapping operation of the string bits to the right hand side of the crossover site of both individuals. Crossover operations synthesize bits of knowledge gained from both parents exhibiting better than average performance. Thus, the probability of a better offspring is greatly enhanced; the third operator is the ‘mutation’ operator. This operator acts as a background operator and is used to explore some of the invested points in the search space by randomly flipping a 'bit' in a population of strings. Since frequent application of this operator would lead to a completely random search, a very low probability is usually assigned to its activation.

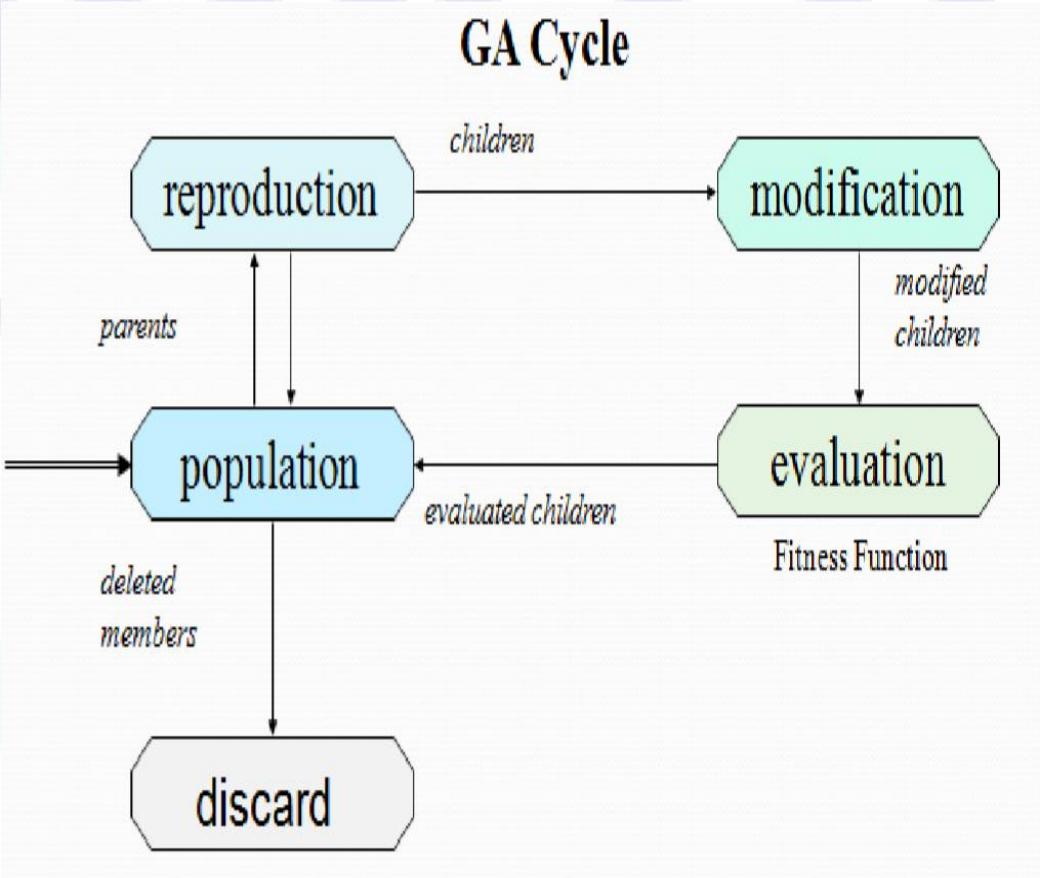

Figure 2: Genetic Algorithm Cycle

3. Methodology

The Optimal DG placement and sizing to reduce the power loss in distribution system using GA based method takes the following steps which is presented in a flow chart in Fig. 3.

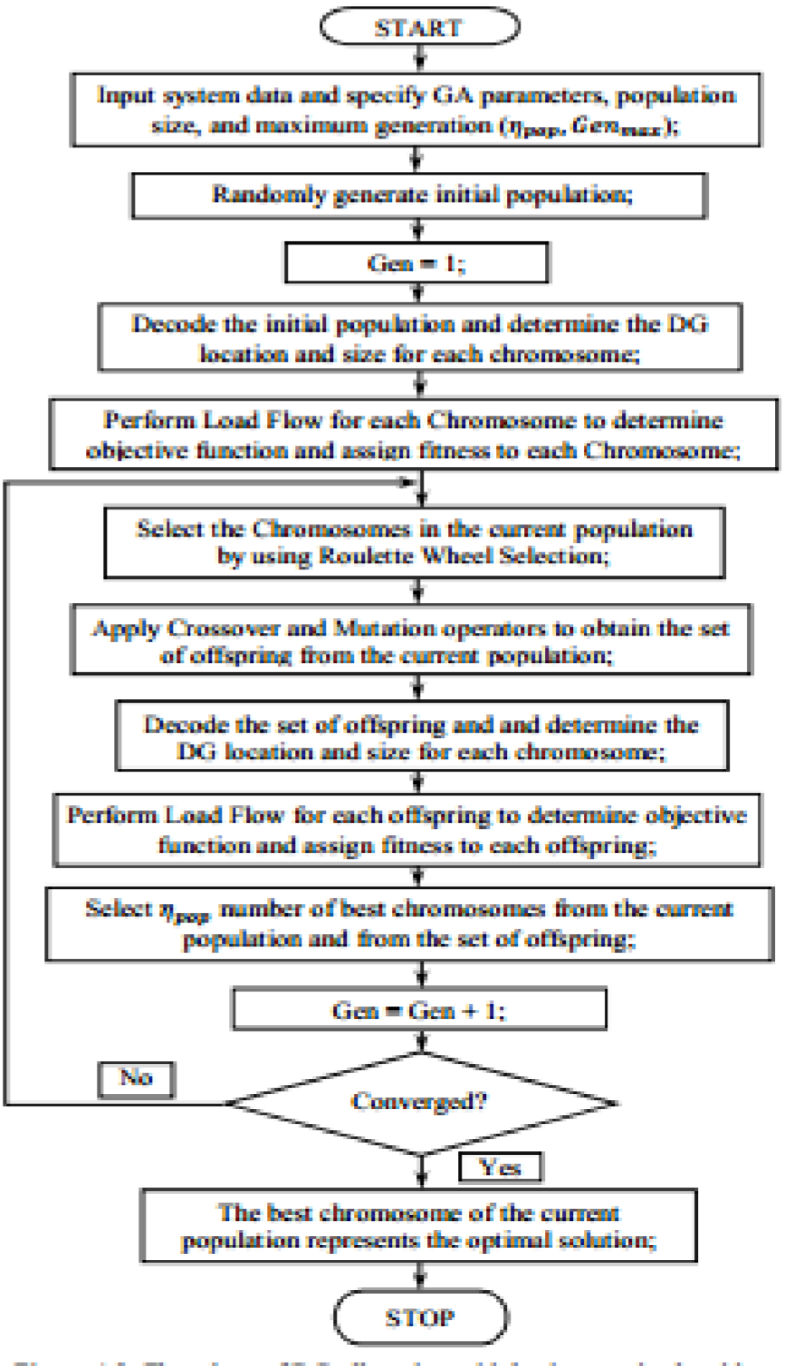

Figure 3: Methodology of the Tas

4. Results and Discussion

The simulation results are carried out for two types of DG (Type 1: which injects real power like photovoltaic cell or fuel cell, Type 2: which injects reactive power source, like synchronous condenser or capacitor). Figure 2. Shows the single line diagram of IEEE 33 radial distribution system, having one main feeder and three laterals. The total demand of the system is 3720 KW real power and 2300 KVAr reactive power.

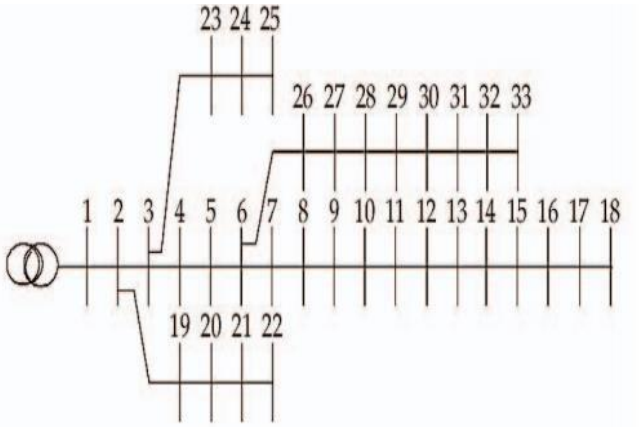

Figure 4: IEEE 33 Bus Radial Distribution System

The upper and lower limit of the voltage profile of the system are taken as 0.90 volts to 1.05 volts. Bus 1 is slack bus, which has maximum voltage for both case (Base case and after DG placement). Before installation of the DG at system, the voltage is found about 0.9038 volts at bus 18, which is minimum of all node voltage whereas after installation of type-1 DG, voltage is improved to 0.9424 volts. However, after installation of type-2 DG, voltage at bus 18 is found 0.9286 volts.

Table 1: Voltage of the system before and after DG installation

Test System		Base case		After DG placement	
		Voltage(P.U)		Voltage(P.U)	
		Min	Max	Min	Max
IEEE 33 Bus	Type 1 DG	0.9038@ bus18	1.00@ bus1	0.942 @bus 18	1.00@ bus1
	Type 2 DG	0.9038@ bus 18	1.00@ bus1	0.9286 @bus 18	1.00 @bus1

From the analysis of table-1 it can be seen that type-1 DG gives better option for improvement of the voltage of the system than type-2 DG installed in the system.

Table-2 describes the optimal placement and sizing of DG with respect to real and reactive power loss for two different type of DG installation. After installation of type -1 DG, the power losses reduces from 211 kw to 111 kw which is about 47.39 % of active power loss reduction whereas the reactive power at this DG is reduced from 143 kVar to 81.7 kVar which is about 39.58 % of reactive loss reduction. For second type of DG, the active power loss reduces from 211 kw to 170.8 kw which is about 19.06 % of active power loss reduction whereas the reactive power at this DG is reduced from 143 KVar to 118.6 KVar which is about 17.06 % of reactive loss reduction. It can be noted that optimal placement of DG is bus 6 and optimal size of

DG is 2.5907 Mw for DG type-1 whereas optimal placement for DG type-2 is bus 30 and optimal size is 1.258 MVar.

Table 2: Optimal DG size Power loss of the system before and after DG

Test System IEEE 33 Bus	Base case		DG size	After DG		Loss Reduction	
	Power Loss			Power Loss			
	Ploss(K	Qloss(Kvar)	Type -1(Mw) Type -2 (Mvar)	Ploss(Kw)	Qloss(Kvar)	Ploss(%)	Qloss(%
Type-1 DG	211	143	2.5907@ bus6	111	81.7	47. 39	39.58
Type-2 DG	211	143	1.258@ bus30	170.8	118.6	19. 05	17.06

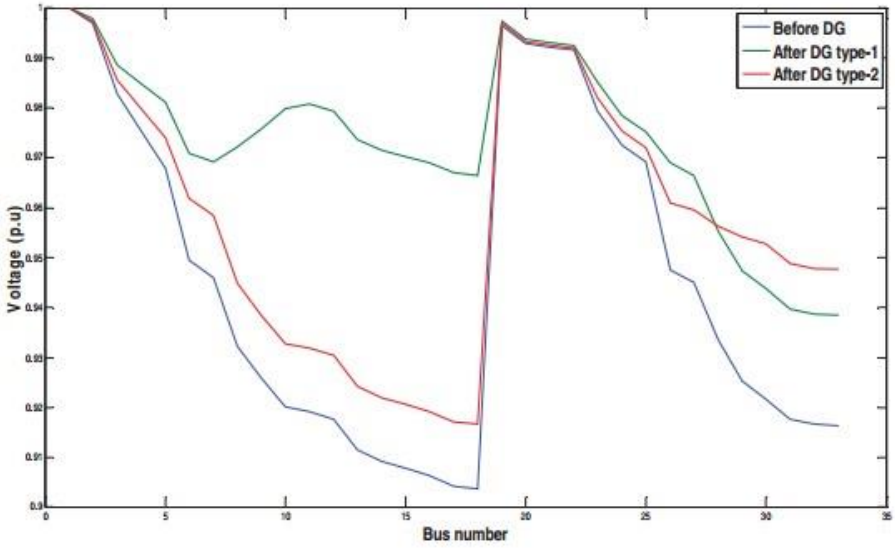

Figure 5: Voltage Profile of IEEE Bus system before and after DG Installation

Moreover, Fig. 6 and Fig. 7 are representing the real and reactive power loss on each branch of the system respectively. It can be observed on fig. 6 and fig. 7 that before DG installation the real power loss is maximum on buses 2,5,3, 4 and reactive power losses is maximum on buses 5,2,27,3 whereas after installation of different type of DG, the power losses is reduced significantly.

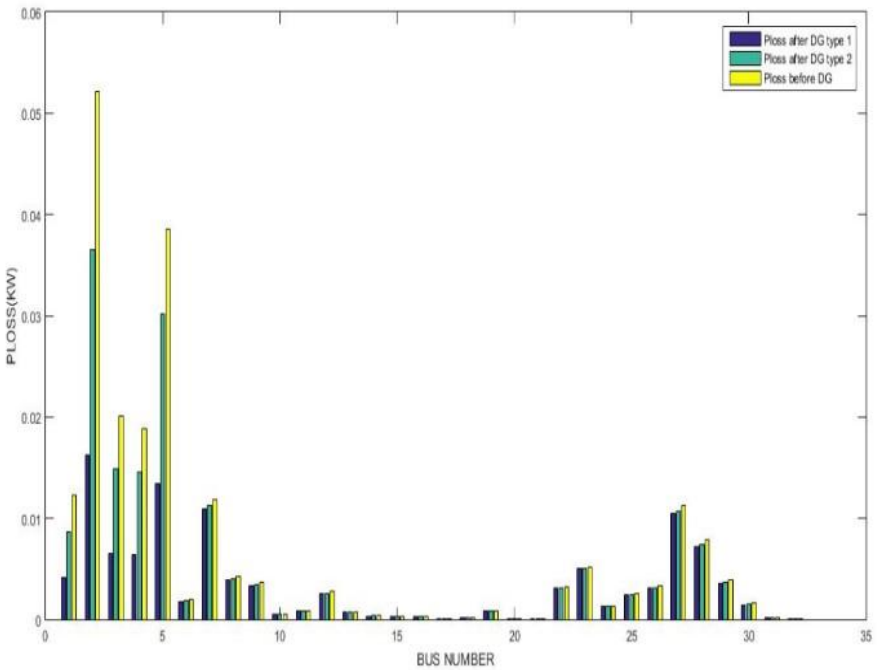

Figure 6: Real Power loss before and after DG

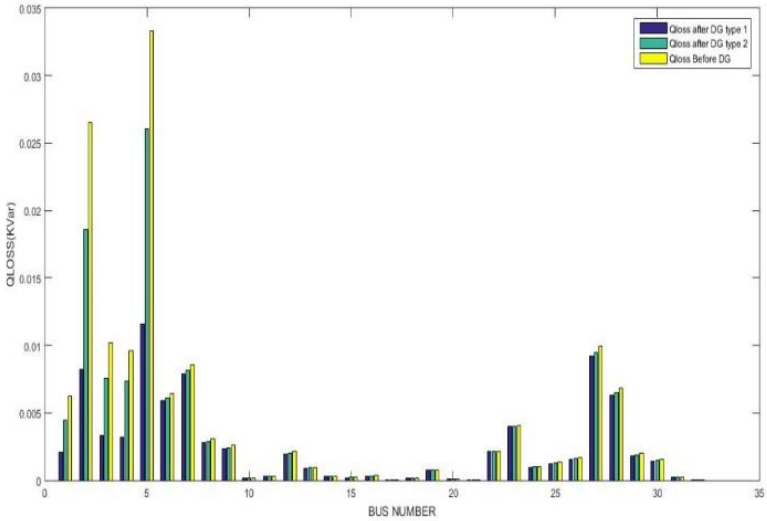

Figure 7: Reactive Power loss before and after DG

5. Conclusion

In this Project work, a methodology for the optimal location and sizing of DG for power loss reduction in IEEE-33 bus system using Genetic algorithms has been proposed. The programming has been done using MATLAB environment.

This project utilizes the optimization approach called Genetic Algorithm for placement and sizing of DG problem in distribution system. The main purpose is to reduce the system power losses and improve the voltage profile. The algorithm has been tested on IEEE 33 bus system for two type of Dg i.e active power source DG(type-1) and reactive power source DG (type-2). The result shows that type-1 DG reduces 47.39 % of active power loss whereas type-2 DG reduces 19.05 % of active power loss. Similarly, for voltage, type-1 DG increases 4.27 % percentage voltage whereas type-2 DG increases 1.79 %. Hence, it can be asserted that type-1 DG minimize more power losses and improve voltage profile of the system as compared to DG type-2. Moreover, it can be observed that this method has a fast convergence response.

References

[1] G. Pepermans, J. Driesen, D. Haeseldonckx, R. Belmans, W. D'haeseleer, (2005). "Distributed Generation:Definition, Benefits and Issues". *Energy Policy*, 33: 787–798.

[2] W.El-Khattam, K.Bhattacharya, Y.Hegazy, M.M.A. Salama,(2004). "Optimal Investment Planning for Distributed Generation in a Competitive Market," *IEEE Transactions on Power Systems*, Vol.19, No. 3, pp 1674-1684.

[3] G. P. Harrison, A. Piccolo, P. Siano, A. R. Wallace, "Exploring the Tradeoffs Between Incentives for Distributed Generation Developers and DNOs," *IEEE Transactions on Power Systems*, Vol. 22, No.2, pp. 821 -828, May 2007.

[4] D. Rizy, F. Li, H. Li, S. Adhikari, and J. Kueck (2010)., "Properly understanding the impacts of distributed resources on distribution systems," in Power and Energy Society General Meeting, IEEE.

[5] O. T. Mithulananthan, Nadarajah and L. V. Phu, (2007).“Distributed generator placement in power distribution system using genetic algorithm to reduce losses,” Thammasat International Journal of Science and Technology, vol. 9, pp. 55–62.

[6] N. Acharya, P. Mahat, and N. Mithulananthan,(2006). “An analytical approach for DG allocation in primary distribution network,” International Journal of Electrical Power & Energy Systems, vol. 28, no. 10, pp. 669–678

[7] S. Kansal, V. Kumar, and B. Tyagi, "Optimal placement of different type of DG sources in distribution networks," International Journal of Electrical Power & Energy Systems, vol. 53, pp. 752-760, 2013.

[8] V. A. Evangelopoulos and P. S. Georgilakis, "Optimal distributed generation placement under uncertainties based on point estimate method embedded genetic algorithm," IET Generation, Transmission & Distribution, vol. 8, pp. 389-400, 2014.

[9] M. Aman, G. Jasmon, A. Bakar, H. Mokhlis, and M. Karimi, "Optimum shunt capacitor placement in distribution system—A review and comparative study," Renewable and Sustainable Energy Reviews, vol. 30, pp. 429-439, 2014.

[10] S. Devi and M. Geethanjali, "Optimal location and sizing determination of Distributed Generation and DSTATCOM using Particle Swarm Optimization algorithm," International Journal of Electrical Power & Energy Systems, vol. 62, pp. 562-570, 2014.

Simulation and Analysis of Harmonic Impact of Electric Vehicle Charging on the Electric Power Grid

Subrat Aryal[1], Anil Kumar Panjiyar[2]

[1]*Electrical Engineering, Pulchowk Campus, Lalitpur, Nepal*
[2]*Electrical Engineering, Advanced College of Engineering & management, Lalitpur, Nepal*

[1]subb.rat@gmail.com
[2]anil.panjiyar@pcampus.edu.np

Abstract

Due to ever increasing use of electric vehicle in the world, an electric utility must be able to meet the both energy demand and peak demand caused by charging of EV's. Not only the peak demand and energy demand fulfillment, a utility must be able to maintain its THD within prescribed limit. Or in other words the EV penetration in the power system has the ability to disturb the voltage and current waveforms of the system. So in order to make the system healthy we must be able to make the supply side of EV battery charging circuit to be harmonic free. The harmonic compensation can be either done by use of active filter or by use of passive filter. Active filter can filter out any amount of harmonic content as per design and is however costlier. With clever design passive filter can be beneficial in removing particular harmonic content or fixed harmonic component. In this project rather implementing the filter multiple EV chargers are simulated and the harmonic obtained in the supply side is studied. Different kind of chargers both single phase and three phase chargers are simulated and the result is studied thereby. For the study purpose MATLAB/SIMULINK software is used.

1. Introduction

Power quality is one of the emerging issue to be addressed by a power system engineer. It is desirable that the system voltage and frequency limit not be violated beyond its prescribed limit. Similarly, the harmonics content of the system should be fundamental as can be possible by any means. That is harmonic distortion in the system has various impacts such as heating of cables and wires, overloading of transformer, overloading of the cable, it may affect the PCC voltage etc. The EV chargers can be either single phase chargers or three phase chargers. The electric vehicle needs to be charged for their daily purpose. This can be either charged at home or can be charged at the charging station which are fed by various feeder. The battery charger acts as the highly nonlinear load due to the use of the semiconductor devices used in the charger circuit [1]. Hence this semiconductor device will cause the supply to inject harmonics in the charger circuit. This will deviate the voltage and the current waveforms from sine wave and this will create the problem. The total harmonic distortion should be within the acceptable limit. According to the IEEE standard THD should be maintained within 5%. If the THD is not maintained, then this might cause the power quality problems. Due to ever increasing electric vehicle it is important to study the impacts of EVs and their chargers have on the electric grid. Basically it depends on the configuration of the electric chargers for different types of harmonic distortion. For this different EV chargers needs to be simulated [6]. In this project, the simulation model of electric vehicle charging station is built and the characteristics of harmonics generated during charging process are analyzed. Furthermore, the multiple charging station has been simulated and the harmonic injected by the supply side has been proposed to be investigated.

Furthermore, the analysis is done to study the voltage and the current harmonics. Depending upon ***state-of-charge(SOC)***, ***charge duration (or charge algorithm),*** and ***charging start time*** of the individual equipment, THD may vary. Due to non-coincidence of above quantity current harmonics will not be just algebraic sum but involves consideration of both the magnitudes and phase angles of individual harmonic components. Hence due to this Harmonic phase cancellation effect will take place. For the study purpose simulation model of electric vehicle charging station [9](*both single phase and three phase)* is built and the characteristic of harmonics generated during charging process are analyzed[5]. Furthermore, the multiple EV charger has been simulated and the harmonic injected by the supply side is investigated.

As shown in the figure 1, The EVk denotes the kth electric vehicle being charged from the charging station. The block EVk denotes either single phase or three phase EV charger.

For proper simulation, the three phase source is taken from the Matlab/Simulink which generates the electric power at 11kv. This is connected to 3 phase distribution line having R/X ratio almost 10. This feeder is then connected to a 11/0.2 kV Delta-Star Distribution transformer. This transformers LT will provide 3 phase four wire for charging purpose. Hence from this 3 phase four wire we can now connect any kind of chargers of different configuration and hence study will be easy.

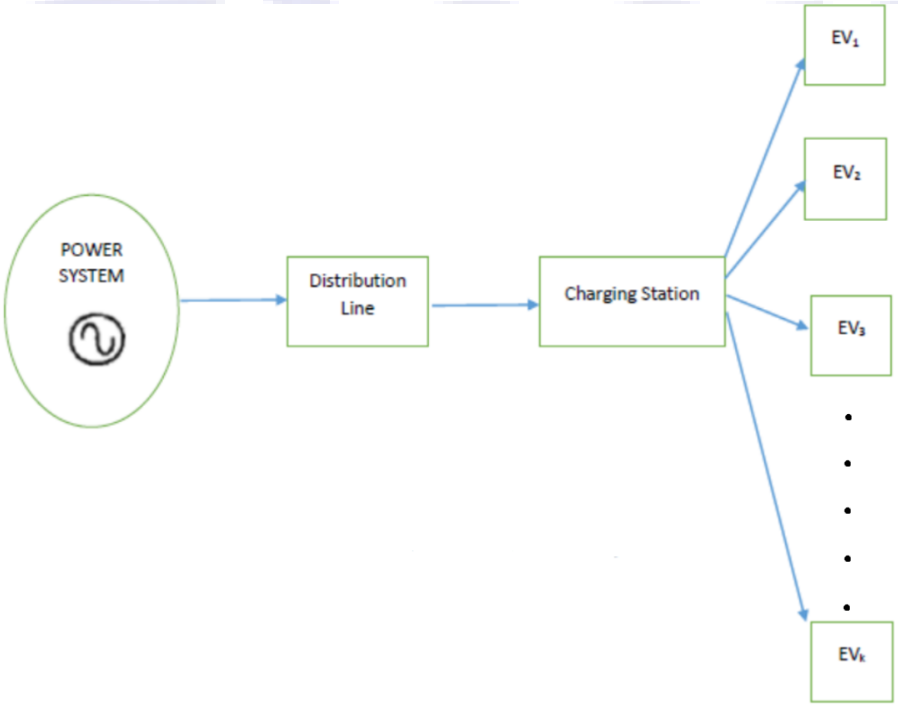

Figure 1: Schematic of Ev charger from Distribution line.

2. Objectives

- To study the harmonic impact of sample individual chargers.
- To simulate multiple chargers on a distribution system and analyze the harmonic impact.

3. Literature Review

Electric vehicle (EV) chargers are highly nonlinear power system load [2]. They present a potential problem to power systems in the forms of excessive harmonic currents and poor power factor. Thus it is important to

analyze the effect of EV chargers on power system harmonic current and then to take some measures to improve the loading factor of power systems and acquire better power quality [3].

The general structure diagram of high power charger is as shown in the figure 2. At first the input AC supply is rectified into DC with the help of Rectifier circuit. The rectifier used can be either controlled or uncontrolled one. The rectifier itself can be either half wave or bridge type rectifier. This rectifier is then connected to filter circuit and then to the DC-DC converter. Finally, battery is connected to the system.

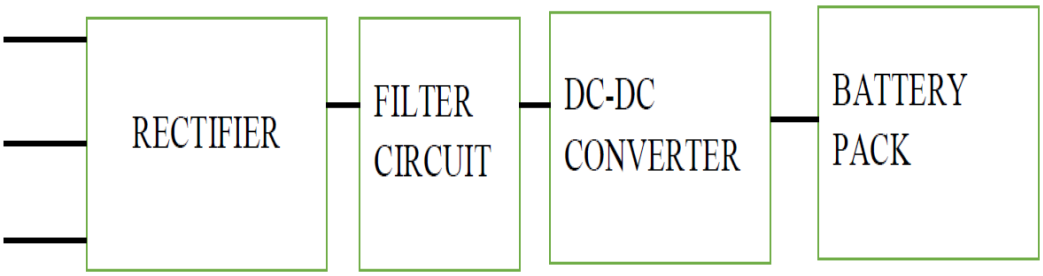

Figure 2: Block Diagram of Battery charger circuit

However, in this simulation study we have not taken the DC-DC converter and simply made the charger circuit and simulation was done.

4. Methodology

STEP 1: Completion of literary review and figuring out in steps the exact method of accomplishing the project.
STEP 2: At first the only one single phase EV battery charger circuit is modelled in Matlab/Simulink. The THD introduced by such charger is studied.
STEP 3: Then after the only one three phase EV battery charger circuit is modelled in Matlab/Simulink. THD introduced due to such charger is also studied.
STEP 4: Then after the distribution feeder feeding different charging station is modelled in the matlab.
STEP 5: For purpose of study, at a time multiple single phase EV chargers only is then charged through this distribution system. And then the current and the harmonics is checked and analyzed. From the result we can compare what will be the significant change in the harmonic distortion as we go on increasing the number of similar type of charger in parallel.
STEP 6: Similarly, at a time multiple three phase EV chargers are then charged through this distribution system. The THD study is made. And then the current and the harmonics is checked and analyzed. From the result we can compare what will be the significant change in the harmonic distortion as we go on increasing the number of similar type of charger in parallel.
STEP 7: Finally, all the combination of single phase and three phase EV chargers are then simulated in the same distribution system at same time and the harmonic study is carried out. That is we connect the larger number of different charger in parallel and charged by the same source and then the harmonics are studied. After checking the result, we can come up to the solution to make the supply side harmonics free
STEP 8: If harmonics still remains present and is not within the acceptable limits filter circuitry must be designed.

5. Results and Discussion

i. Single Phase Charger(*Bridge)*

At first we will see what will be the case when we take only one phase being connected to charger. The battery nominal voltage is adjusted to 50VDC and the system line to line voltage is 200V AC. Here the remaining phase are at no load. This is done only for study purpose. The following results were obtained while simulating this system for 30seconds.

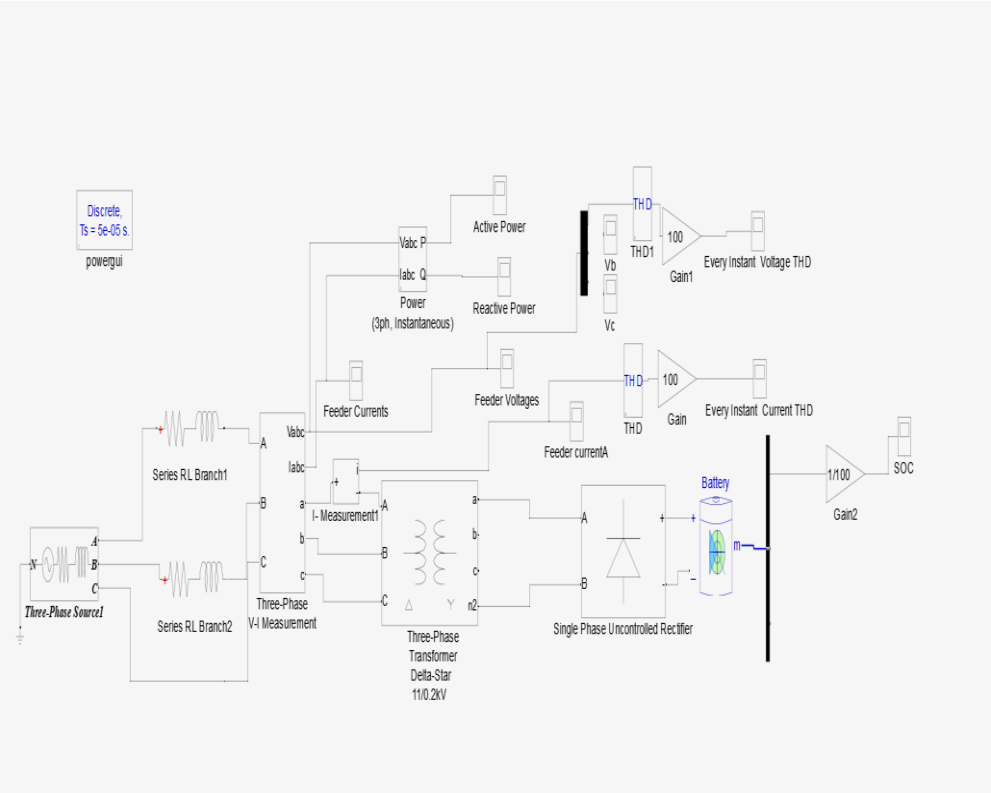

Figure 3: Single phase bridge EV charger

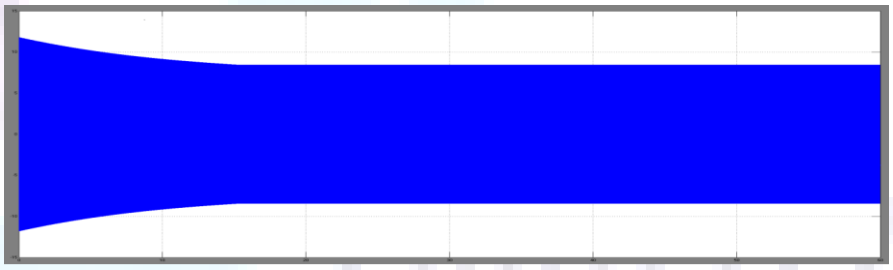

Figure 4: Overall current injected by the supply side

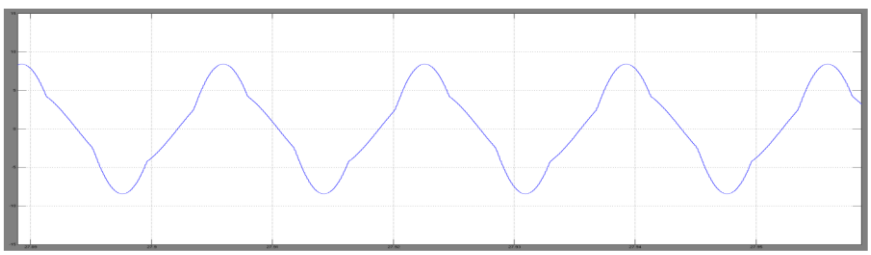

Figure 5: Portion of the supply current

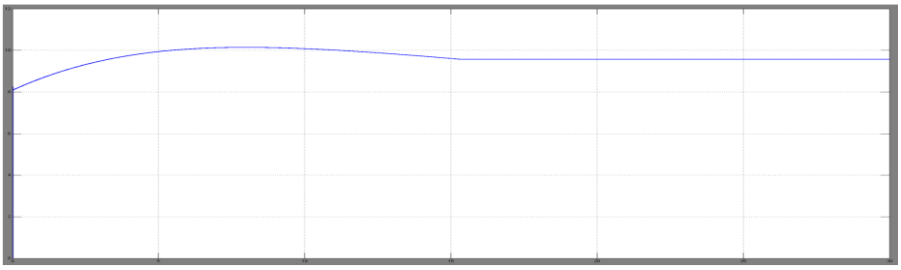

Figure 6: Current THD

Here in this case we can see that the THD has settled down to almost 9.5%. This THD was obtained in Phase A supply current when only that particular phase A was being connected to the charger. Now we will see what will be the case if all the phases are connected to the identical chargers as shown.

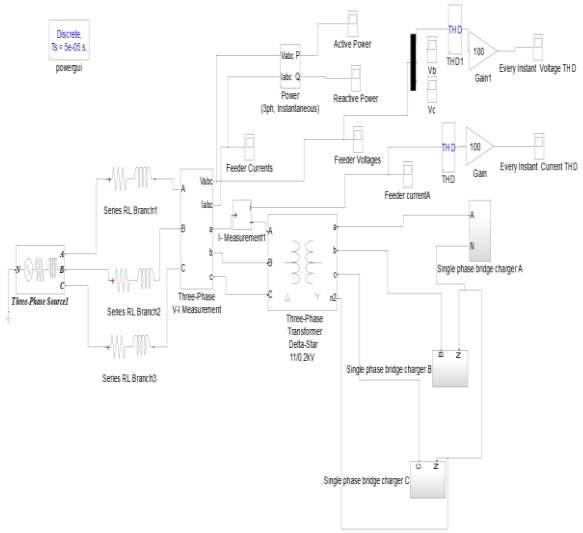

Figure 7: All the phase is connected to single phase bridge type EV charger

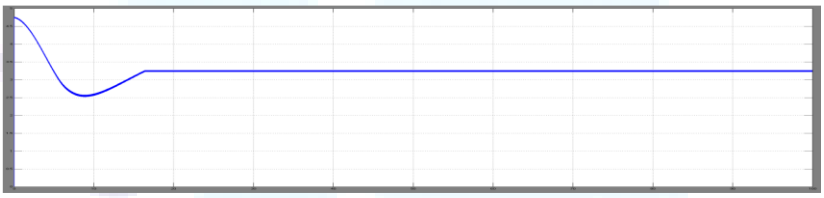

Figure 8: THD of the above simulated system

As we see from the above analysis the THD is drastically improved if the transformer is balanced loaded in each phases. In the first case it was found that THD was almost 9.5 % when only one Phase A was connected. However, in second case when we connected all the phase to the similar charger and it was found that the THD of supply current of Phase was almost 3.3%. This was obtained from the simulation result.

ii. Single Phase Charger (*half wave)*

Here we have connected only one single phase half wave EV battery charger in Phase A, keeping Phase B and Phase-C at no load condition. In next simulation we have considered the balanced loading and analyzed the THD. Similarly, we have again considered the unbalance Single phase chargers being fed by the distribution transformers.

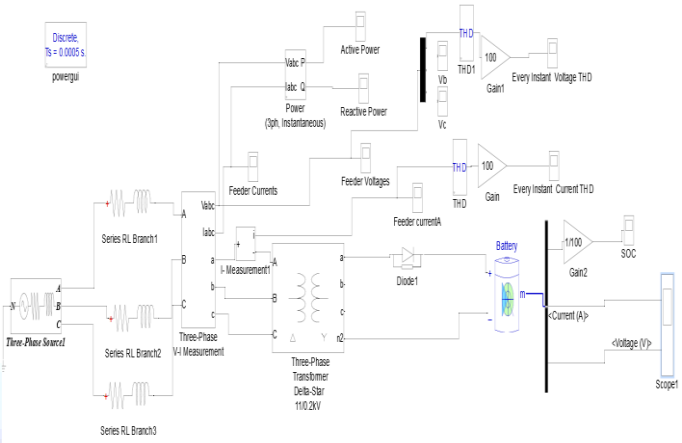

Figure 9: Single Phase Half wave EV battery charger Simulink model

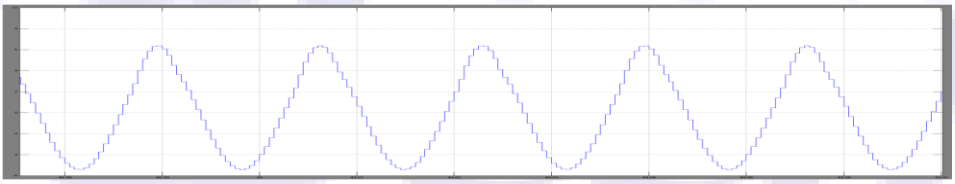

Figure 10: Current Drawn by phase A

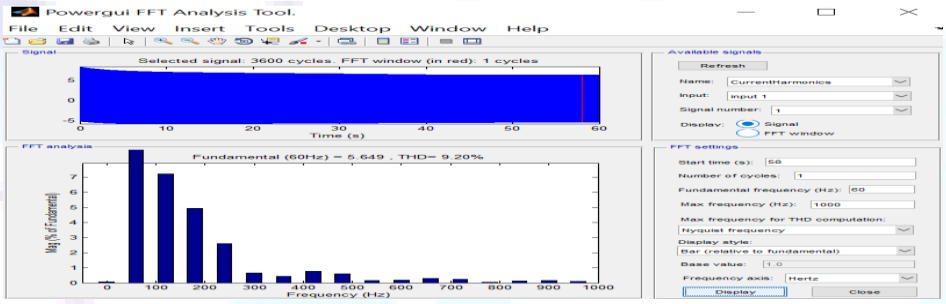

Figure 11: FFT analysis of Current at steady state condition *(***THD=9.20%)**

Now we will again see what will be the case if all the phases are connected to the identical chargers as shown.

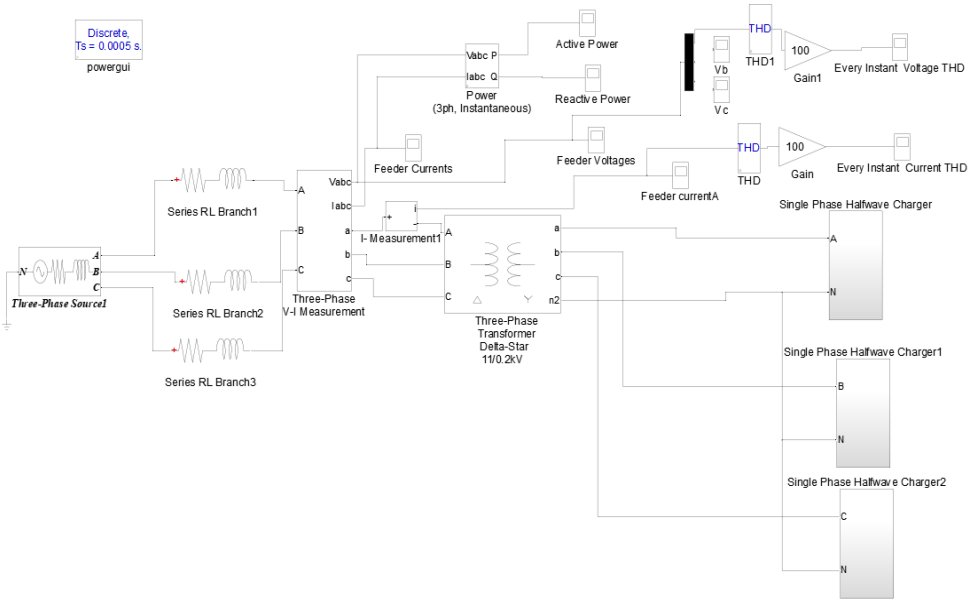

Figure 12: Single Phase Half wave EV battery charger connected in all phases Simulink model

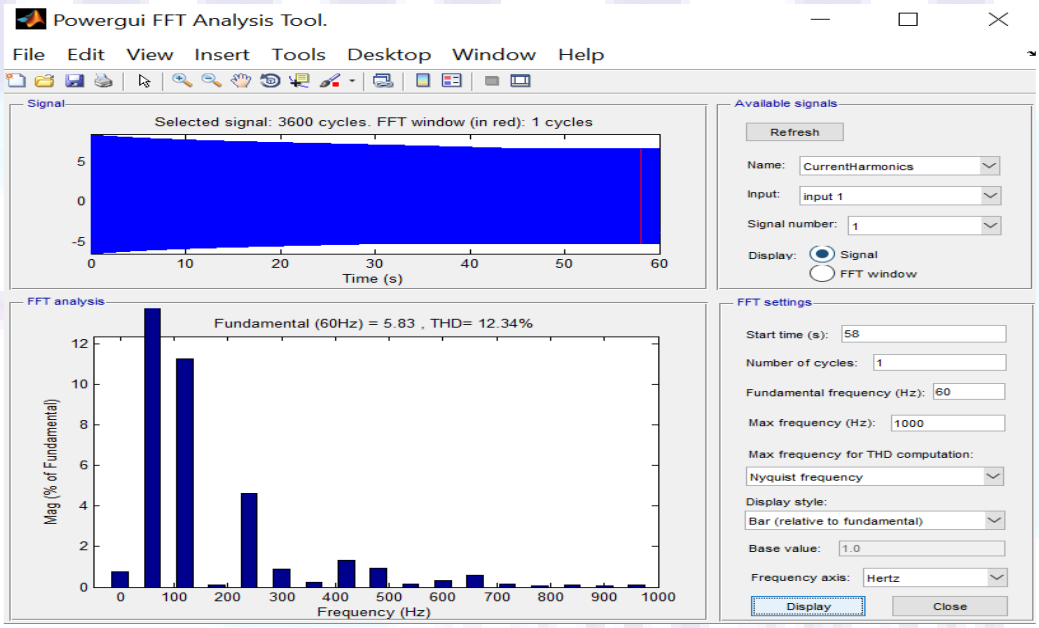

Figure 13: FFT analysis of Phase a Current at steady state condition **(THD=12.34%)**

Comparing this two result THD is slightly increased if we connect identical half wave chargers in all phases.

iii. Multiple single phase charger(bridge) simulation

For studying this, at first balanced loading on each phase of transformer was considered and simulation was carried out. Initially only one EV charger was connected to each phase of the system. After 30sec of the simulation 6 identical charger was connected to the system with the help of breaker. Similarly after 60sec of the simulation another 18 identical charger was again connected to the system. After then THD analysis of current and voltage was done. Some important observation that were obtained are discussed below.

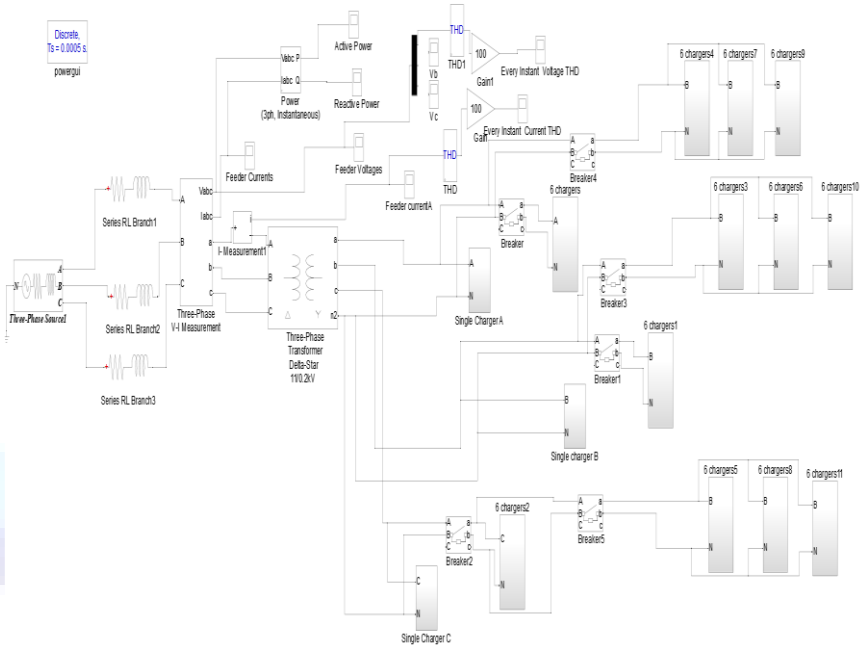

Figure 14: Overall simulation with multiple single phase bridge type charger

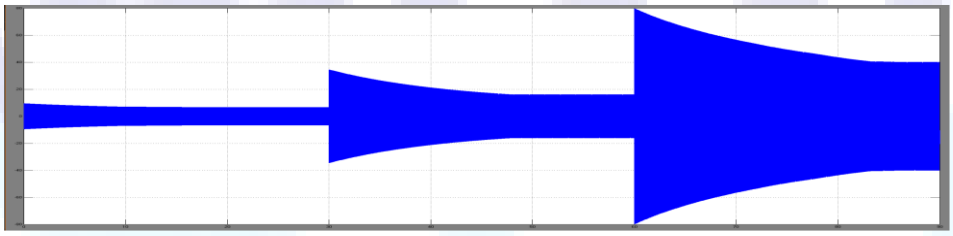

Figure 15: Current waveforms with breaker operation at 30sec and 60sec respectively

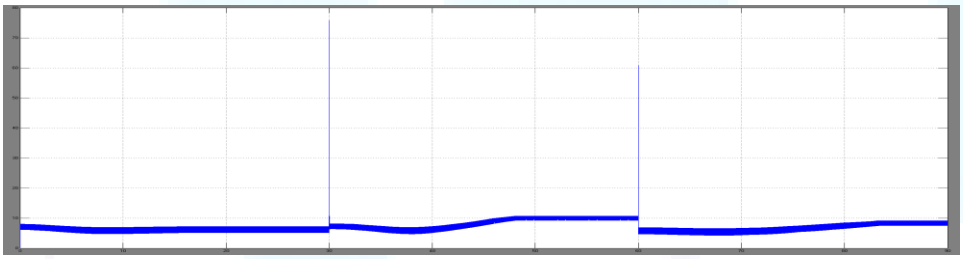

Figure 16: Current THD vs Time with breaker operation at 30sec and 60sec respectively

Here we can see that the THD obtained is about 3.27% when each of the phase was connected to only one bridge charger. However, when the additional 6 identical chargers was connected to the system with help of breaker the THD increased to about 8.23%. Hence this showed that additional charger increased system harmonics to some higher level. But as we go on increasing the additional amount of chargers the result was quite different and current THD began to decrease. That is when additional 18 chargers were connected to the system at about 60sec of the simulation period the THD was drastically dropped down to 6.94%. If we increase additional chargers further, then the THD will obviously reduce from this latter value. However, the voltage THD was obtained to be increased as shown in the figure below. This was also due to the fact that the SOC of chargers were different during breaker operations.

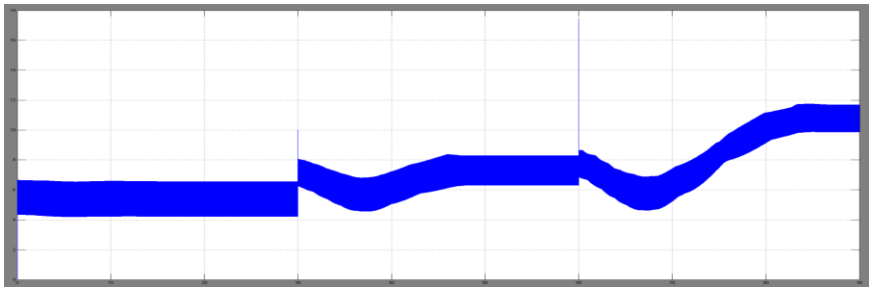

Figure 17: Voltage THD variation with time

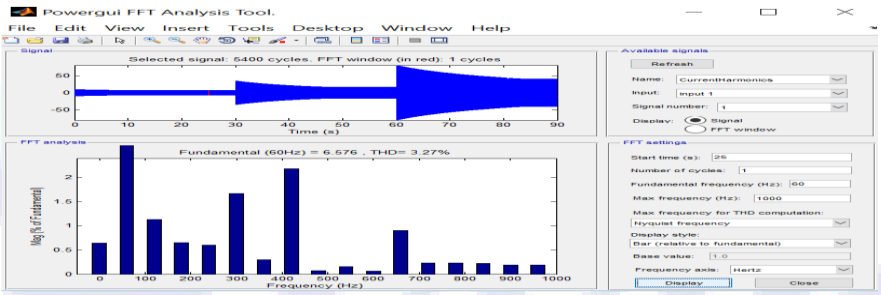

Figure 18: FFT of the supply current with only one EV charger

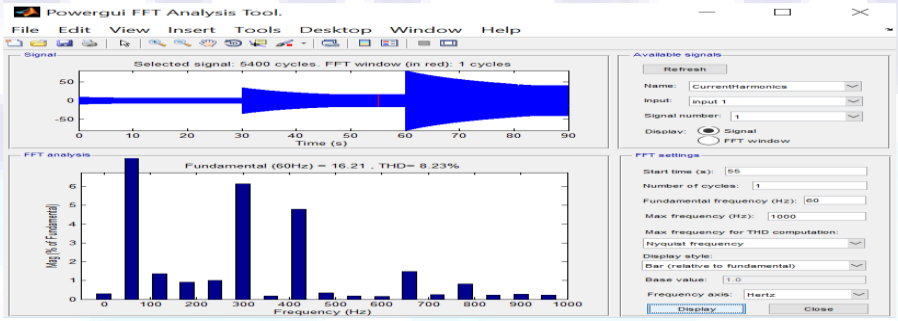

Figure 19: FFT of the supply current with 7 EV charger with additional 6 charger connected at 30sec

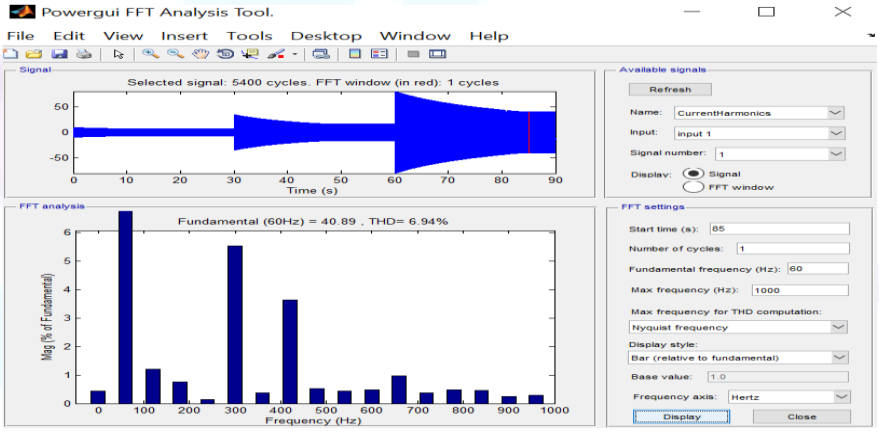

Figure 20: FFT of the supply current with 25 EV charger with additional 18 charger connected at 60sec

Now if we consider the unbalanced loading in this same case we obtained the following results.

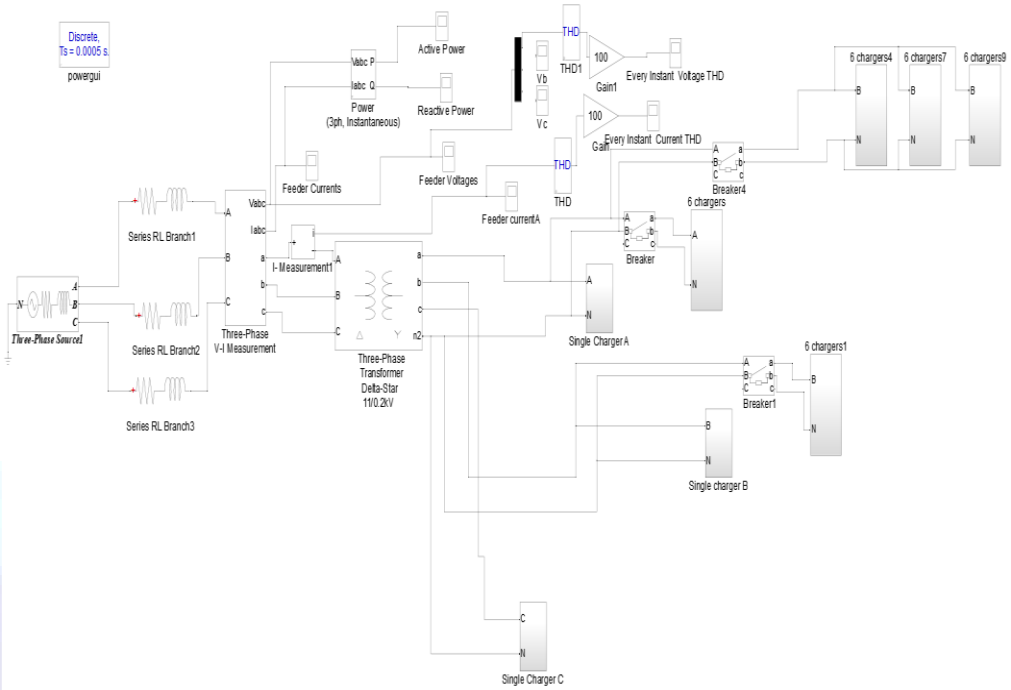

Figure 21: Simulation of bridge type single phase charger with unbalanced loading of EV chargers

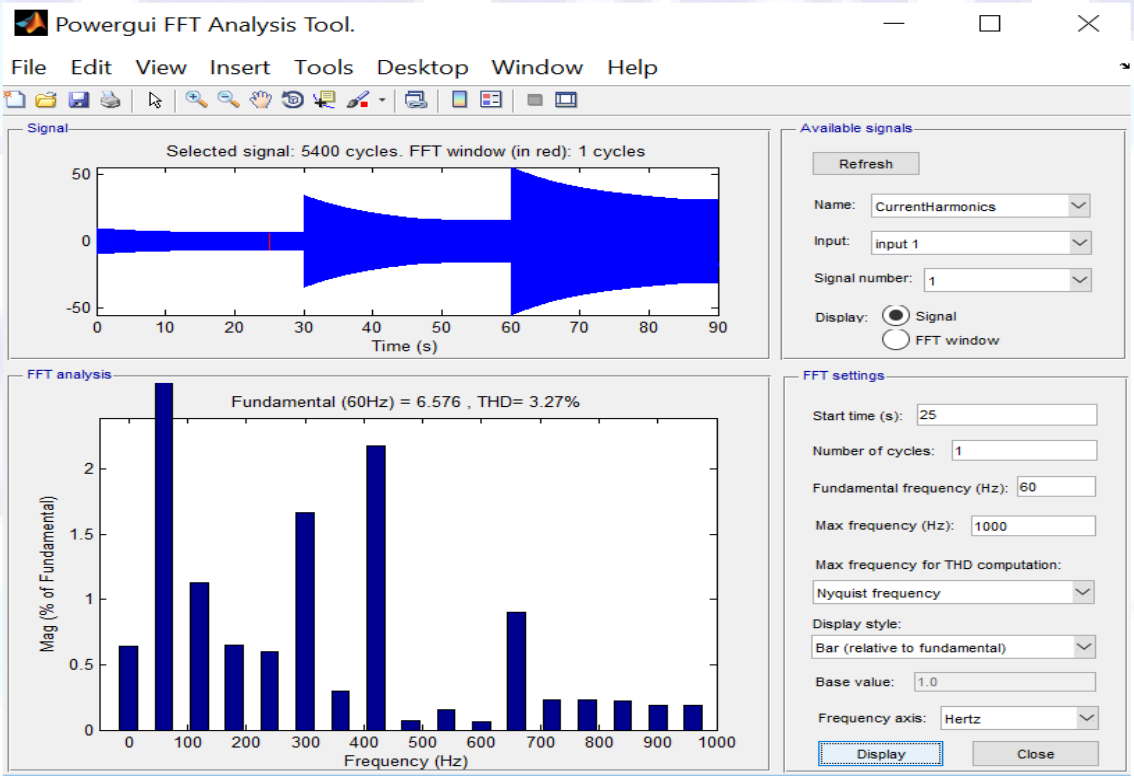

Figure 22: FFT analysis with 3 identical chargers in each phase

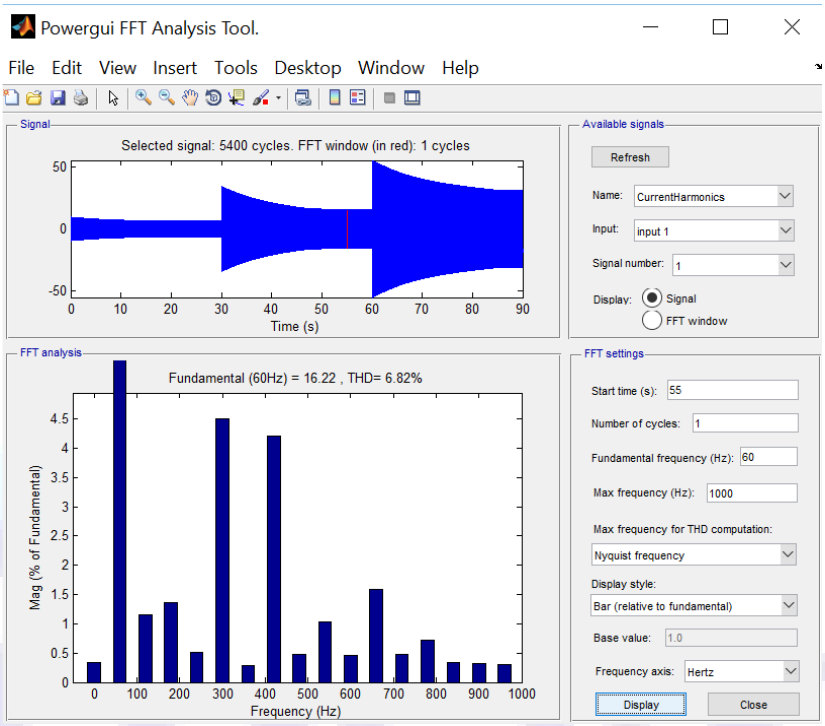

Figure 23: FFT analysis with additional 6 chargers in Phase A and Phase B and no change in Phase C i.e. Unbalanced Loading

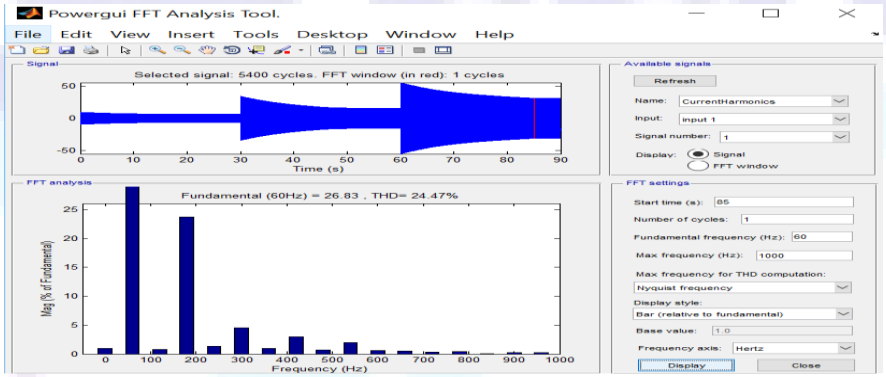

Figure 24: FFT analysis with additional 18 chargers in Phase A and additional 6 chargers in Phase B and no change in Phase C i.e. Unbalanced Loading

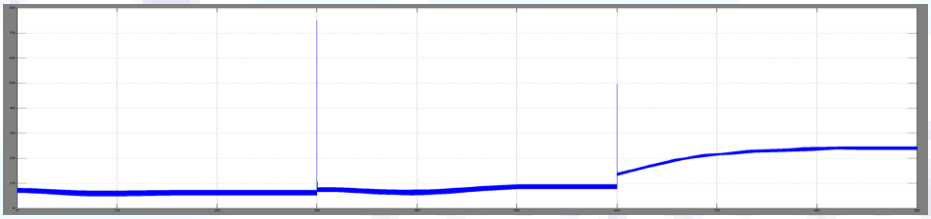

Figure 25: Current THD variation of PHASE A for the above given simulation diagram

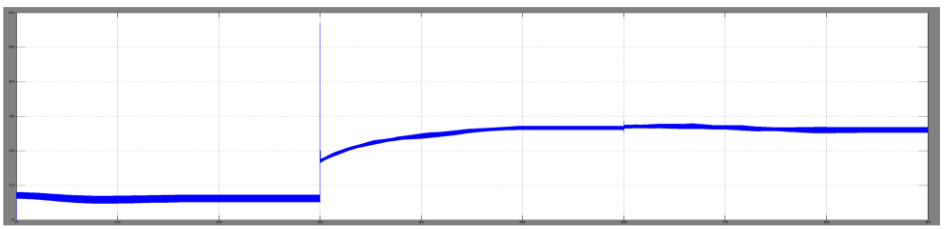

Figure 26: Current THD variation of PHASE B for the above given simulation diagram

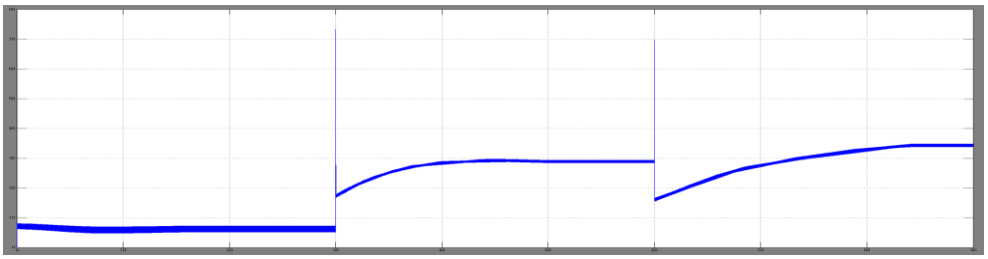

Figure 27: Current THD variation of PHASE C for the above given simulation diagram

Hence from the above observation we can see that in case of an unbalanced loading the THD is likely to be increased in the lightly loaded phase. Here in this case the Phase C is lightly loaded and hence the current THD of the phase C is also drastically increased. The Current THD in the individual phase are as shown as obtained from the FFT analysis and above.

THD at Phase A= 3.27 %, when All Phase Balanced. THD at Phase A= 6.28 %, unbalanced case when phase A and B equally loaded. THD at Phase A= 24.47 %, unbalanced case when Phase A is heavily loaded. THD at Phase B= 3.27 %, when All Phase Balanced. THD at Phase B= *25.31*%, unbalanced case when phase A and B equally loaded. THD at Phase B=24.88%, unbalanced case when Phase A is heavily loaded. THD at Phase C=3.23%, when All Phase Balanced.

THD at Phase C=28.13%, unbalanced case when phase A and B equally loaded.

THD at Phase C=*34.70* %, unbalanced case when Phase A is heavily loaded.

This showed THD is also highly dependent on the balanced condition. Unbalanced condition detoriates the THD of the lightly loaded phase in this case.

iv. *Multiple single phase charger (half wave) simulation*

Here we simulated the single phase half wave EV charger in all the phases. At first until 50sec only one EV charger is connected in the individual phases. After 50sec additional 6 chargers are connected in the each of the phases. Similarly, at the 70 sec of simulation period additional 18 chargers were connected to the distribution transformer for study purpose. The harmonic during this stated period are shown in the figures below under this heading.

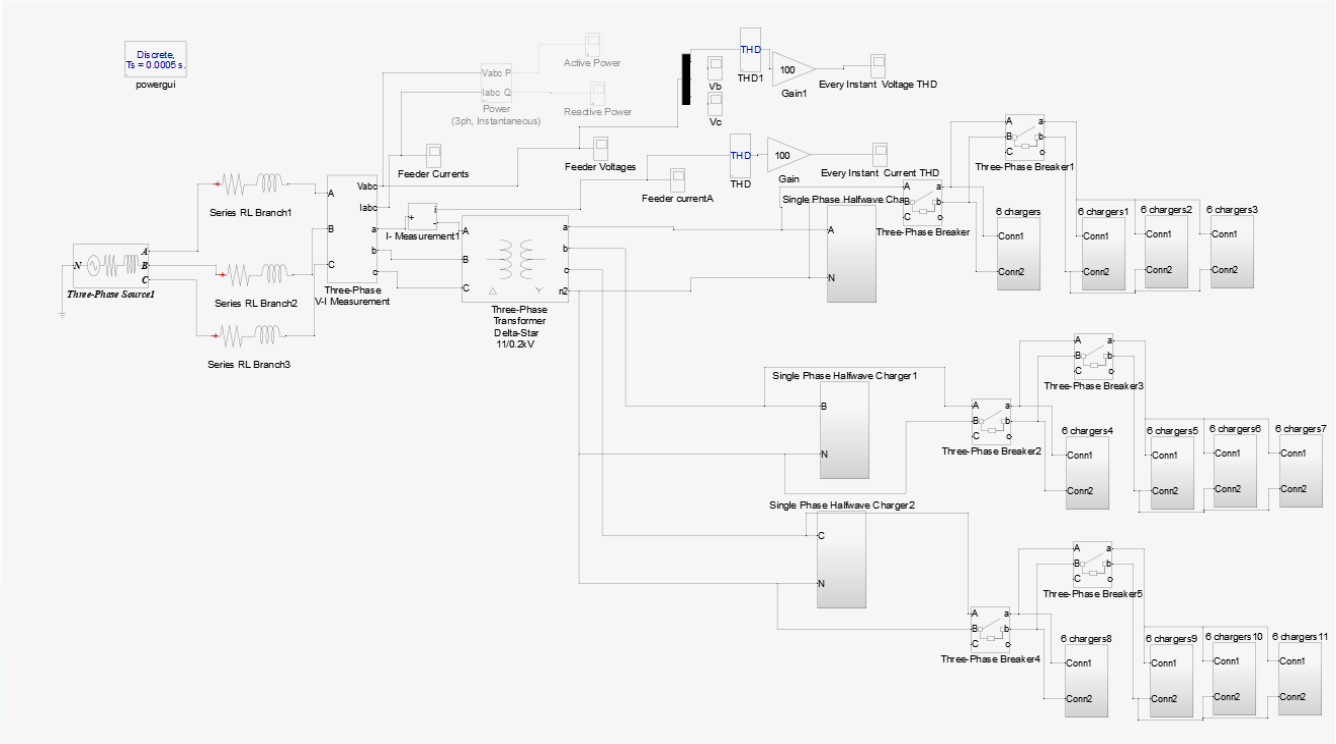

Figure 28: Simulation of Multiple halfwave type single phase charger with balanced loading of EV chargers

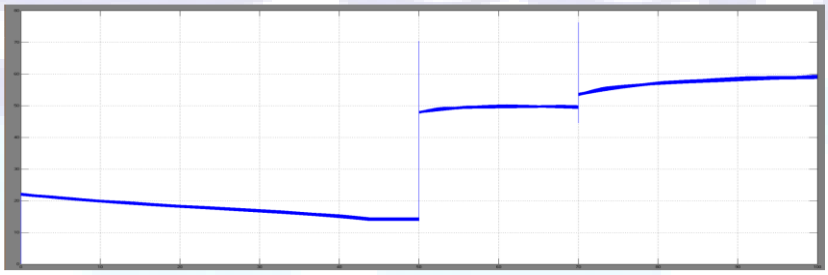

Figure 29: THD of the Phase A current when breaker operates at 50sec and 70sec

Here we can see that the current THD is increased when the number of Half wave EV chargers operating in parallel is increased gradually.

i. Combined multiple single phase charger(Halfwave and Bridge) Simulation

Here under this we have simulated the combined half wave and full wave single phase EV battery charger. For this at first all the three phases are connected with 6 full wave battery charger. After 30sec of the simulation period another 6 numbers of half wave chargers are introduced in the system. Finally at 100sec of simulation study we have again introduced 6 bridge rectifier and 6 half wave rectifier in parallel. That is at 100sec of simulation study we have altogether 12 full wave chargers and 12 half wave chargers being connected to the each of the phases. The simulation results are also shown below.

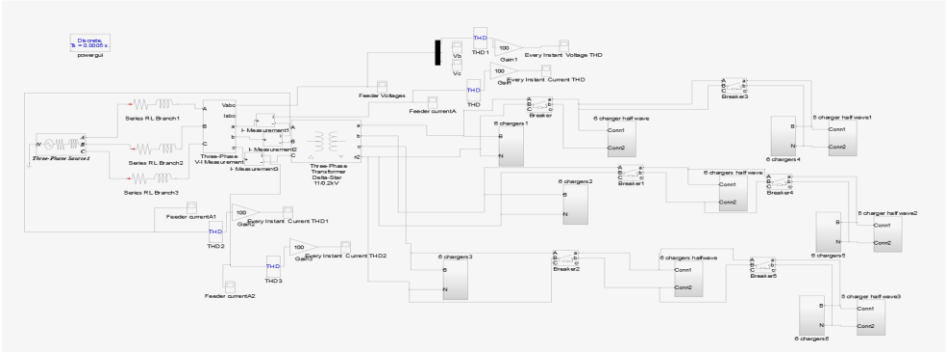

Figure 30: Combined Full wave and Half wave single phase EV battery charger

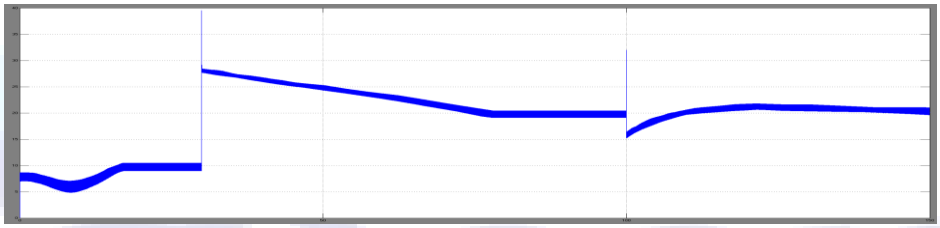

Figure 31: Phase A Current THD variation with time

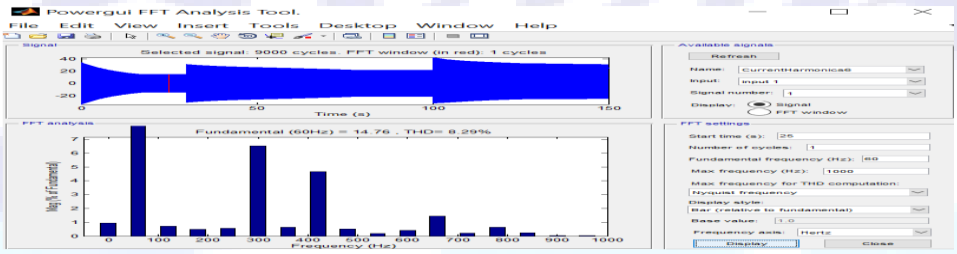

Figure 32: FFT due to 6 full wave chargers connected on each phase

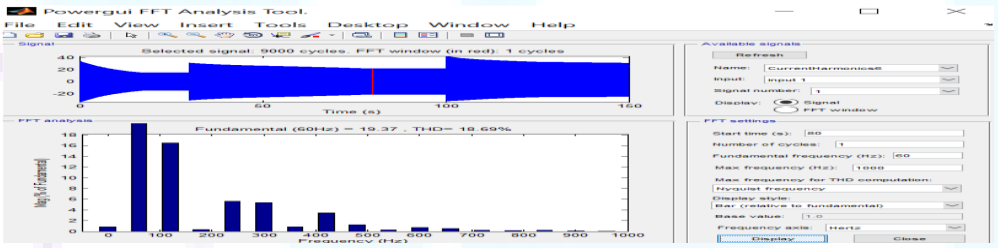

Figure 33: FFT due to 6 full wave chargers and additional 6 half wave chargers connected on each phase at 30sec

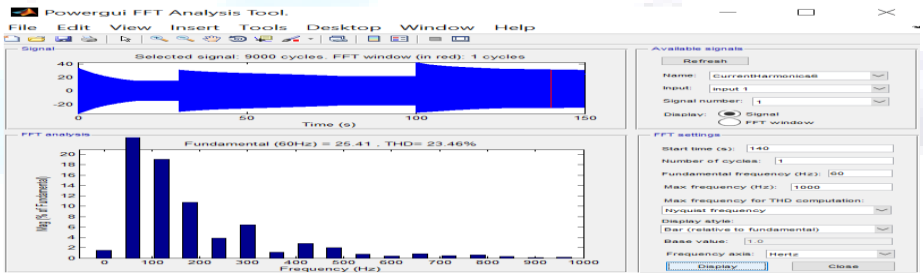

Figure 34: FFT due to additional 6 full wave chargers and additional 6 half wave chargers connected on each phase at 100sec (Total chargers 12 half wave and 12 full wave)

Hence this result showed that the THD is increased if we incorporate the half wave chargers in the system which has previously use full wave single phase chargers. Or in other words the THD rises if both single phase

chargers (half wave and full wave) are more in the system. Here the final value of THD is about 23.46% when the 12 half wave and 12 full wave chargers are operated simultaneously at about 100sec.

ii. Single Three phase charger Simulation

Here the line to line voltage of system considered is 200V AC and battery nominal voltage is 50V dc.

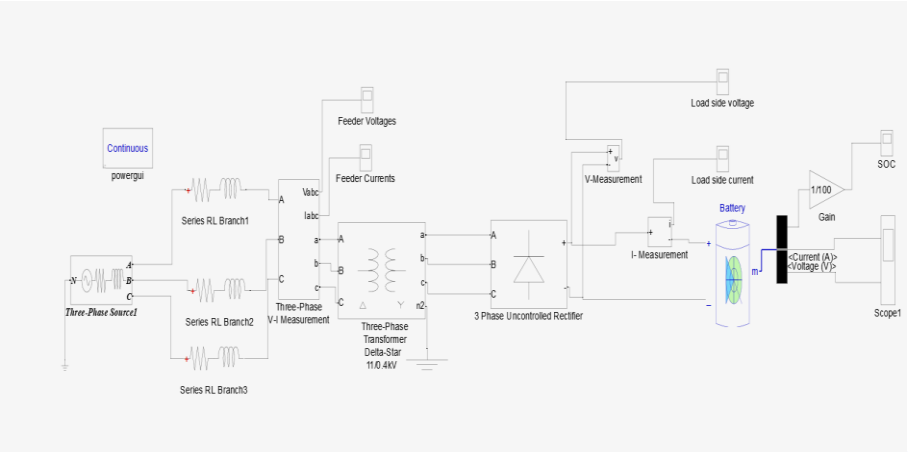

Figure 35: Simulink model of Battery charger with uncontrolled rectifier

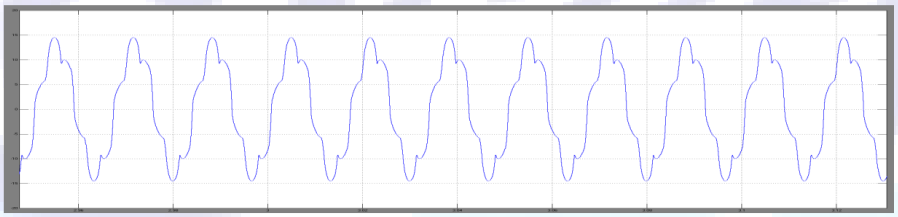

Figure 36: HV side Current Vs Time

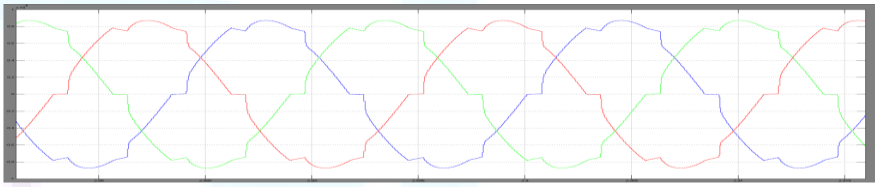

Figure 37: Feeder Voltages Vs Time HV side

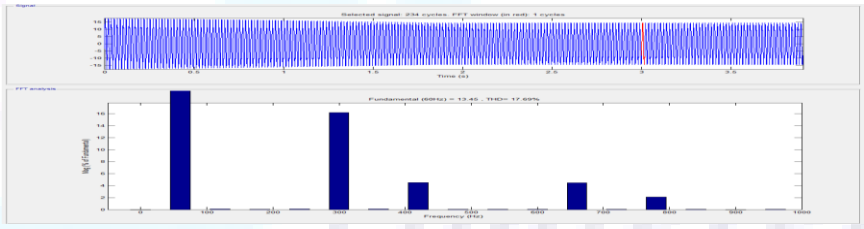

Figure 38: FFT Analysis of injected current of three phase uncontrolled battery charger circuit

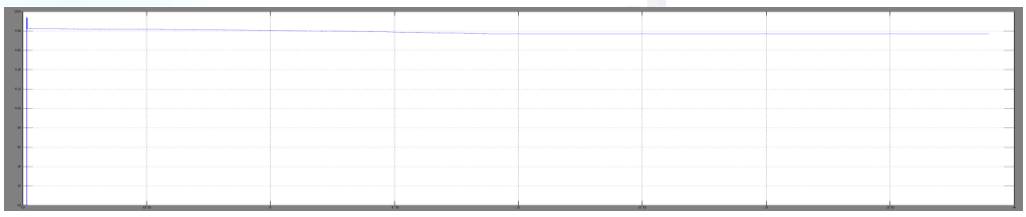

Figure 39: THD Variation with time

From this we can see that THD is **17.69%** when only one three phase bridge type EV charge is connected to the supply.

For studying this, at first only one three phase bridge type charger was connected to the distribution transformer. Then after 4sec of simulation additional 2 EV chargers were connected to the system with the help of Breaker. Similarly, after 8sec of simulation additional 20 EV charger were brought into the system with the help of the three phase breaker. And again after 16sec of simulation additional 20 EV charger were connected. That is at 16sec the system was serving altogether of 43 EV chargers. The simulation results are discussed here below.

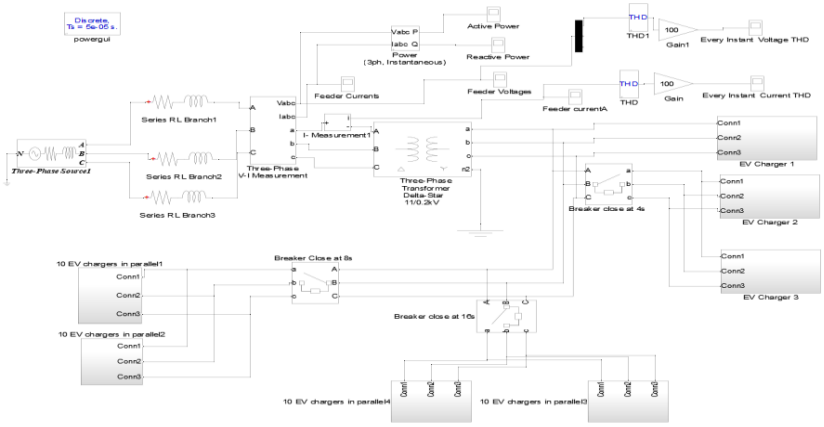

Figure 40: Overall Simulation with Multiple 3 Phase EV charger

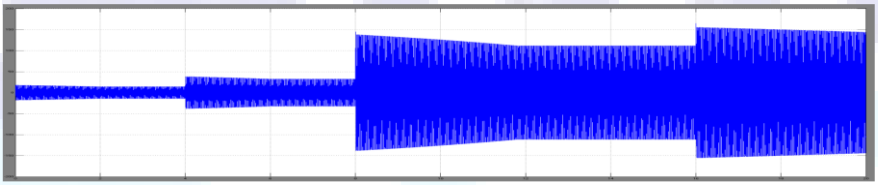

Figure 41: Current waveform with breakers operation at 4s, 8s and 16s respectively

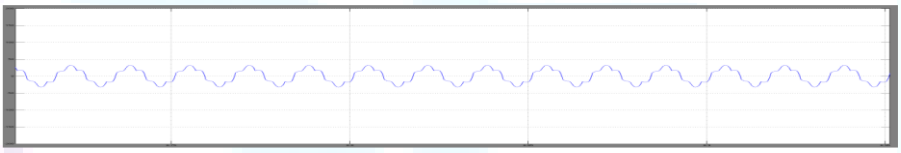

Figure 42: HV side Current Vs Time with 3 EV chargers

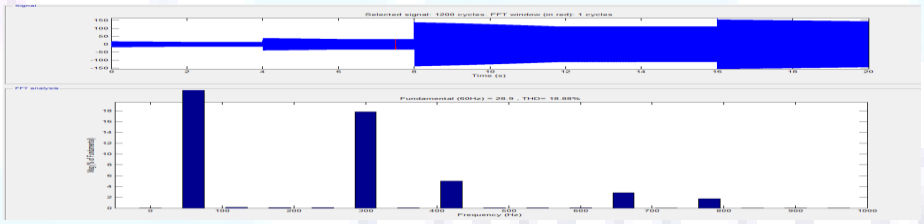

Figure 43: FFT Analysis of injected current of Multiple EV charger for breaker operation beyond 4s with all total 3 EV chargers in operation

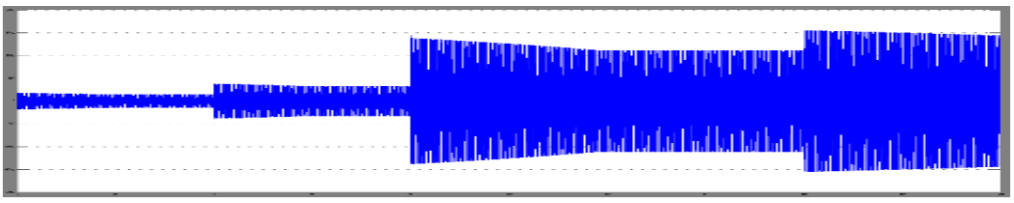

Figure 44: Portion of HV side Current Vs Time with 23 EV chargers and breaker closed at 8s

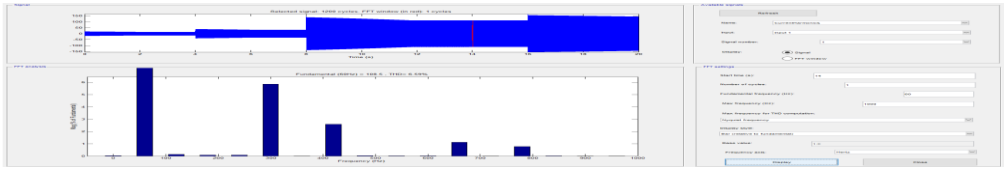

Figure 45: FFT for breaker operation beyond 8s for 23 EV chargers

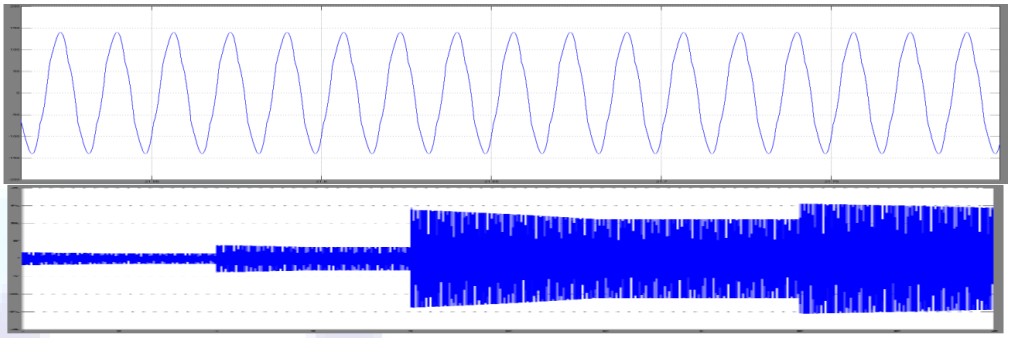

Figure 46: Portion of HV side Current Vs Time with 43 EV chargers and breaker closed at 16s

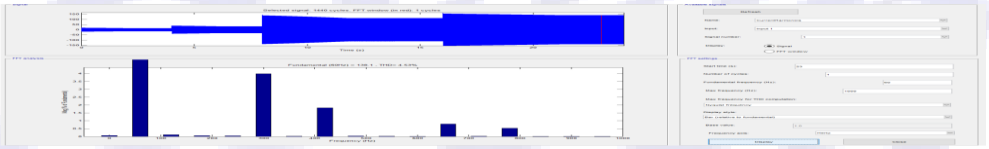

Figure 47: FFT for breaker operation beyond 16s for 43 EV chargers

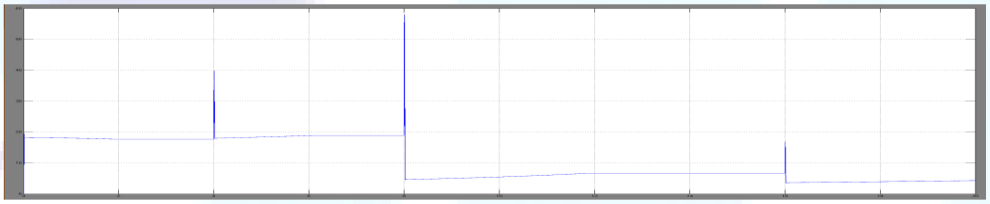

Figure 48: Current THD variation with time with breaker operation at 4s, 8s and 16s respectively

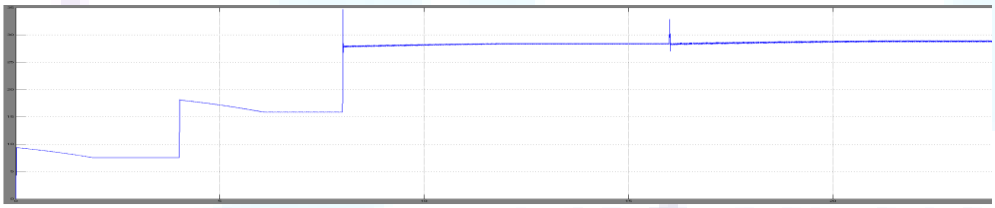

Figure 49: Voltage THD variation with time with breaker operation at 4s, 8s and 16s respectively

Here in this case we found that initially when only one three phase charger was connected to the system the supply current THD was about 17.8%. Now when the additional two EV chargers were connected at 4sec the THD was increased slightly to 18.88%. Similarly, when additional 20 EV chargers were again brought into the system through help of breaker the THD dropped down to 6.69%. This THD was again dropped to 4.53% when additional 20 EV chargers were further brought into system at 16sec of simulation. Hence we can say that current THD was decreased with the increase in number of EV chargers when the state of being charged was different.

iii. Combined single phase and three phase charger simulation

Here up to 16 second 43 three phase EV charger are connected to the system. For this we have already studied the harmonic behavior in the previous section. But here we again introduced the single phase chargers at the period of 22 sec. About 6 half wave chargers and 6 full wave chargers were introduced in the system. This was done only to see the effect that can be introduced by the single phase chargers on THD when they are combine operated with the three phase chargers.

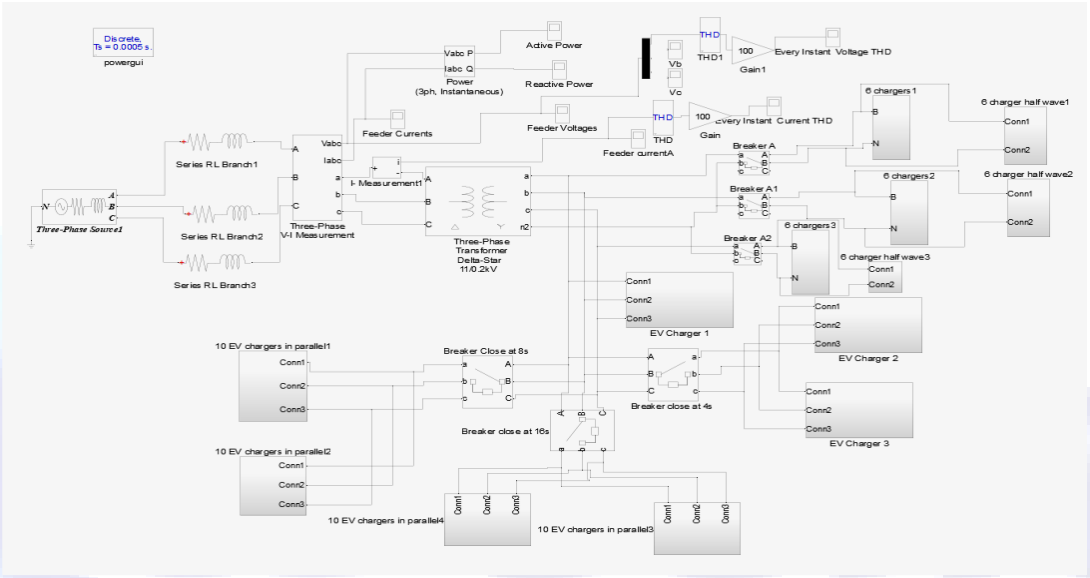

Figure 50: Combined operation of single phase and three phase EV chargers

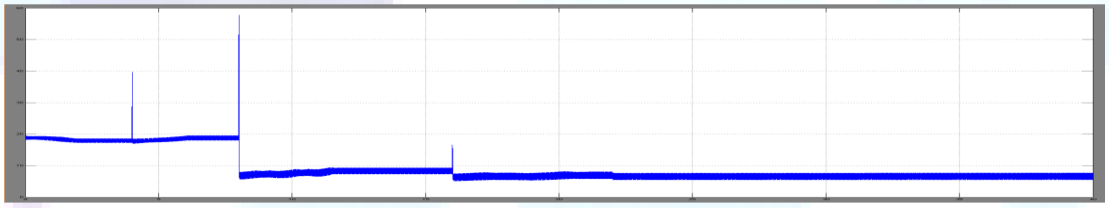

Figure 51: Current THD vs time of phase A

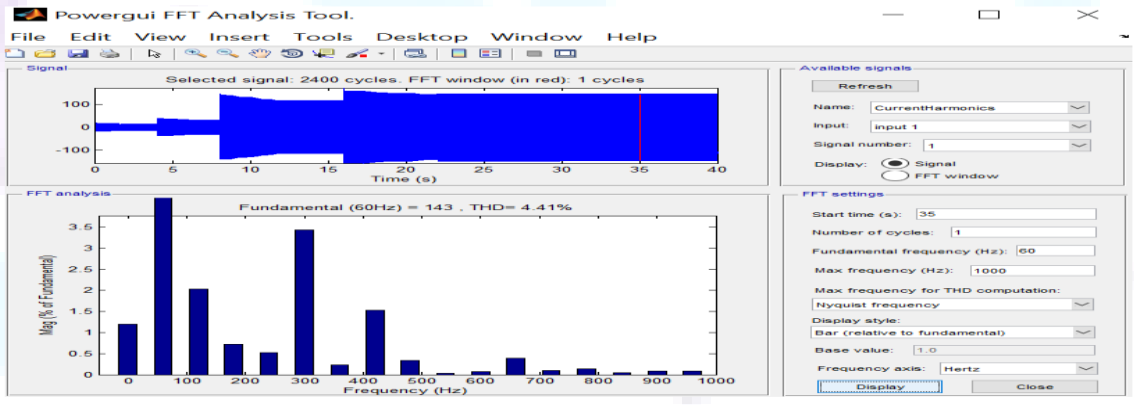

Figure 52: FFT analysis for the given simulation study

Here we can see introducing the single phase chargers where there are more number of 3 phase chargers have almost negligible effect in THD variation. Since 3 phase chargers are more in this case the THD variation is not more due to more cancellation effect introduced by this charger.

6. Conclusion

From this above results we can conclude that the current THD is dependent upon the type of chargers involved. And also it was noted that in case of three phase charger, increasing the number of charger at certain intervals of simulation period tends to decrease the THD. As this was obtained because of the fact that the SOC of new incomer charger will be different than the previously charged one. Hence in this case the the current harmonics will not be just the algebraic sum but involves the consideration of of both the magnitudes and phase angles of individual harmonic components. Hence due to this Harmonic phase cancellation effect will take place. Also it was noted that if the number of single phase half wave chargers were introduced in the system THD level rises. Depending upon the loading condition, the type of chargers involved, the nominal voltage level of battery, the voltage level of supply and the SOC of the batteries involved the THD can vary.

References

[1] J. C. Gomez and M. M. Morcos, "Impact of EV battery chargers on the power quality of distribution systems," IEEE Trans. Power Delivery, vol.18, pp. 975-981, July, 2003.

[2] Yanxia Lu and Jiuchun Jiang, "Harmonic-study of electric vehicle chargers," 2005 IEEE International Electrical Machines and Systems Conf., vol. 3, pp. 2404-2407, Sep, 2005.

[3] Yanxia Lu, Xiumin Zhang, and Xiaowen Pu, "Harmonic Study of Electric Vehicle Chargers," Proceedings of the CSU-EPSA, vol. 18, pp. 51-54, June, 2006.

[4] C.C. Chan and K.T. Chau, "An overview of power electronics in electric vehicles," IEEE

[5] Transactions on Industrial Electronics, Vol. 44, No. 1, February 1997, pp. 3-13.

[6] Zhensheng Chen, "Harm of Harmonic in Power Supply System and Suppressing Technique,"Electric Switchgear. vol. 6, pp.1-5, Nov, 2003.

[7] Aiqiang Pan,Yongwei Zhu, "Harmonic Research of Electric Vehicle Fast Chargers"2016 IEEE PES Asia-Pacific Power and Energy Conference.

[8] Joao P. Trovao and Paulo G. Pereirinha, Leonor Trovao and Humberto M. Jorge"Electric Vehicle Chargers Characterization:Load Demand and Harmonic Distortion"

[9] Lauri Kutt, Eero Saarijarvi, Matti Lehtonen"Electric Vehicle Charger Load Current Harmonics variation due to supply voltage level differences-Case Example"

[10] Agustin Andres Malano, Sascha Muller, Jan Meyer"Harmonic Interaction of Electric Vehicle Chargers in a Central Charging Infrastructure".

Part VIII: Applied Sciences

Design Modification, Fabrication and Testing of Hydraulic Ram Pump: A Case Study of Kalleri, Dhading

Chiranjivi Dahal[1], Ganesh Gajurel[1], Suraj Shrestha[1], R.B. Adhikari[1], R.K. Chaulagain[1]

[1]*Department of Automobile and Mechanical Engineering, Thapathali Campus, IOE, TU, Kathmandu, Nepal*

dchrennp@gmail.com

Abstract

A hydraulic ram is a cyclic water pump powered by water power. The objective of study was to find the existing problem, so as to increase the overall efficiency and delivery flow rate of the ram pump. The methodology included analysis of the field data, design modification in existing pump and testing of new pump. A site at Kalleri, Dhading was chosen for the designing parameter. Implementing the design modification, the modified ram pump was fabricated. The testing of modified ram pump was carried out at Kalleri, where existing pump was running with 82.88% hydraulic efficiency with 200 liter/minute drive flow. This pump was delivering 633 kiloliters of water monthly. The modified pump with drive flow of 200 liters per minute had shown hydraulic efficiency of 84.9%, delivering 648 kiloliters of water monthly. The test was carried out in dry season with lower drive flow rate of 200 liters per minute than the designed one of 265 liters per minute. Thus, efficiency can be increased if the pump will be tested at drive flow greater than 200 liters per minutes.

Keywords: *flow rate, efficiency, modifications, water power*

1. Introduction

A hydraulic ram uses water power to operate. It takes in water at one hydraulic head (pressure) and higher flow rate, and outputs water at a higher hydraulic head and lower flow rate. The device uses the water hammer effect to develop pressure that allows a portion of the input water that powers the pump to be lifted to a point higher than where the water originally started. It is very useful in places where water volume requirement is not large and electrical power is unavailable because power required to operate pump is only kinetic energy of water itself. A hydraulic ram is a structurally simple unit consisting of two moving parts. These are the impulse valve (or waste valve) and the delivery (check) valve. The unit also consists of an air chamber and an air valve. The operation of a hydraulic ram is intermittent due to the cyclic opening and closing of the waste and delivery values. The closure of the waste valve creates a high pressure rise in the drive pipe. The high pressure inside the pump system forces fluid to pass through one-way delivery valve. An air chamber is required to transform the high intermittent pumped flows into a continuous stream of flow. The air valves allow air into the hydraulic ram to replace the air absorbed by the water due to the high pressure and mixing in the air chamber. After the pressure inside the system falls to normal the waste valve reopens.

The study was aimed at understanding the working of ram pump and its characteristics. Different sizes of

pumps installed at different sites were studied and analyzed. Problem finding as well as data collection were done during field visits. Data analysis was carried and compared to standard data and values. After the analysis, a modified design is given to address the problems and minimize losses. Section 3 covers the problem identification and section 4 covers the results of modified design.

2. Literature Review

Whitehurst [1] for the first time in 1775 invented ram which operated manually by the opening and closing of the stopcock. This hydraulic ram was able to raise water to a height of 4.9m. The first automatic hydraulic ram was invented by Montgolfier [1] in 1796 for raising water in his paper mill. His work was improved upon by Pierce [2] , who designed the air or sniffer valve to introduce air into the air chamber and this hydraulic ram, which is 300 mm in diameter is reported to have pumped 1700 l/min to a height of 48m. Easton and James [3] were the first to produce hydraulic rams

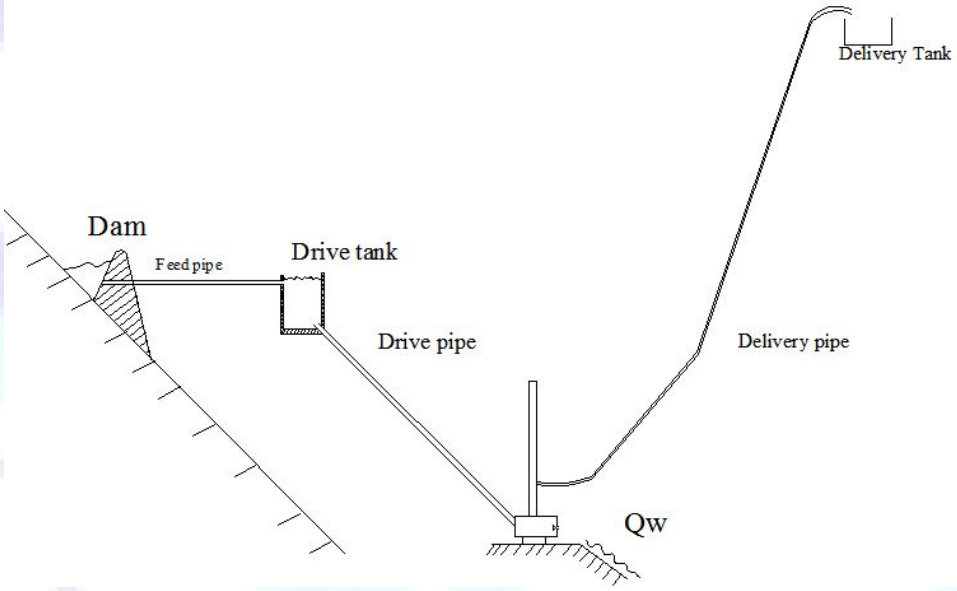

Figure 15: Ram Pump working cycle

in large scale for commercial purpose. Their rams were used for supplying water to large country houses, farms and village communities. A general description of the hydraulic ram which solved most of the design problems was undertaken by F. Molyneux. [4] He had used impulse valve which was a weighted rubber ball, and would be very difficult to tune.

Working instructions and drawings on how to construct a small, simple hydraulic ram from commercially available water pipe fittings has been given by V.I.T.A., USA. [5] The ram described had a supply head H= 6.5 m, delivery head h = 14 m, supply discharge Q= 35litres/min, delivery discharge q = 7litres/min. It is thus only used for small water supplies. The impulse valve is designed to act on a sprung mechanism; the delivery valve is a simple clack valve. In Nepal United Mission for Nepal established Development and Consultancy Services (DCS) developed ram pump based water supply schemes during the 1980s [6]. Between 1983 and 1989, sixteen schemes to supply water for domestic use were installed using DCS 'sown design of locally manufactured ram pump.

3. Methodology

The parameter such as drive pipe length, delivery pipe length, drive head, and delivery head can be classified as pump input parameter. These parameters vary according to size of pump and they were collected through field visits to particular site. The technique used for flow measurement was bucket method. Similarly, head measurement was done by level pipe method and length of pipe was measured by measuring tape. The input parameter discussed above for different site are shown in table below:

Table 3: Pump Input Characters

S.N.	Site name	Pump size (inch)	Drive head H, (m)	Delivery head ,h (m)	Drive pipe length (m)	Delivery pipe length (m)
1.	Kalleri	3	5	56.5	30	550
2.	Balthali	4	3	43.0	25	150
3.	Sankhu	3	4	80.0	22	350
4.	Bhimtar	1	6	45.0	30	400
5.	Sera	4	3	30.0	25	120

Drive flow and delivery flow are the parameters that are obtained after pump runs and certain mechanical work is done on pump. The **Table *4***: Pump output *Characters* Table ***4*** shows the pump output characters. These data were obtained from field visits to particular sites.

Table 4: Pump output Characters

S.N.	Site Name	Drive Flow, Q (LPM)	Delivery Flow, q (LPM)	Volumetric Efficiency	Overall efficiency	Power (W)
1	Balthali	603	26.00	4.31%	60.36%	295.9
2	Sankhu	251	9.00	3.59%	70.82%	164.2
3	Kalleri	265	20.00	7.55%	83.02%	216.7
4	Bhimtar	22	1.43	6.50%	45.50%	21.6
5	Sera	650	36.00	5.54%	66.46%	318.8

The overall efficiency (also called hydraulic efficiency) of a better pump lie in between 70-80 % theoretically [7]. Table 2 clearly shows that most of the pump are running satisfactorily. But only a single pump of Kalleri could be said as performing well with 83% efficiency. With same design parameters and manufacturing techniques other pumps with below 80% efficiency could be increased if all the installation parameters are revised before installing on the site. Factors those effect the efficiency of pump are head ratio, flow ratio, and condition of pump itself.

Table 5: Flow ratio and head ratio for various sites

S.N.	Site Name	Pump Chamber Size	Flow ratio (Q/q)	Head Ratio (H/h)
1	Balthali	4"	23.0	14.3
2	Sankhu	3"	27.8	20.0
3	Kalleri	3"	13.3	6.9
4	Bhimtar	1"	15.4	7.5
5	Sera	4"	18.0	10.0

With the data analysis obtained from field visits, following were the conclusions obtained:

1. The delivery pipe used was polyethylene pipe. So, at many sites, pipes were found with bends and coiling at several lengths. These bends are responsible for the head loss and eventually pump performance.
2. The inlet geometry in the pump body was found to be with sudden enlargement comprising to remarkable head loss. The delivery flow is directly related to the pressure developed in the pump chamber and same is the relation of pressure to the drive head. So, the drive head loss effects the performance of the pump.
3. The water entering check valve from the pump body and delivery supply entry at air chamber has flown from higher area to smaller area and has higher velocities. Since head loss occurs in sudden contraction and is directly proportional to the square of velocity there occurs head loss in remarkable amount comprising to decrease in delivery flow rate and overall efficiency.

3.1. Modifications in existing design

The existing design was modified to obtain more efficient pump. The proposed modifications included circular inlet to be replaced with conical inlet.

Table 6: Head loss comparison with various inlet geometry

S.N	**AIDFI ram with circular inlet**	**Modified ram with conical inlet**
1.	Velocity at pipe end v_1=9.28m/s	Velocity pipe end v_1=9.28m/s)
2.	Velocity at pump inlet v_2=3.71m/s)	Velocity at pump inlet v_2=3.71m/s)
3.	head loss at inlet=0.5 $\times(v_1^2 - v_2^2)/2\times g$ =1.84m	head loss at inlet=0.115 $\times(v_1^2 - v_2^2)/2\times g$ =0.424m
Total	=1.84m	=0.424m

Expected delivery flow is calculated as:

Assumed η=85%

$\eta=(q\times h)/(Q\times H)$ $q=0.85\times265\times5/5$

q=20.47 LPM

Thus, expected delivery flow will be 20.47 LPM with pump efficiency 85 %.

Similarly, new volumetric efficiency can be calculated as

= 20.47/265

=7.76%

Expected monthly increase in delivery water

= (20.47-20) ×60×24×30

=20304liters

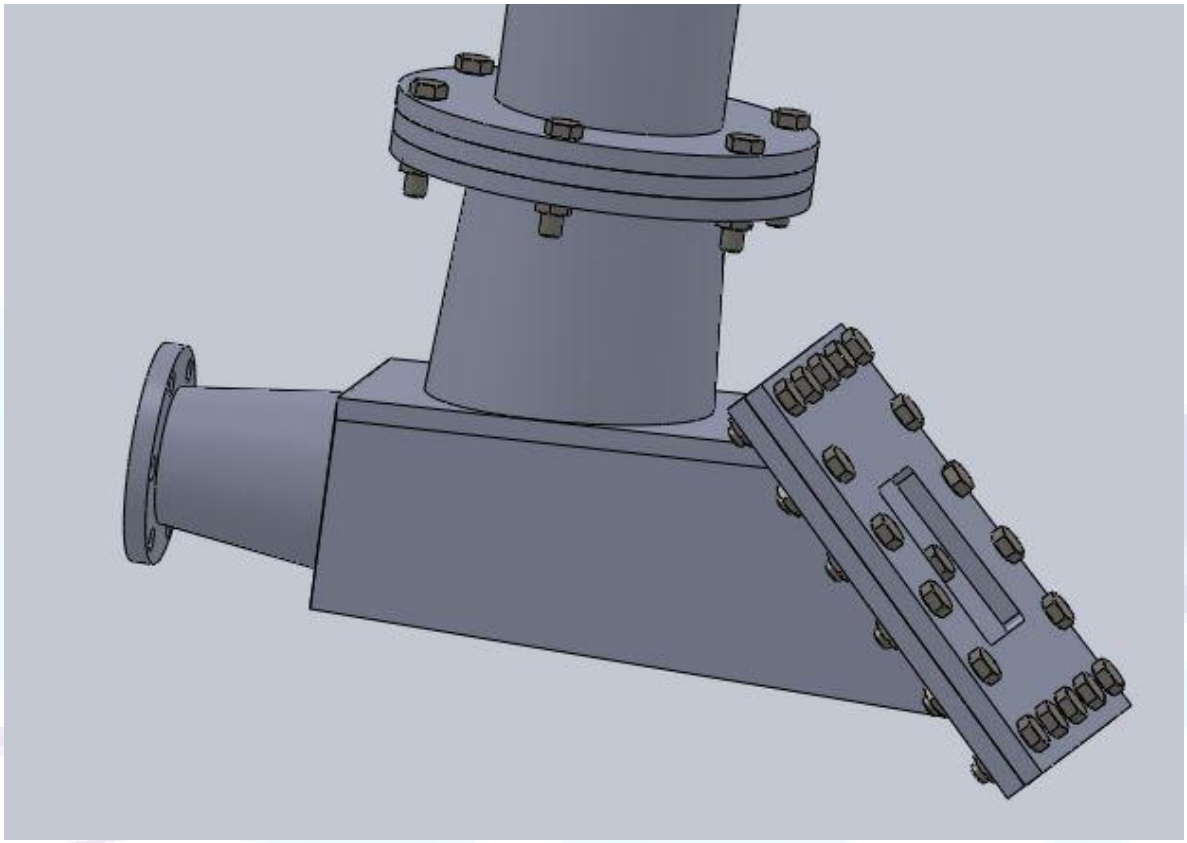

Figure 16: Modified Ram Pump with conical inlet and outlet

4. Results

After the implementation of the proposed modifications in the hydraulic ram pump the results obtained are as follows:

Site chosen for testing: Kalleri, Dhading

Table 7: Existing Site Parameters

S.N.	Parameters	Measured data
1	Drive pipe length	25m
2	Delivery pipe length	550m
3	Drive head	5m
4	Delivery head	56.5m
5	Drive flow	200 LPM
6	Delivery flow	14.67 LPM
7	Drive pipe diameter	75mm
8	Delivery pipe diameter	50mm

Table 8: Comparisons between designed and tested data for modified ram pump

S.N	Parameters	Designed	Tested	Remarks
1.	Drive Discharge	265 LPM	200 LPM	Less
2.	Delivery Discharge	20.47 LPM	15.00 LPM	Less
3.	Drive velocity	1.00 m/s	0.755 m/s	Less
4.	Rise in Head	146.00m	124.63m	Less
5.	Drag force on waste valve	45.01 N	45.00 N	Less
6.	Surge head	124.2 m	115.0.m	Less
7.	Hydraulic efficiency	85.0 %	84.9 %	Less
8.	Volumetric efficiency	7.8 %	7.5 %	Less
9.	Increase in water (monthly)	20304 liters	14256 liters	Less

The table 6 shows the comparison between designed data and tested data for modified ram pump. Here, the designed data was based on water available at monsoon season when stream was fully swollen, whereas test was carried out in dry season. Thu s, reduction in drive discharge effected all the other parameter.

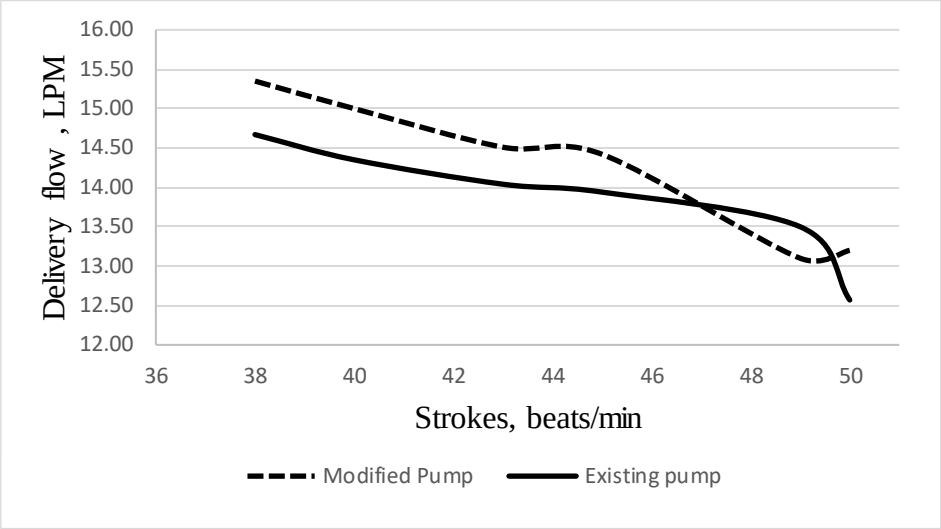

Figure 17: Delivery flow vs strokes

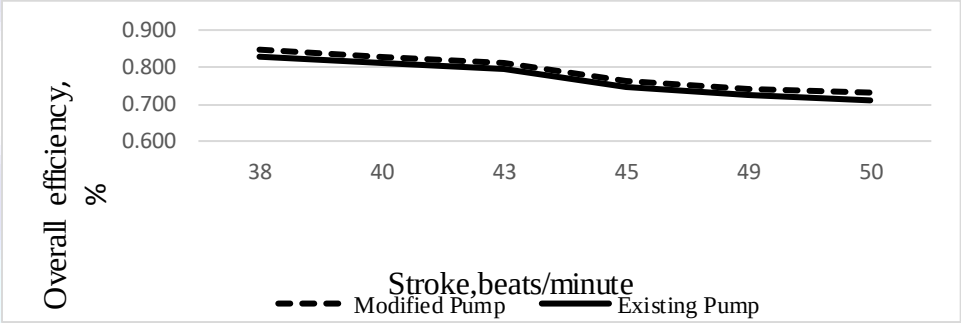

Figure 18: Efficiency comparison of existing and modified ram pump

Monthly Increase in delivery water

= (15-14.67) ×60×24×30

= 14256 litres

The figure 3 clearly shows maximum delivery flow rate occurs when strokes of waste valve was 38 beats per minute. Increasing the strokes from 38 to higher resulted in decrease in delivery flow. The tuning bolt was provided for adjusting the stroke or frequency of waste valve by setting the position of waste valve at certain angle when waste valve was in open state. Shorter the length of the bolt protruded inside longer was the stroke and water hammer effect. When the plug was down, more waste water was able to flow out increasing the velocity of the drive water. As a consequence, the high velocity water caused a strong water hammer effect. Furthermore, if stokes were reduced to 38 and less delivery would certainly increase but the dimension of waste valve limits in reducing the stroke less than 38. The hinge bolts head blocked the waste valve from further opening so maximum possible stroke is limited to 38.

5. Conclusion

Two major modifications were proposed in the existing ram pump system. But the modification done here was the replacement of cylindrical inlet with conical inlet in the pump inlet geometry. The modified pump was fabricated as per the draft. Testing of the modified pump was carried out at the site of Kalleri, Dhading. The input and output parameters were measured and noted. The data collected during the test were analyzed. The expected efficiency of the project was 85 % but the overall efficiency of modified pump was found to be

84.9%. Whereas volumetric efficiency was 7.4%. The deigned pump was expected to increase 20304 liters of water per month but the modified pump increased 14,256 liters of water per month.

There is possibility of increasing the efficiency, it could be done by decreasing the strokes nearer to 30 per minute. The other modifications could be replacement of outlet geometry from cylindrical to conical. Thus, it can be concluded that the result of modification was satisfactory and nearer to the expected result.

Acknowledgment

The authors would like to thank Centre for Rural Technology, Nepal for the support in fabrication and testing of pump.

References

[1] R. &. L. B. &. K. A. Fatahi-Alkouhi, "Determine The Efficiency of Hydraulic Ram-Pumps.," in *IAHR World Congress*, Netherlands, 2015.

[2] S. MOHAMMED, "Design and Construction of a Hydraulic Ram Pump.," *Leonardo Electronic Journal of Practices and Technologies.*, vol. 6, no. 11, pp. 59-70, 2007.

[3] N.G.Carj, "Hydraulic Ram Pump," *The Engineer*, 1967.

[4] F. Molyneux, "Fluid Handling," 1993, p. 274.

[5] VITA, "Using Water Resources," *Village Technology Handbook*, p. 143, 1970.

[6] T. D. J. T. H. T. A. V. S. P. B. G. P. D. Fountain, Hydraulic Ram Pumps (A guide to ram pump water supply systems), S C Fountain, 1991.

[7] E. Rajput, A textbook of HYDRAULICS MACHINES, Delhi: S.CHAND, 2011.